

**Site investigation SFR  
Deformation zone modelling**

**Model version 0.1**

Philip Curtis, Golder Associates AB

Jesper Petersson, Vattenfall Power Consultant AB

Carl-Axel Triumph, Hans Isaksson, GeoVista AB

April 2009

**Svensk Kärnbränslehantering AB**

Swedish Nuclear Fuel  
and Waste Management Co

Box 250, SE-101 24 Stockholm  
Phone +46 8 459 84 00



# **Site investigation SFR Deformation zone modelling**

## **Model version 0.1**

Philip Curtis, Golder Associates AB

Jesper Petersson, Vattenfall Power Consultant AB

Carl-Axel Triumph, Hans Isaksson, GeoVista AB

April 2009

*Keywords:* AP SFR-08-21, P-report SKBDoc id 12225824, Review statement SKBDoc id 1225826, Appendix SKBDoc id 1225822, Geological modelling, SFR version 0.1, Project SFR extension.

This report concerns a study which was conducted for SKB. The conclusions and viewpoints presented in the report are those of the authors. SKB may draw modified conclusions, based on additional literature sources and/or expert opinions.

Data in SKB's database can be changed for different reasons. Minor changes in SKB's database will not necessarily result in a revised report. Data revisions may also be presented as supplements, available at [www.skb.se](http://www.skb.se).

A pdf version of this document can be downloaded from [www.skb.se](http://www.skb.se).

# Abstract

This report presents the results of the work with the initial, deterministic deformation zone model (version 0.1), which is part of the ongoing investigations for the future expansion of the final repository for low and middle level radioactive operational waste, SFR. The modelling project will supply the basis for site-adapted design, in addition to a general assessment of the site suitability. The modelling work during version 0.1 follows SKB's established methodology using the Rock Visualisation System (RVS). The main input to this model version is older geological data from the construction of SFR, including eleven drill cores, which were remapped according to the Boremap system. The prime criterion for the selection of the drill cores for remapping was their cross-cutting relationship with inferred fracture zones in the previous structural models for SFR. In addition, there has been a revision of lineaments based on the interpretation of high resolution measurements of the magnetic total field covering most of the SFR area.

For version 0.1, a single deformation zone model has been delivered, with a volume corresponding to the regional model volume. The combined 'Master' model contains all the deformation zones modelled to date. The deformation zones falling inside the volumetrically more limited local model volume have been modelled without any minimum size constraint, while the deformation zones falling inside the regional model volume have been modelled with a minimum size constraint of 1,000 m trace length at the ground surface. This format is selected to facilitate further work by the hydrogeological modelling group, the primary end users of version 0.1.

The current model follows the earlier established conceptual understanding of the tectonic history of the Forsmark area. At the end of model version 0.1, the overall confidence level concerning the deformation history and the broad tectonic framework of the region is judged to be high. However, the overall confidence level in the rock volume of specific interest to the SFR project, lying between deformation zones ZFMWNW0001 and ZFMNW0805A, is judged to be at best medium since new drilling results, focusing on this rock volume, have not yet been incorporated into the model.

While certain details concerning particular deformation zones have been modified, there is nothing resulting from the current modelling work that has any significant impact on the earlier reported results for the Forsmark project for the final repository for spent nuclear fuel.

# Sammanfattning

Denna rapport presenterar arbetet med den inledande deterministiska deformationszonsmodellen (version 0.1), som är en del av de pågående undersökningarna för den framtida utbyggnaden av slutförvaret för låg- och medelaktivt radioaktivt driftavfall, SFR. Modelleringsprojektet kommer att utgöra grunden för platsspecifik projektering, samt en generell utvärdering av platsens lämplighet. Modelleringsarbetet under fas 0.1 följer SKB:s vedertagna metodik med användandet av RVS. Den aktuella modellversionen är i huvudsak baserad på äldre geologisk data från byggnationen av SFR inklusive elva borrhälar som genomgått förnyad kartering i enlighet med Boremap-systemet. Urvalet av borrhälar för omkartering är främst baserat på huruvida de skär tolkade sprickzoner i tidigare strukturmodeller för SFR. Dessutom har det skett en revision av lineament baserad på tolkningen av högupplösta mätningar av det magnetiska totalfältet som täcker större delen av SFR-området.

För version 0.1 har en enda deformationszonsmodell levererats, vars volym motsvarar den regionala modellvolymen. Denna integrerade 'master' modell innehåller alla deformationszoner som hittills modellerats. Deformationszoner belägna inom den lokal modellvolymen har modellerats utan några undre storleksbegränsningar, medan deformationszoner i den regionala modellvolymen har modellerats med en undre storleksbegränsning på 1 000 m för den projicerade längden på markytan. Formatet har valts för att underlätta arbetet för den hydrogeologiska modelleringsgruppen, som är slutanvändare av version 0.1.

Föreliggande modell följer vedertagen konceptuell förståelse av den tektoniska historien i Forsmarksområdet. Den övergripande konfidensnivån för deformationshistorien och regionens tektoniska ramverk bedöms mot slutet av modellfas 0.1 vara hög. För den bergmassa som ligger mellan deformationszonerna ZFMWNW0001 och ZFNW0805A bedöms dock den övergripande konfidensnivån i bästa fall vara medelhög, eftersom resultaten från de nya borrhälar inte inkorporerats i modellen.

Medan några detaljer för enskilda deformationszoner har modifierats har arbetet under den aktuella modelleringsfasen inte haft någon inverkan på tidigare rapporterade resultat från platsundersökningen i Forsmark för slutförvaret för utbränt kärnbränsle.



# Contents

<b>1</b>	<b>Introduction</b>	9
1.1	Background	9
1.2	Objective and scope	9
1.3	Geological setting	10
1.4	Model volumes	11
<b>2</b>	<b>Previous structural models</b>	13
2.1	Previous structural models for SFR	13
2.2	Conceptual understanding of deformation zones based on the Forsmark site investigation	16
<b>3</b>	<b>Overview of available geological and geophysical data</b>	19
3.1	Data quality	19
3.2	Geological tunnel mapping from SFR	19
3.3	Borehole data	20
3.4	Surface geophysics	22
<b>4</b>	<b>Evaluation of primary data</b>	25
4.1	Geological tunnel mapping within SFR	25
4.2	Borehole data	26
4.2.1	Deviation measurements for boreholes from the construction of SFR	26
4.2.2	Geological data from the construction of SFR	26
4.2.3	Updated geological mapping and geological SHI of existing SFR boreholes	27
4.2.4	Comparison between old SFR interpretations and geological SHI	29
4.2.5	Geological and geophysical borehole data from the Forsmark site investigation	30
4.3	Surface geophysics	31
4.3.1	Background	31
4.3.2	Revision of lineaments	31
4.3.3	Comparison between lineaments from SFR version 0.1 and the Forsmark site investigation	34
4.3.4	Modelling of low magnetic anomalies connected to lineaments	37
4.3.5	Geological significance of lineaments	38
4.3.6	Low velocity anomalies in refraction seismic data	38
4.3.7	Reflectors in reflection seismic data	40
<b>5</b>	<b>Model for deterministic deformation zones</b>	43
5.1	Methodology and modelling assumptions	43
5.2	General character of different sets of zones	48
5.2.1	The vertical to steeply dipping WNW to NW set	48
5.2.2	Other vertical to steeply dipping deformation zones	51
5.2.3	Gently dipping deformation zones	51
5.3	Assignment of properties	51
5.3.1	Orientation, length (size) and thickness	54
5.3.2	Deformation style	54
5.3.3	Alteration	54
5.3.4	Other properties	55
5.4	Geometric model	55
5.4.1	Regional and local models	55
5.4.2	DZ thickness classes	56
5.4.3	Deformation zone depth cut-off classes	56
5.5	Confidence assessment and the future handling of key uncertainties	57
	<b>References</b>	59

<b>Appendix 1</b>	Specification of available data	63
<b>Appendix 2</b>	Previous structural overview mapping of the existing SFR facility	65
<b>Appendix 3</b>	Technical borehole data	75
<b>Appendix 4</b>	WellCad logs from the geological single-hole interpretation of remapped drill cores	77
<b>Appendix 5</b>	Lineaments SFR model version 0.1	89
<b>Appendix 6</b>	Modelling of anomalies in the magnetic total field adjacent to lineaments – SFR version 0.1	97
<b>Appendix 7</b>	Deformation zones on a borehole by borehole and tunnel by tunnel basis	127
<b>Appendix 8</b>	Basis for interpretation of all deformation zones and property tables for deformation zones focused on during model version 0.1	141

# 1 Introduction

## 1.1 Background

During 2008, the Swedish Nuclear Fuel and Waste Management Company (SKB) initiated an investigation programme for a future expansion of the final repository for low and middle level radioactive operational waste, SFR. The motivation for the expansion was to provide room for the demolition waste from the closed reactors (Barsebäck, Studsvik and Ågesta) and the increased amount of operational waste caused by the extended operating time of the remaining nuclear power plants.

The programme was preceded by the site investigations for a deep repository for spent nuclear fuel, henceforth denoted the Forsmark site investigation /SKB 2008a/, and some systematisation and evaluation of the material from the construction of the nuclear power plant and SFR. Based on these data, a site descriptive model, version 0, was compiled for geology, rock mechanics, hydrogeology and hydrogeochemistry /SKB 2008b/. The version 0 model forms the framework for the current model version 0.1. The work follows SKB's established methodology for modelling /Munier et al. 2003/ using the Rock Visualisation System (RVS) /Curtis et al. 2007/. The main input to this model version is older geological data from SFR and a revision of lineaments based on the interpretation of high resolution measurements of the magnetic total field covering most of the SFR area /Isaksson et al. 2007/.

Model version 0.1 will serve as a platform for the modelling work by other geo-disciplines and further drilling activities. It will be updated as the SFR site investigations proceed. The subsequent model version 1.0 will be based on the completed revision of lineaments, a further re-examination and integration of earlier SFR drilling and tunnel mapping results as well as the results from the surface and underground based boreholes of the current drilling campaign. In addition to the deformation zone model, model version 1.0 will include a geometrical rock domain model. The final geological model, version 1.0, is intended to provide a foundation for the detailed design and the long-term safety assessment.

The investigations for the expansion of SFR differ in several aspects from the preceding Forsmark site investigation. Since it is desired that the new storage capacity will connect with the existing facility, the target area for the location of the extension is already well defined. Thus, the current SFR investigations will supply the basis for site-adapted design in addition to a general assessment of the site suitability. Moreover, the requirements on the rock mass and hydrogeological situation are somewhat lower for the SFR repository compared to the final repository for spent nuclear fuel.

## 1.2 Objective and scope

The general aim of the geological modelling work is to provide deterministic deformation zone and rock domain models that fulfil the needs of the repository design and safety assessment groups. Since the deterministic geological models form the framework for the modelling work by other disciplines, including rock mechanics, hydrogeology and hydrogeochemistry, it is developed successively, in tandem with the other models as new data from the SFR site investigation become available.

The specific aim with the version 0.1 modelling work was to produce a deterministic deformation zone model based on a reassessment of existing data from SFR and the Forsmark site investigation. Although this process has been initiated in version 0.1, due to the amount of data involved and changes in the ambition level for handling these data, the process is incomplete and will continue during version 1.0, along with the integration of new investigation data in particular from new boreholes. An important part in this work is to focus attention on the uncertainties and coverage of the available data from the construction of SFR and to support the planning for the ongoing field investigations. It needs to be emphasised that there are large uncertainties in model version 0.1 and in many aspects the confidence is low. The main reasons for this are the lack of primary data and the variable quality of the data. These points are addressed further in section 3.1.

### 1.3 Geological setting

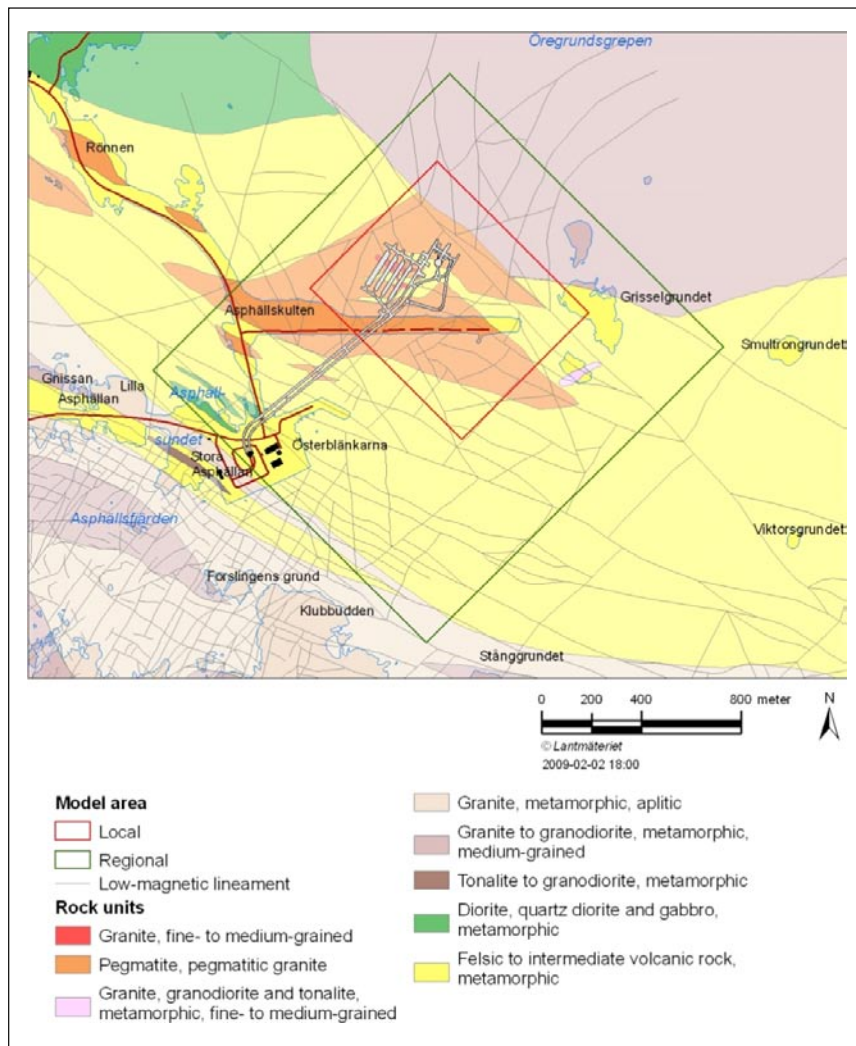
The SFR facility is located in northern Uppland close to the Forsmark nuclear power plant within the municipality of Östhammar, about 120 km north of Stockholm. The area forms part of a crustal segment in the Fennoscandian Shield generally affected by high ductile strain that extends several tens of kilometres across the Palaeoproterozoic bedrock in northern Uppland /Söderbäck (ed) 2008/. This crustal segment consists of subvertical belts affected by high ductile strain that strike WNW-ESE to NW-SE and anastomose around tectonic lenses affected by lower ductile strain (Figure 1-1). The deformation initiated under amphibolite-facies metamorphic conditions at mid-crustal levels during the Svecokarelian orogeny, and continued at lower metamorphic grade with the retrograde development of more discrete, subvertical deformation zones with similar strike, along which both ductile and brittle strain was focussed. Other orientation sets of brittle deformation zones, which are subvertical or gently dipping, formed during the later stages of or after the Svecokarelian orogeny.

The SFR area is situated within a high-strain belt that forms the north-easterly margin to the so-called Forsmark tectonic lens /SKB 2008a/. The north-western part of this tectonic lens hosts the target area for siting a potential repository for spent nuclear fuel. The strongly deformed rocks in the SFR area consist of a heterogeneous package of mainly felsic to intermediate metavolcanic rocks intercalated with biotite-bearing metagranite. Locally, these rocks have been intruded by considerable amounts of younger, often pegmatitic granite (Figure 1-2) during the waning stages of the Svecokarelian orogenic activity. Extensive geochronological data in the Forsmark area indicate that the bedrock formed and was affected by ductile deformation under amphibolite-facies conditions between 1.89 and 1.85 Ga, while ductile deformation along the more discrete zones continued until at least 1.8 Ga /Hermansson et al. 2007, 2008ab/. The bedrock had cooled sufficiently to respond to deformation in a brittle manner sometime between 1.8 and 1.7 Ga /Söderlund et al. 2009/.

The felsic to intermediate metavolcanic rock and biotite-bearing metagranite, which are the major components in the older igneous suite, exhibit a penetrative foliation and are, in part, also lineated or banded, forming heterogeneous banded, foliated and lineated (BSL) tectonites. Due to the intense strain and recrystallization, these rocks are generally difficult to separate. Other subordinate rock types in this suite are amphibolite and aplitic metagranite. Lithological contacts between these rocks are generally aligned parallel to the ductile tectonic foliation.



**Figure 1-1.** Map showing the structural framework in the Forsmark area with ductile high-strain belts that anastomose around tectonic lenses of lower ductile strain. The major retrograde deformation zones surrounding the Forsmark tectonic lens are also shown. Modified after /Stephens et al. 2007/.



**Figure 1-2.** Bedrock geological map of the area around SFR based on the bedrock geological map, Forsmark stage 2.2 /Stephens et al. 2007/ produced during the Forsmark site investigation. The inferred low magnetic lineaments in the area, based on model stage 2.3 in the Forsmark site investigation /Isaksson et al. 2007/, and the local and regional SFR model areas are also shown. The paler shades for each colour on the map indicate that the corresponding rock unit is covered by water.

Granite in the younger igneous suite occurs typically as dykes and minor bodies that are only partly affected by the ductile deformation and metamorphism. Most contacts are discordant to the ductile deformation in the older meta-igneous rocks. The grain-size is highly variable in the rocks of this suite and may range from fine-grained to coarse-grained pegmatitic in a single occurrence. Another conspicuous feature is the anomalously high uranium content in the younger granites. More details regarding the character of individual rock types are provided in /Stephens et al. 2007/.

The Singö deformation zone forms a regionally important, composite ductile and brittle zone in the SFR area. A conceptual model for the formation and reactivation of deformation zones in the Forsmark area has been provided in /Stephens et al. 2007/ and is summarised in section 2.2.

## 1.4 Model volumes

In accordance with the geoscientific execution programme /SKB 2008b/, the modelling work has been performed on two different scales, one regional and one local. The local model covers the existing SFR facility and the rock volume for the planned SFR extension. The SFR model areas as well as the local model area in the Forsmark site investigation are shown in Figure 1-3. The SFR local

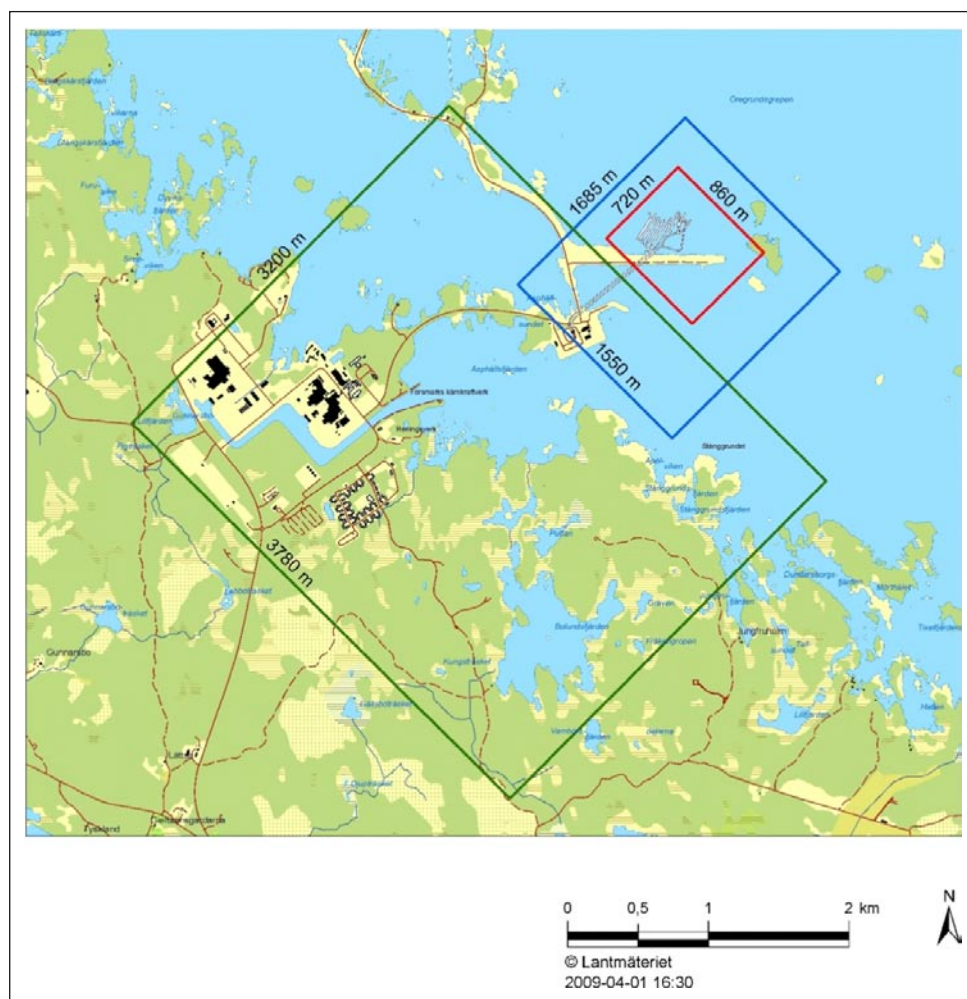


model volume extends from elevation +100 masl (metres above sea level) to –300 masl, while the regional model volume extends from +100 masl to – 1,100 masl. The coordinates defining the model areas are provided in Table 1-1.

A single deformation zone model has been delivered in model version 0.1, with a volume corresponding to the regional model volume as defined above. The combined ‘Master’ model contains all the deformation zones modelled to date. However, the local model volume has been included and those deformation zones falling within the local model volume have been modelled following the local model size constraints as well as the larger zones that are modelled in accordance with the regional model constraints. This format has been selected to facilitate further work by the hydrogeological modelling group who are the primary end users of version 0.1. Since the information density varies, the confidence in the description will generally vary within the model volume. For version 1.0 separate local and regional models as well as a combined model will be delivered to facilitate the work by the various end users.

**Table 1-1. Coordinates defining the model areas for SFR in metres. RT90 (RAK) system.**

Regional model volume		Local model volume	
<i>Easting</i>	<i>Northing</i>	<i>Easting</i>	<i>Northing</i>
1631920.0000	6701550.0000	1632550.0000	6701880.0000
1633111.7827	6702741.1671	1633059.2484	6702388.9854
1634207.5150	6701644.8685	1633667.2031	6701780.7165
1633015.7324	6700453.7014	1633157.9547	6701271.7311



**Figure 1-3.** Regional (blue) and local (red) model areas for SFR model version 0.1 relative to the local model area used in the Forsmark site investigation, model stage 2.2 (green).

## 2 Previous structural models

### 2.1 Previous structural models for SFR

The first conceptual model of the fracture zones around SFR was presented by /Carlsson et al. 1985, 1986/, with the purpose of providing input to a performance assessment study of the facility. The model was based on geological and hydrogeological data, with complementary information from refraction seismic investigations and aerial photographs. The central concept was a number of steeply to moderately dipping deformation zones, dividing the rock mass around SFR into three distinct blocks (Figure 2-1. a) and b) Two alternative models for the eight most prominent fracture zones at repository depth. Interpretation based on borehole logs and tunnel mapping. c) Vertical profile along one of the access ramps (tunnel BT) to SFR showing the position of gently dipping zones. The three blocks in the rock mass, as discussed in the text, are marked by I, II and III. a), b) and c) are redrawn after /Carlsson et al. 1985/.), which were further subdivided by gently dipping zones with high hydraulic conductivity. These blocks are:

Block I defined by zones 3 (ZFMNNE0869), 7 and 8 (ZFMNW0805A).

Block II defined by zones 3 (ZFMNNE0869), 6 (ZFMNNW1209) and 7.

Block III defined by zones 3 (ZFMNNE0869) and 6 (ZFMNNW1209).

The zone names in accordance with the designation system adopted during the Forsmark site investigation and used herein are given in parentheses. To be consistent with earlier terminology used at Forsmark, the following dip terminology has been applied within the SFR project:

Vertical to steeply dipping:  $\geq 70^\circ$

Moderately dipping:  $70^\circ\text{--}45^\circ$

Gently dipping:  $\leq 45^\circ$

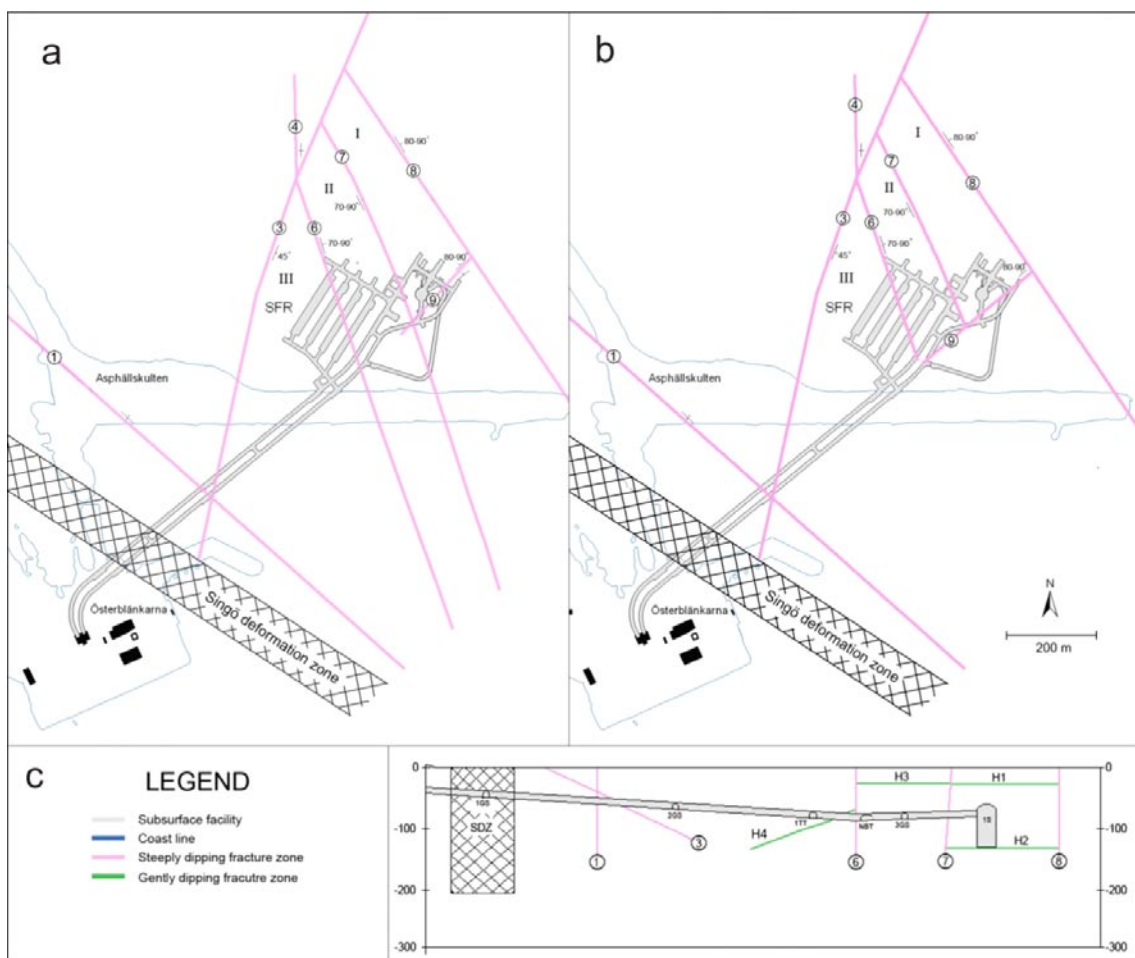
The model includes eight steeply dipping zones, exceeding one metre in thickness. The most prominent of the zones is the regional Singö deformation zone (ZFMWNW0001). In addition, there are a large number of less prominent steep zones ( $< 1$  m in thickness), which have not been included in Figure 2-1. a) and b) Two alternative models for the eight most prominent fracture zones at repository depth. Interpretation based on borehole logs and tunnel mapping. c) Vertical profile along one of the access ramps (tunnel BT) to SFR showing the position of gently dipping zones. The three blocks in the rock mass, as discussed in the text, are marked by I, II and III. a), b) and c) are redrawn after /Carlsson et al. 1985/. It should be noted that there is considerable difference in the assessment of zone thickness used during the SFR construction work compared with that currently used by SKB. Earlier thickness definitions focused on the rock quality from an engineering viewpoint, while current SKB methodology focuses on a geological thickness that is often significantly larger. This difference is described more fully in section 4.2.4.

The model includes two alternative interpretations, with insignificant differences for the eight more prominent zones (cf. Figure 2-1. a) and b) Two alternative models for the eight most prominent fracture zones at repository depth. Interpretation based on borehole logs and tunnel mapping. c) Vertical profile along one of the access ramps (tunnel BT) to SFR showing the position of gently dipping zones. The three blocks in the rock mass, as discussed in the text, are marked by I, II and III. a), b) and c) are redrawn after /Carlsson et al. 1985/. a) and b). The gently dipping zones (denoted by 'H' followed by a number), as shown in Figure 2-1. a) and b) Two alternative models for the eight most prominent fracture zones at repository depth. Interpretation based on borehole logs and tunnel mapping. c) Vertical profile along one of the access ramps (tunnel BT) to SFR showing the position of gently dipping zones. The three blocks in the rock mass, as discussed in the text, are marked by I, II and III. a), b) and c) are redrawn after /Carlsson et al. 1985/. c), are truncated by the more steeply dipping zones that define the three blocks. The north-eastern block (Block I) is intersected by two inferred, gently dipping zones between  $-20$  and  $-40$  (H1), and between  $-90$  and  $-140$  (H2) masl, the central block (Block II) by one zone between  $-15$  and  $-35$  masl (H3) and the south-western (block III) by one zone (H4) that strikes  $N75^\circ E$  and dips  $25^\circ$  towards the NNW. The most well-defined of these gently dipping zones, zone H2, is characterized by high hydraulic conductivity, an increased

frequency of sub-horizontal fractures and, locally, significant amounts of clay. The other gently dipping zones are mainly manifested by high hydraulic conductivity, whereas their geological character is less significant and described as ‘zones of released joints’ /Carlsson et al. 1985/. In model version 0.1, H1 and H3 are inferred to be unloading or stress relief structures, due to their orientation and shallow depth. However, additional efforts will be made to better characterize these features, based on archive data, in version 1.0.

An evaluation by /Christiansson 1986/, based on additional borehole data, resulted in a more comprehensive characterisation of some of the larger zones close to SFR, as well as an extension of zone H2 through the central block (Block II). It was inferred that H2 (ZFM871) terminated against zones 3 (ZFMNNE0869), 6 (ZFMNNW1209), 8 (ZFMNW0805A) and, towards the south-east, against zone 9 (ZFMNE0870A/B) in the model (cf. Figure 2-1. a) and b) Two alternative models for the eight most prominent fracture zones at repository depth. Interpretation based on borehole logs and tunnel mapping. c) Vertical profile along one of the access ramps (tunnel BT) to SFR showing the position of gently dipping zones. The three blocks in the rock mass, as discussed in the text, are marked by I, II and III. a), b) and c) are redrawn after /Carlsson et al. 1985/. Moreover, the dip of zone 3 (ZFMNNE0869) was changed from 35–45° to 70–80°, based on borehole intersections.

Seven of the most prominent zones, as shown in Figure 2-1. a) and b) Two alternative models for the eight most prominent fracture zones at repository depth. Interpretation based on borehole logs and tunnel mapping. c) Vertical profile along one of the access ramps (tunnel BT) to SFR showing the position of gently dipping zones. The three blocks in the rock mass, as discussed in the text, are marked



**Figure 2-1.** a) and b) Two alternative models for the eight most prominent fracture zones at repository depth. Interpretation based on borehole logs and tunnel mapping. c) Vertical profile along one of the access ramps (tunnel BT) to SFR showing the position of gently dipping zones. The three blocks in the rock mass, as discussed in the text, are marked by I, II and III. a), b) and c) are redrawn after /Carlsson et al. 1985/.

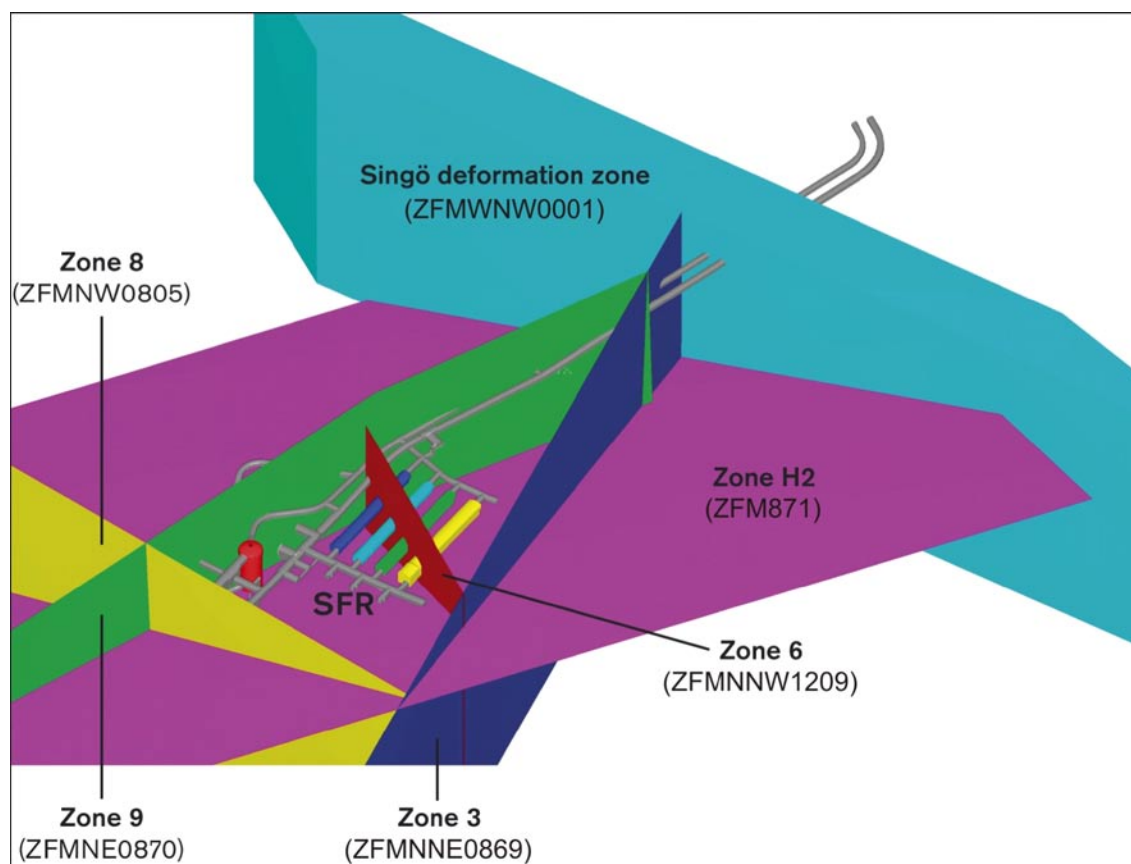


by I, II and III. a), b) and c) are redrawn after /Carlsson et al. 1985/. (i.e. Singö as well as zones 1, H2, 3, 6, 8 and 9), were included in a performance assessment study for the SFR facility /SKB 1987/. An updated study, with no formal revision of the fracture zones, was reported by /SKB 1993/.

A review of the original conceptual model was performed by /Axelsson et al. 1995/. The major findings were that there were uncertainties in the fracture zone model and that other interpretations were possible. An alternative model was therefore presented by /Axelsson and Hansen 1997/, based on a review of geophysical, geological and hydrogeological data. The zones affected by this work are H2, 6, 8 and 9, which were revised according to the following (Figure 2-2):

<i>Zone H2 (Zone 871)</i>	Extended beyond zones 3, 6, 8 and 9, probably also beyond the Singö fault zone.
<i>Zone 6 (Zone ZFMNNW1209)</i>	Shortened and terminated before it reaches the drift tunnel.
<i>Zone 8 (ZFMNW0805A)</i>	Reduced to a relatively unimportant zone from a hydraulic viewpoint.
<i>Zone 9 (ZFMNE0870)</i>	Extended to end in zone 3.

Thus, the original concept with a modelled termination of the gently dipping zones against the nearest, more steeply dipping zone was abandoned by the extension of zone H2. This interpretation formed the basis for the hydraulic modelling work by /Holmén and Stigsson 2001/ that gave input to the latest performance assessment study for SFR /SKB 2001/. It must be emphasized that all zone indications given by /Carlsson et al. 1986/ for H2, 3, 6, 8 and 9 were adopted by /Axelsson and Hansen 1997/ without any changes in borehole or tunnel positions. However, /Axelsson and Hansen 1997/ included additional intercepts and extended some of the earlier defined zones. Hence, the model represents an



**Figure 2-2.** Deformation zones in the local structural model updated by /Axelsson and Hansen 1997/. The general layout of the SFR tunnel systems is also shown. The zones are marked both according to the SFR terminology and the system established during the Forsmark site investigation /SKB 2004/. View towards south.

alternative interpretation, based on the same data, as pointed out by /Axelsson and Hansen 1997/. For SFR version 0.1, the most recent interpreted zone intercepts, defined in /Axelsson and Hansen 1997/, have been taken as providing the starting point for the modelling work. The interpreted borehole and tunnel interceptions with the zones, as defined in /Axelsson and Hansen 1997/, have been logged in Sicada to ensure traceability. However, further review of details provided in /Carlsson et al. 1985, 1986/ and other possibly existing SFR documentation will continue in version 1.0. In particular, there will be a focus on searching for information to confirm the existence and characterization of H1, H3 and H4.

## 2.2 Conceptual understanding of deformation zones based on the Forsmark site investigation

A description of the deformation zones inside the larger model volumes (local and regional) used in the Forsmark site investigation was presented in the final geological model stage 2.2 during the site investigation work /Stephens et al. 2007/ and complementary stage 2.3 data were evaluated in /Stephens et al. 2008a/. An integrated site descriptive model was presented in /SKB 2008a/. The oldest discrete master structures in the area are the steeply dipping, WNW-ENE and NW-SE zones (e.g. Singö deformation zone), generally referred to as the WNW to NW set. These zones initiated their development in the ductile regime and continued to be active as faults in the brittle regime. Together with the broader structural belts with the same orientation, which developed earlier under higher-grade metamorphic conditions, they account for a pronounced structural anisotropy in the bedrock. In addition to the conspicuous WNW to NW zones, there are three distinctive sets of brittle deformation zones (fracture zones) in the area:

- Vertical to steeply dipping fracture zones that strike ENE-WSW (NE-SW) and NNE-SSW, generally referred to as the ENE to NNE set including ENE(NE) and NNE sub-sets.
- Vertical and steeply dipping fracture zones that strike NNW-SSE, generally referred to as the NNW set.
- Gently dipping ( $\leq 45^\circ$ ) fracture zones that, relative to all the other sets, contain a higher frequency of open fractures and non-cohesive fault rocks.

Kinematic data along major zones of the WNW to NW master set shows that these zones have been affected by brittle deformation under different stress regimes. Also the ENE to NNE set is inferred to have developed under different stress regimes with evidence of both sinistral and dextral movement along minor, steeply dipping faults that strike ENE to NE inside the zones and a dominance of sinistral displacement along the NNE minor faults. Subordinate dip-slip movement has also occurred. The NNW set, on the other hand, shows evidence for a predominant sinistral strike-slip displacement, as well as minor dextral strike-slip and dip-slip movements. The gently dipping zones reveal evidence of both reverse dip-slip and subordinate strike-slip senses of movement, suggesting development in one or more compressive regimes. However, fault-slip data are absent along some of them and these structures are possibly join zones /SKB 2008a/.

A concept where the four different sets of deformation zones formed initially in response to compressive tectonic regimes, during the later part of the Svecokarelian orogeny, was presented already in early model versions /SKB 2005, 2006/, and was further refined in the final geological model /Stephens et al. 2007, SKB 2008a/. This concept involved dextral strike-slip displacement in low-temperature ductile and subsequently brittle regimes along the steeply dipping, WNW to NW master set and possibly even the steeply dipping NNW set (Figure 2-3). This was followed by continued dextral strike-slip displacement along these structures in the brittle regime, in combination with sinistral strike-slip displacement along the steeply dipping ENE(NE) and NNE sub-sets (Figure 2-3). Bulk crustal shortening in a NW-SE to N-S direction during the later part of the Svecokarelian orogeny was inferred.

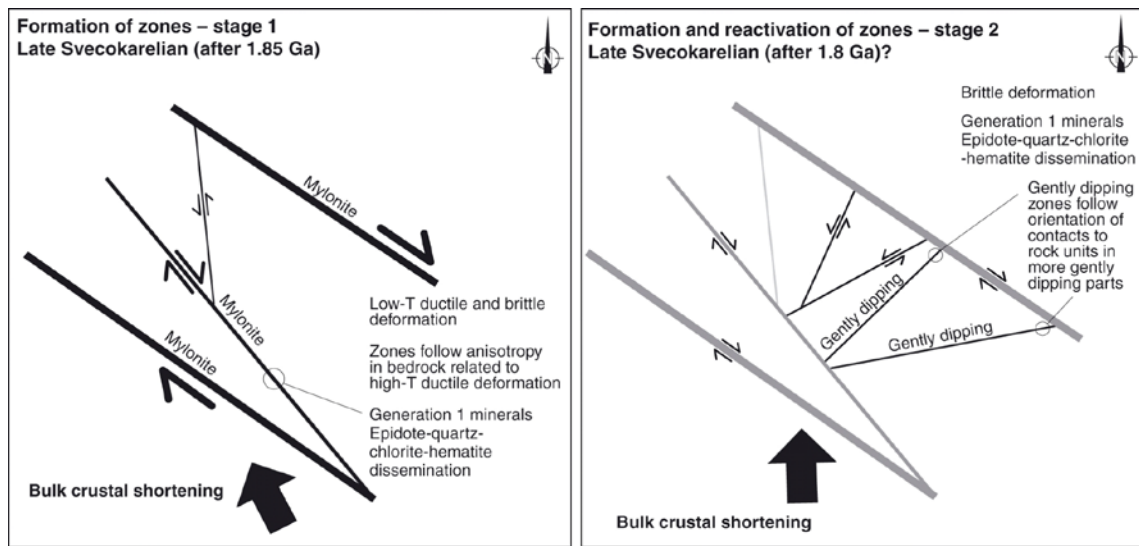
The modelled truncation of the gently dipping zones is based on the conceptual hypothesis that these structures formed after the steeply dipping master set of WNW to NW zones, and more or less at the same time as the steeply dipping ENE(NE) sub-set, NNE sub-set and at least some of the steeply dipping NNW set in the brittle regime (Figure 2-3). For this reason, the gently dipping zones were

extended in space as far as the nearest steeply dipping zone in the 3D modelling work /Stephens et al. 2007/. It was proposed that the gently dipping zones, at least in the south-eastern part of the Forsmark candidate area, followed arrays of amphibolite boudins in the predominant metagranite. Furthermore, the markedly lower frequency of these hydrogeologically important structures in the target area (north-western part of the candidate area) was related to the steeper dips of the ductile structures in this area, i.e. the structural anisotropy in the bedrock.

All the four sets of deformation zones underwent reactivation in the brittle regime during the subsequent geological evolution. For example, sinistral strike-slip displacement has been documented along the zones in the WNW to NW master set (see review in /Stephens et al. 2008a/). Furthermore, the reactivation of fractures in the bedrock as joints, due to the effects of loading and unloading cycles during the later part of the Proterozoic and Phanerozoic time periods, has been recognized. This type of reactivation with changes in aperture along fractures is most conspicuous in fractures along the gently dipping zones and along fractures in the near-surface realm in the target area at Forsmark.

In the current stress regime with the minimum principal stress at a high angle to the gently dipping zones, the flat-lying fractures within these zones will be the most susceptible to dilatational strain and reactivation. Consequently, they are most likely to bear groundwater. The steeply dipping ENE(NE) and NNE sub-sets of deformation zones, on the other hand, which are oriented at a high angle to the maximum principal stress at the current time, are the least favoured for reactivation as dilatational joints and hence should bear least groundwater /Stephens et al. 2007/. Hydrogeological data confirm these predictions /Follin 2008/.

The relevant reports for the previous structural models for SFR and the modelling work during the Forsmark site investigation, including the final document of the site investigation referred to as SDM-Site Forsmark, are listed in Appendix 1.



**Figure 2-3.** Two-dimensional cartoon illustrating the regional-scale dynamics during the initial development of the master, steeply dipping WNW and NW zones and the subordinate sets of brittle deformation zones in response to late stage Svecokarelian tectonic activity. After /SKB 2008a/.

## **3 Overview of available geological and geophysical data**

### **3.1 Data quality**

Although there is a considerable quantity of geological documentation from the construction of SFR, the data quality is highly variable, and there are, moreover, uncertainties in the methodology used to obtain the data. The basis for the current modelling methodology established by SKB is quality-assured data available in the SKB databases Sicada and GIS. However, at this stage there are also data from the construction of SFR, used in this modelling work, which lack this quality-assurance.

A part of the version 0.1 modelling work has been to review the older SFR data and to identify which data can be the subject of further processing and quality checks, with the aim of reaching a level where it can be included in the Sicada and GIS databases for use in version 1.0. Where possible, data from the Forsmark site investigation and the remapping and geological single-hole interpretation (SHI) of selected older SFR boreholes, performed during version 0.1, have been given precedence over older, less controlled data. Thus, where possible, intercepts between boreholes and deformation zones, upon which previous structural models of SFR were built, have been replaced by correlations based on the occurrence of possible deformation zones in the SHI of the same boreholes. However, issues arise particularly with the old tunnel data and their earlier interpretations, which are difficult to review in a meaningful way, yet are, at the same time, a very important source of information and inherently give a valuable indication of the character of a particular deformation zone in a different manner to that indicated by a borehole intercept. In the same way, it is not considered reasonable to discount documented experience from the construction phase of SFR, even if the reporting does not correspond to current SKB quality standards.

One important issue that has arisen is the contrast in the methodology used during the SFR construction work and that used currently by SKB for the definition of what constitutes a deformation zone and how a zone's thickness is defined. The fracture zones included in the previous structural models of SFR were generally identified on the basis of the frequency of open fractures and hydrogeological information /cf. Carlsson et al. 1986/. An extreme example is ZFMNE0870A/B (SFR zone 9) which is an open, persistent, water-bearing joint. This structure was consequently interpreted as a zone, since it was significant for the rock excavation, support and grouting. In a structural geological sense, this structure would probably not constitute a zone that qualifies for deterministic modelling using current SKB methodology. This should not be taken in any way to infer that the earlier judgments were better or worse than the current definitions but rather they were based on a very different approach.

This difference becomes clearer when zone thickness is specifically considered in the modelling work. The earlier SFR zone thicknesses were largely based on the presence and frequency of open fractures. This differs considerably from the definition established by SKB /Munier et al. 2003/, with core and damage zones that take into account both sealed fractures, alteration and other features in addition to open fractures, which will generally result in a much greater thickness compared with the earlier applied methodology. Bearing in mind these differences, an attempt has been made in model version 0.1 to avoid the mixing of borehole intercepts from previous reported structural models with up-to-date SHI interpreted possible deformation zones when defining individual zone thicknesses. Consequently, while a particular deformation zone's existence and overall geometry may be based on a mixture of older and newer data, the zone thickness is based first and foremost on SHI data.

A summary of the available bedrock geological and geophysical data and their treatment in SFR model version 0.1 is presented in Appendix 1.

### **3.2 Geological tunnel mapping from SFR**

Geological maps at the scale 1:200 covering all underground openings were generated during the construction of SFR /Christiansson and Bolvede 1987/. These maps provide details regarding rock



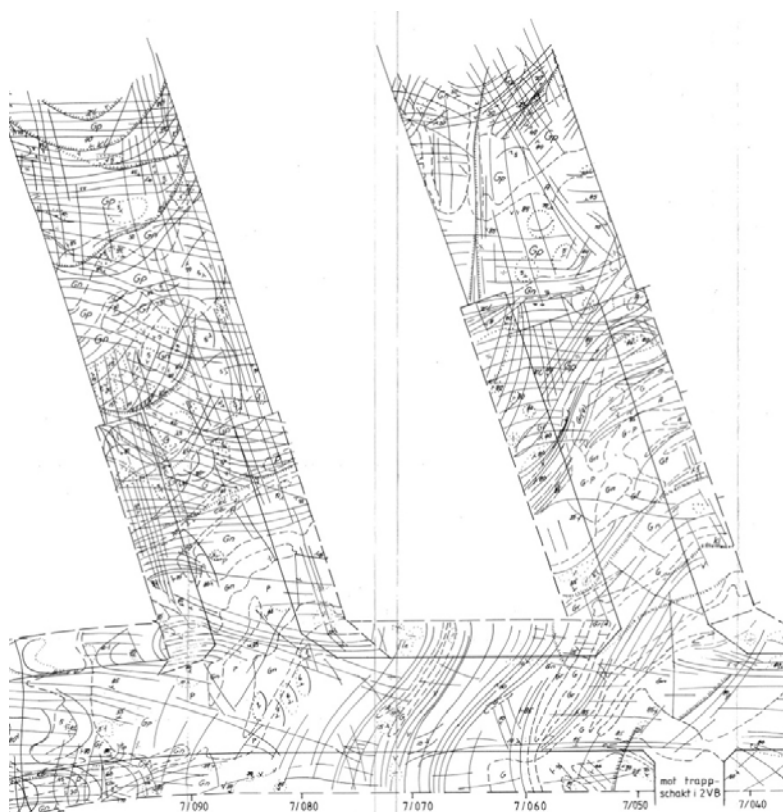
type, fractures, other tectonic structures and water seepage (Figure 3-1). In addition, there is a compilation of the structural data from SFR at a scale of 1:2,000 (Appendix 2). This compilation focuses on brittle structures and includes mapped crush zones, brittle shear zones and gouge-filled fractures of varying width (down to less than 2 dm), as well as occurrences of closely spaced, parallel fractures and slickensides. A general description of the various brittle features is presented in /Christiansson and Bolvede 1987/, along with a description of the mapping methodology.

An updated geological mapping of the lower construction tunnel (NBT), located in the lowermost eastern part of SFR, has been performed during 2008 /Berglund 2009/. This mapping included documentation of fracture zones. However, the results from the mapping have not yet been made available from the SKB database Sicada. It is intended to review and incorporate these results during the version 1.0 modelling.

### 3.3 Borehole data

An extensive drilling campaign, resulting in a total of 60 cored boreholes, was performed both at the surface and along underground excavations during the construction of the SFR facility (Figure 3-2). Technical data concerning the drilling activities, including the coordinates of the drill sites and the length, bearing and inclination of the boreholes are presented in Appendix 3. Relevant data reports are listed in Appendix 1.

Logs and protocols from the geological core mapping exist for the majority of the boreholes that were completed during the earlier investigation and construction of the existing SFR facility /Christiansson 1986, Christiansson and Magnusson 1985a, b, Hagkonsult 1983/. Available protocols concern mainly the rock type with a few notes on brittle structures. Fracture protocols with systematic quantitative data are more sparse. Borehole logs that typically exist include (1) rock type, (2) fracture filling, (3) fractures oriented along the drill core, (4) RQD, (5) fracture frequency and



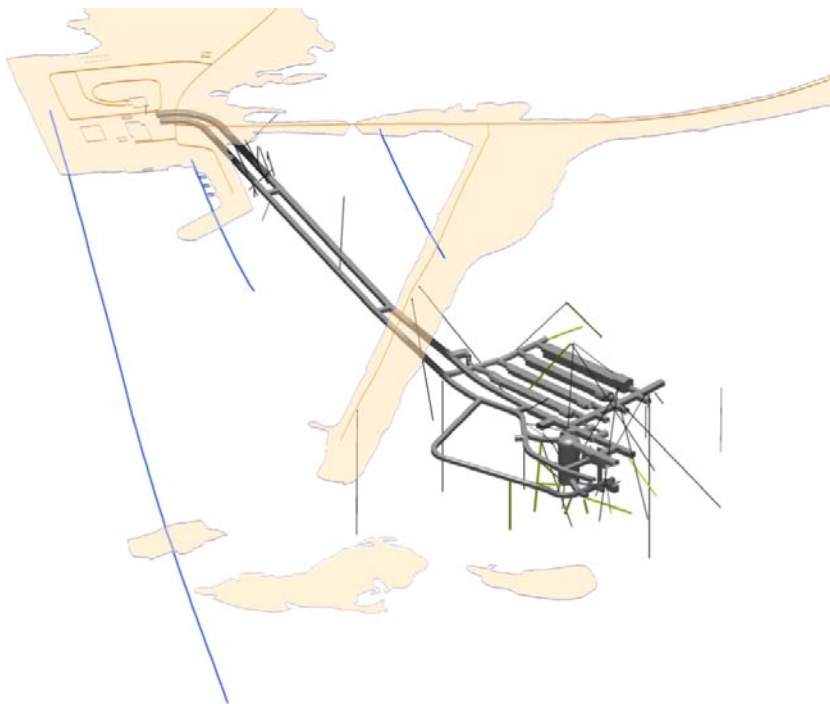
**Figure 3-1.** Example from the detailed geological mapping of tunnels at SFR showing rock type, fractures, other tectonic structures and water seepage. The tunnels are presented in 2D by 'folding out' the walls. Detail taken from Drawing -20 in /Christiansson and Bolvede 1987/.

(6) weathering. However, the methodology applied for the mapping of fractures is unclear and the different companies involved in the mapping appear to have used different methods and truncation levels. The inferred intercepts between the boreholes and fracture zones included in the previous structural models of SFR are provided in /Carlsson et al. 1985, 1986, Christiansson 1986/ and summarized in /Axelsson and Hansen 1997/.

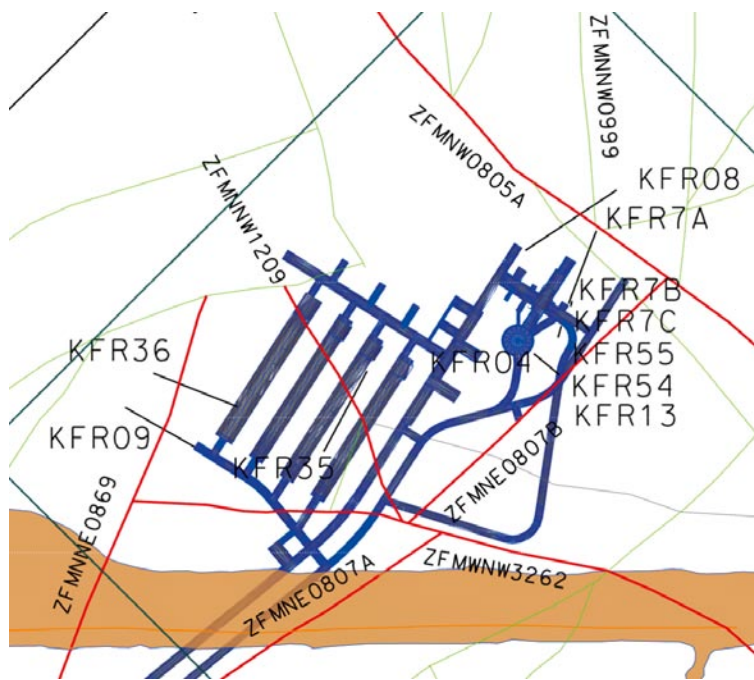
Based on the experiences from the preceding Forsmark site investigation (see Appendix in /Stephens et al. 2008b/), it was decided that eleven drill cores obtained in connection with the construction of SFR should be remapped according to the so-called Boremap system, despite that no BIPS-logging have been done. The prime criterion for the selection of the drill cores from KFR04, KFR08, KFR09, KFR13, KFR35, KFR36, KFR54, KFR55, KFR7A, KFR7B and KFR7C was their cross-cutting relationship with inferred fracture zones in the previous structural models for SFR (cf. /Axelsson and Hansen 1997/). The renewed mapping provided input to a so-called geological single-hole interpretation (SHI).

Since no BIPS-images are available for the boreholes, it has not been possible to obtain absolute orientations for geological structures and only relative measurements are available, based on the deviation from the drill core centre-line axis. Thus, the methodology has differed from the one adopted by SKB for use during the Forsmark site investigation. The remapping of the eleven drill cores generally focused on the location and mineralogy of broken and unbroken fractures, as well as crush zones, breccias and sealed networks. In addition, rock type, alteration and any ductile structures present were documented. The results of the mapping and geological SHI are presented in /Petersson and Andersson 2008/ and /Petersson et al. 2009/, respectively. Tabular summaries of the SHI are provided in Appendix 4.

In addition, one cored borehole (KFM11A) and two percussion boreholes (HFM34 and HFM35), which were drilled during the Forsmark site investigation, are relevant to the current SFR site investigation. All three boreholes were drilled within or in close proximity to the Singö deformation zone and penetrate the western part of the regional model volume (Figure 3-2). An evaluation of the geological, geophysical and SHI data from KFM11A and to some extent HFM34 and HFM35 was presented in /Stephens et al. 2008a/.



**Figure 3-2.** Three-dimensional image showing the position of all boreholes drilled inside regional model volume version 0.1. The three boreholes drilled during the Forsmark site investigation are marked in blue, whereas the boreholes from the construction of SFR are marked in green (remapped using the Boremap system) or black (no remapping using the Boremap system).



**Figure 3-3.** Surface projections of the eleven remapped SFR boreholes in relation to the ground surface traces (light brown) of the modelled deformation zones (red), lineaments (green) and SFR facility (blue).

### 3.4 Surface geophysics

The first detailed geophysical data from the Forsmark area were gathered already during the planning of the nuclear power plants. Since then, geophysical investigations at different scales and for different tasks have been carried out in the area, which have resulted in data of several types with variable spatial resolution and distribution. The intensity in gathering of geophysical data culminated during the Forsmark site investigation, between 2002 and 2007. An overview of the geophysical data used in the Forsmark site investigation is provided in /Stephens et al. 2007/.

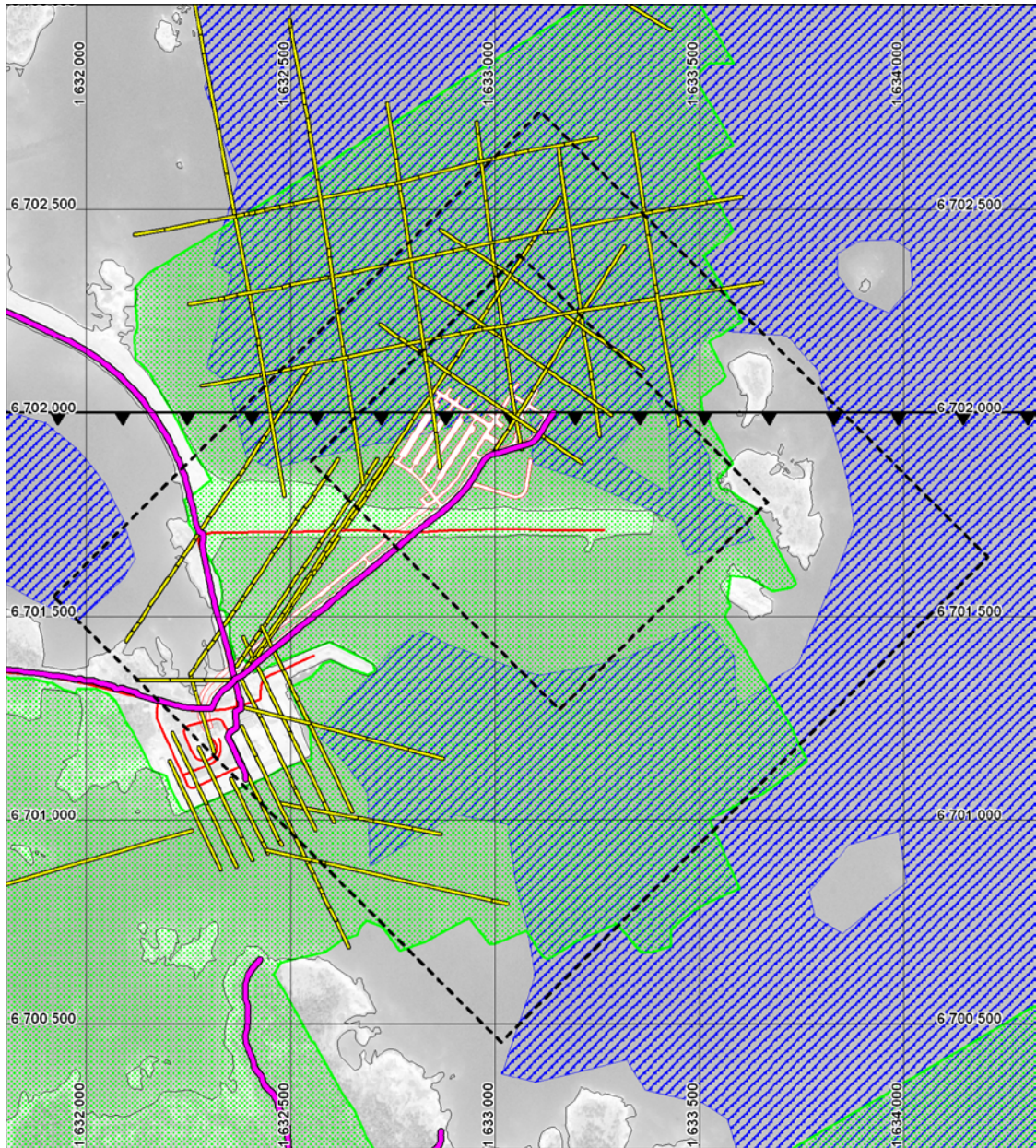
During the Forsmark site investigation, the focus was directed on the identification of structural information from magnetic total field data and reflection seismic data. The main source of magnetic data was the dense measurements from the ground survey on land, sea and lakes. However, the helicopter-borne survey also provided information on the magnetic total field, but with lower spatial resolution. At sea, and also quite near the shore, a marine geological survey provided data on the bedrock topography. Campaigns with refraction seismics, both on land and in the sea, resulted in models for the bedrock topography and the P-wave velocity distribution in the bedrock. Only two of the reflection seismic profiles (profiles 5b and 8) cover part of the SFR model areas /Juhlin and Palm 2005/.

The characteristics of available magnetic data are presented in Table 3-1 and the surface coverage of all the available geophysical data is presented in Figure 3-4. Relevant data reports for the surface geophysical measurements and lineament interpretation are listed in Appendix 1.

**Table 3-1. Characteristics of magnetic surveys in the Forsmark area (after /Stephens et al. 2007/).**

Type of survey	Contractor	Line spacing	Station spacing	Survey direction	Survey elevation	Grid resolution
Airborne, fixed-wing	SGU	200 m	17 or 40 m	EW	60 m (30 m older data)	40 * 40 m
Airborne, helicopter	NGU	50 m	3 m	NS and EW	45 m	10 * 10 m
Ground on land, sea and lake	GeoVista AB	10 m	5 m (2–3 m in the marine survey)	150°/330°	ca. 1.5–2 m	4 * 4 m





**Figure 3-4.** Coverage of available geophysical data around the SFR model areas (black, dashed lines). The whole area is covered by the SGU fixed-wing airborne survey and the NGU helicopter-borne NS-directed survey (Table 3-1). The NGU helicopter-borne EW-directed survey was carried out south of the jagged line at co-ordinate North 6702000. The detailed ground magnetic survey was carried out in the green shaded area and bedrock topography from the marine geological survey is available in the blue-hatched area. Refraction seismic profiles are shown with a yellow-black line. Reflection seismic profiles are shown with a magenta-black line.



## 4 Evaluation of primary data

### 4.1 Geological tunnel mapping within SFR

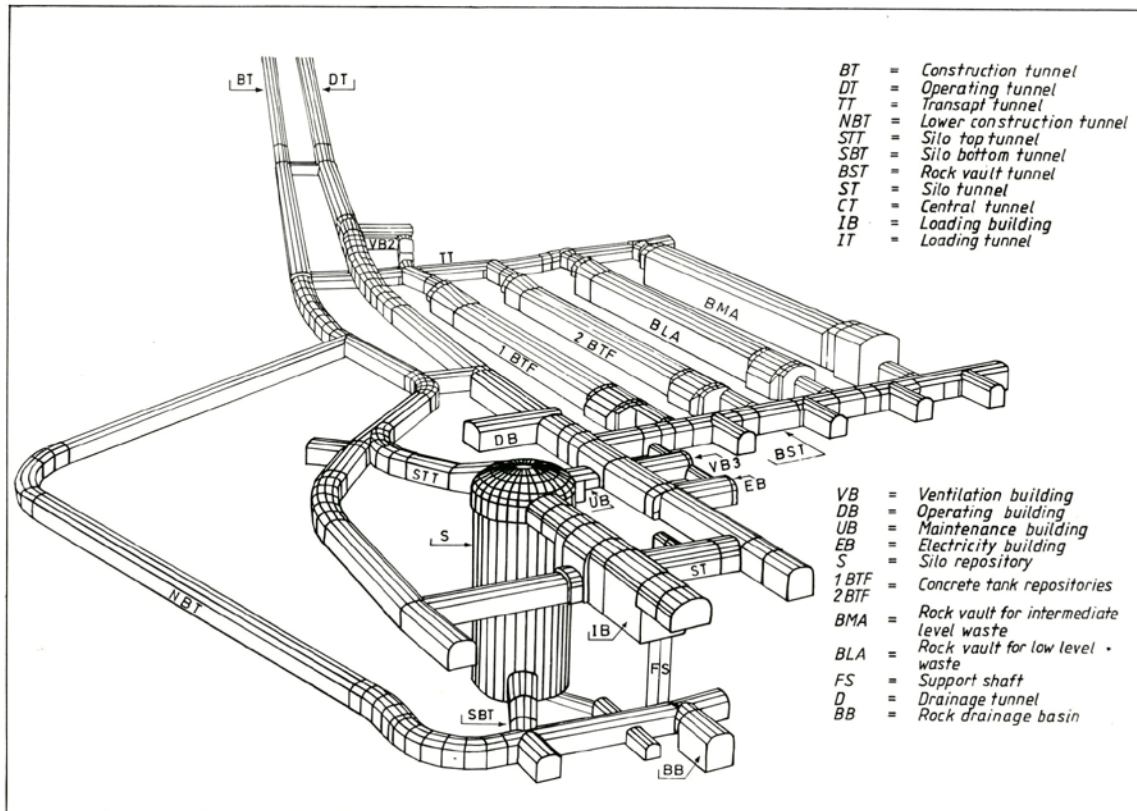
All the tunnel mapping drawings from /Christiansson 1986/ have been digitally scanned, georeferenced in ArcGis and attached to the RVS model. The overview drawings at the scale 1:2000 (see Appendix 2) have formed a primary input to the modelling of deformation zone intersections at the SFR underground facility, whereas the detailed maps at the scale 1:200 have been used to provide supporting details. It should be noted that the geometries of all the underground openings presented in the drawings are ‘as planned’ i.e. they are theoretical rather than ‘as built’. This together with deliberate generalizations involved in the mapping methodology /cf. Christiansson and Bolvede 1987/ means that the positions of all recorded features are only approximate. These drawings have been used in combination with as-built tunnel centre-line and laser scanned tunnel section survey data to estimate the zone tunnel intersection positions in 3D.

Although there exists a documented methodology for the tunnel mapping work, and even detailed sketches for some zones, the correlation between the structures represented in the overview mapping and the results of the fracture mapping presented in the detailed tunnel mapping is often unclear. Clearly identified ‘established’ fracture zones in the overview drawings are often difficult to identify in the detailed drawings.

Numerical information regarding the intercepts of deformation zones H2 (ZFM871), 3 (ZFMNNE0869), 6 (ZFMNNW1209), and 9 (ZFMNE0870A) along tunnels that were included in the previous structural models for SFR are presented in /Axelsson and Hansen 1997/. They are shown here in Table 4-1. This is complemented by Figure 4-1, which shows a view of SFR with ID codes used for the different tunnels and caverns. Similar to the SFR drill core data, these intercepts are based on increases in fracture frequency and, occasionally, an increased hydraulic conductivity. This information has, in some cases, been used in the SFR model version 0.1 to cover deficiencies in the scanned drawings.

**Table 4-1. Listed intercepts of fracture zones included in the structural model by /Axelsson and Hansen 1997/.**

Zone	Tunnel	Chainage	Orientation	Width [m]	Characteristics
Zone H2 (ZFM871)	NBT	8/405–435	WSW/20°S	6.0	Large inflow.
Zone 3 (ZFMNNE0869)	DT	1/470–1/495	NNE/steep W	10	–
	BT	5/390–5/420	NNE/steep W	10	–
Zone 6 (ZFMNNW1209)	BT	No observation		–	–
	DT	1/930	NNW/steep W	0.5	–
	1BTF	0/100	NNW/steep W	0.5	–
	2BTF	0/085	NNW/steep W	2	–
	BLA	0/060	NNW/steep W	0.5	–
	BMA	0/030	NNW/steep W	1	–
Zone 9 (ZFMNE0870A/B)	DT	1/530–1/570	ENE/steep SE	< 1	Water-bearing clayey gouge w chl and ca. Branches of from zone 3.
	Connection at DT	1/610	ENE/steep	< 1	Water-bearing gouge.
	BT	5/640–5/690	ENE/80°SE		Water-bearing gouge w clay and mylonite.
	BT	6/025–050	ENE/steep	< 1	Water-bearing gouge w clay and mylonite.
	STT	6/800–820	ENE/steep	3	Fractured zone w mylonite and clay.
	ST	4/090	ENE/90°	3	Increased jointing.
	NBT	8/025	ENE/70°SE	< 1	Two branching water-bearing gouges.
	NBT	8/290–8/350	ENE/80°–85°NE	3	Water-bearing gouge with clay, ca and Fe.



**Figure 4-1.** View of SFR with abbreviations used for the different tunnels and caverns. After /Carlsson et al. 1986/.

In addition to the fracture zones discussed by /Axelsson and Hansen 1997/, there are a number of inferred deformation zones marked on Drawing -103 of /Christiansson and Bolvede 1987/. The separation of zones with different characteristics is comprehensive in this drawing, as shown in Appendix 2, though there is no detailed explanation of the legend. All fracture zones included by /Carlsson et al. 1985, 1986/ and /Axelsson and Hansen 1997/ are defined as 'fault zone, partly crushed and altered bedrock, sealings'. However, there are additional zones marked on Drawing -103, which were not included in the structural model of /Axelsson and Hansen 1997/. Information regarding intercept position and orientation for all brittle structural features marked on Drawing -103, which might be of interest for the modelling work are listed in Appendix 2. These features, denoted 'tunnel deformation zone' (tDZ), include crush zones, brittle shear zones and gouge-filled fractures of varying width, as well as occurrences of closely spaced, parallel fractures and slicken-sides. Totally, there are 145 tunnel deformation zones in Drawing -103.

## 4.2 Borehole data

### 4.2.1 Deviation measurements for boreholes from the construction of SFR

Although deviation measurements were carried out for most cored boreholes drilled during the construction of SFR /e.g. Hagkonsult 1982, 1983/, there are no calculated deviations available in the SKB database Sicada. Instead, the orientations of the boreholes have been defined by the bearing and inclination of the top-of-casing. The deviations given in /Hagkonsult 1982, 1983/ are all less than one metre from the theoretical orientation.

### 4.2.2 Geological data from the construction of SFR

Efforts were made to check the consistency of the original drill core mapping with the aim of calibrating these earlier results in the context of modern day SKB standards. However, a comparison

between the new, remapped and the original frequencies of broken fractures did not show the expected concordance in any of the drill cores; both higher and lower frequencies were registered. To a certain degree, some of the differences are probably due to handling and transportation of the drill cores between the two mapping occasions, which has most likely broken previously unbroken fractures, along with the fact that drilling-induced fractures were recorded during the original mapping rather than being discounted as is done in modern SKB practice. Consequently, it was concluded that the earlier recorded fracture frequencies are insufficient on their own to fulfil the current standards of input data required for a formal geological single-hole interpretation (SHI). It is planned for the model version 1.0 that all available drill core from the earlier SFR investigation and construction phase will be inspected, photographed and overview remapped in accordance with SKB's methodology or, if an older mapping is available, rock coded with the aim of establishing input to a simplified geological SHI. However, for model version 0.1 only SHI information from eleven remapped boreholes (see section 4.2.3) is available and this is complemented by the deformation zone intercept positions from other boreholes as defined in /Axelsson and Hansen 1997/.

Inferred borehole intercepts for the fracture zones included in the previous structural models of SFR are provided in /Carlsson et al. 1985, 1986, Christiansson 1986/ and summarized in /Axelsson and Hansen 1997/. As pointed out in section 2.1, all zone indications given by /Carlsson et al. 1986/ for H2, 3, 6, 8 and 9 were adopted by /Axelsson and Hansen 1997/ without any changes in borehole or tunnel positions. However, /Axelsson and Hansen 1997/ included additional intercepts and extended some of the earlier defined zones.

The existence and width of these intercepts are generally based on a significant increase in the frequency of broken fractures and, in some cases, an increased hydraulic conductivity /cf. Carlsson et al. 1985, 1986/. This differs significantly from the methodology used to define possible deformation zones by the geological SHI methodology as currently implemented by SKB. The geological SHI provides an integrated synthesis of the geological data from the drill core mapping and geophysical borehole data with the aim of identifying rock units and possible deformation zones. The geological SHI analysis of fracture frequencies is not restricted to broken fractures, but also includes sealed fractures, sealed fracture networks, open and partly open fractures, and crush zones. In addition, current SHI practice gives equal weight to the presence and character of ductile deformation structures when defining deformation zones, in contrast to earlier judgements where such structures were to a certain extent ignored. Thus, there are significant differences in the methodologies to define the existence and boundaries of possible deformation zones in the geological SHI compared with those used to define fracture zones in the early structural models for SFR. In addition, there are unresolved uncertainties and deficiencies in the primary data that hamper the direct application of the SHI methodology.

Notwithstanding these difficulties, it was decided to use the earlier inferred borehole intercepts summarized by /Axelsson and Hansen 1997/, as direct input to the version 0.1 modelling work, where data from geological SHI were not available. However, these data are only available for the fracture zones included in previous structural models for SFR. The intercepts listed in /Axelsson and Hansen 1997/ and used in their model are presented in Table 4-1. Furthermore, the boreholes with geological SHI are indicated in this table. All the intercepts listed are given relative to a local, site established, elevation level rather than as borehole lengths. Generally, only the approximate central intercept position of a deformation zone is listed in /Axelsson and Hansen 1997/ with the exception of H2 (ZFM871) where there are levels for both upper and lower intercept surfaces.

The approximate centres of the intercepts, including those for H2 (ZFM871), have been recalculated to borehole lengths and used as input to the modelling as documented for individual zones in Appendix 8.

#### **4.2.3 Updated geological mapping and geological SHI of existing SFR boreholes**

The drill cores from boreholes KFR04, KFR08, KFR09, KFR13, KFR35, KFR36, KFR54, KFR55, KFR7A, KFR7B and KFR7C were remapped in connection with SFR modelling version 0.1 /Petersson and Andersson 2008/. The aim of the renewed mapping of these drill cores was to provide input to a geological SHI. The latter forms a key link between the borehole (in this case drill core)

**Table 4-1. Inferred borehole intercepts for fracture zones defined in previous structural models for SFR. Data from /Axelsson and Hansen 1997/. Boreholes where the drill cores have been subjected to updated Boremap-mapping and geological SHI are marked in red.**

Deformation zone	Upper surface level [–m]	Lower surface level [–m]	Level of approx. center [–m]	BH length of approx. center	Width of intercept
<b>KFR02</b>					
Zone H2 (ZFM871)	300	290	295	119.5	10.0
Zone 9 (ZFMNE0870A/B)	–	–	380	35.0	–
<b>KFR03</b>					
Zone H2 (ZFM871)	331	322	326	91.1	9.0
Zone 9 (ZFMNE0870A/B)	–	–	365	53.0	–
<b>KFR04</b>					
Zone H2 (ZFM871)	335	326	330	95.5	9.0
Zone 9 (ZFMNE0870A/B)	–	–	400	23.0	–
<b>KFR05</b>					
Zone H2 (ZFM871)	343	340	341	86.5	3.0
<b>KFR08</b>					
Zone 8 (ZFMNW0805A)	–	–	407	80	18.9
<b>KFR09</b>					
Zone 3 (ZFMNNE0869)	–	–	415	79.5	8.2
<b>KFR10</b>					
Zone 3 (ZFMNNE0869)	–	–	350	101.5	*
<b>KFR11</b>					
Zone 8 (ZFMNW0805A)	–	–	400	80	13.9
<b>KFR12</b>					
Zone H2 (ZFM871)	387	370	385	27.5	19.3
<b>KFR13</b>					
Zone H2 (ZFM871)	335	333			2.0
	316	314	315	64.5	2.0
<b>KFR21</b>					
Zone H2 (ZFM871)	384	378	381	119	5.7
<b>KFR22</b>					
Zone H2 (ZFM871)	372	363	367	153	7.3
<b>KFR24</b>					
Zone H2 (ZFM871)	377	372	375	149	5.2
Zone 8 (ZFMNW0805A)	–	–	385	137	2.1
<b>KFR25</b>					
Zone H2 (ZFM871)	404	391	398	141.5	16.0
Zone 8 (ZFMNW0805A)	–	–	375	174	4.9
<b>KFR31</b>					
Zone H2 (ZFM871)	349	346	347	230	2.4
<b>KFR32</b>					
Zone H2 (ZFM871)	387	370	378	174.5	19.3
<b>KFR33</b>					
Zone 6 (ZFMNNW1209)	–	–	465	58	2.1
<b>KFR35</b>					
Zone 6 (ZFMNNW1209)	–	–	460	57.5	2.8
<b>KFR36</b>					
Zone 3 (ZFMNNE0869)	–	–	430	104	4.7
<b>KFR37</b>					
Zone H2 (ZFM871)	343	332	337	188	8.7
<b>KFR38</b>					
Zone H2 (ZFM871)	354	351	352	180	2.9
<b>KFR53</b>					
Zone 9 (ZFMNE0870A/B)	–	–	405	30.0	–
<b>KFR54</b>					
Zone 9 (ZFMNE0870A/B)	–	–	390	38.0	–
<b>KFR55</b>					
Zone 9 (ZFMNE0870A/B)	–	–	365	48.0	–
<b>KFR56</b>					
Zone 8 (ZFMNW0805A)	–	–	445	68	?
<b>KFR57</b>					
Zone H2 (ZFM871)	396	390	393	16.5	6.0
Zone 6 (ZFMNNW1209)	–	–	400	12.5	
<b>KFR7A</b>					
Zone H2 (ZFM871)	365	364	365	74.5	–
<b>KFR7B</b>					
Zone H2 (ZFM871)	355	351	353	14.0	6.5
<b>KFR7C</b>					
Zone H2 (ZFM871)	359	346	352	15.0	7.8

\* Penetrates only part of Zone 3 (ZFMNNE0869).

data and the modelling work. However, deficiencies in the available geological data, not least the absence of orientation data, the lack of radar data and the availability of geophysics for only one of the boreholes (KFR04) enforced serious deviations from the established geological SHI methodology. In addition, it was decided to inspect data from hydrogeological borehole tests in connection with the geological SHI work. The identification of the possible deformation zones and rock units was carried out independently for each borehole, based on an analysis of available primary data and an inspection of the drill core.

The results of the geological SHI for existing boreholes (/Pettersson et al. 2009/ and Appendix 4) form a key input to the present modelling work. For the possible deformation zones, the following features were documented:

- The specific geological criteria and, for KFR04, also geophysical criteria used to identify the possible deformation zone.
- $\alpha$ -angle and mineralogy of fractures inside the possible zone.
- Rock types affected by the possible zone.
- Confidence in the interpretation on the basis of: 3 = high, 2 = medium and 1 = low.

Possible deformation zones of brittle character have been identified in the geological SHI work primarily on the basis of fracture frequency, rock alteration and, where available, single point resistivity (i.e. for KFR04). In contrast to the established methodology, where sealed, open and partly open fractures are differentiated in the analysis of anomalously high fracture frequencies, it was only possible to distinguish between broken and unbroken fractures, due to the lack of BIPS images and the overview character of the fracture data. Thus, the remapping of the eleven drill cores has identified unbroken fractures, broken fractures, sealed fracture networks and crush zones. The most prominent alteration along these zones is 'oxidation' as manifested by a red staining associated with sub-microscopic hematite dissemination in the feldspars.

The positions of the possible deformation zones along the eleven remapped drill cores are presented in Table 4-2 (cf. Appendix 4). Their identification during the geological SHI provides potential fixed data points for the position of zones at depth. Thus, the possible deformation zones form a direct input to the modelling work.

#### **4.2.4 Comparison between old SFR interpretations and geological SHI**

A comparison between the inferred borehole intercepts, as presented in Table 4-1, and the results of the geological SHI (Table 4-2) has been made for the eleven remapped drill cores. From this comparison it can be concluded that the majority of the old borehole intercepts are included in the possible deformation zones as defined during the geological SHI. However, there are two exceptions: (1) neither of the two possible deformation zones interpreted in KFR04 correlate with the intercept for H2 (ZFM871) listed by /Axelsson and Hansen 1997/ at approximately 95.5 m borehole length, and (2) neither of the two possible deformation zones interpreted in KFR55 correlate with the intercept for Zone 9 (ZFMNE0870A/B) listed by /Axelsson and Hansen 1997/ at approximately 48.0 m borehole length. In all other cases, where the old intercepts are included, the drill core length of the old borehole intersects are consistently less than the corresponding possible deformation zones from the geological SHI. Both these observations reflect differences in the definition of the zone concept.

The difference in the zone definition between the previous structural model and that used in the geological SHI becomes most evident for Zone 9 (ZFMNE0870A/B). In /Axelsson and Hansen 1997/ it has been described as "a water bearing gouge-filled joint, occasionally with increased fracturing on one or both sides". Features of such limited extent, more or less only detected by their hydrogeological properties, are usually not defined as possible deformation zones during the geological SHI, if they are not associated with increased fracture frequency and hydrothermal alteration. Thus, the results of the geological SHI cannot be used directly to define the position of narrow, transmissive features such as Zone 9 (ZFMNE0870A/B). Similarly, /Axelsson and Hansen 1997/ list an intercept between KFR04 and H2 (ZFM871) that lies outside the two SHI possible deformation zones interpreted in KFR04. However, inspection of the mapping data /cf. Pettersson and Andersson 2008/ reveals that there are fractures with the characteristics associated with H2 (ZFM871) at the position of the old intercept, but they are too few to give rise to an interpreted possible deformation zone with present SHI methodology.



**Table 4-2. Position of possible deformation zones defined by the geological SHI for KFR04, KFR08, KFR09, KFR13, KFR35, KFR36, KFR54, KFR55, KFR7A, KFR7B and KFR7C /Petersson et al. 2009/**

DZ	Sec_up [m]	Sec_low [m]	Borehole length of PDZ	Confidence in interpretation	Comment
<b>KFR04</b>					
DZ1	0	3	3	1	Brittle, chlorite.
DZ2	14	63	49	2	Brittle, laumontite, calcite, breccia, one crush.
<b>KFR08</b>					
DZ1	3	19	16	1	Brittle, chlorite, calcite, laumontite.
DZ2	41	104.4	63.4	3	Brittle, brittle-ductile, calcite, chlorite, adularia, fault breccias, cataclasite, 19 crushes.
<b>KFR09</b>					
DZ1	0	58.7	58.7	3	Brittle, calcite, chlorite, adularia, seven crushes.
DZ2	69	74.3	5.3	3	Brittle, calcite, chlorite, adularia.
<b>KFR13</b>					
DZ1	20	30	10	3	Brittle, laumontite, calcite, breccias, one crush.
DZ2	36	41	5	1	Brittle, laumontite, chlorite.
DZ3	47.5	61	13.5	2	Brittle, laumontite, chlorite.
DZ4	61	68	7	1	Brittle, chlorite, calcite and clay minerals.
<b>KFR35</b>					
DZ1	32.7	70	37.3	3	Brittle, adularia, calcite, fault breccias, cataclasite, six crushes.
<b>KFR36</b>					
DZ1	45	115.5	70.5	3	Brittle, adularia, calcite, laumontite, nine crushes.
<b>KFR54</b>					
DZ1	0	2.5	2.5	3	Brittle, chlorite, calcite.
DZ2	27	40	13	3	Brittle, clay minerals, laumontite.
<b>KFR55</b>					
DZ1	0	3.3	3.3	2	Brittle, laumontite, calcite, one minor crush.
DZ2	8	38	30	3	Brittle, clay minerals, laumontite
<b>KFR7A</b>					
DZ1	3.5	74.75	71.25	3	Brittle and brittle-ductile, clay minerals, calcite, fault breccias, cataclasite and 19 crushes.
<b>KFR7B</b>					
DZ1	0	17	17	3	Brittle, calcite, chlorite, clay minerals, four crushes.
<b>KFR7C</b>					
DZ1	6	32	26	3	Brittle, clay minerals five crushes.

Since all other borehole intercepts of the previously inferred fracture zones are consistently less and overlapped by the wider possible deformation zones identified during the geological SHI, it is generally concluded that the old fracture zones typically represent the most highly fractured, transmissive part of the possible deformation zones of the geological SHI. This is an important outcome of the comparison that needs to be considered in the evaluation of other data upon which the original structural models are based, especially inferred intercepts of fracture zones along tunnels.

#### **4.2.5 Geological and geophysical borehole data from the Forsmark site investigation**

In total, there are three boreholes from the Forsmark site investigation that penetrate the SFR regional model volume. These include one cored borehole, KFM11A, and two percussion boreholes,

HFM34 and HFM35. None of the data from these boreholes were directly included in the current modelling work due to time constraints. Inspection of the borehole geological SHI, along with the lineaments and tunnel mapping results, indicated that a more extensive detailed review was required than anticipated. The necessary review will need to include how the Singö deformation zone should be modelled, with possible influence on the planned update of the Forsmark geological models. However, the evaluation of the geological SHI of the boreholes in /Stephens et al. 2008a/ has been used to generally verify the interpretations in SFR model version 0.1. All data from these three boreholes will be included in SFR modelling version 1.0.

## **4.3 Surface geophysics**

### **4.3.1 Background**

SFR lies within the regional model area of the earlier Forsmark site investigation. Hence, the bedrock models for rock domains and deformation zones developed during the site investigation form the natural starting point for building a more detailed model of the bedrock containing the SFR facility and its extension.

The structural part of the bedrock model at Forsmark has been developed successively as more information from the site investigation activities became available. The identification of lineaments from different sources of data /Isaksson 2003, Isaksson et al. 2004, Isaksson and Keisu 2005, Isaksson et al. 2006a, b, Isaksson et al. 2007/ has provided an important input for the modelling of steeply dipping deformation zones /SKB 2005, Stephens et al. 2007, Stephens et al. 2008a/. However, following the completion of the initial site investigation phase (model version 1.2), uncertainties were recognised in the interpretation of the geological significance of topographic lineaments /SKB 2006/. For this reason, attention was focused on the modelling of steeply dipping deformation zones using lineaments defined by magnetic minima. The detailed surveys of the magnetic total field on land and at sea provided information of very high resolution during the subsequent complete site investigation phase (model stages 2.1, 2.2 and 2.3). This strategic decision to focus on features in the maps of the magnetic field was supported by observations of wall rock alteration associated with zone intersections in boreholes, as well as on the results of excavation work at the site.

As the SFR facility forms part of the Forsmark area, and as the geological setting is comparable, the fundamental conclusions from the preceding site investigation have been implemented in the development work during the SFR model version 0.1. Hence the primary focus for the modelling of steeply dipping deformation zones is again on the data of the magnetic total field and the identification of lineaments defined by magnetic minima.

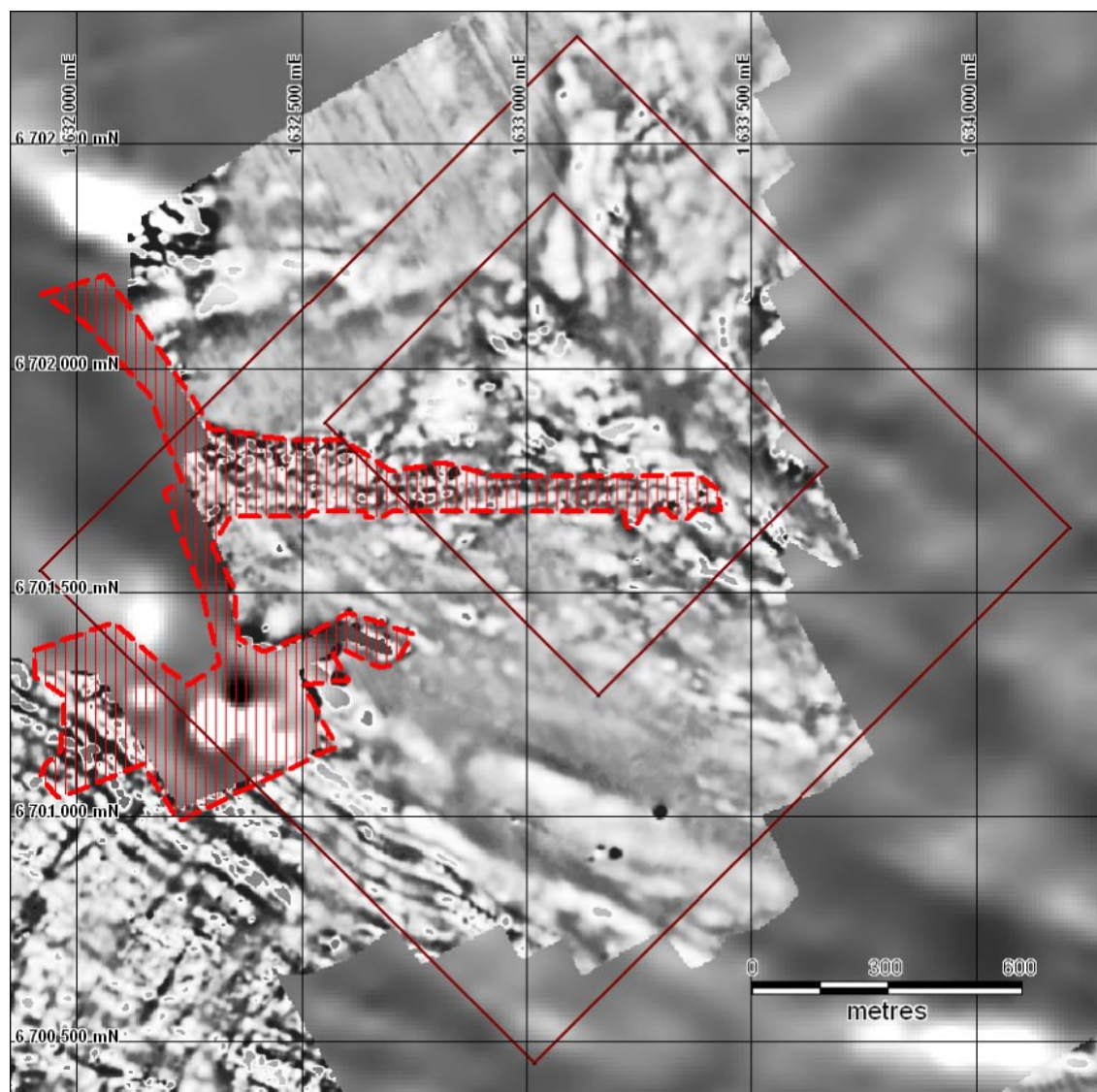
The latest interpretation of lineaments from the Forsmark site investigation, stage 2.3, was reported in /Isaksson et al. 2007/. This interpretation was presented after the use of lineaments in the final geological models for Forsmark in the stage 2.2 work /Stephens et al. 2007/. However, the implications of the new lineament interpretation for the geological models were addressed in model stage 2.3 /Stephens et al. 2008a/ and in the final descriptive model for the site /SKB 2008a/. In the current first phase of the geological modelling of the SFR regional and local model volumes, a revision of stage 2.3 lineaments from the Forsmark site investigation has been carried out. The current revision was required due to the different scale and area of focus of the SFR project compared with the Forsmark site investigation project. The revision has resulted in changes to some of the lineaments that were recognized during the earlier work, as well as in entirely new lineaments. Some of the magnetic anomalies connected to the lineaments have been modelled using a modern programme package (Encom ModelVision Pro ver 8.0). The lineaments used in model version 0.1 have been delivered to Sicada (field note number SFR92).

### **4.3.2 Revision of lineaments**

While the local model in the Forsmark site investigation has addressed a relatively large area of approximately 12 km<sup>2</sup>, the regional model area for SFR model version 0.1 is much smaller (approximately 2.6 km<sup>2</sup>). In spite of this difference, the lineaments from the Forsmark site investigation form the natural framework for any revision of SFR regional model area lineaments. The identification

of lineaments during the site investigation focused on detailing the area south and southwest of the Singö deformation zone (ZFMWNW0001) inside the local model area, while north and north-east of the zone, outside the local model area, only lineaments with trace lengths longer than 3,000 m were included in the final, stage 2.2 geological model /Stephens et al. 2007/. Shorter lineaments in the area around SFR, identified with the help of the ground high-resolution magnetic data, were only identified during stage 2.3 of the investigation and evaluated in /Stephens et al. 2008a/. However, in the modelling of the bedrock surrounding the SFR facility, the effort is now concentrated on evaluating the lineaments from the site investigation, at a scale and in an area adapted to the needs for SFR model version 0.1. This change of focus implies that the revision of lineaments is carried out in a more detailed scale in comparison with earlier work. It should be noted that the local and regional model areas of SFR host piers and roads, which cause disturbances in the magnetic field (Figure 4-2). The revision has taken these disturbances into account and has resulted in the rejection of a few of the earlier interpreted lineaments that impinge on these disturbed areas.

An explicit aim of the revision work has been to maintain consistency across the boundary between the areas within and outside the SFR regional model area. Hence, lineaments from the Forsmark site investigation entering the SFR regional model area have generally been maintained without



**Figure 4-2.** The SFR model areas (regional and local) shown in brown on a map of the first vertical derivative of the magnetic total field from measurements on land, at sea and via helicopter (for details see Figure 3-4). Area of disturbance caused by civil installations, affecting the magnetic total field, is shown in dashed red.



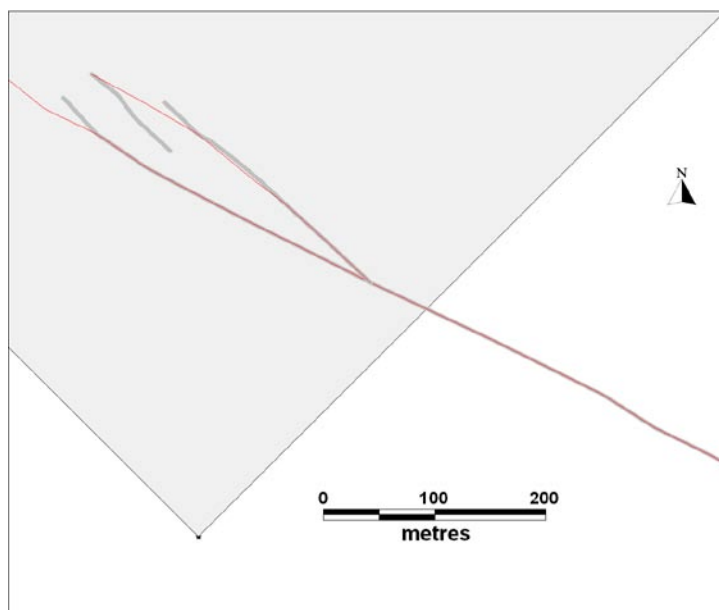
any changes outside the model area, while inside the model area, changes in length, path or locality are allowed; some parts of lineaments may also have been deleted (Figure 4-3). This conservative approach at the margin is aimed at simplifying future studies on the interaction between both model sets. However, in a few cases, detailed interpretation of data showed the need to slightly adjust former lineaments that were situated directly outside the SFR regional model area.

Based on this approach, the main focus has been to revise lineaments in the magnetic data from the detailed ground survey, with a demand on a more detailed scale in the modelling, as compared with the Forsmark site investigation. To a limited degree, low velocity zones from the refraction seismic profiles and depressions in the bedrock surface have also provided an input to the revision process. The revision activity has resulted in 123 lineaments based on magnetic minima (Figure 4-4) that are found entirely or partly within the SFR regional and, consequently, local model areas.

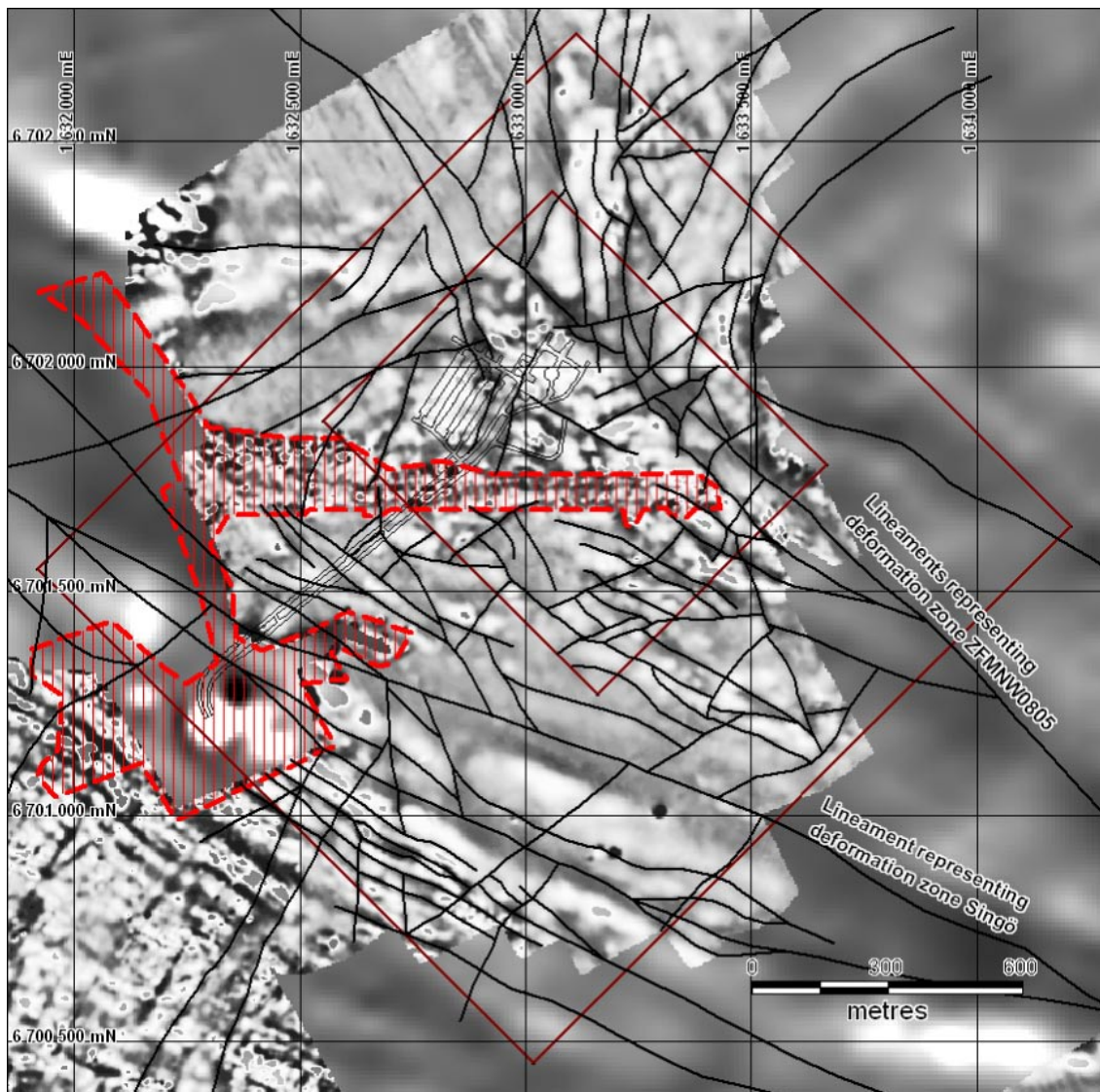
Comparable to what was utilized during the Forsmark site investigation, a table of attributes connected to each lineament is presented in Appendix 5. The lineaments in SFR version 0.1 consist of two groups; the first group contains lineaments that have been imported directly from the latest version of lineaments in the Forsmark site investigation /Isaksson et al. 2007/, the second group contains lineaments that have been modified from previously identified lineaments in the Forsmark site investigation, or are entirely new lineaments. The names and attributes in the first group are preserved from the site investigation, while the second group has new names (MSFR0800X) and also new attributes.

As mentioned above, some parts of the SFR regional and local model areas show disturbances in the magnetic total field data due to piers and roads. The most severely disturbed areas are marked in Figure 4-4. In these areas, the density of lineaments is lower due to the high noise level.

In the southern part of the SFR regional model area, a broad significant low magnetic feature is present (see Figure 4-4) that corresponds to the Singö deformation zone /Stephens et al. 2007/. In the revised lineament interpretation, this zone is represented by a thin line drawn close to the centre of the feature. In the north-eastern part of the SFR local model area, a similarly broad but apparently much more complex low magnetic feature is also present and also corresponds to a deformation zone, ZFMNW0805 /Stephens et al. 2007/. Both these features are examples of deformed domains in the bedrock, i.e. rock volumes that could possibly be better represented by volumes rather than by thin sheets. This is a possible task for further analysis that should include other data than solely geophysics to investigate how such features are best represented in the model.



**Figure 4-3.** The figure illustrates the consistency between lineaments of different generations along the border of the SFR regional model area, version 0.1. Lineaments from the Forsmark site investigation are shown as thin red lines and those from the SFR model version 0.1 as thick grey lines. The SFR regional model area is marked in grey.

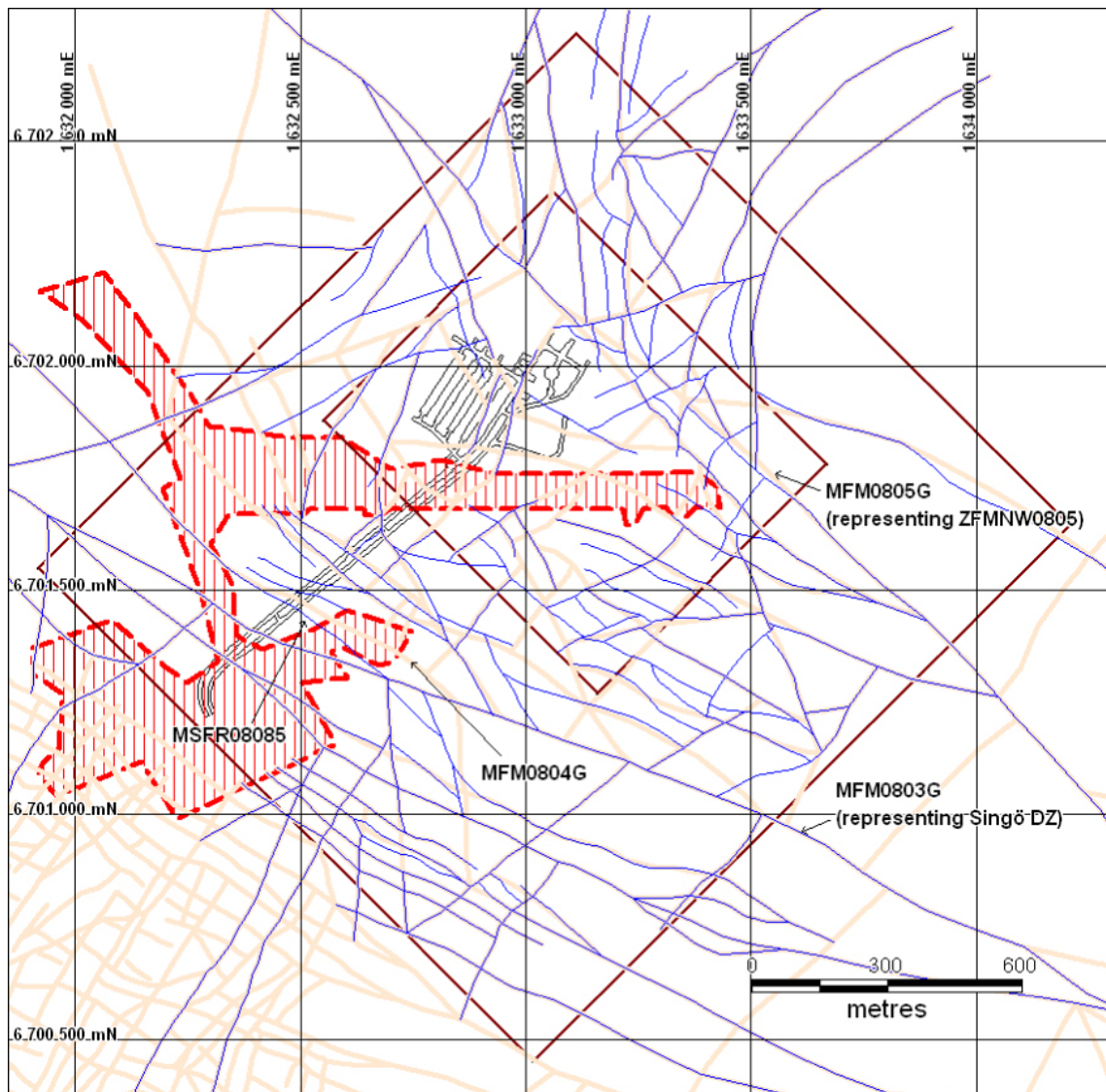


**Figure 4-4.** Map of the first vertical derivative of the magnetic total field from measurements on land, at sea, and from helicopter, showing the 123 lineaments based on magnetic minima that have been identified (black lines). Only lineaments that are partly or entirely within the SFR regional and local model areas (brown lines) are shown. Prominent low magnetic features in the southern and north-eastern parts of the SFR regional model area correspond to the Singö deformation zone (ZFMWNW0001) and zone ZFMNW0805 in /Stephens et al. 2007/. The areas where data used in the lineament identification are disturbed by installations and constructions connected to the piers and roads are also shown (dashed red).

### 4.3.3 Comparison between lineaments from SFR version 0.1 and the Forsmark site investigation

The relationship between the lineaments in SFR model version 0.1 and the previous lineaments from the Forsmark site investigation is described in Appendix 5 and shown in Figure 4-5. Some of the lineaments from the Forsmark site investigation have not been included in SFR model version 0.1. The motivation behind each exclusion is described in Appendix 5.

The lineaments of version 0.1 have been drawn with high fidelity to the features observed in maps of enhanced versions of the magnetic field. Using the terminology applied in the Forsmark site investigation /Isaksson and Keisu 2005/, the lineaments of SFR model version 0.1 should be considered as “coordinated” rather than “linked”. In the process of maturing the lineament map to a map of deformation zones both direct geological knowledge and theory must be applied. In order not to introduce unnecessary constraints in the process, the lineaments have been drawn without



**Figure 4-5.** Lineaments from the Forsmark site investigation (light pink) compared with the lineaments interpreted in connection with SFR version 0.1 (blue). The SFR regional and local model areas are shown in brown. Lineaments from the site investigation commented in the text below are labelled. The hatched red area marks disturbances in the magnetic total field from civil installations.

any geological guidance in the work with SFR model version 0.1; hence they should be considered as relatively immature. The termination of the lineaments is a task for the subsequent geological modeling of the lineaments into deformation zones.

In the southern part of the regional model area, most of the previous lineaments are also considered valid for the SFR model version 0.1. Only minor differences are observed.

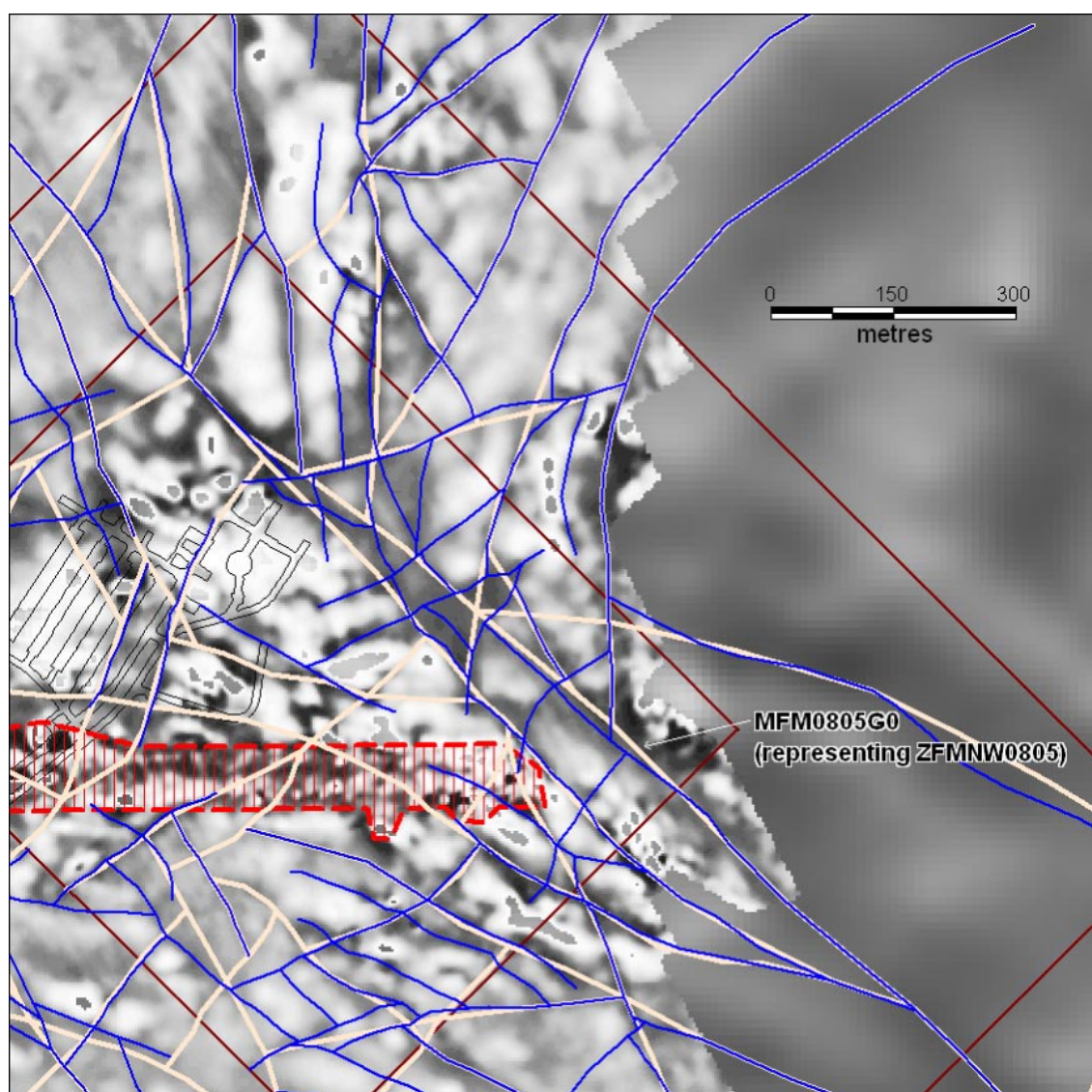
In the central and western parts of the SFR local model area, some of the lineaments from the Forsmark site investigation are not directly inherited into SFR model version 0.1, instead their appearance may have been changed. In some cases, they may even have been excluded from the SFR model version 0.1. The main reason for this difference is the disturbance of the magnetic total field caused by civil installations and constructions, which prevent meaningful identification of lineaments at the appropriate scale.

One of the prominent low magnetic features found in the SFR model areas is associated with the Singö deformation zone (ZFMWNW0001). During the Forsmark site investigation, the identification of lineaments based on dense measurements of the magnetic total field on land and at sea, in the vicinity of the Singö deformation zone, implied changes of some of the former lineaments. As a



consequence, the south-eastern part of lineament MFM0804G replaced lineament MFM1127 (representing deformation zone ZFMWNW1127) /Stephens et al. 2008a/. On this basis, it was possible to redraw the south-eastern part of deformation zone ZFMNW0002 to follow lineament MFM0804G. In SFR model version 0.1, the lineament MFM0804G has been re-evaluated one more time and the south-eastern part of MFM0804G has been redrawn so that it connects to MFM0803G0 at a position about 170 m towards the north-west. The modified version of the former lineament MFM0804G is now called MSFR08085. It is important to keep in mind that the final geological models for Forsmark only had access to the stage 2.2 and earlier interpretations. The implications of the subsequent stage 2.3 lineament interpretation on the Forsmark geological models were evaluated in /Stephens et al. 2008a/. No revised geological models, based on revised lineaments, were produced during stage 2.3.

Lineament MFM0805G0 transects the SFR local model area with a continuous north-westerly trend in the interpretation presented in the Forsmark site investigation /Isaksson et al. 2007/. The detailed revised interpretation of the magnetic data, carried out here, has divided this apparently continuous structure into a more complex one. A detailed image that demonstrates the complexity introduced in the lineament version 0.1 is shown in Figure 4-6.



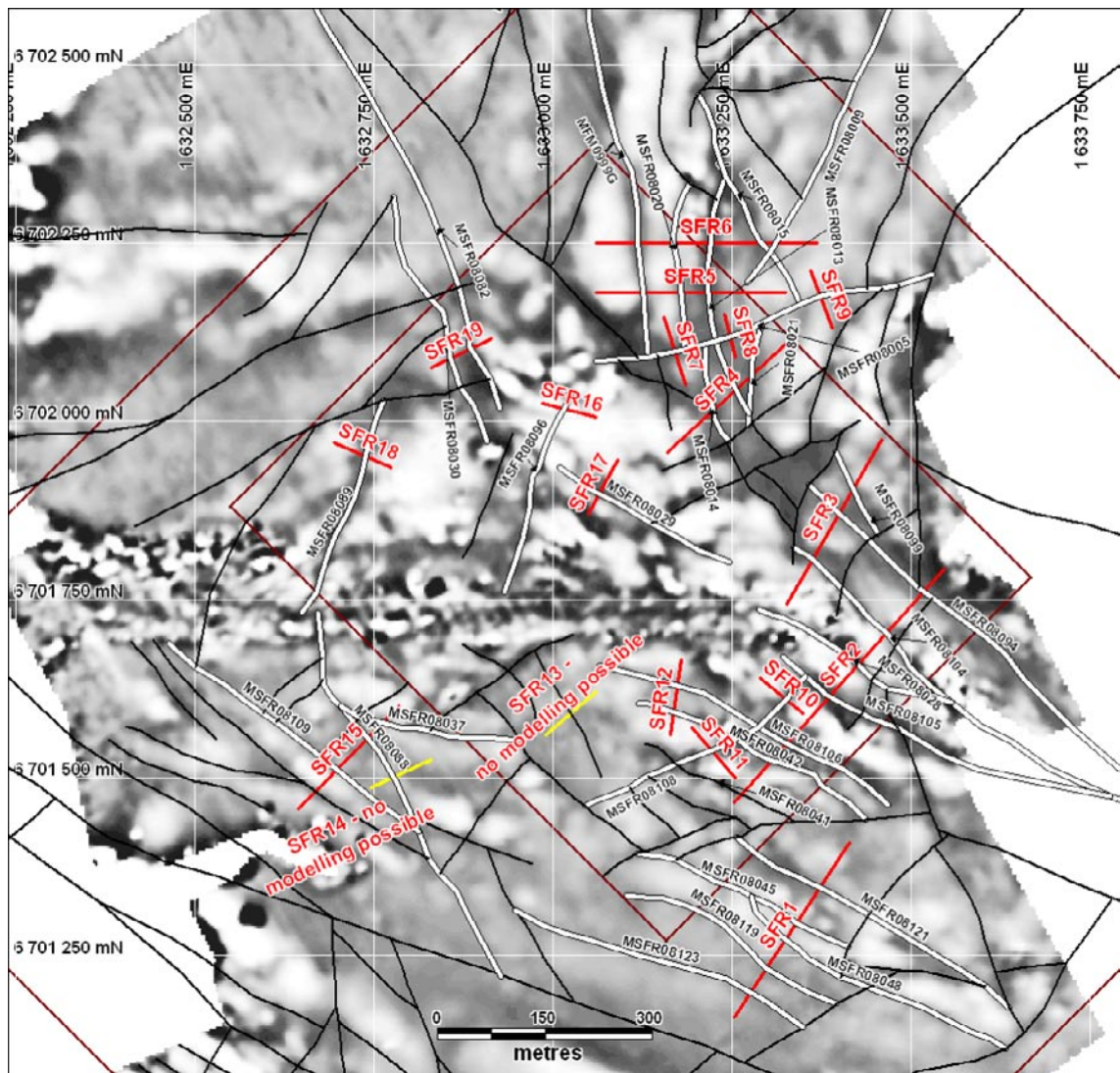
**Figure 4-6.** The lineaments from the Forsmark site investigation (light pink) compared with the lineaments from SFR model version 0.1 (blue). The SFR regional and local model areas are shown in brown. The lineament MFM0805G0 from the site investigation appears to be fairly continuous in the data if observed in regional scale while the detailed scale shows complexity. The implication is that the possible deformation zone connected with these lineaments probably has a complex geometry.

#### 4.3.4 Modelling of low magnetic anomalies connected to lineaments

Forward modelling of the magnetic total field data from the detailed ground survey has been performed in order to estimate the geometries of the sources to the low magnetic anomalies associated with the lineaments, i.e. principally the approximate thickness and dip of the possible deformation zone (Appendix 6).

In total, 19 profiles traversing lineaments were selected for modelling. Seventeen (17) profiles were modelled while two were abandoned due to problematic data or weak anomalies. The location of all profiles is shown in Figure 4-7. The preliminary results of the modelling of profiles are presented in Appendix 6. Due to the overall irregular pattern seen in the magnetic map and the weakness of many of the anomalies, it was considered that further confirmatory profiles need to be modelled across the targeted lineaments, along with attempted correlation with borehole data from version 1.0, before the results of this work are integrated into the model.

When studying the modelling results, it is important to observe that some of the modelled anomalies are fairly faint. The interplay between a weak anomaly from the source of interest (the possible deformation zone represented by the lineament) and anomalies caused by “geological noise”, such as



**Figure 4-7.** The location of the 19 profiles selected for modelling (red lines). The lineaments in SFR model version 0.1 addressed by the modelling work are marked with thick black-white lines, and labelled. An enhanced version of the magnetic total field image (1st vertical derivative) with the remaining inferred lineaments (black lines) is shown in the background.



an irregular magnetisation in a specific lithological unit, may lead to modelling results with a low level of confidence. Thus, a significant magnetic anomaly in combination with normal variations in the magnetic field over the area can be characterized and modelled with a higher degree of confidence, whereas a small anomaly in the same area introduces a higher degree of uncertainty in the resulting model.

#### **4.3.5 Geological significance of lineaments**

The Singö deformation zone (ZFMWNW0001) is a prominent feature that intersects the southern part of the SFR regional model volume. It intersects tunnels and boreholes and is consequently relatively well studied and characterized. According to the parameter setting of lineaments from the site investigation, more than half of its length is detected in topographical data (bedrock topography) while the whole structure is easily observed in magnetic total field data (see Figure 4-2). The deformation zone is intersected by refraction seismic profiles that show decreased P-wave velocity over broad sections along the profiles. As it is associated with a prominent low magnetic anomaly, it illustrates the diagnostic strength of magnetic data to predict tectonic structures in the bedrock.

Excavation work and drilling activities inside the Forsmark tectonic lens have addressed a number of lineaments detected as low magnetic features /Stephens et al. 2007/. The work has led to several conclusions of which some are summarized below.

- Lineaments defined by discordant magnetic minima primarily represent fracture zones.
- Lineaments defined by discordant magnetic minima could also represent dykes of granite and pegmatite.
- Lineaments defined by concordant minima connections are related primarily to lithological contrasts that are aligned parallel to the ductile foliation in the bedrock. However, the occurrence of minor fracture zones along the tectonic foliation cannot be excluded as a contributory factor to these lineaments.

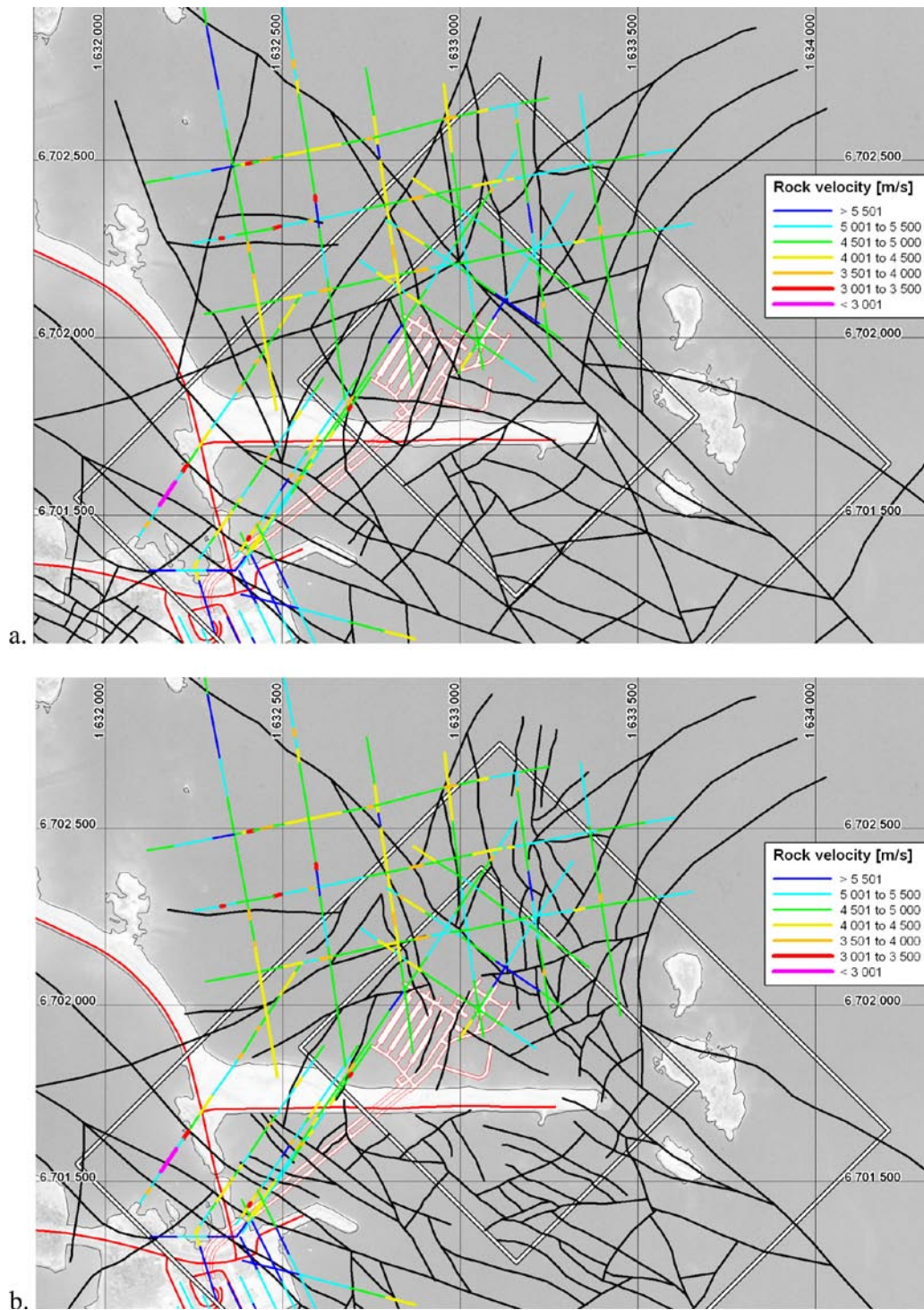
These conclusions are only applicable inside the Forsmark tectonic lens. The character of concordant minima connections inside the ductile high-strain belts outside the lens, including a large part of the SFR regional model area, is uncertain. Some of these lineaments are known to be and many have been modelled as regionally significant deformation zones /Stephens et al. 2007/.

Based on these considerations, a pragmatic interpretation is that lineaments in the magnetic total field data in the SFR model areas with a length in the order of 1,000 m or more primarily represent deformed rock but when lineaments much shorter than this are considered then sources emanating from lithological factors are increasingly likely. The straightforward method to validate a lineament map is to control the lineaments against solid geological observations whether in outcrops, trenches, boreholes or tunnels.

#### **4.3.6 Low velocity anomalies in refraction seismic data**

Seismic refraction surveys were carried out in 1981 to support the design work for the original SFR facility. The aim of the surveys was to identify deformation zones and estimate sea bottom sediment thicknesses /Hagkonsult 1982/. The basic precept was that low velocity anomalies in the bedrock may represent steeply dipping, brittle deformation zones that contain an anomalous concentration of open fractures or sections with incohesive rock. The position of the profiles and the measured seismic velocities are presented in Figure 4-8.

As can be seen in Figure 4-8, the seismic velocities in the bedrock are generally greater than 4,000 m/s. /Isaksson 2007/ evaluated the correlation between low velocity anomalies  $\leq 4,000$  m/s, low magnetic lineaments and deformation zones (Forsmark stage 2.2). The analysis showed that there is only moderate correlation between low velocity anomalies and low magnetic lineaments or modelled deformation zones. However, both survey methodology and geological conditions need to be considered in the assessment of the relatively poor correlation. These two features are reported in more detail in /Isaksson 2007/ and /Stephens et al. 2007/. Of particular note is the fact that the geophone spacing of 5 m limits the resolution for the identification of anomalies. For the SFR local model area, in particular, where the minimum lineament length for consideration is 300 m, it is unlikely that such short lineaments will have identifiable low velocity anomalies. Thus, it is difficult



**Figure 4-8.** Profiles from seismic refraction surveys performed in 1981 to support the design work for the original SFR facility /Hagkonsult 1982/. a) Presents the velocities in relation to the Forsmark site investigation version 2.3 interpreted lineaments and b) the SFR version 0.1 lineaments.

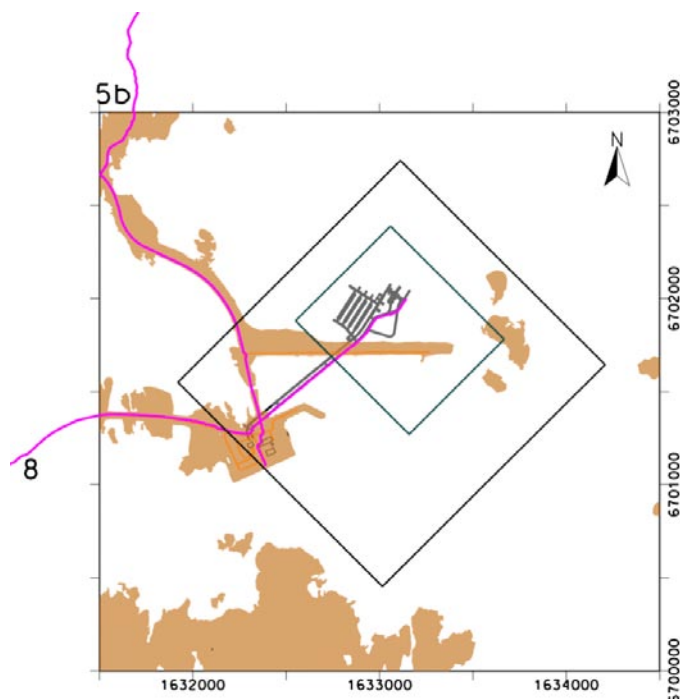
to resolve individual narrow low velocity sections. The velocity provided in the data is probably an average over longer sections composed of both intact and lower quality bedrock. In addition, it is noteworthy that /Carlsson and Christiansson 2007/ reported that the Quaternary deposits in the area include glacial till some of which is, at least locally, very compact and even required blasting during excavation. Seismic investigations made during the geophysical explorations showed a seismic velocity of around 4,500 m/s in some cases that would possibly mask any underlying lower velocity anomaly associated with a narrow deformation zone.

For these reasons and based on others discussed in /Isaksson 2007/ and /Stephens et al. 2007/, it can be stated, in summary, that the presence of a well defined low velocity anomaly can only be expected to be associated with larger steeply dipping, brittle deformation zones and even then there are various reasons to explain the absence of such an anomaly. The low velocity anomalies that do not match low magnetic lineaments and/or deformation zones and that are, as yet, not explained may represent unidentified fracture zones. Alternatively, they may be related to local, narrow depressions in the bedrock surface that correlate with fractured near-surface bedrock or are simply filled with less compact Quaternary cover material. This is supported by the pattern of anomalies seen across the SFR regional model area where generally clearly defined low velocity anomalies are lacking. Seismic refraction anomalies are addressed in the individual deformation zone descriptions presented in Appendix 8.

#### 4.3.7 Reflectors in reflection seismic data

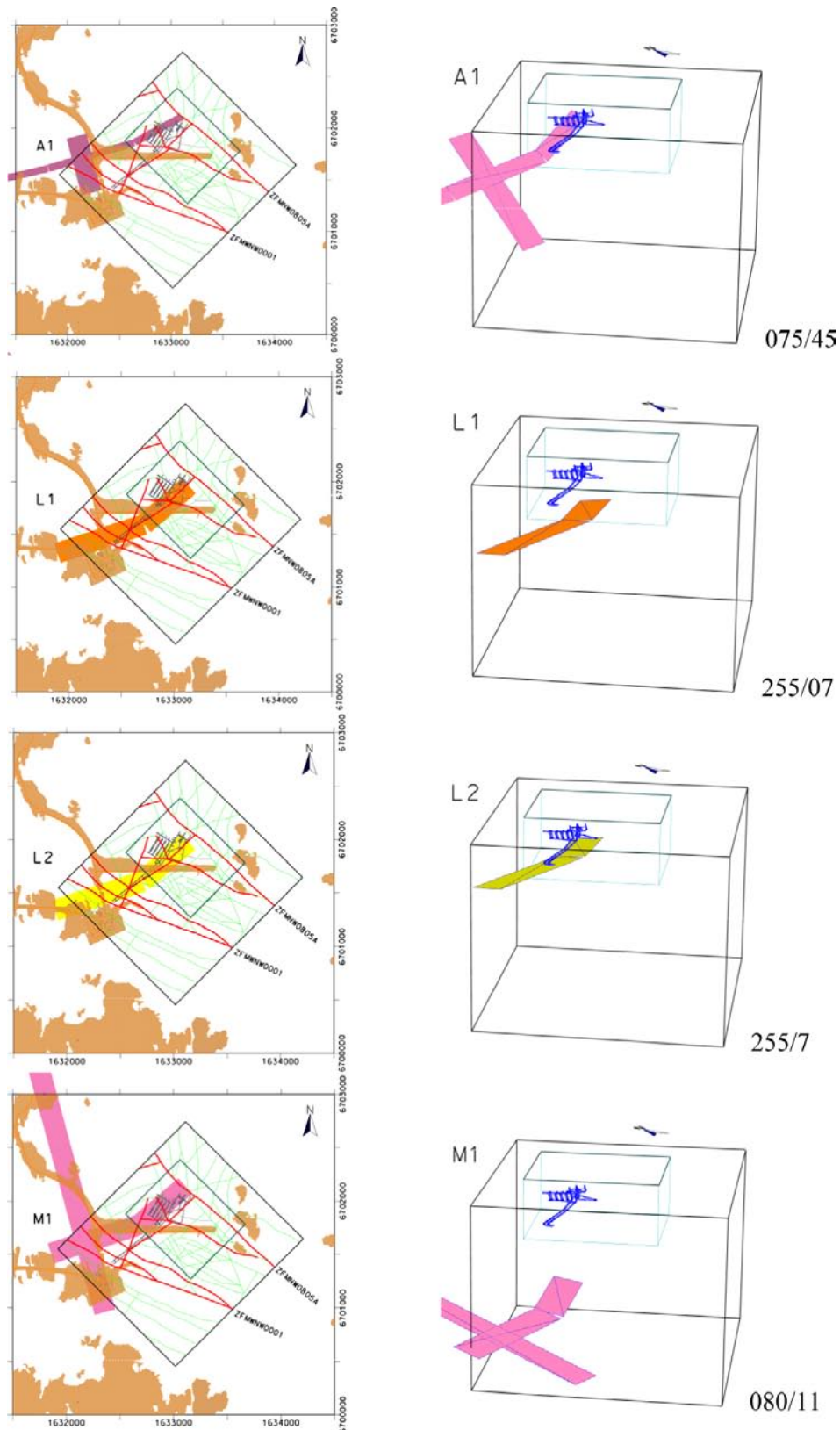
Surface reflection seismic data proved to be an important tool in the modelling of gently dipping, brittle deformation zones at the Forsmark site /SKB 2005, 2006/. Such data were obtained and interpreted during two separate stages in connection with Forsmark model versions 1.2 and 2.1 /Juhlin et al. 2002, Juhlin and Bergman 2004, Juhlin and Palm 2005/. Approximately 40 km of high-resolution (10 m shot and receiver spacing) reflection seismic data were shot. The positions of the profiles 5b (LFM000817) and 8 (LFM000818) that lie in and around the SFR regional model area are shown in Figure 3-4 and Figure 4-9. In order to permit their use in the modelling work, the reflections were placed in three-dimensional space with the help of the method described in /Cosma et al. 2003/. The results of this exercise are presented in /Cosma et al. 2003, Balu and Cosma 2005, Cosma et al. 2006/. The seismic reflector geometries will be studied in detail in version 1.0. However, those reflector geometries that are close to or intercept the SFR regional model volume (A1, L1, L2 and M1) have been imported for reference into the version 0.1 RVS deformation zone model and are shown in Figure 4-10. All the relevant reflectors are of confidence class 2 (probable).

Reflector A1 is extensive and has been inferred to be present on both sides of the Singö deformation zone (ZFMWNW0001). However, for model version 1.0, it is considered that the A1 observations on profiles 5b and 8 need to be reassessed and modelled separately from the other observations that lie at much greater distance from SFR. There are possible correlations between this reflector and lineaments MSFR08092 and MSFR08034 (updates from version 2.3 MFM0137BG and MFM0137A0 /Isaksson et al. 2007/) that need to be further investigated. In addition, after remodelling with a focus on SFR, a possible correlation with ZFM871 also needs to be considered.



**Figure 4-9.** Seismic reflection profile 5b (on land) and profile 8 (on land and along the tunnel).





**Figure 4-10.** Seismic reflector position plots with strike/dip based on /Cosma et al. 2006/.

Reflectors L1 and L2 dip very gently to the north though their currently modelled extent is questionable and will be reviewed during model version 1.0. Reflector M1 dips gently to the south-east. Although it is situated well below the base of the local model volume, it is possible it may be significant from a hydrogeological viewpoint, if found to correlate with a brittle structure.

## 5 Model for deterministic deformation zones

### 5.1 Methodology and modelling assumptions

For version 0.1, a single deformation zone model has been delivered, with a volume corresponding to the regional model volume as defined in Figure 1-1. This combined 'Master' model contains all the deformation zones modelled to date. Due to the immature state of the current lineament interpretation the proposed minimum size criterion of a surface trace length of 300 m for deterministic modelling has not been strictly applied for deformation zones falling within the local model volume. Inferred deformation zones with trace lengths as short as 95 m have been included in the model where supporting geological data from the existing SFR facility was available. For the part of the regional model volume lying outside of the local model volume a minimum inferred deformation zone trace length of 1,000 m has been applied as a criterion for deterministic modelling.

The 'Master' model format has been selected to facilitate further work by the hydrogeological modelling group who are the primary end users of this model version. For version 1.0, separate local and regional models as well as a combined model will be delivered to facilitate the work by the various end users.

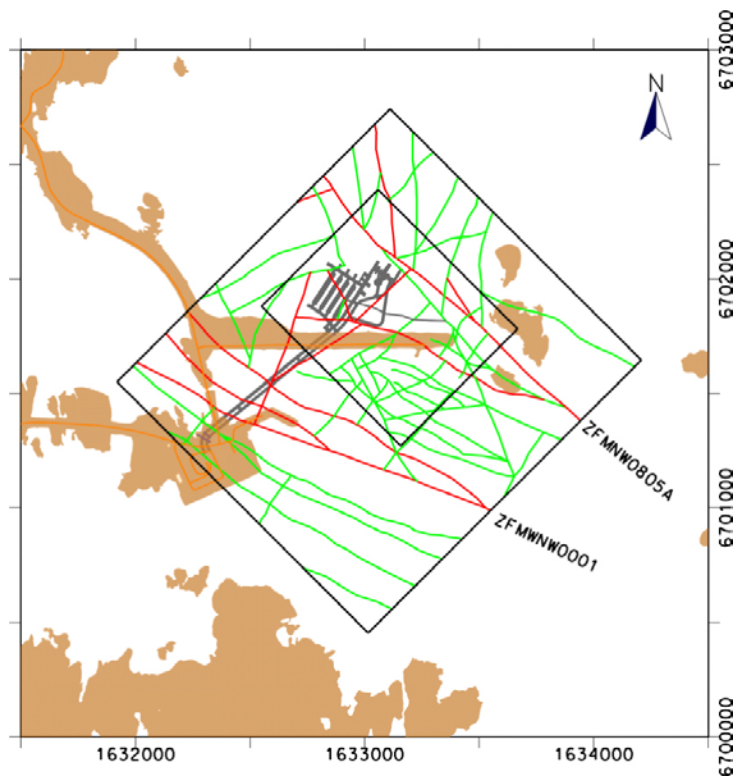
The set of fundamental assumptions underlying the current deformation zone modelling has been inherited from the methodology as outlined in /Munier and Hermanson 2001, Munier et al. 2003/. It is assumed that:

- Deformation zones can be interpreted through direct data from surface field observations, tunnels and boreholes. The confidence in geological character and possible extent (length and thickness) of deformation zones inferred from direct data sources is higher than that for deformation zones identified from indirect observations (see bullets 2 and 3 below).
- Deformation zones can be interpreted through indirect sources of data such as geophysical maps (magnetics, VLF, slingram, gravimetric), topography, seismic reflections and refractions.
- Lineaments, in particular geophysical and to a limited extent topographical, provide information about the location and extent at the surface of potential deformation zones (see section 4.3 for details).
- Different sources of data can complement each other and increase the confidence in the interpreted deformation zone. Several types of observations, both direct and indirect, also increase the degree of detail in which the deformation zone can be described.
- Interpreted deformation zones can be interpolated between points of observation, if there are reasonable data to suggest the validity of such interpolation.
- Deformation zones are variable in their thickness and can be modelled honouring an inferred generalised thickness.
- Within the limits of the regional or local model volumes, deformation zones interpreted at the ground surface can be extended downwards to a depth equal to the interpreted length of the mapped surface trace. This means, for example, that deformation zones longer than 1,000 m at the ground surface are extended to the bottom of the regional model volume (-1,100 masl).
- Each interpreted deformation zone has been ranked according to the confidence in its existence as being high, medium or low. Deformation zones that have high confidence ratings are based on direct data sources from boreholes and tunnels, complemented by indirect data sources mostly in the form of lineament indications.
- Deformation zones ranked with medium confidence are based solely on indirect information such as clear topographic, magnetic and/or surface geophysical anomalies which cannot be disregarded as being other linear structures in the landscape, such as Quaternary deposits, ditches, power lines, roads, forest fire lanes, or other man-made features. A zone based solely on seismic reflection data is also included in this group.
- Interpreted deformation zones with assigned low confidence are only supported by indirect sources of information such as lineament indications of weaker strength, from topography, magnetics or electromagnetic methods.

The lineament map used in SFR model version 0.1 and its development is described in section 4.3 and forms the basis for the surface interpretation of steeply dipping deformation zones (see also /Stephens et al. 2007/). During the deformation zone modelling work, the lineaments, particularly their overall continuity, has been continually reviewed and the background data re-examined. The following text explains in more detail various terms and methodological aspects in the SFR version 0.1 modelling work.

The current deformation zone model addresses deformation zones in the regional and local model areas as presented in Figure 5-1 and Figure 5-2, respectively. For SFR model version 1.0, it is intended that the local scale model shall contain deformation zones that are inferred to be 300 m or longer in length at the ground surface, i.e. minor, local major and regional deformation zones according to the terminology of /Andersson et al. 2000/. No such minimum size criterion have been applied in the current local model volume, since the lineament review is still ongoing and a number of apparently smaller structures have been included in the deterministic model. In addition, there are currently deformation zones interpreted from the drilling investigations that have not been correlated with any surface lineament or neighbouring boreholes. These zones will be addressed in SFR model version 1.0. The version 1.0 regional scale model will contain deformation zones that are inferred to be 1,000 m or longer in length at the ground surface, i.e. local major and regional deformation zones.

In the cases where a deformation zone can be correlated with a lineament and borehole data, the strike of the deformation zone is assumed to be the same as the trend of the matching lineament. The dip is inferred by matching the lineament to the borehole intercept(s) and is documented as the average dip angle of the deformation zone, along its entire extent. The matching process is largely geometrical, since any borehole position and orientation is generally sited with the aim of intercepting a particular lineament that is initially assumed to be a steeply dipping deformation zone. However, earlier experience from Forsmark has shown that certain deformation zone orientations have associated characteristics that can be used to further support SHI borehole DZ and lineament correlation. Deformation zones observed only at the surface, which lack information on their sub-surface extents and geometry, are assumed to be vertical. The steeply dipping deformation zones



**Figure 5-1.** Intersection at the current ground surface of deformation zone traces inside the regional model area. The regional deformation zones ZFMNW0001 and ZFMNW0805A form the general SW and NE boundaries of the SFR tectonic block. Confidence in existence: high=red, medium=green, low=grey.



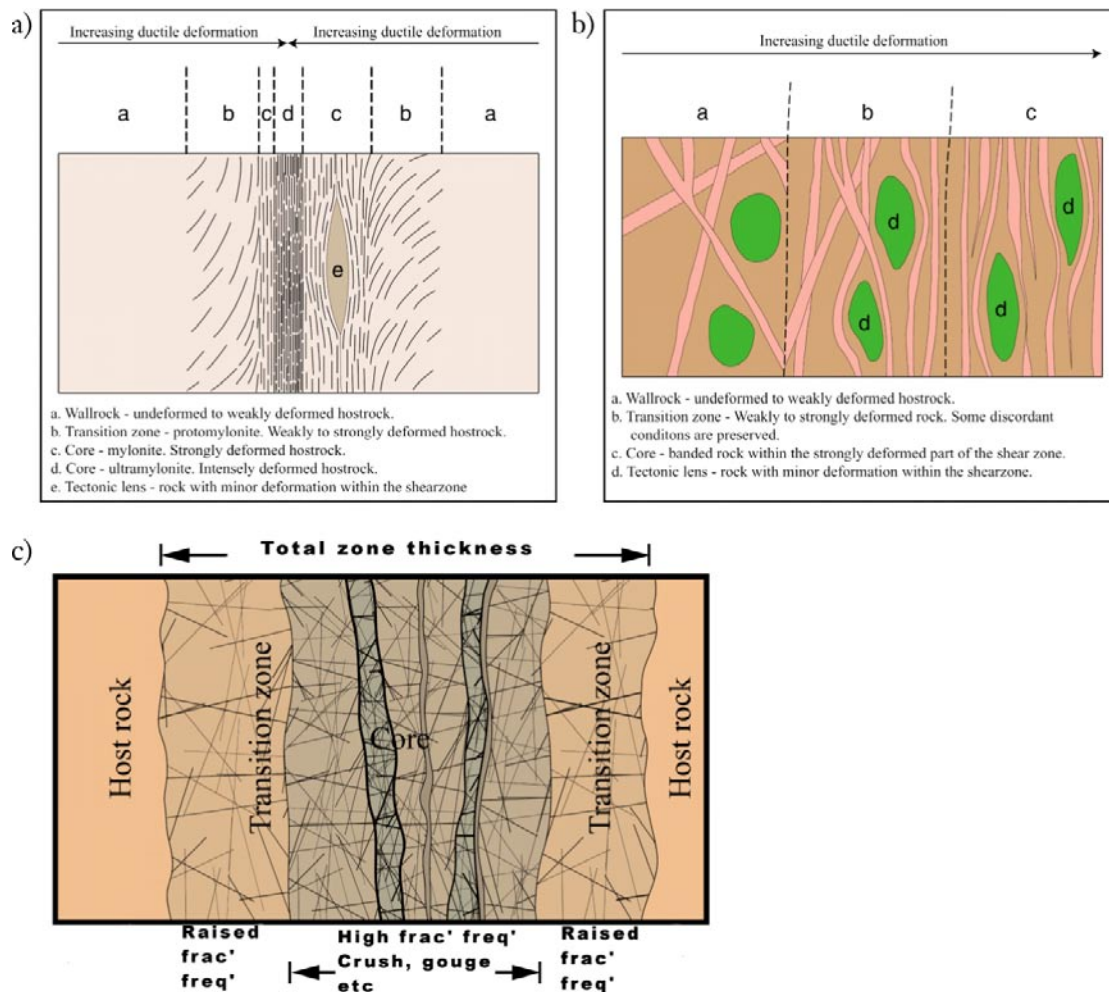
**Figure 5-2.** Intersection at the current ground surface of deformation zone traces with focus on the local model area. Confidence in existence: high=red, medium=green, low=grey.

are assumed to terminate, along their strike direction, against deformation zones as indicated by the lineament map. Thus, generally the length of such zones at the ground surface is represented by the length of the corresponding lineament. In certain cases, due to scale issues, the version 0.1 lineament study has clearly represented a lineament included in the Forsmark version 2.3 modelling work by an assembly of much shorter lineaments. Where both lineament sets have been interpreted to correspond to the same structure, but at different scales, a compromise has been made and the overall length quoted for a deformation zone corresponds to the entire longer lineament length, including those parts lying outside the local or regional model boundaries. An example involving deformation zone ZFMNW0805A and its associated lineaments is presented in section 4.3.3.

During the Forsmark site investigation and modelling work, gently dipping deformation zones have been detected by an integration of data from boreholes with the interpretation of seismic reflectors /Stephens et al. 2007/. During SFR model version 0.1, only a preliminary assessment of the existing seismic reflection data has been made (section 4.3.7) and those reflector geometries defined by /Cosma et al. 2006/ that intercept the SFR regional model volume have been imported into the RVS model without modification. The conceptual tectonic history described in /Stephens et al. 2007/ suggests that the gently dipping deformation zones in the Forsmark models terminate, both along their strike and in the down-dip direction, against regional or local major, vertical and steeply dipping deformation zones. The SFR version 1.0 modelling work will follow this concept and the modelled extent of the gently dipping zones will be constrained on the basis of the lateral extent of the supporting investigation evidence and the subsequent termination against the nearest steeply dipping zone outside the volume where this evidence exists.

The concept of deformation zone core and damage zones for brittle deformation zones is well established and has been presented earlier (/Munier et al. 2003/ and Figure 5-3). In contrast to the original representation, the use of absolute fracture frequencies to define a damage zone or zone core boundary position has not been applied. Elevated fracture frequencies in a relative sense are implied in the definition of such brittle deformation zones, but the strict application of fixed threshold values is considered unhelpful. The prime criterion used to define a zone core is a highly increased fracture frequency relative to the damage zone, often together with the occurrence of crushes, breccias and/or cataclasites. It should also be noted that deformation zone geometries are often complex, discontinuous and asymmetrical.





**Figure 5-3.** a) Schematic example of a ductile shear zone in homogeneous rock, which is deformed under low- to medium-grade metamorphic conditions. The increasing degree of deformation is reflected in the formation of protomylonite, mylonite and ultramylonite. The zone may contain less deformed rock volumes, often shaped as lenses. The example shows sinistral shear. (b) Schematic example of a ductile shear zone (or belt) in heterogeneous rock, which is deformed under low- to high-grade metamorphic conditions. The host rock consists of e.g. tonalite (brown) intruded by an ultramafic rock (green) and a swarm of granitic dykes (pink). (c) Schematic illustration of a brittle deformation zone. Transition zone = damage zone in current terminology.

The current SKB zone definition differs considerably from that of the previous structural models of SFR, where fracture zones were identified on the basis of the frequency of open fractures and hydrogeological information (see /Carlsson et al. 1985, 1986/). Mixing borehole intercepts defined in previous structural models together with SHI interpreted possible deformation zones is considered reasonable when assessing the evidence for the existence and orientation of a deformation zone. However, conscious efforts have been made to avoid associated inconsistencies in the judgment of zone thickness due to the different mapping methodologies. For model version 0.1, unless otherwise noted, zone thicknesses have been estimated on the basis of the SHI borehole intercepts.

For SFR modelling version 1.0, it is intended to remap all available drill cores from earlier SFR boreholes. This exercise will include the identification of the existence and width of any possible deformation zone intercepts in accordance with a simplified variant of SKB's current methodology. The process will allow a review of the earlier interpretations made and an update in accordance with SKB current practice. This was not possible during model version 0.1, since currently only about a quarter of the old SFR boreholes have been subject to geological SHI. However, predicted geometrical intercepts between the current modelled zones and all boreholes, even those boreholes that have not been reviewed yet, have been included in Appendix 7 and will be further investigated during version 1.0.



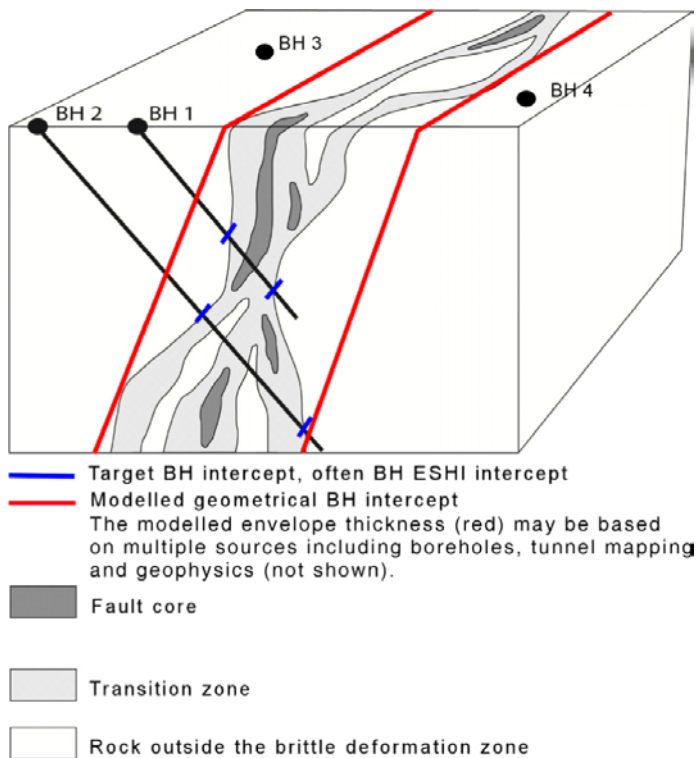
For model version 0.1, it was decided to use both borehole and tunnel intercepts from the previous structural models and possible deformation zone from the SHI work to estimate thickness in the following manner:

- The thicknesses of zones H2 (ZFM871), 3 (ZFMNNE0869), 6 (ZFMNNW1029) and 8 (ZFMNW0805A) are based on the identification of possible deformation zones in the SHI.
- The character and thickness of zone 9 (ZFMNE0870A/B) are based on the reported tunnel intercept in /Axelsson and Hansen 1997/, since it is this extensive intercept that dominates the basis for the existence of the zone rather than borehole data.

Two specific borehole related terms are quoted in the deformation zone descriptions and accompanying property tables, namely *Target borehole intercept* and *Geometrical borehole intercept* (Figure 5-4). These two parameters underlie much of the resulting modelled 3D deformation zone geometries.

A *target borehole intercept* is the interpreted position of a deformation zone in a specific borehole and is described by an upper and lower borehole length (sec\_up/sec\_low). In general, target intercepts conform to the geological SHI possible deformation zone intercepts but, in certain cases, adjustments have been made on the basis of other information or interpretation, related to information away from the specific borehole. These positions correspond to where the blue lines cross the boreholes as shown in Figure 5-4. A *target tunnel intercept* is defined in the same manner, but by chainage intervals along a tunnel centre line rather than borehole length.

A *geometrical borehole intercept* is the intercept between a modelled zone and a specific borehole as they exist in the RVS model. In the case of a zone modelled with thickness, any such intercept is described by the intercept positions of the outer surfaces of the modelled structure and specifically by an upper and lower borehole length (sec\_up/sec\_low). These positions correspond to where the red zone boundary lines cross the boreholes, as shown in Figure 5-4, and are of importance for the estimation of modelled thickness. A *Geometrical tunnel intercept* is defined in the same manner, but by chainage intervals along a tunnel centre line rather than borehole length.



(redrawn after Caine et al. 1996)

**Figure 5-4.** Three-dimensional cartoon illustrating a conceptual geometric model for a brittle deformation zone at Forsmark (after /Stephens et al. 2007/). Note the variable character of the deformation zone along the two borehole intersections (BH).

As described earlier, the modelled thickness of a particular deformation zone is generally based on information from a number of sources from both the surface and at depth and sometimes includes more than one borehole. The physical location and inferred orientation of deformation zone target intercepts, deformation indicators from any tunnel mapping evidence, and geophysical information in the form of seismic reflection, seismic refraction, magnetic and resistivity anomalies may be taken into account to assign an overall 'envelope thickness' for a deformation zone defined in 3D. This envelope thickness aims to contain at least the majority of the core(s), damage zone(s) and possible splays of each deformation zone. It is this envelope thickness that defines the deformation zone in the 3D RVS deterministic deformation zone model along with a, generally centrally located, zero thickness middle plane. The *geometrical intercepts* in boreholes or tunnels listed in the deformation zone descriptions and property tables (Appendix 7 and 8) relate to where the deformation zone envelope surfaces intercept the various boreholes/tunnels and are described by an upper and lower borehole length (sec\_up/sec\_low) for each borehole or start and end chainage for each tunnel. A summary of all deformation zone intercepts on a borehole by borehole and tunnel by tunnel basis are presented in Appendix 7.

Any estimate of deformation zone length, like thickness, is also closely related to the scale of interpretation. The quoted lengths in the property tables refer to total deformation zone length and include the known extents outside of the regional and local model boundaries. For the purposes of the deterministic modelling, within the local model volume, deformation zone length generally corresponds to the length of an associated linked lineament. However, all of the associated lineaments in the local model area are still under review and further adjustments are likely to be made during model version 1.0. The lineament review referred to is a process performed with reference to the original background data and lineament interpreters.

## **5.2 General character of different sets of zones**

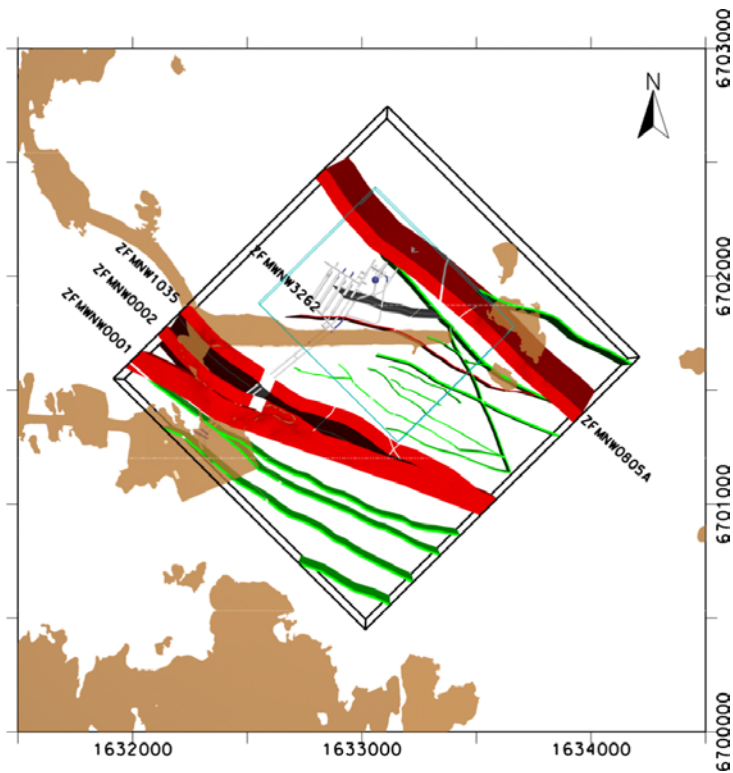
At least three sets of vertical to steeply dipping deformation zones can be distinguished in the regional model volume. The most conspicuous set consists of deformation zones referred to as the WNW to NW set (Figure 5-5). In addition, there are two sets that consist of vertical to steeply dipping zones referred to as the NNW (Figure 5-6) and NNE to ENE (Figure 5-7) sets. The latter includes a significant portion of the deformation zones, but the set is somewhat less well defined in terms of orientation than the other two. There are also two gently dipping zones (Figure 5-8).

The geological information is mostly limited to deformation zones in the steeply dipping WNW to NW set, as well as one gently dipping zone. Borehole and/or tunnel data are available for three zones in the vertical to steeply dipping NNW and NNE to ENE sets. However, these data are somewhat restricted and even ambiguous for some of the zones. They are insufficient for the characterisation of these sets.

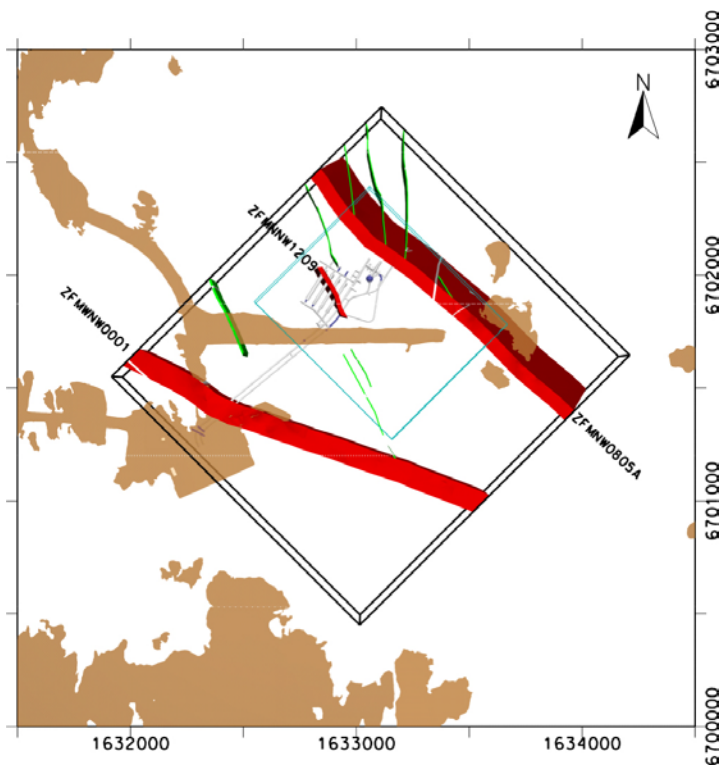
Based on the available data, it can be concluded that the geological characterization of the vertical to steeply dipping NNW and NNE to ENE sets, as defined in SDM Forsmark stage 2.2, is applicable to the SFR model volume. However, it must be emphasized that only a few of the boreholes that were subjected to geological SHI intersect these sets, and information of fracture orientations is not available for any of the boreholes.

### **5.2.1 The vertical to steeply dipping WNW to NW set**

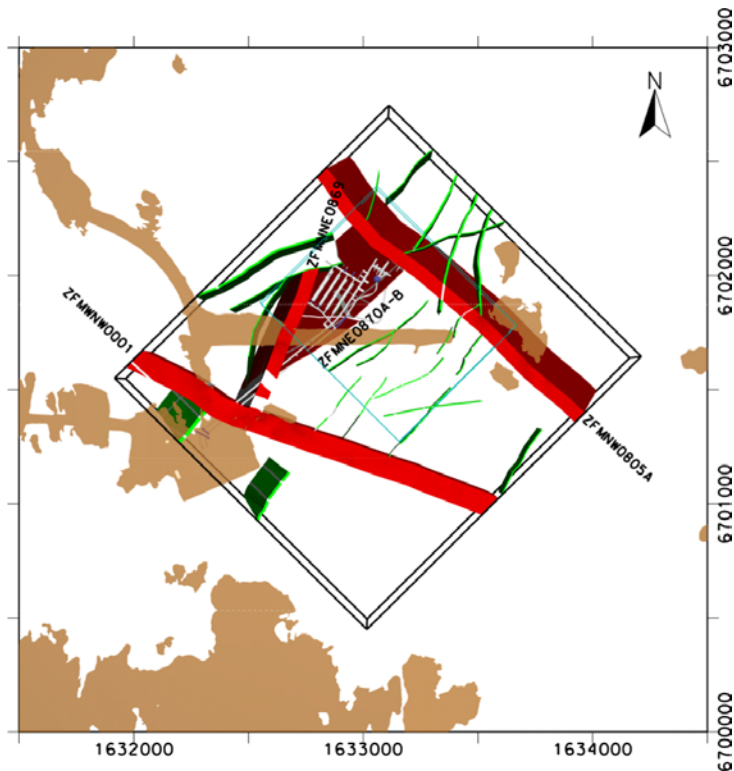
The zones in the vertical to steeply dipping WNW to NW set are generally composite features, characterized by an initial development in the ductile regime followed by brittle reactivation. It is the only set that exhibits ductile deformation. The majority of the fractures are sealed and mylonites, cataclasites and cohesive breccias occur locally, especially in the most prominent zones in this set (i.e. ZFMWNW0001 and ZFMNW0805A). The bedrock within these zones is typically affected by a varying degree of oxidation. Epidote, quartz, adularia, chlorite and calcite dominate the mineral fillings and coatings along fractures in these zones.



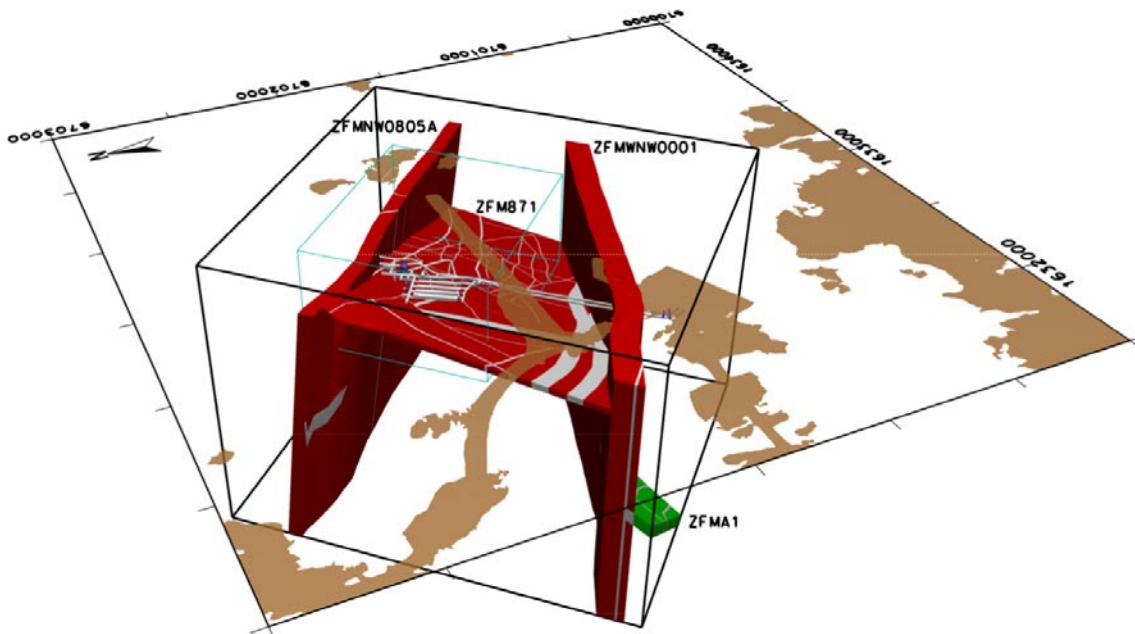
**Figure 5-5.** Three dimensional model that shows the vertical and steeply dipping deformation zones that strike WNW-ESE and NW-SE (WNW to NW set) inside the local and regional model volumes. The colours of the zones refers to the confidence of existence where red = high, green = medium and grey = low confidence in existence. Only one zone with low confidence exists in the 0.1 model version.



**Figure 5-6.** Three dimensional model that shows the vertical and steeply dipping deformation zones that strike NNN-SSE and N-S (NNW set) inside the local and regional model volumes. ZFMWNW0001 (Singö deformation zone) and ZFMNW0805A are included as reference. The colours of the zones refers to the confidence of existence where red = high and green = medium.



**Figure 5-7.** Three dimensional model that shows the vertical and steeply dipping deformation zones that strike NNE-SSW, NE-SW and ENE-WSW (NNE to ENE set) inside the local and regional model volumes. ZFMWNW0001 (Singö deformation zone) and ZFMNW0805A are included as reference. The colours of the zones refers to the confidence of existence where red = high and green = medium.



**Figure 5-8.** Three dimensional model that shows the gently dipping deformation zones (ZFMA1 and ZFM871) inside the local and regional model volumes. ZFMWNW0001 (Singö deformation zone) and ZFMNW0805A are included as reference. The colours of the zones refers to the confidence of existence where red = high and green = medium.

### **5.2.2 Other vertical to steeply dipping deformation zones**

Notwithstanding the limited material, all other vertical to steeply dipping deformation zones formed in the brittle regime and are generally dominated by sealed fractures. However, there are records of 'mylonite' in some of these deformation zones (e.g. ZFMNE0870A and B) /cf. Christiansson 1986/, but comparison with data from remapped drill cores suggests that the term refers to brittle rather than ductile features, such as cataclasite. Adularia, laumontite, chlorite and calcite are conspicuous along the fractures in these zones, whereas clay minerals are less frequent. The most common type of bedrock alteration associated with these zones is oxidation of varying intensity.

### **5.2.3 Gently dipping deformation zones**

A gently dipping deformation zone (ZFM871), which provides data that characterizes the gently dipping set at SFR, is located just beneath the silo at SFR. It was referred to as zone H2 during the SFR construction work (Figure 5-8). The geological information for ZFM871 is relatively extensive due to intersection with several cored boreholes and the NBT (lowermost tunnel in SFR). It is characterized by a high frequency of sub-horizontal, open fractures and incoherent crush material. Chlorite, calcite and especially clay minerals, stained by hematite and/or Fe-hydroxide, are conspicuous along the fractures in ZFM871. Argillitic alteration and oxidation occur locally along the zone.

## **5.3 Assignment of properties**

A summary of the basic geometrical properties of each of the 58 deformation zones that intercept the regional scale deformation zone model is presented in Table 5-1. The basis for the interpretation of all the deformation zones in the regional model volume, along with descriptions of the thirteen deformation zones focused on during model version 0.1, including their geological properties, are presented in Appendix 8. Some general remarks on the properties of deformation zones that are located inside the local scale model are provided below.



**Table 5-1. Summary table showing geometry of deformation zones inside the regional model volume.**

DZ Name	Strike (°)	Dip (°)	Thickness (m)	Length (m)	Lower cut off depth (-masl)	Comment
Gently dipping DZs						
zfm871_zoneh2_SFR*	071	19	24	1,200	–	No clearly identified magnetic lineament
ZFMA1**	082	45	40	–	–	No surface interception
Steeply dipping DZs						
NNE to ENE set						
ZFMNNE0725	201	84	12	1,757	1,100	Medium confidence-until further review.
zfmNNE0869_zone3_SFR*	201	86	60	694	1,100	Increased depth class since longer/deeper zones terminate against it.
ZFMNNE2308	214	80	15	1,382	1,100	
zfmNNE3110	031	90	5	125	500	
zfmNNE3117	019	90	1	94	500	
ZFMNNE3130	030	90	5	411	750	Increased depth class since longer/deeper zones terminate against it.
zfmNNE3146	028	90	5	385	1,100	Increased depth class since longer/deeper zones terminate against it.
zfmNNE3264	031	90	10	1,107	1,100	
zfmNNE3265	018	90	10	1,166	1,100	
zfmNNE	034	90	10	1,015	1,100	
zfmNNE3271	016	90	5	262	500	
zfmNNE8027	032	90	5	222	500	
zfmNE0870A_zone9a_SFR*	238	75	1	468	750	Note: two sections, A and B.
zfmNE0870B_zone9b_SFR*	227	73	1	340	750	
zfmNE3112	049	90	5	231	1,100	Increased depth class since longer/deeper zones terminate against it.
zfmNE3134	041	90	5	463	500	
zfmNE3137	040	90	5	325	500	
zfmNE3141	036	90	5	239	750	Increased depth class since longer/deeper zones terminate against it.
ZFMNE3153	041	90	5	581	1,100	Length class uncertain. To be reviewed in v1.0.
zfmNE8026	039	90	5	199	500	
zfmENE3109	062	90	5	362	500	
zfmENE3115	056	90	5	547	1,100	Increased depth class since longer/deeper zones terminate against it.
zfmENE3135	081	90	5	444	500	
zfmENE3151	073	90	5	413	500	
zfmENE8031	067	90	5	545	1,100	Increased depth class since longer/deeper zones terminate against it.
zfmENE8034	064	90	10	650	1,100	Length class uncertain. To be reviewed in v1.0.
WNW to NW set						
ZFMWNW0001_SFR_Singö*	120	90	100	30,000	1,100	

DZ Name	Strike (°)	Dip (°)	Thickness (m)	Length (m)	Lower cut off depth (-masl)	Comment
ZFMWNW0813	114	90	10	2,708	1,100	
zfmWNW0835	114	90	10	1,068	1,100	
ZFMWNW0836	117	90	10	4,368	1,100	
ZFMWNW1035*	121	80	60	1,615	1,100	
ZFMWNW1056	110	90	10	2,758	1,100	
ZFMWNW2496	123	90	10	2,399	1,100	
zfmWNW3145	282	85	5	456	500	No indication of existence in SFR tunnels.
ZFMWNW3259	114	90	10	1,467	1,100	
zfmWNW3262*	111	90	5	1,171	1,100	
zfmWNW3267	124	90	5	731	750	
ZFMWNW3268	110	90	5	586	750	
zfmWNW8028	119	90	5	306	500	
zfmWNW8037	100	90	5	258	1,100	Depth class to be reduced to 500 m in v1.0.
zfmWNW8041	117	90	5	240	500	
zfmWNW8042	116	90	5	368	500	
zfmWNW8043	120	90	5	868	750	
ZFMNW0002*	123	90	58	18,000	1,100	
zfmNW0805A_zone8_SFR*	314	83	60	3,643	1,100	Note: two sections, A and B.
zfmNW0805B*	133	90	10	1,111	1,100	
NNW set						
zfmNNW0999*	170	90	5	692	1,100	Increased depth class since longer/deeper zones terminate against it.
zfmNNW1034	157	90	5	707	750	
zfmNNW1209_zone6_SFR*	151	88	20	253	500	
zfmNNW3111	147	90	5	206	500	
zfmNNW3113	172	90	5	381	500	
zfmNNW3119	155	90	5	648	1,100	Increased depth class since longer/deeper zones terminate against it.
zfmNNW3140	151	90	5	196	750	Increased depth class since longer/deeper zones terminate against it.
ZFMNNW3148	153	90	10	1,130	1,100	
zfmNNW3155	153	90	5	609	1,100	Increased depth class since longer/deeper zones terminate against it.
zfmNS3154***	180	90	5	757	1,100	Increased depth class since longer/deeper zones terminate against it.

\* a separate more detailed property table exists in Appendix 8.

\*\* ZFM, upper case indicates that the entire zone lies outside of the local model volume.

\*\*\*zfm, lower case indicates that some part of the DZ falls within the local model volume.

	High confidence (in existence)
	Medium confidence (in existence)
	Low confidence (in existence)

### **5.3.1 Orientation, length (size) and thickness**

The orientation of the deformation zones in the zone descriptions and property tables, i.e. the quoted strike and dip in Table 5-1 and Appendix 8, is the average modelled value provided in RVS based on the input modelling constraints. This means that these values are relevant to the scale of the modelled objects since orientation, like most other parameters, is closely linked to the scale of observation. In practice, the presented strike is an average value of the trend of the associated surface lineament that has been used as input data to RVS and the dip has been constrained by the modeller, or calculated based on the resultant geometry from a series of control points, mostly borehole intercepts.

The length of the deterministic zones is presented in Table 5-1 and Appendix 8. This entity implies the overall traceable length of the surface expression of the interpreted deformation zone at the regional model scale. The assessment of geological length at this scale is not terminated along, or restricted to, the local or regional scale model boundaries. It is anticipated that such length estimates only give a rough indication of deformation zone size, since such values clearly vary with the elevation of measurement and the interplay with neighbouring (intersecting and truncating) deformation zones. Any estimate of deformation zone or lineament length implicitly involves a judgement of continuity related to the scale of assessment and the realization that deformation zone geometries are not fully continuous in reality. For the local SFR model version 0.1, no minimum deformation zone trace length has been strictly applied since the associated lineaments are still under review. For model version 1.0, it is anticipated that a minimum cut off length of 300 m will be applied in the local model. Structures with a surface trace length of less than 300 m will not be modelled deterministically. Lineaments with lengths greater than 1,000 m have been taken to represent local major or regional deformation zones, whereas lineaments shorter than 1,000 m have been assumed to represent minor deformation zones. For the regional model, a minimum deformation zone trace length of 1,000 m will be applied in model version 1.0.

The estimates of deformation zone thickness presented in Table 5-1 and Appendix 8 refer to true thickness. More specifically, the single thickness values given in the property tables in Appendix 8 refer to modelled true thickness. This means that a value has been assigned that aims to provide a representative overall thickness applicable over the entire length of the zone in the deterministic model. This modelled deformation zone thickness makes use of the geometrical intercepts listed in the property tables and defined in Figure 5-4. It is based on all available data, both from surface and at depth. In the case of the current model version, the presented range of deformation zone thickness is generally based on an inspection of tunnels and boreholes along with any available surface-based, geophysical data. The surface geophysical surveys, namely magnetic data, provide some indication as to how the relative thickness of a deformation zone varies laterally and by inference with depth. It is accepted that this type of surface expression is, in fact, linked to an apparent rather than a true thickness but it is still considered to provide the best estimate with consideration made to likely lateral variations in deformation zone dip. The forward modelling of magnetic data (preliminary results presented in Appendix 6) will provide input to thickness estimates for version 1.0. The thickness estimates include deformation zone cores, damage zones and, to a certain extent, local splays. The widths of the low velocity anomalies from seismic refraction surveys are taken as giving an indication of the presence and thickness of more highly fractured rock associated with brittle deformation zone cores, whereas the magnetic anomalies are interpreted as giving an indication of the variation in thickness of hydrothermal alteration, typically intimately associated with both the highly fractured core and the damage zones.

### **5.3.2 Deformation style**

An indication as to whether an individual deformation zone has a ductile, brittle or composite ductile and brittle character is indicated in the property tables and deformation zone descriptions presented in Appendix 8.

### **5.3.3 Alteration**

Red staining caused by a fine-grained dissemination of hematite is associated with a majority of the deformation zones. This type of alteration and the occurrence of other types of alteration are listed in the property tables in Appendix 8.

### **5.3.4 Other properties**

Currently the interpretations are preliminary and the model is at an early stage of development. However, it is intended that descriptions of the following properties with the following formats will be included in SFR model version 1.0:

#### ***Fracture orientation***

The Terzaghi-corrected fracture pole concentrations from ‘best source’ borehole intercepts will be presented. By ‘best source’ is implied that, where possible, a borehole is selected which has the cleanest interception with the target deformation zone, rather than using information from a borehole that intercepts the deformation zone obliquely, or where interference from other structures is suspected. In some cases, uncorrected measurements from tunnel mapping will be presented.

#### ***Fracture frequency***

Terzaghi-corrected fracture frequency will be presented. Open and sealed fracture frequencies will be presented separately in an attempt to provide at least a general indication of fracture condition and character within the deformation zone. The estimates take into account sections of the core that have been mapped as sealed networks. This will be carried out by taking the inferred number of fractures as being equal to the sealed section length/rock piece length, per sealed network section. However, the presented fracture frequencies will not take into account sections of crush, which are provided separately for clarity (see below).

#### ***Crush zone***

The number and overall combined thickness of crush zones will be provided. The total crush thickness will be estimated in order to provide a better indication of true thickness. It should be pointed out that the assessment is simplistic and it should be appreciated that the internal architecture of a deformation zone is likely to be complex and crush zones need not necessarily run parallel to the overall deformation zone orientation. As for fracture orientation and fracture frequency, a ‘best source’ borehole intercept(s) will be selected.

#### ***Fracture mineralogy of deformation zones***

Fracture fillings identified in the deformation zones during Boremap logging will be listed in the property tables.

#### ***Kinematic properties of deformation zones***

For the Forsmark site investigation, a focused kinematic study was performed based on measurements of kinematic indicators identified during detailed mapping of the drill core. Considering the objective of the deformation zone model, it was decided at the outset of model version 0.1 that the SFR investigation programme would not include additional studies of kinematic indicators.

## **5.4 Geometric model**

In this section, some of the basic geometrical methods used in the modelling work are described in order to assist the end users in understanding how the SFR model version 0.1 has been constructed. It should be noted that the appropriateness of all these methods will be reviewed and this may lead to modifications in their application in future model versions. A brief outline of the key issues for review is also presented.

### **5.4.1 Regional and local models**

The regional and local model volumes, resolution and scale issues are described in section 1.3 and Figure 1-3. As discussed in section 5.1, the lineament cut off lengths for the regional and local models have not been strictly applied in the current model version and the review of the interpreted



lineaments is incomplete. For these reasons and to assist the Hydrogeology and Design groups, the principle end users of the model version 0.1, a single Master deformation zone model, integrating both the regional and local models has been created as the end product for this modelling version. For future model versions, after the lineament review and a final length cut-off criterion is established, separate local and regional model versions will be produced.

**5.4.2 DZ thickness classes**

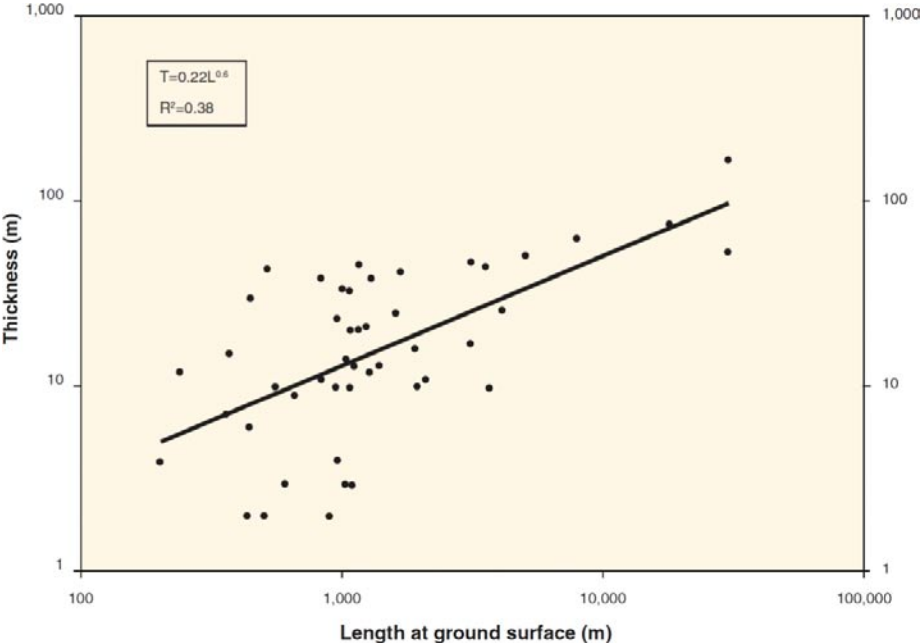
A deformation zone thickness-length correlation chart is presented in Figure 5-9. The background and limitations to this analysis were presented in /Stephens et al. 2007/. This correlation was utilized during the Forsmark version 2.2 modelling work to define the thickness of deformation zones that were based solely on interpreted lineaments where more direct information was lacking. The vast majority of lineaments of most relevance to the SFR modelling work fall within the lower range of 100 to 2,000 m. As can be seen in the chart, the application of this correlation in such a size range is highly questionable. For this reason, the presented thickness-length correlation has not been applied in the current modelling step. Instead, the following simple group classification has been applied where no information concerning thickness is available and where a thickness has not been defined by the earlier Forsmark version 2.2 modelling work:

Zone (lineament) length (m)	Zone thickness (m)
≥1,000	10
999–100	5
≤100	1

The issue of deformation zone thickness versus length and its application specifically in the SFR project will be evaluated in model version 1.0.

**5.4.3 Deformation zone depth cut-off classes**

A requirement of the version 0.1 modelling has been the application of a deformation zone termination depth versus length classification. Earlier SKB modelling work has followed the general principle that a deformation zone should be modelled to a depth equal to the length of the zone’s



*Figure 5-9. Power law correlation diagram between thickness and ground surface length of deterministic deformation zones, based on Forsmark model stage 2.2 data.*

surface trace. This principle, in combination with the selected local and regional model modelling scales and model volume lower boundaries, means in practice that any zone included in the local model would terminate at the base of the local model volume and, in the case of the SFR regional model constraints, any zone included in the regional model would terminate at the base of the regional model volume. In this way, the systematic division between stochastic and deterministic modelling is maintained. The requirement for a more strict termination depth versus length in the combined regional and local ‘*Master*’ version 0.1 deformation zone model has led to use of the following, general classification grouping:

Zone (lineament) length (m)	Cut-off depth (–masl)
≥1,000	1,100
999–500	750
≤500	500

Individual deformation zone lengths and cut-off depths for all zones in the model are presented in Table 5.1. As documented in Table 5-1, if a longer zone that belongs to a deeper cut-off depth class terminates against a shorter zone that belongs to a shallower class, then the cut-off depth of the shorter zone has been increased. The requirement for this classification and in particular the application of these groupings will be evaluated further during version 1.0.

## 5.5 Confidence assessment and the future handling of key uncertainties

The overall confidence level concerning the deformation history and the broad tectonic framework of the region is judged high, based on the detailed work associated with the Forsmark site investigation and the modelling work as reported in /Stephens et al. 2007/ and elsewhere.

The confidence levels of all deformation zones included in the local model volume are indicated by colours in Table 5-1. Confidence levels and key properties associated with the deformation zones, such as dip, length and thickness, are included in the deformation zone descriptions and property tables in Appendix 8. However, the overall confidence level in the rock volume lying between zones ZFMWNW0001 and ZFMNW0805A is judged to be at best medium at the current time. This is based on the fact that, although the existing tunnel and borehole mapping and associated data from the investigation and construction of the SFR facility are available, the quality of these data is variable and low by current SKB standards. In addition, these data have not been fully utilized in the current model and much more needs to be done for SFR modelling version 1.0. It is planned to remap all available drill core from the earlier SFR boreholes in accordance with SKB’s standard simplified mapping methodology (overview mapping). At the same time, independent from earlier SFR interpretations, any possible deformation zones will be identified and described. It is planned that the results of this mapping exercise will be logged in Sicada as *preliminary geological single-hole interpretation*. In this way, the quality of the older borehole data will be raised as will any modelling interpretations that rely primarily on this data.

While an improved modelling of the regional zones ZFMWNW0001 and ZFMNW0805A is desirable, it is the specific rock volume lying between these zones and to the south of the existing SFR tunnels that needs to be the focus in the version 1.0 modelling work. For the version 0.1 modelling work, there is extremely little data available for this specific rock volume and the overall confidence in the model is low in this area.

In addition to old borehole data, it is suspected that additional archive data, notes and reports from the SFR construction and investigations exist that have not yet been identified and fully utilized. Further efforts will be made to locate such material and integrate the results into the model and its description in version 1.0.

While the detailed magnetic survey results could be expected to provide a sound basis for the interpretation of lineaments, the actual bedrock rock mass that exists generates no clear systematic linear pattern of anomalies in the focused area for the new facility (Figure 5-10). In addition, the

existence of the man-made pier, marine electric cable and the existing SFR facility all locally distort the magnetic field. These facts, in combination with the scale needed for any detailed design work, means that interpretation of resulting lineaments, in particular the shorter ones (< 1,000 m), as consistently representing discrete minor deformation zones, can only be carried out, in most cases, with a low degree of confidence.

As described in section 4.3.4, in order to maximize the utilization of the available magnetic data, forward modelling has been performed of the magnetic total field from the detailed ground survey in order to estimate the geometries of the sources to the low magnetic anomalies associated with the lineaments, i.e. principally the approximate thickness and dip of the possible deformation zones. In order to ensure a reasonable level of confidence, confirmatory profiles still need to be modelled across the targeted lineaments before these results are integrated into the deformation zone model. However, it is hoped that in the cases where high quality borehole data is available from the new boreholes, correlation with the modelled anomalies will be possible and consequently such profile modelling can also be used to support the modelled orientation of inferred deformation zones where direct high quality borehole information is lacking. If successful, the application of this modelling technique will provide at least a limited increase in confidence throughout the model volume during version 1.0.

The existence and position of any gently dipping deformation zones in the SFR local model volume is a key issue due to their geometry and water transporting, brittle open character as indicated by earlier Forsmark and SFR investigations and construction. Such zones are important from both rock excavation and hydrogeological points of view. For the Forsmark modelling work /Stephens et al. 2007/, the results from seismic reflection surveys provided key evidence for the existence and orientation of such zones. There are difficulties associated with performing new seismic reflection survey work relevant to the SFR local model volume, due to the shallow depth of the sea in this area in addition to the relatively shallow depth of interest for the SFR project (< 200 m). Special efforts are currently being made to reassess how a meaningful additional survey could be performed. A limited coverage of the rock volume of interest is provided by existing seismic reflection data (see section 4.3.7). The relevant reflector geometries resulting from this earlier survey have been imported into the version 0.1 model and a detailed assessment of their possible character will be made during version 1.0. Currently the existence and orientation of gently dipping zones remains a key uncertainty.

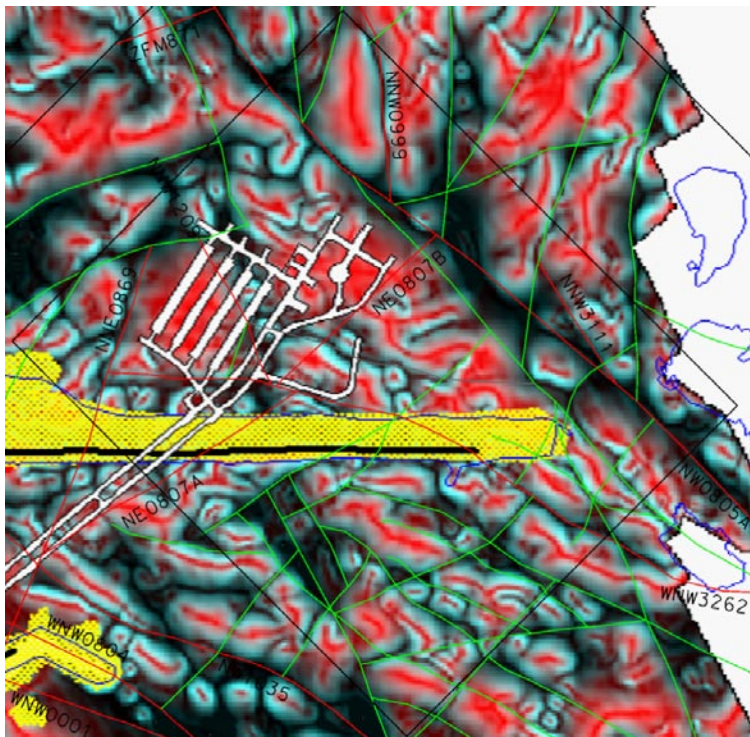


Figure 5-10. Pattern of magnetic anomalies with a focus on the SFR local model area.

## References

- Andersson J, Ström A, Svemar C, Almén K-A, Ericsson L-O, 2000.** What requirements does the KBS-3 repository make on the host rock? Geoscientific suitability indicators and criteria for siting and site evaluation. SKB TR-00-12, Svensk Kärnbränslehantering AB.
- Axelsson C-L, Ekstav A, Lindblad Påsse A, 1995.** SFR – Utvärdering av hydrogeology. Golder Associates AB, SKB PM Facilities 95/12, Reg. No. A4343.
- Axelsson C-L, Hansen L M, 1997.** Update of structural models at SFR nuclear waste repository, Forsmark, Sweden SKB R-98-05, Svensk Kärnbränslehantering AB.
- Balu L, Cosma C, 2005.** Estimation of 3D positions and orientations of reflectors based on an updated interpretation of Stage 1 reflection seismic data. Preliminary site description Forsmark area – version 1.2. SKB R-05-39, Svensk Kärnbränslehantering AB.
- Berglund J, 2009.** Site investigation SFR. Geological mapping and laser scanning of the lower construction tunnel. SKB P-09-XX, Svensk Kärnbränslehantering AB.
- Caine J S, Evans J P, Forster C B, 1996.** Fault zone architecture and permeability structure. *Geology* 24, 1025–1028.
- Carlsson A, Christiansson R, 2007.** Construction experiences from underground works at Forsmark. Compilation report. SKB R-07-11, Svensk Kärnbränslehantering AB.
- Carlsson L, Carlsten S, Sigurdsson T, Winberg A, 1985.** Hydraulic modeling of the final repository for reactor waste (SFR). Compilation and Conceptualization of Available Geological and Hydrogeological Data. Edition 1. SKB SFR 85-06, Svensk Kärnbränslehantering AB.
- Carlsson L, Winberg A, Arnefors J, 1986.** Hydraulic modeling of the final repository for reactor waste (SFR). Compilation and Conceptualization of Available Geological and Hydrogeological Data. SKB SFR 86-03, Svensk Kärnbränslehantering AB.
- Carlsten S, Döse C, Samuelsson E, Gustafsson J, Petersson J, Stephens M, Thunehed H, 2007.** Forsmark site investigation. Geological single-hole interpretation of KFM11A, HFM33, HFM34 and HFM35. SKB P-07-109, Svensk Kärnbränslehantering AB.
- Christiansson R, 1986.** Geologisk beskrivning av zoner kring slutförvaret. SKB SFR 86-02, Svensk Kärnbränslehantering AB.
- Christiansson R, Magnusson K-Å, 1985a.** Hydrogeologiskt program. Beskrivning av den geologiska miljön kring kärnborrhålen HK1–4. SKB SFR 85-03, Svensk Kärnbränslehantering AB.
- Christiansson R, Magnusson K-Å, 1985b.** Geologisk miljö kring Silo 1. SKB SFR 85-07, Svensk Kärnbränslehantering AB.
- Christiansson R, Bolvede P, 1987.** Byggnadsgeologisk uppföljning. Slutrapport. SKB SFR 87-03, Svensk Kärnbränslehantering AB.
- Claesson L-Å, Nilsson G, 2007.** Forsmark site investigation. Drilling of flushing water well HFM33 and monitoring wells HFM34 and HFM35 at drill site DS11. SKB P-07-11, Svensk Kärnbränslehantering AB.
- Claesson L-Å, Nilsson G, Ullberg A, 2007.** Forsmark site investigation. Drilling of the telescopic borehole KFM11A at drill site DS11. SKB P-07-45, Svensk Kärnbränslehantering AB.
- Cosma C, Balu L, Enescu N, 2003.** Estimation of 3D positions and orientations of reflectors identified during the reflection seismic survey at the Forsmark area. Site descriptive modelling Forsmark Stage 2.1. SKB R-03-22, Svensk Kärnbränslehantering AB.
- Cosma C, Balu L, Enescu N, 2006.** Estimation of 3D positions and orientations of reflectors identified during the reflection seismic survey. Site descriptive modelling Forsmark Stage 2.1. SKB R-06-93, Svensk Kärnbränslehantering AB.
- Curtis P, Elfström M, Markström I, 2007.** Rock Visualization System. Technical description (RVS version 4.0). SKB R-07-44, Svensk Kärnbränslehantering AB.



- Döse C, Samuelsson E, 2007.** Forsmark site investigation. Boremap mapping of percussion drilled borehole HFM33-37. SKB P-07-106, Svensk Kärnbränslehantering AB.
- Follin S, 2008.** Bedrock hydrogeology Forsmark. Site descriptive modelling, SDM-Site Forsmark. SKB P-08-95, Svensk Kärnbränslehantering AB.
- Glamheden R, Maersk Hansen L, Fredriksson A, Bergkvist L, Markström I, Elfström M, 2007.** Mechanical modelling of the Singö deformation zone. Site descriptive modelling Forsmark stage 2.1. SKB R-07-06, Svensk Kärnbränslehantering AB.
- Hagkonsult, 1982.** Geologiska undersökningar och utvärderingar för lokalisering av SFR till Forsmark. SKB SFR 81-13. Svensk Kärnbränslehantering AB.
- Hagkonsult, 1983.** Geologiska undersökningar och utvärderingar för förvarstrymmen i berg. SKBF/KBS 83-5, Svensk Kärnbränslehantering AB.
- Hermansson T, Stephens M B, Corfu F, Andersson J, Page L M, 2007.** Penetrative ductile deformation and amphibolite-facies metamorphism prior to 1851 Ma in the western part of the Svecofennian orogen, Fennoscandian Shield. *Precambrian Research* 153, 29–45.
- Herrmannsson T, Stephens M B, Corfu F, Page L M, Andersson J, 2008a.** Migratory tectonic switching, western Svecofennian orogen, central Sweden: Constraints from U/Pb zircon and titanite geochronology. *Precambrian Research* 161, 250–278.
- Herrmannsson T, Stephens M B, Page L M, 2008b.** <sup>40</sup>Ar/<sup>39</sup>Ar hornblende geochronology from the Forsmark area in central Sweden: Constraints on late Svecofennian cooling, ductile deformation and exhumation. *Precambrian Research* 167, 303–315.
- Holmén J G, Stigsson M, 2001.** Modelling of future hydrogeological conditions at SFR, Forsmark. SKB R-01-02, Svensk Kärnbränslehantering AB.
- Isaksson H, 2003.** Forsmark site investigation. Interpretation of topographic lineaments 2002. SKB P-03-40, Svensk Kärnbränslehantering AB.
- Isaksson H, Thunehed H, Keisu M, 2004.** Forsmark site investigation. Interpretation of airborne geophysics and integration with topography. Stage 1 (2002). SKB P-04-29, Svensk Kärnbränslehantering AB.
- Isaksson H, Keisu M, 2005.** Forsmark site investigation. Interpretation of airborne geophysics and integration with topography. Stage 2 (2002–2004). An integration of bathymetry, topography, refraction seismics and airborne geophysics. SKB P-04-282, Svensk Kärnbränslehantering AB.
- Isaksson H, Pitkänen T, Keisu M, 2006a.** Forsmark site investigation. Ground magnetic survey and lineament interpretation in an area northwest of Bolundsfjärden. SKB P-06-85, Svensk Kärnbränslehantering AB.
- Isaksson H, Thunehed H, Pitkänen T, Keisu M, 2006b.** Forsmark site investigation. Detailed ground and marine magnetic survey and lineament interpretation in the Forsmark area – 2006. SKB P-06-261, Svensk Kärnbränslehantering AB.
- Isaksson H, 2007.** Correlation between refraction seismic data, low magnetic lineaments and deformation zones (model stage 2.2). In Stephens MB and Skagius K (editors), *Geology – Background complementary studies. Forsmark modelling stage 2.2.* SKB R-07-56, Svensk Kärnbränslehantering AB.
- Isaksson H, Thunehed H, Pitkänen T, Keisu M, 2007.** Forsmark site investigation. Detailed ground and marine magnetic survey and lineament interpretation in the Forsmark area, 2006–2007. SKB R-07-62, Svensk Kärnbränslehantering AB.
- Juhlin C, Bergman B, Palm H, 2002.** Reflection seismic studies in the Forsmark area – stage 1. R-02-43, Svensk Kärnbränslehantering AB.
- Juhlin C, Bergman B, 2004.** Forsmark site investigation. Reflection seismics in the Forsmark area. Updated interpretation of Stage 1 (previous report R-02-43). Updated estimate of bedrock topography (previous report P-04-99). P-04-158, Svensk Kärnbränslehantering AB.
- Juhlin C, Palm H, 2005.** Forsmark site investigation. Reflection seismic studies in the Forsmark area, 2004: Stage 2. R-05-42, Svensk Kärnbränslehantering AB.

- Keisu M, Isaksson H, 2004.** Forsmark site investigation. Acquisition of geological information from Forsmarksverket. Information from the Vattenfall archive, Räcksta. SKB P-04-81, Svensk Kärnbränslehantering AB.
- Mattsson H, Keisu M, 2007a.** Forsmark site investigation. Interpretation of geophysical borehole measurements from KFM10A, KFM08C, HFM30, HFM31, HFM33, HFM34, HFM35 and HFM38. SKB P-06-258, Svensk Kärnbränslehantering AB.
- Mattsson H, Keisu M, 2007b.** Forsmark site investigation. Interpretation of geophysical borehole measurements from KFM02B, KFM08D and KFM11A. SKB P-07-125, Svensk Kärnbränslehantering AB.
- Munier R, Hermanson J, 2001.** Metodik för geometrisk modellering. Presentation och administration av platsbeskrivande modeller. SKB R-01-15, Svensk Kärnbränslehantering AB.
- Munier R, Stenberg L, Stanfors R, Milnes A G, Hermansson J, Triumf C-A, 2003.** Geological Site Descriptive Model. A strategy for the model development during site investigations. SKB R-03-07, Svensk Kärnbränslehantering AB.
- Nielsen U T, Ringgaard J, 2007a.** Forsmark site investigation. Geophysical borehole logging in boreholes KFM08C, KFM10A, HFM30, HFM31, HFM33, HFM34, HFM35 and HFM38. SKB P-07-05, Svensk Kärnbränslehantering AB.
- Nielsen U T, Ringgaard J, 2007b.** Forsmark site investigation. Geophysical borehole logging in boreholes KFM011A and KFM09B. Forsmark site investigation. SKB P-07-92, Svensk Kärnbränslehantering AB.
- Petersson J, Berglund J, Andersson U B, Wängnerud A, Danielsson P, Ehrenborg J, 2007.** Forsmark site investigation. Boremap mapping of telescopic drilled borehole KFM11A. SKB P-07-104, Svensk Kärnbränslehantering AB.
- Petersson J, Andersson U B, 2008.** Site investigation SFR. Overview Boremap mapping of drill cores from KFR04, KFR08, KFR09, KFR13, KFR35, KFR36, KFR54, KFR55, KFR7A, KFR7B and KFR7C. SKB P-08-02, Svensk Kärnbränslehantering AB.
- Petersson J, Curtis P, Bockgård N, Simeonov A, 2009.** Site investigation SFR. Geological single-hole interpretation of KFR04, KFR08, KFR09, KFR13, KFR35, KFR36, KFR54, KFR55, KFR7A, KFR7B and KFR7C. SKB P-09-32, Svensk Kärnbränslehantering AB.
- SKB, 1987.** SKB Slutförvar för reaktoravfall – SFR. Slutlig säkerhetsrapport SFR1. 1987-09-30, Svensk Kärnbränslehantering AB.
- SKB, 1993.** SKB Slutförvar för radioaktivt driftavfall – SFR1. Slutlig säkerhetsrapport. Revised edition – May 1993. 1993-05-14, Svensk Kärnbränslehantering AB.
- SKB, 2001.** SKB Slutförvar för radioaktivt driftavfall – SFR1. Slutlig säkerhetsrapport. 2001-06-30, Svensk Kärnbränslehantering AB.
- SKB, 2002.** Forsmark – site descriptive model version 0. SKB R-02-32, Svensk Kärnbränslehantering AB.
- SKB, 2004.** Preliminary site description Forsmark area – version 1.1. SKB R-04-15, Svensk Kärnbränslehantering AB.
- SKB, 2005.** Preliminary site description Forsmark area – version 1.2. SKB R-05-18, Svensk Kärnbränslehantering AB.
- SKB, 2006.** Site descriptive modelling Forsmark stage 2.1. Feedback for completion of the site investigation including input from safety assessment and repository engineering. SKB R-06-38, Svensk Kärnbränslehantering AB.
- SKB, 2008a.** Site description of Forsmark at completion of the site investigation phase. SDM-Site Forsmark. SKB TR-08-05, Svensk Kärnbränslehantering AB.
- SKB, 2008b.** Geovetenskapligt undersökningsprogram för utbyggnad av SFR. SKB R-08-67, Svensk Kärnbränslehantering AB.

**Stephens M B, Fox A, Simeonov A, Isaksson H, Hermanson J, Öhman J, 2007.**

Geology Forsmark. Site descriptive modelling. Forsmark stage 2.2. SKB R-07-45, Svensk Kärnbränslehantering AB.

**Stephens M B, Simeonov A, Isaksson H, 2008a.** Bedrock geology Forsmark. Modelling stage 2.3. Implications for and validation of the deterministic geological models based on complementary data. SKB R-08-64, Svensk Kärnbränslehantering AB.

**Stephens M B, Bergman T, Isaksson H, Petersson J 2008b.** Bedrock geology Forsmark. Modelling stage 2.3. Description of the bedrock geological map at the ground surface. SKB R-08-128, Svensk Kärnbränslehantering AB.

**Söderbäck B (ed), 2008.** Geological evolution, palaeoclimate and historical development in the Forsmark and Laxemar-Simpevarp areas. Site descriptive modelling, SDM-Site. SKB R-08-19, Svensk Kärnbränslehantering AB.

**Söderlund P, Hermansson T, Page L M, Stephens M B, 2009.** Biotite and muscovite  $^{40}\text{Ar}$ - $^{39}\text{Ar}$  geochronological constraints on the post-Svecofennian tectonothermal evolution, Forsmark site, central Sweden. *International Journal of Earth Sciences* 98, 1835–1851.

## Specification of available data

<b>Available bedrock geological and geophysical data and their treatment in SFR model stage 0.1</b>			
Data specification	Reference to data report	Reference in Sicada/GIS	Usage in version 0.1 analysis/modelling
<b>Ground geophysical data and lineament interpretation</b>			
High-resolution ground magnetic measurements	/Isaksson et al. 2006a/	AP PF400-05-082	Identification of magnetic lineaments and input for DZ modelling
	/Isaksson et al. 2006b/	AP PF400-06-034	
	/Isaksson et al. 2007/	AP PF400-06-034	
Interpretation of topographic, bathymetric and helicopter-borne geophysical data. Lineament assessment	/Isaksson et al. 2004/	AP PF400-02-047	Identification of magnetic lineaments and input for DZ modelling
	/Isaksson and Keisu 2004/	AP PF400-02-047	
Correlation between refraction seismics, lineaments and DZ's	/Isaksson 2007/		Input to DZ modelling
Reflectors identified during reflection seismic survey	/Balu and Cosma 2005/		Not used in the present model version.
	/Cosma et al. 2006/		
	/Cosma et al. 2003/		
	/Juhlin et al. 2002/	AP PF400-03-84	
	/Juhlin and Bergman 2004/	AP PF400-03-84	
	/Juhlin and Palm 2005/	AP PF400-04-78	
<b>Data from core-drilled boreholes</b>			
Technical data	/Hagkonsult 1981/		Siting and orientation of the boreholes in the modelling work
	/Hagkonsult 1983/		
	/Carlsson et al. 1986/		
	/Keisu and Isaksson 2004/	AP PF400-02-048	
	/Claesson et al. 2007/	AP PF400-06-006	
		AP PF400-06-025	
	/Claesson and Nilsson 2007/	AP PF400-06-027	
Older geological mapping including fracture logging	/Hagkonsult 1983/		Input to DZ modelling
	/Christiansson and Magnusson 1985a/		
	/Christiansson and Magnusson 1985b/		
	/Christiansson 1986/		
Boremap mapping (KFR04, KFR08, KFR09, KFR13, KFR35, KFR36, KFR54, KFR55, KFR7A, KFR7B, KFR7C, KFM11A, HFM34, HFM35)	/Petersson and Andersson 2008/	AP SFR-07-004	Used in geological SHI and as input to DZ modelling
	/Petersson et al. 2007/	AP PF400-06-094	
	/Döse and Samuelsson 2007/	AP PF400-06-115	
Geophysical logging (KFR01, KFR02, KFR03, KFR04, KFR19 and KFR20, KFM11A, HFM34, HFM35)	/Christiansson and Magnusson 1985a/		Data for KFR04 used in updated geological mapping and SHI
	/Christiansson and Magnusson 1985b/		
	/Mattsson and Keisu 2007a/	AP PF400-06-074	
	/Mattsson and Keisu 2007b/	AP PF400-07-018	
	/Nielsen and Ringgaard 2007a/	AP PF400-06-050	
	/Nielsen and Ringgaard 2007b/	AP PF400-06-103	
Geological SHI (KFR04, KFR08, KFR09, KFR13, KFR35, KFR36, KFR54, KFR55, KFR7A, KFR7B, KFR7C, KFM11A, HFM34, HFM35)	/Petersson et al. 2009/	AP SFR-07-005	Input to DZ modelling
	/Carlsten et al. 2007/	AP PF400-07-016	



**Data from tunnel mapping**

Geological tunnel mapping and interpretation of fracture zones /Christiansson and Bolvede 1987/ Input to DZ modelling in proximity to the SFR facility

**Previous models**

SFR structural models /Carlsson et al. 1985/  
/Carlsson et al. 1986/  
/Christiansson 1986/  
/Axelsson and Hansen 1997/ Input to DZ modelling of zones H2, 3, 6, 8 and 9

Forsmark SDM versions and stages 0, 1.1, 1.2, 2.1, 2.2 and 2.3. SDM-Site Forsmark /SKB 2002/  
/SKB 2004/  
/SKB 2005/  
/SKB 2006/  
/Stephens et al. 2007/  
/Stephens et al. 2008a/  
/Stephens et al. 2008b/  
/SKB 2008a/  
/SKB 2008b/ The approved models are stored in the SKB model database Conceptual understanding and comparison

SFR SDM version 0 /SKB 2008b/ Introduction to available data

---

## Previous structural overview mapping of the existing SFR facility

This appendix summarises the brittle structural data from the underground openings of SFR, as presented in a series of drawings by /Christiansson and Bolvede 1987/. The documentation includes two overview drawings (–103 and –104) at the scale 1:2,000 and 23 maps at the scale 1:200 that provide supporting details. There is also a documented methodology for the tunnel mapping work as well as detailed sketches for some of the zones. However, the correlation between the structures represented in the overview mapping and the results presented in the detailed fracture mapping is unclear in some cases.

All the tunnel mapping drawings have been digitally scanned, georeferenced in ArcGis and delivered to the SKB SDE GIS database. The drawings have subsequently been attached to the RVS model. Only the two overview mappings, which have formed a primary input to the modelling work, are included here. A number of different brittle features have been marked on Drawing –103. The classification system applied includes mapped crush zones, brittle shear zones and gouge-filled fractures of varying width, as well as occurrences of closely spaced, parallel fractures and slickensides, though there is no detailed explanation of the legend in the drawing.

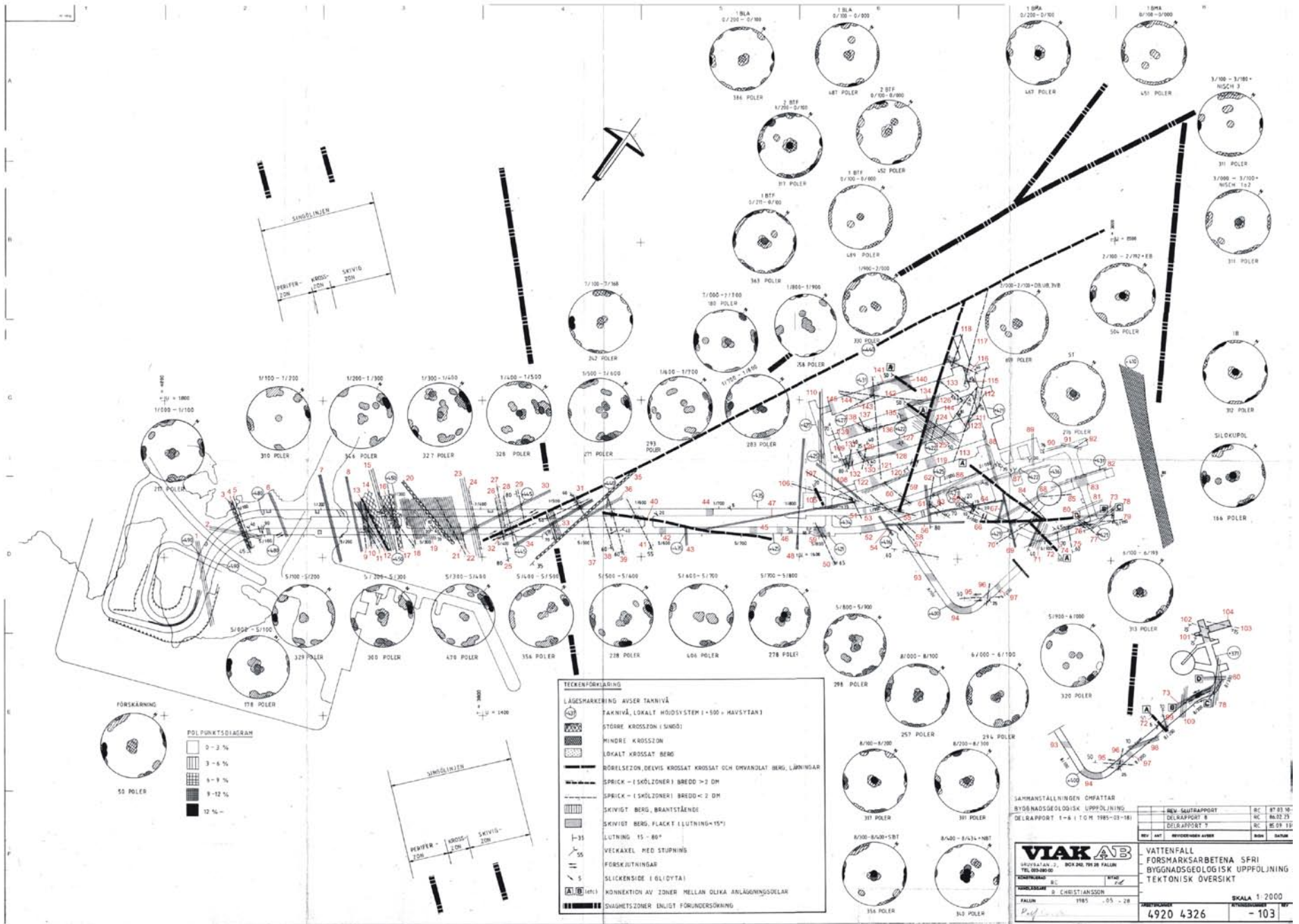
Table A2-1 lists the brittle features marked on Drawing –103, which are judged to be relevant to the scale of the current modelling work. Quantitative information regarding all these features is listed in Table A2-2. Each brittle feature is given an ID that consists of a number accompanied by the abbreviation tDZ (tunnel deformation zone). Numbers are marked in red on Drawing –103. 145 tDZ's have been logged and each is defined by type (cf. Table A2-1), location (facility and chainage) and orientation. The abbreviations used for the various SFR tunnels and caverns are presented in Figure 4-1 that shows a view of SFR from the north-east. In addition, Table A2-2 contains information on whether individual tDZ's were used in the previous structural models for SFR.

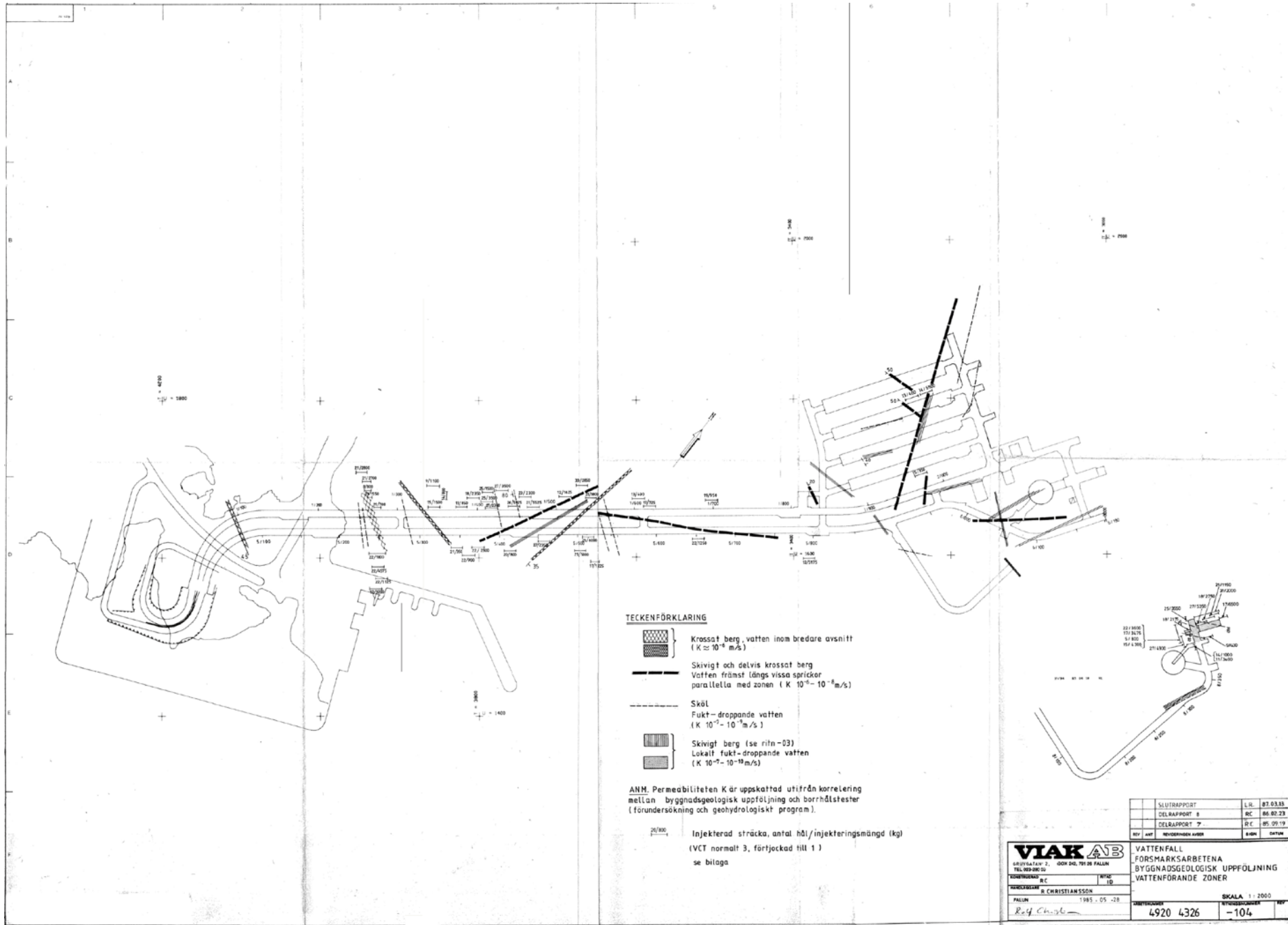
### Contents

Drawing –103	Brittle structures 1:2,000 /Christiansson and Bolvede 1987/
Drawing –104	Water bearing structures, grouting overview 1:2,000 /Christiansson and Bolvede 1987/
Table A2-1.	Abbreviations for brittle structures listed in Table A2-2. Translated from the legend in Drawing –103 of /Christiansson and Bolvede 1987/
Table A2-2.	Tunnel intercepts for the more prominent brittle structures included in Drawing –103 of /Christiansson and Bolvede 1987/

**Table A2-1. Abbreviations for brittle structures listed in Table 2. Translated from legend in overview drawing –103 of /Christiansson and Bolvede 1987/.**

Abbrev.	Structure (english)	Struktur (swedish)
tDZ	Tunnel deformation zone	Tunneldeformationszon
MCZ	Major crush zone (Singö)	Större krosszon (Singö)
mCZ	Minor crush zone	Mindre krosszon
FZ	Brittle shear zone, locally crushed and altered rock, sealings	Rörelsezon, delvis krossat och omvandlat berg, läkningar
GF	Gouge-filled fracture, > 2 dm wide	Sprick – (skölzoner), bredd > 2 dm
gF	Gouge-filled fracture, < 2 dm wide	Sprick – (skölzoner), bredd < 2 dm
SPF	Closely spaced, sub-vertical parallel fractures	Skivigt berg, brantstående
GPF	Closely spaced, gently dipping parallel fractures	Skivigt berg, flackt (lutning < 15°)







**Table A2-2. Tunnel intercepts for the more prominent brittle structures included in drawing –103 of /Christiansson and Bolvede 1987/.**

Zone ID	Zone typ	DT	BT	1 BTF	2 BTF	BLA	BMA	STT	ST	NBT	TT	BST	IB	S	EB	UB	BB	Modelled zone	Orient.
tDZ1	SPF	1+030– 1+044																	296°/90°
tDZ2	SPF	1+065	5+085																050°/90°
tDZ3	gF	S-crete	5+070																120°/90°
tDZ4	mCZ	S-crete	5+076																105°/45°
tDZ5	gF	S-crete	5+072																120°/90°
tDZ6	SPF	1+143	S-crete																118°/90°
tDZ7	SPF	1+212	5+189															Singö zone (ZFMWNW0001)	105°/80°
tDZ8	SPF	1+243	5+220															Singö zone (ZFMWNW0001)	115°/90°
tDZ9	gF	1+255	5+228															Singö zone (ZFMWNW0001)	115°/90°
tDZ10	gF	1+257	5+229															Singö zone (ZFMWNW0001)	115°/90°
tDZ11	gF		5+231															Singö zone (ZFMWNW0001)	110°/90°
tDZ12	gF	1+259	5+234															Singö zone (ZFMWNW0001)	110°/90°
tDZ13	GF	1+260	5+238															Singö zone (ZFMWNW0001)	105°/90°
tDZ14	MCZ (Singö)	1+258– 1+271	5+238– 5+249															Singö zone (ZFMWNW0001)	115°/90°
tDZ15	SPF	1+275	5+248															Singö zone (ZFMWNW0001)	115°/90°
tDZ16	MCZ (Singö)	1+278– 1+295	5+267– 5+283															Singö zone (ZFMWNW0001)	110°/90°
tDZ17	gF	1+291	5+268															Singö zone (ZFMWNW0001)	125°/90°
tDZ18	gF	?	5+280															Singö zone (ZFMWNW0001)	125°/90°
tDZ19	SPF	1+309– 1+372	5+297– 5+347															Singö zone (ZFMWNW0001)	105°/90°
tDZ20	mCZ	1+322	5+302															Singö zone (ZFMWNW0001)	100°/90°
tDZ21	gF	1+355	5+339															Singö zone (ZFMWNW0001)	100°/90°
tDZ22	gF		5+345															Singö zone (ZFMWNW0001)	115°/90°

Zone ID	Zone typ	DT	BT	1 BTF	2 BTF	BLA	BMA	STT	ST	NBT	TT	BST	IB	S	EB	UB	BB	Modelled zone	Orient.
tDZ23	SPF	1+395	5+370																120°/90°
tDZ24	gF	1+389	5+370																120°/90°
tDZ25	gF	1+420	?																130°/90°
tDZ26	SPF	1+422	5+398																120°/90°
tDZ27	gF	1+425																	110°/90°
tDZ28	gF	1+433	5+416																120°/90°
tDZ29	gF	1+449																	115°/80°
tDZ30	SPF	1+430	5+355																25°/80°
tDZ31	FZ	1+475	5+400															Zone 3 (ZFMNNE0869)	Dextral 205°/75°
tDZ32	gF	1+478	5+414																150°/75°
tDZ33	SPF	1+490	5+465																125°/70°
tDZ34	SPF	1+525	5+450																195°/80°
tDZ35	mCZ	1+534	5+484																355°/35°
tDZ36	SPF	1+540																	015°/90°
tDZ37	gF		5+505																110°/90°
tDZ38	gF		5+530																110°/55°
tDZ39	gF	1+564	5+545																110°/55°
tDZ40	FZ	1+535– 1+570 1+610*	5+640– 5+690															Zone 9 (ZFM- NE0870B)	050°/80°
tDZ41	gF	1+594	5+579																100°/55°
tDZ42	GPF		5+600																125°/20°
tDZ43	SPF		5+630																130°/80°
tDZ44	GPF	1+680																	145°/25°
tDZ45	GPF		5+712																130°/50°
tDZ46	GPF		5+750																130°/10°
tDZ47	SPF	1+790	5+690								7+033								210°/85°
tDZ48	SPF	1+800	5+770																135°/85°
tDZ49	GPF		5+785– 5+805																155°/10°
tDZ50	gF		5+795																290°/65°
tDZ51	gF	1+872																	105°/80°
tDZ52	GPF		5+850– 5+872																135°/15°
tDZ53		1+893																	120°/35°

Zone ID	Zone typ	DT	BT	1 BTF	2 BTF	BLA	BMA	STT	ST	NBT	TT	BST	IB	S	EB	UB	BB	Modelled zone	Orient.
tDZ54	SPF		5+880																140°/85°
tDZ55	SPF		5+888– 5+907															Zone 9 (ZFM- NE0870A)	050°/80°
tDZ56	gF	1+906	5+921																070°/90°
tDZ57	gF		5+903							8+000– 8+023									Sinistral 285°/75°
tDZ58	gF	1+914	5+907																100°/90°
tDZ59	FZ	1+930		0+100	0+080	0+060	0+030											Zone 6 (ZFMNNW1209)	Sinistral 165°/90°
tDZ60	gF	1+939																	080°/90°
tDZ61	SPF	1+965	5+942																320°/80°
tDZ62	gF	1+970																	340°/50°
tDZ63	gF		5+951																275°/70°
tDZ64	SPF		5+942– 5+990																035°/90°
tDZ65	gF		5+994																295°/20°
tDZ66	FZ		6+020– 6+050					6+810– 6+820										Zone 9 (ZFM- NE0870A)	235°/75°
tDZ67	SPF		6+040																320°/85°
tDZ68	SPF		6+040												X				015°/90°
tDZ69	SPF		6+060																140°/90°
tDZ70	gF		6+063																020°/70°
tDZ71	SPF		6+093																340°/40°
tDZ72	FZ	2+045	6+095			0+081	0+085	6+823		8+256									135°/55°
tDZ73	SPF		6+095						4+088	8+295– 8+340									020°/90°
tDZ74	gF		6+115																300°/70°
tDZ75	gF		6+129																300°/60°
tDZ76	gF		6+146																225°/80°
tDZ77	gF		6+153																Sinistral 090°/75°
tDZ78	SPF		6+175							8+330– 8+373									135°/90°
tDZ79	gF		6+163																045°/85°
tDZ80	SPF								4+088	8+352								Zone 9 (ZFM- NE0870A)	035°/85°
tDZ81	SPF								4+075										030°/90°
tDZ82	SPF								4+025				X	X					030°/90°

Zone ID	Zone typ	DT	BT	1 BTF	2 BTF	BLA	BMA	STT	ST	NBT	TT	BST	IB	S	EB	UB	BB	Modelled zone	Orient.
tDZ83	GPF													X					215°/05°
tDZ84	gF							6+831											295°/80°
tDZ85	gF														X				220°/85°
tDZ86	SPF	1+985– 2+030																	020°/90°
tDZ87	SPF	2+000– 2+050														X			030°/90°
tDZ88	SPF	2+055										3+040*							315°/85°
tDZ89	SPF	2+110													X				140°/90°
tDZ90	SPF	2+134– 2+160																	030°/85°
tDZ91	SPF	2+160																	235°/80°
tDZ92	gF	2+165– 2+192																	225°/90°
tDZ93	GPF									8+080– 8+090									195°/25°
tDZ94	GPF									8+120– 8+165									060°/40°
tDZ95	gF									8+178									Sinistral 230°/50°
tDZ96	gF									8+183									310°/80°
tDZ97	GPF									8+193– 8+210									090°/05°
tDZ98	SPF									8+222									020°/90°
tDZ99	gF																		
tDZ100	SPF									8+283									125°/90°
tDZ101	gF									X								Zone H2 (ZFM871)	Cf. tDZ60
tDZ102	gF									X							X	Zone H2 (ZFM871)	Cf. tDZ60
tDZ103	gF																X	Zone H2 (ZFM871)	Cf. tDZ60
tDZ104	FZ									8+405– 8+435							X	Zone H2 (ZFM871)	040°/20°
tDZ105	FZ										7+045*								300°/20°
tDZ106	gF										7+051								105°/85°
tDZ107	gF			0+200							7+065								265°/85°
tDZ108	SPF			0+185							7+070								260°/80°
tDZ109	gF					0+015	0+003												120°/70°



Zone ID	Zone typ	DT	BT	1 BTF	2 BTF	BLA	BMA	STT	ST	NBT	TT	BST	IB	S	EB	UB	BB	Modelled zone	Orient.
tDZ110	SPF										7+115– 7+155								320°/85°
tDZ111	gF				0+014														000°/75°
tDZ112	gF										3+086								345°/70°
tDZ113	gF				0+017						3+095								330°/70°
tDZ114	gF										3+104								015°/70°
tDZ115	gF										3+113								240°/65°
tDZ116	gF										3+139								270°/40°
tDZ117	gF										3+139								330°/85°
tDZ118	gF										3+177								330°/80°
tDZ119	GPF			0+070– 0+090															290°/25°
tDZ120	SPF			0+105– 0+165															205°/85°
tDZ121	gF			0+146	0+137	0+129	0+126												320°/80°
tDZ122	GPF			0+135– 0+160															000°/00°
tDZ123	gF			0+035															110°/90°
tDZ124	gF			0+102															165°/90°
tDZ125	SPF				0+044– 0+077	0+083													105°/50°
tDZ126	SPF				0+078	0+055												Zone 6 (ZFMNNW1209)	165°/90°
tDZ127	GPF				0+118														130°/35°
tDZ128	SPF				0+127– 0+157														025°/90°
tDZ129	gF				0+154														330°/50°
tDZ130	gF				0+162														280°/45°
tDZ131	gF				0+175														280°/40°
tDZ132	GPF				0+170– 0+190														000°/00°
tDZ133	gF					0+024													100°/50°
tDZ134	SPF					0+052– 0+062													035°/90°
tDZ135	GPF					0+100– 0+115													080°/40°
tDZ136	gF					0+134													220°/80°

Zone ID	Zone typ	DT	BT	1 BTF	2 BTF	BLA	BMA	STT	ST	NBT	TT	BST	IB	S	EB	UB	BB	Modelled zone	Orient.
tDZ137	gF					0+148													070°/90°
tDZ138	gF					0+149													120°/40°
tDZ139	GPF					0+150– 0+170													000°/00°
tDZ140	SPF						0+075– 0+105												035°/80°
tDZ141	GPF						0+075– 0+105												000°/00°
tDZ142	gF						0+128												240°/80°
tDZ143	gF						0+132												075°/90°
tDZ144	gF						0+146												105°/90°
tDZ145	GPF						0+170– 0+185												000°/00°

\* In connecting facility part without notation.

## Technical borehole data


Table A2-1. Technical borehole data (Coordinate system RT90-RHB70).

BH ID	Old ID	Length (m)	Northing (m)	Easting (m)	Inclination (°)	Bearing (°)
HFM34	n/a	200.75	6,701,325.06	1,632,470.21	-58.59	30.50
HFM35	n/a	200.75	6,701,555.86	1,632,320.51	-59.27	32.96
KFM11A	n/a	851.21	6,701,103.82	1,632,366.75	-60.94	40.25
KFR01	HK1	62.30	6,701,434.83	1,632,453.42	-60.00	230.50
KFR02	HK2	116.80	6,701,770.05	1,632,887.78	-90.00	0.00
KFR03	HK3	101.60	6,701,908.96	1,632,997.74	-90.00	0.00
KFR04	HK4	100.50	6,701,946.04	1,633,055.96	-75.00	98.20
KFR05	HK5	131.40	6,701,946.04	1,633,056.58	-70.00	9.10
KFR06	HK6	39.00	6,701,961.50	1,633,059.01	-63.00	315.60
KFR08	HK8	104.40	6,702,071.23	1,633,066.45	-5.00	56.40
KFR09	HK9	80.24	6,701,881.83	1,632,755.38	-5.00	299.90
KFR10	HK10	107.28	6,701,882.58	1,632,755.89	-45.00	302.50
KFR11	HK11	98.07	6,702,046.91	1,633,110.05	-10.00	72.51
KFR12	HK12	50.26	6,702,057.64	1,632,899.87	-90.00	0.00
KFR13	HK13	76.60	6,701,910.29	1,633,092.89	-90.00	0.00
KFR14	HK14	29.10	6,702,010.36	1,633,031.74	-45.00	135.10
KFR19	KB19	110.17	6,701,908.32	1,633,000.46	13.80	38.20
KFR20	KB20	109.70	6,701,909.55	1,632,998.33	10.44	56.40
KFR21	KB1	250.80	6,702,093.30	1,633,037.21	-90.00	230.51
KFR22	KB2	160.10	6,702,087.50	1,633,033.17	-60.00	213.01
KFR23	KB3	160.20	6,702,184.17	1,632,993.04	-60.00	257.01
KFR24	KB4	159.20	6,702,062.95	1,633,083.74	-57.00	51.51
KFR25	KB5	196.50	6,702,065.30	1,633,077.79	-46.00	0.01
KFR27	KB7	146.50	6,701,714.42	1,633,175.52	-87.60	248.20
KFR31	KB11	242.10	6,701,959.66	1,632,915.47	-43.20	82.11
KFR32	KB12	209.70	6,701,956.59	1,632,915.67	-46.50	24.91
KFR33	KB13	167.00	6,701,958.73	1,632,912.61	-43.80	302.51
KFR34	KB14	142.00	6,701,923.75	1,632,794.20	-49.00	198.11
KFR35	KB15	140.20	6,701,956.28	1,632,915.93	-51.50	208.11
KFR36	KB16	123.90	6,701,922.23	1,632,792.99	-46.00	291.71
KFR37	KB17	204.90	6,702,050.31	1,633,033.49	-62.50	188.51
KFR38	KB18	185.40	6,702,048.62	1,633,035.53	-57.60	92.21
KFR51	KB21	46.85	6,701,898.12	1,632,963.47	35.00	358.76
KFR52	KB22	29.95	6,701,963.94	1,633,066.31	10.00	230.51
KFR53	KB23	40.60	6,701,947.78	1,633,100.54	-27.40	312.64
KFR54	KB24	53.30	6,701,949.71	1,633,102.00	-47.70	309.97
KFR55	KB25	61.89	6,701,930.05	1,633,094.49	-11.00	328.98
KFR56	KB26	81.73	6,702,069.46	1,633,067.51	26.00	87.94
KFR57	KB27	25.38	6,702,050.77	1,632,854.91	-90.00	230.51
KFR61	DS1	70.90	6,701,382.45	1,632,391.99	-44.00	38.41
KFR62	DS2	82.80	6,701,368.43	1,632,401.86	-45.00	42.91
KFR63	DS3	15.08	6,701,226.87	1,632,315.81	-90.00	230.51
KFR64	DS4	41.38	6,701,406.16	1,632,407.71	-60.00	33.91
KFR65	DS5	28.95	6,701,403.62	1,632,406.04	-90.00	230.51
KFR66	DS6	14.18	6,701,420.17	1,632,417.16	-90.00	230.51
KFR67	DS7	35.21	6,701,419.85	1,632,419.75	-65.00	34.61
KFR68	DS8	116.70	6,701,552.67	1,632,530.76	-45.00	82.01
KFR69	DS9	201.20	6,701,713.56	1,632,783.24	-45.40	14.51
KFR70	DS10	172.50	6,701,712.85	1,632,823.74	-51.30	61.81
KFR71	DS101	120.90	6,701,367.83	1,632,363.08	2.00	283.51
KFR72	DS102	100.53	n/a	n/a	n/a	n/a
KFR7A	HK7A	74.70	6,702,020.20	1,633,107.36	-2.00	20.80
KFR7B	HK7B	21.10	6,702,017.62	1,633,109.54	-75.00	11.50
KFR7C	HK7C	34.00	6,701,999.29	1,633,100.63	-70.00	196.00
KFR80	INJ	20.00	6,702,028.08	1,633,056.22	-70.00	196.04
KFR83	SH3	20.00	6,702,061.20	1,632,857.98	-35.00	32.51
KFR84	BT 5/241	29.50	6,701,409.24	1,632,432.52	25.00	308.81
KFR85	BT 5/247 1	12.20	6,701,406.24	1,632,443.03	-5.00	115.31
KFR86	BT 5/247 2	14.70	6,701,406.94	1,632,443.09	-90.00	230.51
KFR87	NBT 1	15.10	6,702,035.75	1,633,042.79	-5.00	212.50
KFR88	NBT 2	30.00	6,702,058.78	1,633,063.72	20.00	338.50
KFR89	SFR1/177	17.00	n/a	n/a	n/a	n/a
n/a	SFR(Silo1)	45.12	n/a	n/a	n/a	n/a









### **WellCad logs from the geological single-hole interpretation of remapped drill cores**

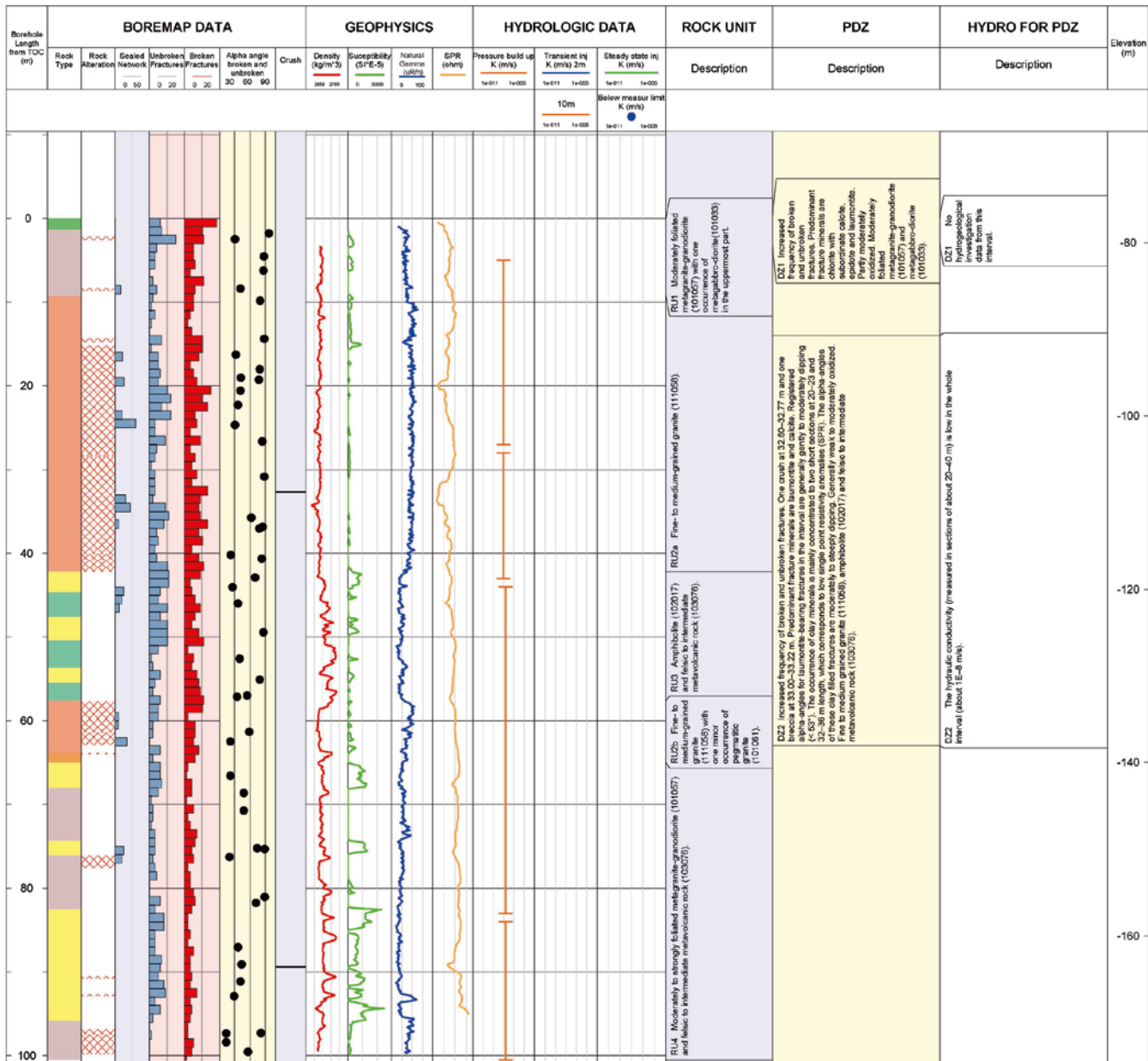
WellCad logs included in this appendix are reproduced from /Petersson et al. 2009/ and summarize the results from the geological SHI of eleven boreholes selected for renewed mapping following the Boremap system /Petersson and Andersson 2008/. The boreholes included are: KFR04, KFR08, KFR09, KFR13, KFR35, KFR36, KFR54, KFR55, KFR7A, KFR7B and KFR7C.



<b>Title</b> GEOLOGY KFR04		<b>Site</b> FORSMARK - SFR		<b>Coordinate System</b> RT90-RHB70	
	<b>Borehole</b>	KFR04	<b>Northing [m]</b>	6701946.04	
	<b>Diameter [mm]</b>	56	<b>Easting [m]</b>	1633055.96	
	<b>Length [m]</b>	100.500	<b>Elevation [m]</b>	-77.18	
	<b>Activity Type</b>	GE038	<b>Bearing [°]</b>	98.20	
	<b>Date of mapping</b>	2007-10-04 09:34:00	<b>Inclination [°]</b>	-74.99	

<b>ROCK TYPE</b>			<b>ROCK ALTERATION</b>		
	Granite, fine- to medium-grained				
	Pegmatite, pegmatitic granite				
	Granite to granodiorite, metamorphic, medium-grained				
	Diorite, quartz diorite and gabbro, metamorphic				
	Amphibolite				
	Felsic to intermediate volcanic rock, metamorphic				



**Title** GEOLOGY KFR08



Site FORSMARK - SFR  
 Borehole KFR08  
 Diameter [mm] 56  
 Length [m] 104.400  
 Activity Type GE038  
 Date of mapping 2007-10-04 09:34:00

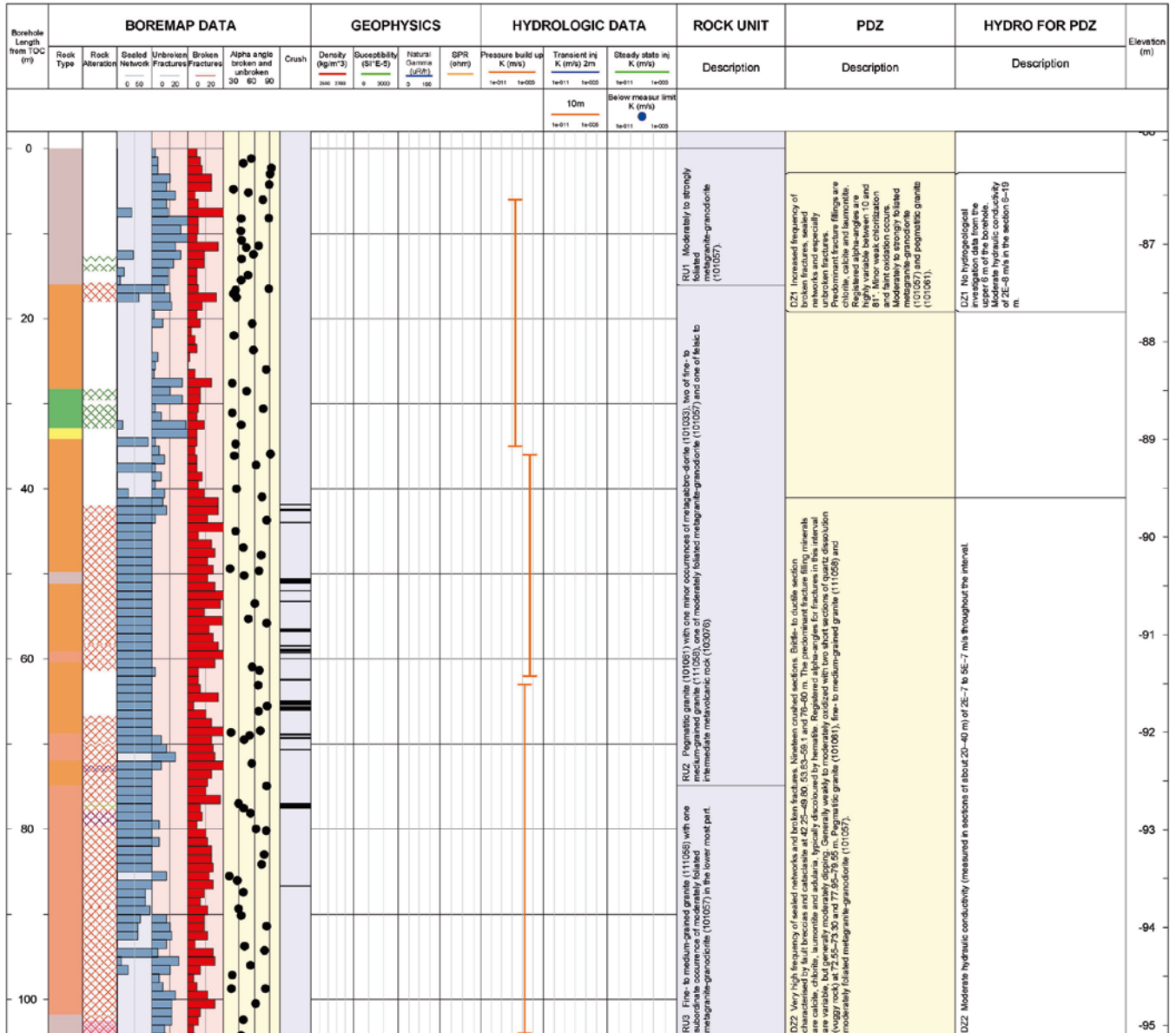
Coordinate System RT90-RHB70  
 Northing [m] 6702071.23  
 Easting [m] 1633066.45  
 Elevation [m] -86.01  
 Bearing [°] 56.40  
 Inclination [°] -4.99


**ROCK TYPE**

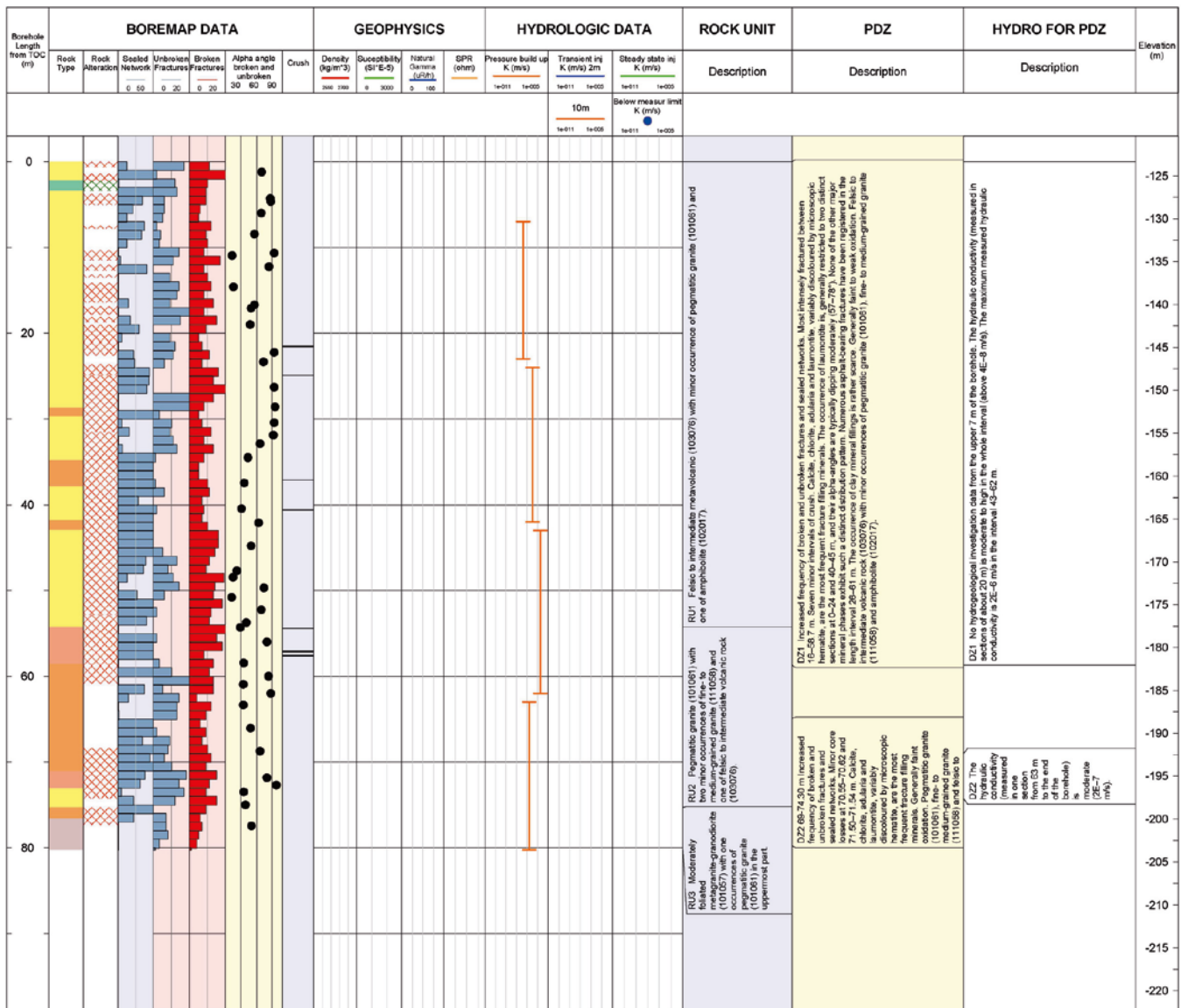
- Granite, fine- to medium-grained
- Pegmatite, pegmatitic granite
- Granite to granodiorite, metamorphic, medium-grained
- Diorite, quartz diorite and gabbro, metamorphic
- Felsic to intermediate volcanic rock, metamorphic

**ROCK ALTERATION**

- Oxidized
- Chloritized
- Epidotized
- Quartz dissolution
- Albitization
- Laumontization



<b>Title</b> GEOLOGY KFR09																
	<b>Site</b>	FORSMARK - SFR	<b>Coordinate System</b>	RT90-RHB70												
	<b>Borehole</b>	KFR09	<b>Northing [m]</b>	6701881.84												
	<b>Diameter [mm]</b>	56	<b>Easting [m]</b>	1632755.38												
	<b>Length [m]</b>	80.240	<b>Elevation [m]</b>	-77.43												
	<b>Activity Type</b>	GE038	<b>Bearing [°]</b>	299.90												
	<b>Date of mapping</b>	2007-10-04 09:34:00	<b>Inclination [°]</b>	-4.99												
<table border="0"> <tr> <td><b>ROCK TYPE</b></td> <td><b>ROCK ALTERATION</b></td> </tr> <tr> <td> Granite, fine- to medium-grained</td> <td> Oxidized</td> </tr> <tr> <td> Pegmatite, pegmatitic granite</td> <td> Chloritized</td> </tr> <tr> <td> Granite to granodiorite, metamorphic, medium-grained</td> <td></td> </tr> <tr> <td> Amphibolite</td> <td></td> </tr> <tr> <td> Felsic to intermediate volcanic rock, metamorphic</td> <td></td> </tr> </table>					<b>ROCK TYPE</b>	<b>ROCK ALTERATION</b>	Granite, fine- to medium-grained	Oxidized	Pegmatite, pegmatitic granite	Chloritized	Granite to granodiorite, metamorphic, medium-grained		Amphibolite		Felsic to intermediate volcanic rock, metamorphic	
<b>ROCK TYPE</b>	<b>ROCK ALTERATION</b>															
Granite, fine- to medium-grained	Oxidized															
Pegmatite, pegmatitic granite	Chloritized															
Granite to granodiorite, metamorphic, medium-grained																
Amphibolite																
Felsic to intermediate volcanic rock, metamorphic																







**Title** GEOLOGY KFR35



**Site** FORSMARK - SFR  
**Borehole** KFR35  
**Diameter [mm]** 56  
**Length [m]** 140.200  
**Activity Type** GE038  
**Date of mapping** 2007-10-04 09:34:00

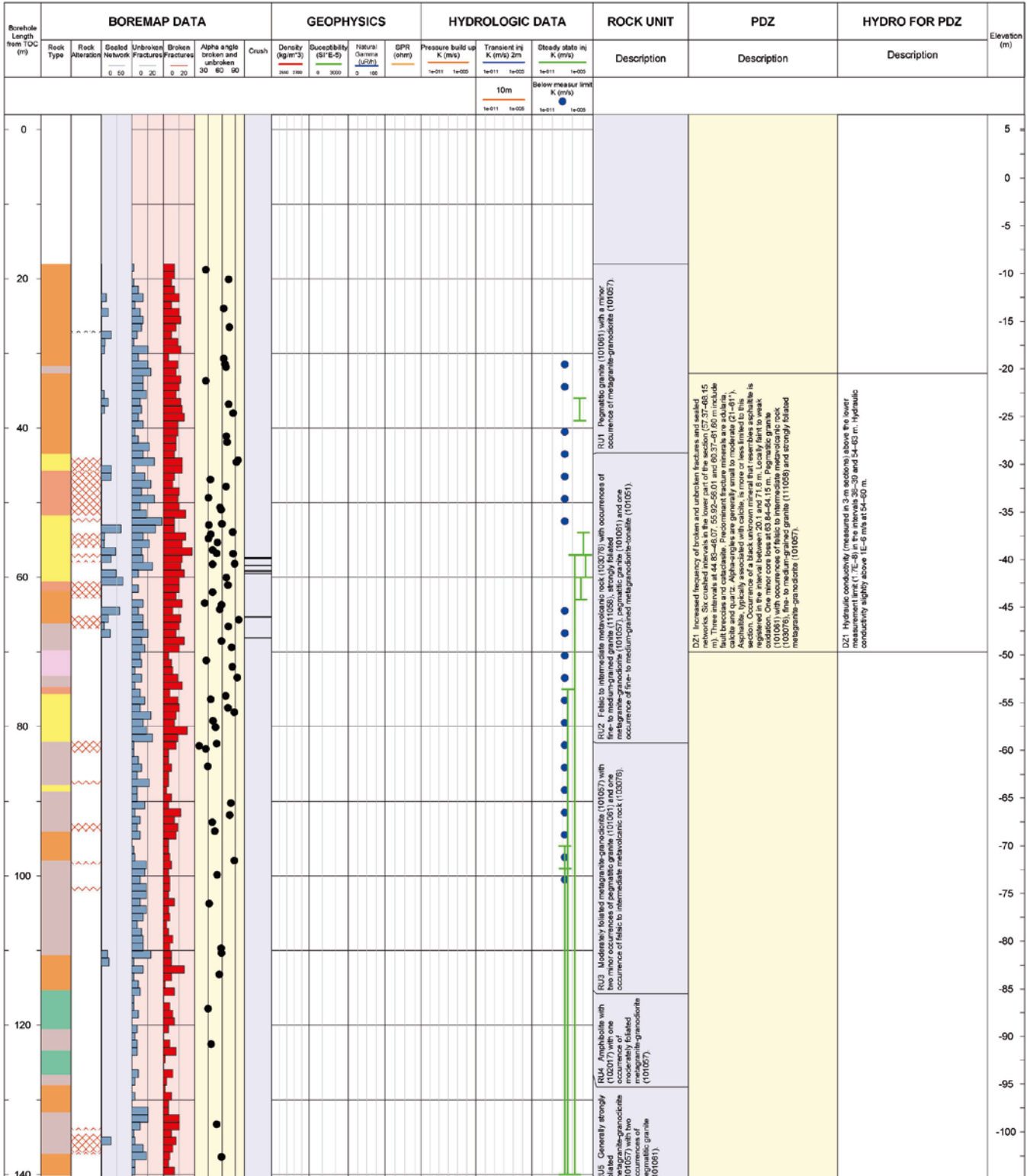
**Coordinate System** RT90-RHB70  
**Northing [m]** 6701956.28  
**Easting [m]** 1632915.93  
**Elevation [m]** 5.10  
**Bearing [°]** 208.11  
**Inclination [°]** -51.49

**ROCK TYPE**

- Granite, fine- to medium-grained
- Pegmatite, pegmatitic granite
- Granite, granodiorite and tonalite, metamorphic, fine- to medium-grained
- Granite to granodiorite, metamorphic, medium-grained
- Amphibolite
- Felsic to intermediate volcanic rock, metamorphic

**ROCK ALTERATION**

- Oxidized
- Carbonatization



**Title** GEOLOGY KFR36



Site FORSMARK - SFR  
 Borehole KFR36  
 Diameter [mm] 56  
 Length [m] 123.900  
 Activity Type GE038  
 Date of mapping 2007-10-04 09:34:00

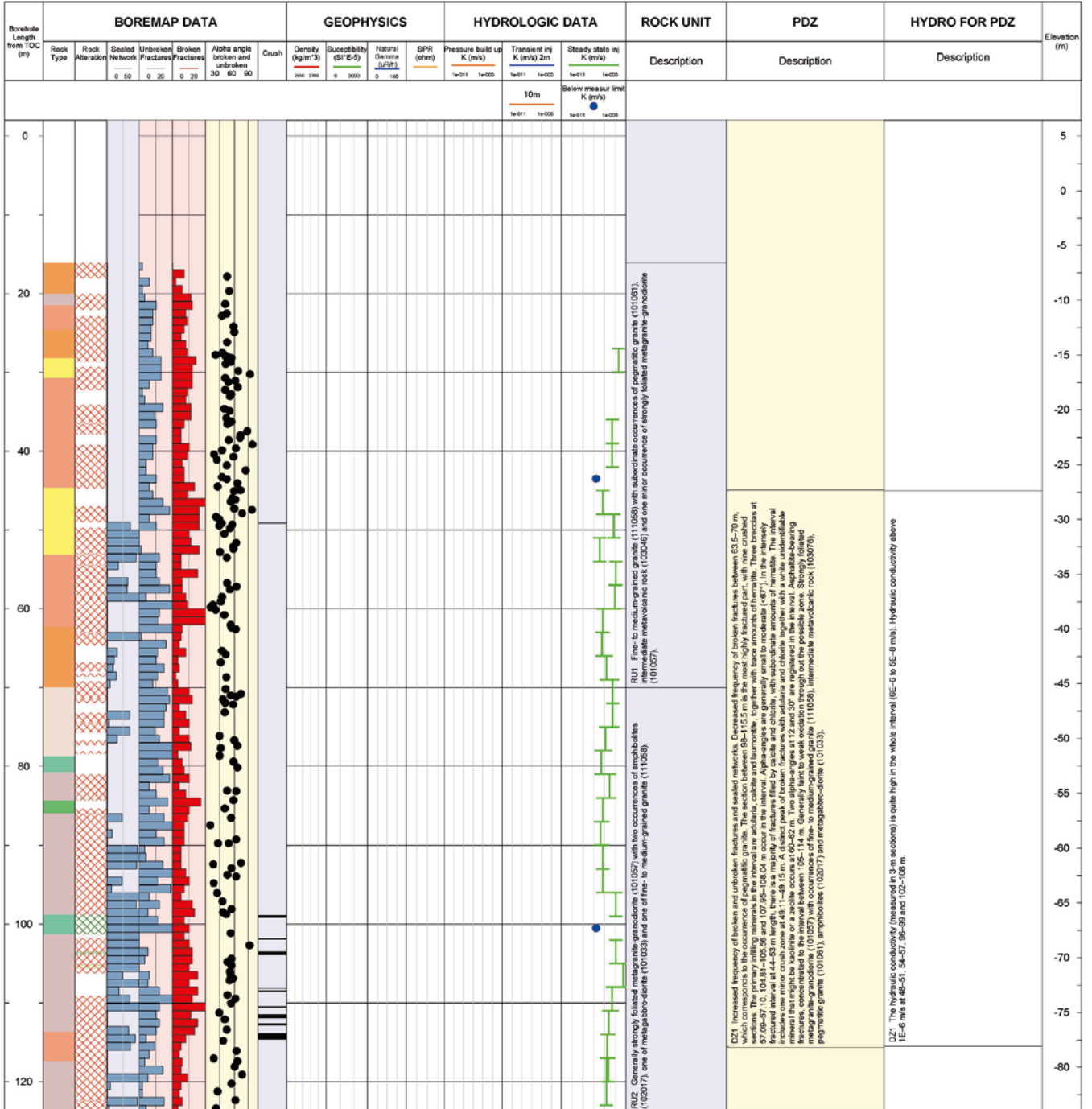
Coordinate System RT90-RHB70  
 Northing [m] 6701922.23  
 Easting [m] 1632792.99  
 Elevation [m] 5.00  
 Bearing [°] 291.71  
 Inclination [°] -45.99

**ROCK TYPE**

- Granite, fine- to medium-grained
- Pegmatite, pegmatitic granite
- Granite, metamorphic, aplitic
- Granite to granodiorite, metamorphic, medium-grained
- Diorite, quartz diorite and gabbro, metamorphic
- Amphibolite
- Felsic to intermediate volcanic rock, metamorphic

**ROCK ALTERATION**

- Oxidized
- Chloritized
- Epidotized
- Steatitization
- Laumontization



Title **GEOLOGY KFR54**



Site FORSMARK - SFR  
 Borehole KFR54  
 Diameter [mm] 56  
 Length [m] 53.300  
 Activity Type GE038  
 Date of mapping 2007-10-04 09:34:00

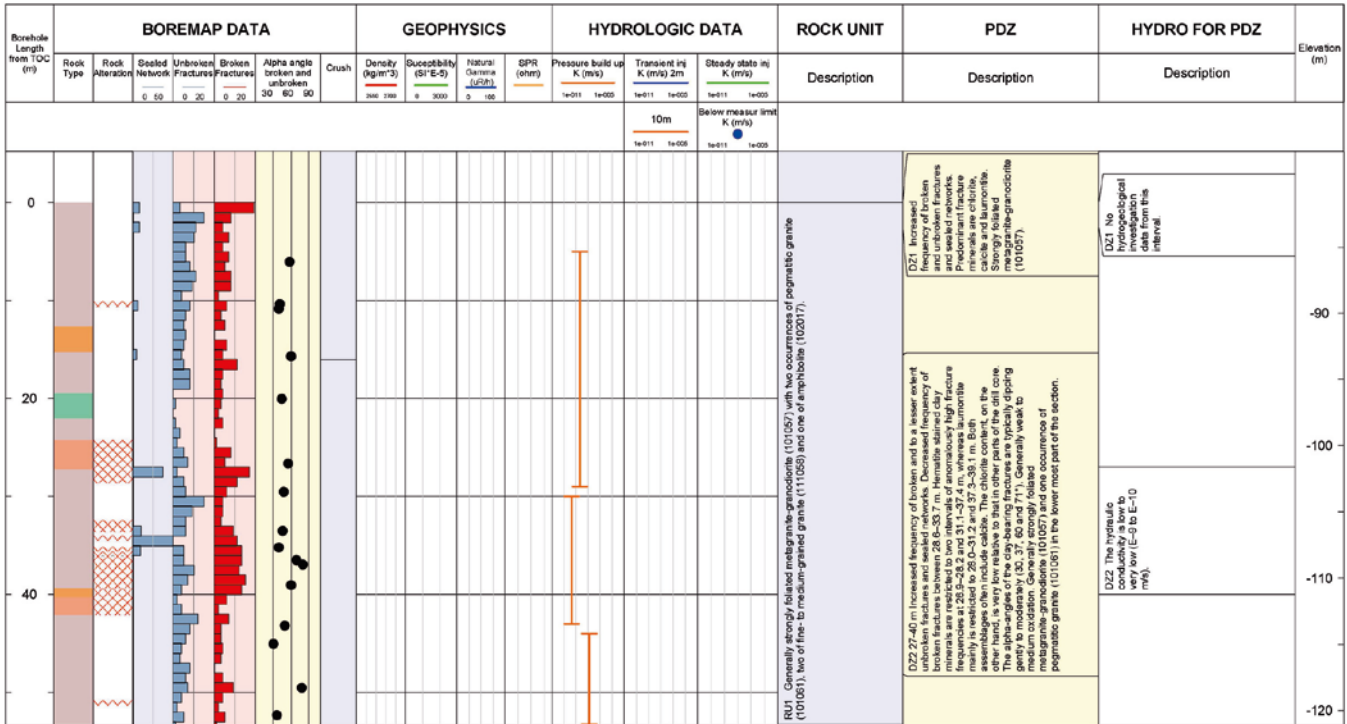
Coordinate System RT90-RHB70  
 Northing [m] 6701949.71  
 Easting [m] 1633102.00  
 Elevation [m] -81.64  
 Bearing [°] 309.97  
 Inclination [°] -47.69






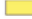




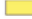




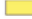
ROCK TYPE

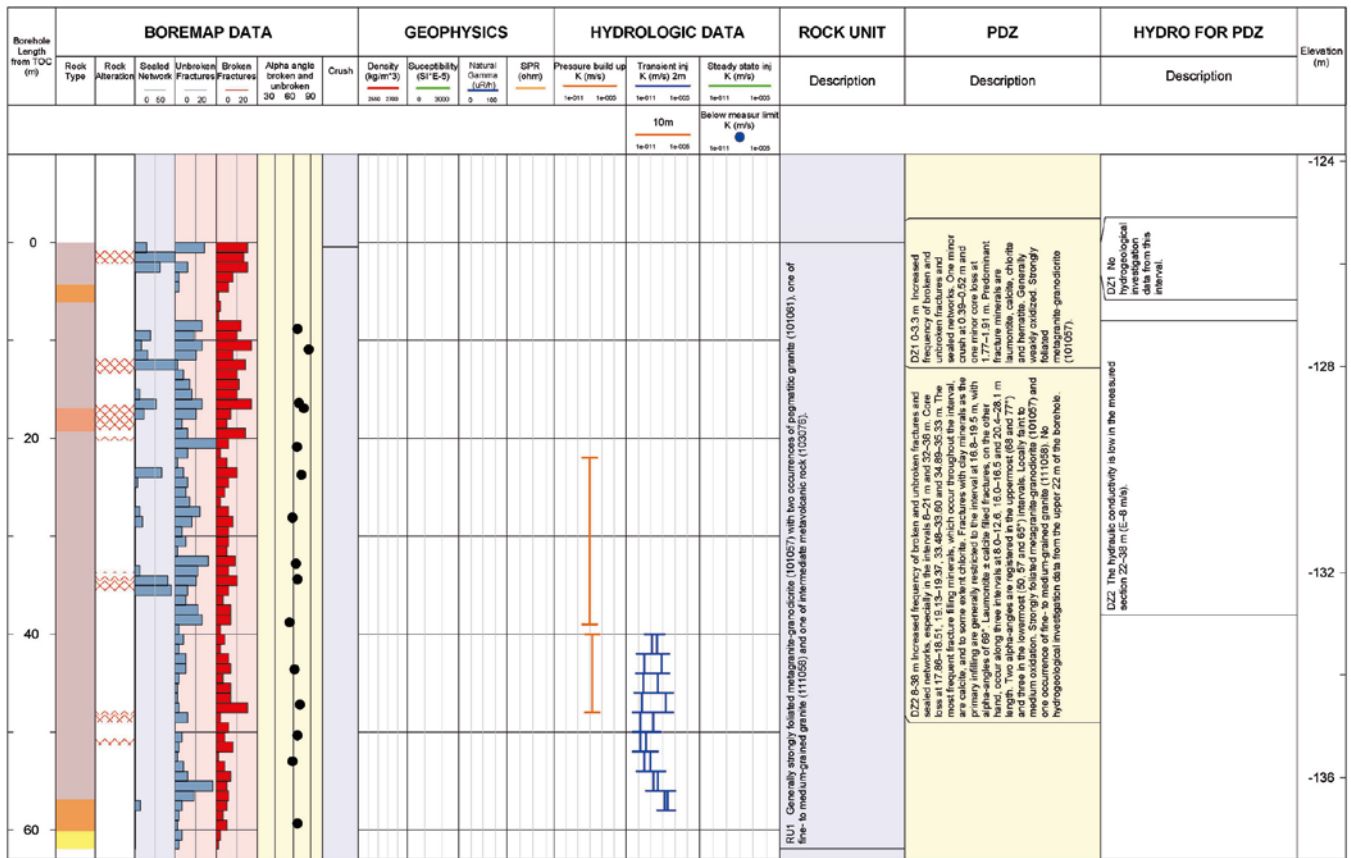
- Granite, fine- to medium-grained
- Pegmatite, pegmatitic granite
- Granite to granodiorite, metamorphic, medium-grained
- Amphibolite

ROCK ALTERATION


- Oxidized
- Argillization












<b>Title</b> <b>GEOLOGY KFR55</b>																								
	<b>Site</b>	FORSMARK - SFR	<b>Coordinate System</b>	RT90-RHB70																				
	<b>Borehole</b>	KFR55	<b>Northing [m]</b>	6701930.05																				
	<b>Diameter [mm]</b>	56	<b>Easting [m]</b>	1633094.49																				
	<b>Length [m]</b>	61.890	<b>Elevation [m]</b>	-125.57																				
	<b>Activity Type</b>	GE038	<b>Bearing [°]</b>	328.98																				
<b>Date of mapping</b>	2007-10-04 09:34:00	<b>Inclination [°]</b>	-10.99																					
<table border="0"> <tr> <td><b>ROCK TYPE</b></td> <td></td> <td><b>ROCK ALTERATION</b></td> <td></td> </tr> <tr> <td> Granite, fine- to medium-grained</td> <td></td> <td> Oxidized</td> <td></td> </tr> <tr> <td> Pegmatite, pegmatitic granite</td> <td></td> <td></td> <td></td> </tr> <tr> <td> Granite to granodiorite, metamorphic, medium-grained</td> <td></td> <td></td> <td></td> </tr> <tr> <td> Felsic to intermediate volcanic rock, metamorphic</td> <td></td> <td></td> <td></td> </tr> </table>					<b>ROCK TYPE</b>		<b>ROCK ALTERATION</b>		 Granite, fine- to medium-grained		 Oxidized		 Pegmatite, pegmatitic granite				 Granite to granodiorite, metamorphic, medium-grained				 Felsic to intermediate volcanic rock, metamorphic			
<b>ROCK TYPE</b>		<b>ROCK ALTERATION</b>																						
 Granite, fine- to medium-grained		 Oxidized																						
 Pegmatite, pegmatitic granite																								
 Granite to granodiorite, metamorphic, medium-grained																								
 Felsic to intermediate volcanic rock, metamorphic																								





<b>Title</b> GEOLOGY KFR7A				
	<b>Site</b>	FORSMARK - SFR	<b>Coordinate System</b>	RT90-RHB70
	<b>Borehole</b>	KFR7A	<b>Northing [m]</b>	6702020.20
	<b>Diameter [mm]</b>	56	<b>Easting [m]</b>	1633107.36
	<b>Length [m]</b>	74.700	<b>Elevation [m]</b>	-132.28
	<b>Activity Type</b>	GE038	<b>Bearing [°]</b>	20.80
	<b>Date of mapping</b>	2007-10-04 09:34:00	<b>Inclination [°]</b>	-1.99

<b>ROCK TYPE</b>		<b>ROCK ALTERATION</b>	
	Granite, fine- to medium-grained		Oxidized
	Pegmatite, pegmatitic granite		Epidotized
	Granite, metamorphic, aplitic		Argillization
	Granite to granodiorite, metamorphic, medium-grained		Albitization
	Amphibolite		

Borehole Length from TOC (m)	BOREMAP DATA						GEOPHYSICS				HYDROLOGIC DATA			ROCK UNIT	PDZ	HYDRO FOR PDZ	Elevation (m)
	Rock Type	Rock Alteration	Sealed Network	Unbroken Fractures	Broken Fractures	Alpha angle broken and unbroken	Density (g/cm <sup>3</sup> )	Susceptibility (SI-E-2)	Natural Gamma (uR/h)	SPR (ppm)	Pressure build up K (m/s)	Transient inj K (m/s) 2m	Steady state inj K (m/s)	Description	Description	Description	
0			0.50	0.20	0.20	30 60 90	2400 2500	8 3000	0 100		1e-011 1e-005	1e-011 1e-002	1e-011 1e-005				-132.5
20																	-133.0
40																	-133.5
60																	-134.0
																	-134.5


  

<p><b>RU1</b> Moderately to moderately altered megacrystic-granodiorite (101057).</p>	<p><b>RU2</b> Pegmatitic granite (101061) and aplitic megacrystic (101053).</p>	<p><b>RU3</b> Moderately to strongly foliated megacrystic-granodiorite (101057), one of pegmatitic granite (101061) and one of amphibolite (102017).</p>	<p><b>DZ1</b> Increased frequency of subvertical fractures, sealed networks and especially linked fractures. Nineteen cracks with the most extensive sections at 49.00–74.45 m. Brittle-ductile section characterized by fault breccias and calcite at 21–24 m and 64.85–71.26 m. Predominant fracture minerals are clay minerals, calcite and Fe-hydroxide/hematite. The registered alpha-angles of clay filled fractures are highly variable, ranging from 0 to 85°. Fractures filled with baronite form screens throughout the drill core with the most extensive occurrence at 26.5–48.8 m length. Most of these fractures are sealed with calcite. The most extensive occurrence of amphibolite is at 49.00–74.45 m. The most extensive occurrence of amphibolite is at 49.00–74.45 m.</p>
---	---	--	---

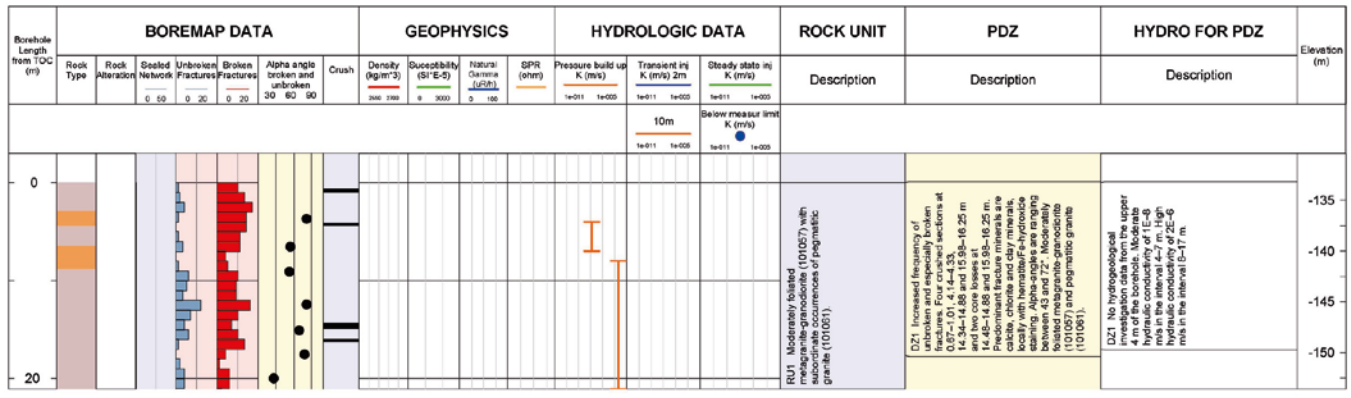
  

<p><b>DZ1</b> Low hydraulic conductivity 6E–9 m/s in the interval 3.5–19 m. Moderate hydraulic conductivity of 5E–7 m/s in the interval 20–47 m. High hydraulic conductivity of 3E–6 m/s in the interval 48–74.45 m.</p>
--

**Title** GEOLOGY KFR7B

	<b>Site</b>	FORSMARK - SFR	<b>Coordinate System</b>	RT90-RHB70
	<b>Borehole</b>	KFR7B	<b>Northing [m]</b>	6702017.62
	<b>Diameter [mm]</b>	56	<b>Easting [m]</b>	1633109.54
	<b>Length [m]</b>	21.100	<b>Elevation [m]</b>	-133.24
	<b>Activity Type</b>	GE038	<b>Bearing [°]</b>	11.50
	<b>Date of mapping</b>	2007-10-04 09:34:00	<b>Inclination [°]</b>	-74.99

<b>ROCK TYPE</b>	<b>ROCK ALTERATION</b>
 Pegmatite, pegmatitic granite  Granite to granodiorite, metamorphic, medium-grained	



**Title** GEOLOGY KFR7C



**Site** FORSMARK - SFR  
**Borehole** KFR7C  
**Diameter [mm]** 56  
**Length [m]** 34.000  
**Activity Type** GE038  
**Date of mapping** 2007-10-04 09:34:00

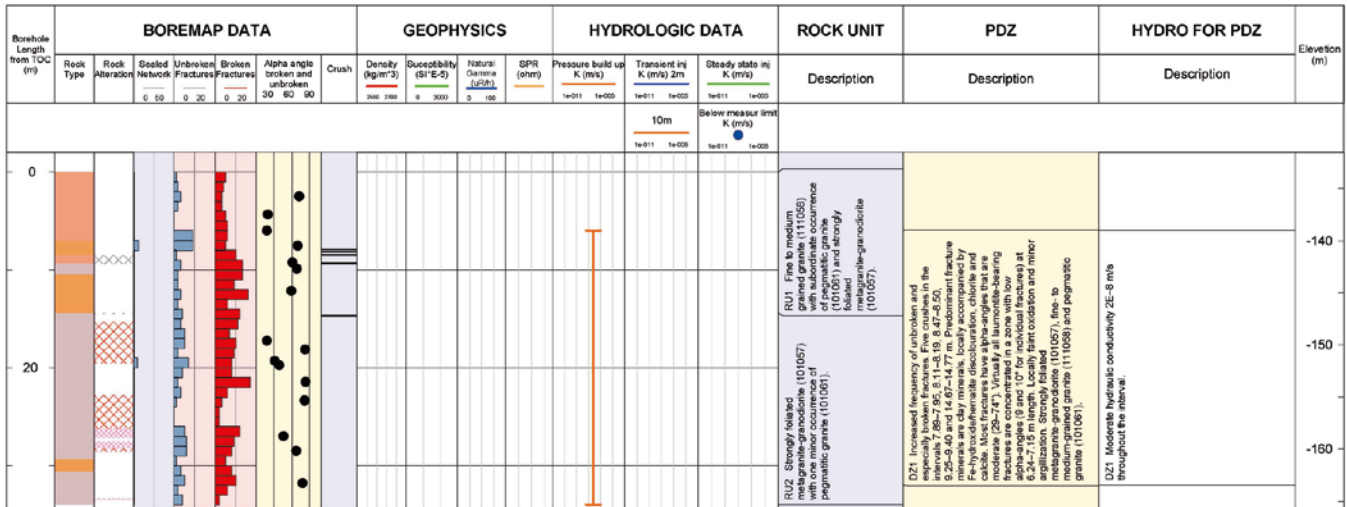
**Coordinate System** RT90-RHB70  
**Northing [m]** 6701999.29  
**Easting [m]** 1633100.63  
**Elevation [m]** -133.39  
**Bearing [°]** 196.00  
**Inclination [°]** -69.99

**ROCK TYPE**

- Granite, fine- to medium-grained
- Pegmatite, pegmatitic granite
- Granite to granodiorite, metamorphic, medium-grained

**ROCK ALTERATION**

- Oxidized
- Argillization
- Albization



## Lineaments SFR model version 0.1

## Contents

Table A5-1.	Name of each lineament and the relation to lineaments interpreted during the Forsmark site investigation.
Table A5-2.	Lineaments from the Forsmark site investigation not included in the SFR model version 0.1.
Table A5-3	Attribute table for the lineaments in SFR version 0.1. The table is based on Table 4-2 in /Isaksson et al. 2007/.

**Table A5-1. Name of each lineament and the relation to lineaments interpreted during the Forsmark site investigation.**

Lineament name in the Forsmark site investigation that wholly or partly is connected to a lineament in SFR v. 0.1	Name of lineament in SFR model version 0.1	Comment
MFM3264G	MSFR08001	As MFM3264G, but slightly changed at S
MFM3265G	MSFR08002	MFM3265G has been divided into 3 discontinuous pieces, MSFR08002 – MSFR08004, with deviating paths as compared to the original
MFM3265G	MSFR08003	MFM3265G has been divided into 3 discontinuous pieces, MSFR08002 – MSFR08004, with deviating paths as compared to the original
MFM3265G	MSFR08004	MFM3265G has been divided into 3 discontinuous pieces, MSFR08002 – MSFR08004, with deviating paths as compared to the original
MFM3151G	MSFR08005	MFM3151G has been changed in length and running route
–	MSFR08006	New
MFM0836G	MSFR08007	As MFM0836G but slightly shortened at west and with slightly deviating running
MFM3153G	MSFR08008	MFM3153G changed at south-west
MFM3266G	MSFR08009	MFM3266G slightly shortened at south
–	MSFR08010	New
MFM3152G	MSFR08011	MFM3152G changed at west
MFM3154G	MSFR08012	MFM3154G, divided into three (MSFR08012–MSFR08014) discontinuous pieces with changed running routes
MFM3154G	MSFR08013	MFM3154G, divided into three (MSFR08012–MSFR08014) discontinuous pieces with changed running routes
MFM3154G	MSFR08014	MFM3154G, divided into three (MSFR08012–MSFR08014) discontinuous pieces with changed running routes
MFM3150G, MFM3154G	MSFR08015	coincides partly with MFM3150G and partly also with MFM3154G
–	MSFR08016	New
–	MSFR08017	New
–	MSFR08018	New
–	MSFR08019	New
–	MSFR08020	New
–	MSFR08021	New
–	MSFR08022	New, but part of the complex tectonic structure which is a result of the interplay between MFM0805G0 and MFM0805G1



Lineament name in the Forsmark site investigation that wholly or partly is connected to a lineament in SFR v. 0.1	Name of lineament in SFR model version 0.1	Comment
–	MSFR08023	New
–	MSFR08024	New, possibly a dislocated southern continuation of MFM0999G
–	MSFR08025	New
–	MSFR08026	New, but possibly part of the complex tectonic structure which is a result of the interplay between MFM0805G0 and MFM0805G1
–	MSFR08027	New
–	MSFR08028	New
–	MSFR08029	New
–	MSFR08030	New
–	MSFR08031	New
–	MSFR08032	New
–	MSFR08033	New, but possibly part of the complex tectonic structure which is a result of the interplay between MFM0805G0 and MFM0805G1
–	MSFR08034	New
–	MSFR08035	New
–	MSFR08036	New
–	MSFR08037	New
–	MSFR08038	New
–	MSFR08039	New
–	MSFR08040	New
–	MSFR08041	New
–	MSFR08042	New
–	MSFR08043	New
–	MSFR08044	New
–	MSFR08045	New
–	MSFR08046	New
–	MSFR08047	New
MFM3268G	MSFR08048	Partly coinciding with MFM3268, deviating at north-west.
MFM1056G	MFM1056G	As original MFM1056G
MFM3133G	MFM3133G	As original MFM3133G
MFM3108G	MFM3108G	As original MFM3108G
MFM2296G	MFM2296G	As original MFM2296G
MFM0725G	MFM0725G	As original MFM0725G
MFM0812	MFM0812	As original MFM0812
MFM2317G	MFM2317G	As original MFM2317G
MFM1201G	MFM1201G	As original MFM1201G
MFM0813G	MFM0813G	As original MFM0813G
MFM0803G0	MFM0803G0	As original MFM0803G0
MFM2496G	MSFR08059	MFM2496G is divided into two discontinuous parts (MSFR08059, MSFR08060) with slightly changed running
MFM2496G	MSFR08060	MFM2496G is divided into two discontinuous parts (MSFR08059, MSFR08060 ) with slightly changed running
MFM3261G	MFM3261G	As original MFM3261G
MFM3254G	MFM3254G	As original MFM3254G
MFM0999G	MFM0999G	As original MFM0999G
MFM3131G	MFM3131G	As original MFM3131G
MFM3257G	MFM3257G	As original MFM3257G
MFM3258G	MFM3258G	As original MFM3258G
MFM3140G	MSFR08067	As MFM3140G but slightly changed at north-west
MFM3126G	MFM3126G	As original MFM3126G
MFM3253G	MSFR08069	As MFM3253G but extended towards south-east

<b>Lineament name in the Forsmark site investigation that wholly or partly is connected to a lineament in SFR v. 0.1</b>	<b>Name of lineament in SFR model version 0.1</b>	<b>Comment</b>
MFM3127G	MSFR08070	replaces northern part of MFM3127G
MFM0814G	MFM0814G	As original MFM0814G
MFM3106G	MSFR08072	As MFM3106G but shortened at north
MFM3259G	MSFR08073	MFM3259G has been divided into three discontinuous pieces MSFR08073 – MSFR08075
MFM3259G	MSFR08074	MFM3259G has been divided into three discontinuous pieces MSFR08073
MFM3259G	MSFR08075	MFM3259G has been divided into three discontinuous pieces MSFR08073
MFM3129G	MSFR08076	MFM3129G is divided into two discontinuous pieces (MSFR08076, MSFR08077)
MFM3129G	MSFR08077	MFM3129G is divided into two discontinuous pieces (MSFR08076, MSFR08077)
MFM3149G	MSFR08078	MSFR08078 deviates a bit from its original (MFM3149G) running route at north-east and south-west and is shorter, and forms two discontinuous sub-sections of MFM3149G, together with MSFR08081
MFM3113G	MSFR08079	As MFM3113G but shortened at south and with changed curvature in most of its length
MFM3271G	MSFR08080	As MFM3271G but changed at its north-eastern part
MFM3149G	MSFR08081	Very short discontinuous sub-segment of MFM3149G, the other part is MSFR08078
MFM3119G	MSFR08082	As MFM3119G but shortened at south-east
MFM3255G	MFM3255G	As original MFM3255G
MFM3146G	MSFR08084	As MFM3146G, but cut at north and slightly deviating from its original route, at south unreliable due to disturbed area
MFM0804G	MSFR08085	As MFM0804G but changed at its south-eastern part where it is moved to another connection point in the Singö line. Earlier it passed more in a severely disturbed area
MFM3252G	MSFR08086	MFM3252G is divided into two discontinuous lineaments MSFR08086 – MSFR08087
MFM3252G	MSFR08087	MFM3252G is divided into two discontinuous lineaments MSFR08086 – MSFR08087
MFM3142G and partly also MFM3143G	MSFR08088	Partly coinciding with MFM3142G, and partly with the southern part of MFM3143G
MFM3143G	MSFR08089	Partly as MFM3143G, but divided into two discontinuous pieces MSFR08089, MSFR08090
MFM3143G	MSFR08090	Partly as MFM3143G, but divided into two discontinuous pieces MSFR08089, MSFR08090
MFM3137G	MSFR08091	As MFM3137G, but shortened
MFM0137BG	MSFR08092	MFM0137BG has been shortened radically at north-east where MSFR08034 forms an alternative route
MFM0805G0	MSFR08093	Short sub-section of MFM0805G0
MFM0805G0	MSFR08094	Sub-section of MFM0805G0, with slightly changed running
MFM0805G0	MSFR08095	This is the north-western sub-segment of MFM0805G0, though with slightly changed running
MFM3116G	MSFR08096	Part of MFM3116G but unreliable as it runs through disturbed area, because of that cut at both south and north
MFM3117G	MSFR08097	Part of MFM3117G but unreliable as it runs through disturbed area, because of that cut at south
MFM0805G1	MSFR08098	Discontinuous part of MFM0805G1, together with MSFR08104 and MSFR08095, almost connects to MSFR08014
MFM3111G	MSFR08099	As MFM3111G but shortened and with slightly deviating running
MFM1034G	MSFR08100	MFM1034G divided into two discontinuous parts (MSFR08100, MSFR08101). The northernmost part of MFM1034G is entirely removed

Lineament name in the Forsmark site investigation that wholly or partly is connected to a lineament in SFR v. 0.1	Name of lineament in SFR model version 0.1	Comment
MFM1034G	MSFR08101	MFM1034G divided into two discontinuous parts (MSFR08100, MSFR08101). The northernmost part of MFM1034G is entirely removed
–	MSFR08102	New
MFM3293G	MSFR08103	South-western portion of MFM3293G
MFM0805G1	MSFR08104	SE part of MFM0805G1 though with slightly changed running
MFM3262G	MSFR08105	SE part of MFM3262G, slightly deviating from original running
MFM0835BG	MSFR08106	The north-western part of MFM0835BG, which is divided into two discontinuous sections, MSFR08106 and MSFR08107
MFM0835BG	MSFR08107	The north-western part of MFM0835BG, which is divided into two discontinuous sections, MSFR08106 and MSFR08107
MFM3109G	MSFR08108	As MFM3109G but prolonged at south-west
MFM3269G	MSFR08109	Partly coinciding with MFM3269G, but changed running route
MFM1035G	MSFR08110	Sub-section of MFM1035G but slightly deviating running route
MFM3118G	MSFR08111	Short sub-section of MFM3118G at its south-western part
MFM1035G	MSFR08112	Short and slightly dislocated sub-section of MFM1035G
MFM3135G	MSFR08113	As MFM3135G but shortened at west and slightly bended
–	MSFR08114	New
MFM3267G	MSFR08115	Sub-section of MFM3267G, but changed running
MFM3115G	MSFR08116	South-western part of MFM3115G
MFM3155G	MSFR08117	This lineament constitutes a north-western continuation of MFM3155G, and partly coincides with the north-western end of the same
MFM1035G	MSFR08118	Dislocated and short north-western section of MFM1035G
MFM3268G	MSFR08119	Sub-parallel and partly coinciding with MFM3268G
MFM3132G	MSFR08120	South-western part of MFM3132G
MFM3267G	MSFR08121	As MFM3267G but discontinuous at the entrance to the local model area (where it continues in MSFR08115), shortened, slightly changed at south-east
MFM3130G	MSFR08122	Coinciding with MFM3130G at its northern half, but deviates severely to the south-west
MFM1035G	MSFR08123	Sub-parallel and partly coinciding with MFM1035G, deviating at west

**Table A5-2. Lineaments from the Forsmark site investigation not included in the SFR model version 0.1, along with the name of each lineament and the reason for exclusion. Comments concerning attribute “uncertainty” refer to the classification made by /Isaksson et al. 2007/.**

Lineament name in the Forsmark site investigation that wholly or partly is not included in SFR v. 0.1	Comment
MFM3134G	This high uncertainty lineament is possible to identify in data at its central section, but is very faint elsewhere
MFM3155G	This lineament is positioned in a broad and short minimum with a signature indicating a possible low magnetic lithological unit and hence, should possibly be considered having a minima connection character. At its south-eastern part it is of high uncertainty and difficult to trace in data
MFM3141G	This high uncertainty lineament is located in an area with a fairly complex anomaly pattern, which combined with its short length has implied exclusion
MFM3115G	More than half of this high uncertainty lineament is excluded at its north-eastern part due to interference from disturbances created by the installations in the area. The south-western part of MFM3115G is associated with MSFR08116
MFM3112G	This high uncertainty lineament is difficult to follow at south-west; at north-east the lineament is excluded due to interference from disturbances created by the installations in the area
MFM3148G	This lineament has a low-moderate uncertainty north-west of the SFR regional model boundary. However, the south-easternmost third of this lineament inside the model area of SFR, has a high uncertainty. It is located in a low-relief area and furthermore disturbed by the installations in the area
MFM3147G	This high uncertainty lineament is only very faintly and discontinuously observed in data, it occurs in a low-relief area and furthermore its strike is semi-parallel with the magnetic survey lines
MFM3144G	This high uncertainty lineament is only very faintly and discontinuously observed in data and furthermore its strike is semi-parallel with the magnetic survey lines
MFM3114G	This high uncertainty lineament is very near to being implemented in the SFR model version 0.1, but it is short and deviating at north-east from the magnetic minimum supposedly used as its indicator
MFM3262G	At south-east this lineament is coinciding with MSFR08105, but for more than half of its length it is not accepted as its trace runs through the area with disturbances from civil installations

**Table A5-3. Attribute table for the lineaments in SFR version 0.1. The table is based on Table 4-2 in /Isaksson et al. 2007/.**

Field name	Name	Description	Further comments on attributes used to describe lineaments
Id_t	Identity	Identity of a lineament.	All lineaments within SFR version 0.1 are given new identities, MSFR08001–MSFR08XXX, with the exception of the lineaments in SFR version 0.1 that were directly imported from the latest version of lineaments within the FSI work /Isaksson et al. 2007/; their original names are preserved. The relation between lineaments in this SFR version 0.1 and lineaments from earlier work within the FSI is partly commented in the attribute “Comment_t” (see below in this attribute table) and in more detail in Tables A5-1 and A5-2.
Origin_t	Origin	Major type of basic data.	Basic data used, or, Method specific or Coordinated lineaments from the latest version within the FSI work /Isaksson et al. 2007/. With exception for the directly imported lineaments from the FSI work, all lineaments in SFR version 0.1 were identified almost uniquely in data describing the magnetic total field (magnetics). In the case of lineaments directly imported from the latest version of the FSI work /Isaksson et al. 2007/, their original values have been left without change.
Class_t	Classification	Classification of a lineament.	Regional (>10 km), local major (1–10 km) and local minor (<1 km). In the case of lineaments directly imported from the latest version of the FSI work /Isaksson et al. 2007/, their original values have been left without change.
Method_t	Method	The type of data in which the lineament is observed.	Magnetics mostly (see also comments related to “Origin_t” above). The principal data sources used are measurements of the magnetic total field, from helicopter, on land and at sea. In the case of lineaments directly imported from the latest version of the FSI work /Isaksson et al. 2007/, their original values have been left without change.
Weight_n	Weight	A combination of uncertainty and number of properties (methods). An overall assessment of the confidence of the lineament. This assessment is based on both the number of properties upon which the lineament has been identified and the degree of uncertainty.	This attribute is not assigned to the lineaments within SFR version 0.1 with exception for the value inherited at the direct import of a lineament from the FSI work /Isaksson et al. 2007/.
Char_t	Character	Character of the lineament in letters	Characteristics of the anomaly representing the lineament, like minima, edge, minima connection, dislocation, or characteristics of the lineament itself. In the case of lineaments directly imported from the latest version of the FSI work /Isaksson et al. 2007/, their original values have been left without change.
Char_n	Character	Character of the lineament translated into an integer.	0 = minima connection, 1 = minima, 2 = edge, 3 = dislocation. In the case of lineaments directly imported from the latest version of the FSI work /Isaksson et al. 2007/, their original values have been left without change.
Uncert_t	Uncertainty	Gradation of the lineament in terms of uncertainty. In effect, this attribute involves both the degree of clarity of the lineament as well as a judgement regarding the possible cause of the lineament	1 = low, 2 = medium, 3 = high. In the case of lineaments directly imported from the latest version of the FSI work /Isaksson et al. 2007/, their original values have been left without change. Further explanation can be found in /Isaksson et al. 2007/.
Comment_t	Comment	Specific comments regarding the lineament	
Process_t	Processing	Data processing performed	Grid, image analysis, GIS
Date_t	Date	Date for the identification	Date
Scale_t	Scale	Scale of the image used in the identification	In SFR version 0.1 the scale used has varied, the value presented is a rough estimate of the average. In the case of lineaments directly imported from the latest version of the FSI work /Isaksson et al. 2007/, their original values have been left without change.



Field name	Name	Description	Further comments on attributes used to describe lineaments
Width_t	Width	Width on average	Not assigned in SFR version 0.1. In the case of lineaments directly imported from the latest version of the FSI work /Isaksson et al. 2007/, their original values have been left without change.
Precis_t	Precision	Spatial uncertainty of position. An estimate of how well the lineament is defined in horizontal position.	In SFR version 0.1 the value is estimated and dependent on scale. In the case of lineaments directly imported from the latest version of the FSI work /Isaksson et al. 2007/, their original values have been left without change.
Count_n	Count	The number of original segments along the lineament.	In SFR version 0.1 the value is always 1. In the case of lineaments directly imported from the latest version of the FSI work /Isaksson et al. 2007/, their original values have been left without change.
Cond_n	Conductivity	Shows how much of the lineament that has been identified by EM and/or VLF.	In SFR version 0.1 no conductivity data have been interpreted, the value is set to 0. In the case of lineaments directly imported from the latest version of the FSI work /Isaksson et al. 2007/, their original values have been left without change.
Magn_n	Magnetic	Shows how much of the lineament that has been identified by magnetics	In SFR version 0.1 the value is 1. In the case of lineaments directly imported from the latest version of the FSI work /Isaksson et al. 2007/, their original values have been left without change.
Topo_n	Topography	Shows how much of the lineament that has been identified by topography, either on the ground surface, sea bottom surface or in the rock surface.	Topography data have only aided to a very limited extent in the identification of lineaments in the work with SFR version 0.1, as a consequence this attribute has been set to 0. In the case of lineaments directly imported from the latest version of the FSI work /Isaksson et al. 2007/, their original values have been left without change.
Topog_n	Ground surface	Shows how much of the lineament that has been identified by topography in the ground surface.	Topography data have only aided to a very limited extent in the identification of lineaments in the work with SFR version 0.1, as a consequence this attribute has been set to 0. In the case of lineaments directly imported from the latest version of the FSI work /Isaksson et al. 2007/, their original values have been left without change.
Topor_n	Rock surface	Shows how much of the lineament that has been identified by topography in the bedrock surface.	Topography data have only aided to a very limited extent in the identification of lineaments in the work with SFR version 0.1, as a consequence this attribute has been set to 0. In the case of lineaments directly imported from the latest version of the FSI work /Isaksson et al. 2007/, their original values have been left without change.
Prop_n	Property	Shows in average, how many properties (complementary investigation methods) that have been identifying the lineament.	In SFR version 0.1 the value is 1 (referring to magnetics). In the case of lineaments directly imported from the latest version of the FSI work, their original values have been left without change. Isaksson et al. 2007 explain this attribute further.
Length_n	Length	The length of the lineament	In metres.
Direct_n	Direction	The average trend of the lineament.	In degrees.
Platform_t	Platform	Measuring platform for basic data.	Ground survey grid.
Sign_t	Signature	Work performed by.	In the work of SFR version 0.1, C-A Triumf GeoVista AB. In the case of lineaments directly imported from the latest version of the FSI work, their original values have been left without change.

### **Modelling of anomalies in the magnetic total field adjacent to lineaments – SFR version 0.1**

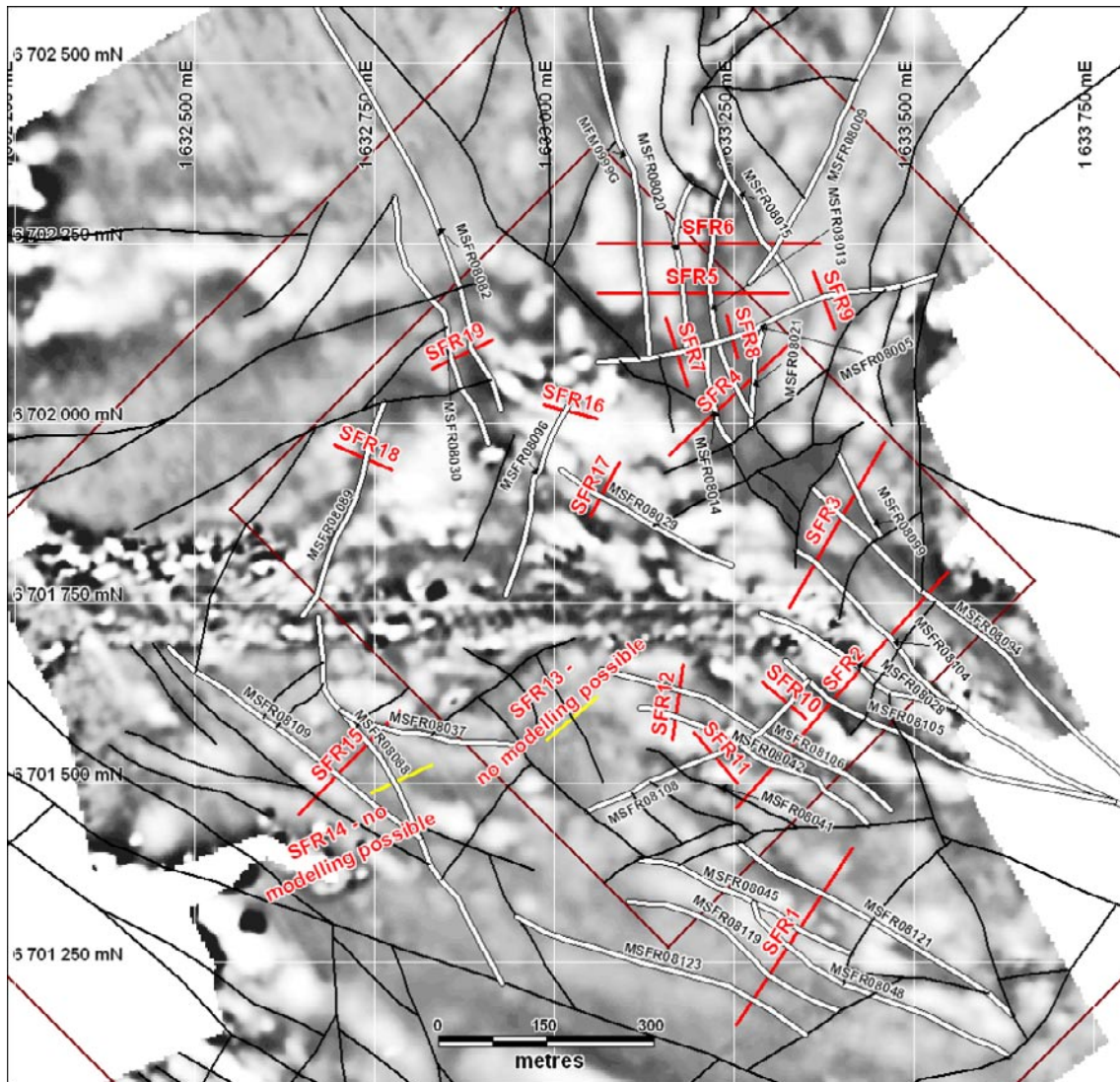
The modelling has been carried out using a background magnetic susceptibility value of  $500 \times 10^{-5}$  SI. The starting model for the low susceptibility body representing the source to the lineament has had a magnetic susceptibility of  $130 \times 10^{-5}$  SI. During the modelling process, this value has changed, but the final value normally differs by less than  $100 \times 10^{-5}$  SI from the initial value. During modelling, high susceptibility source bodies have been introduced in some of the profiles, in order to compensate for local field variations as an alternative to creating a very peculiar “regional” field.

Many of the magnetic anomalies associated with the lineaments are vague. Modelling of anomalies with low amplitude may give a rather low level of confidence in the resulting models. In the results presented below, the source bodies often end at a depth between 100 and 300 m. However, when modelling faint anomalies, the results have a reduced level of confidence already below 50 m. By contrast, modelling of strong anomalies associated with prominent lineaments is expected to yield more diagnostic results even down to depths considerably below 50 m.

The modelling of anomalies in the magnetic field has resulted in three-dimensional source bodies. The bodies have been exported to a DXF format that can be attached to the RVS model, and can be used as a direct aid in the modelling of deformation zones at SFR. This allows the results to be viewed in RVS and integrated into the model. Hence, only limited comments regarding the geometries of the source bodies are included below.

The modelling results from seventeen profiles are presented below. Profiles SFR13 and SFR14 were not possible to model with any significant results and are omitted from the presentation. The location of the nineteen profiles is shown in Figure A6-1. The names of the relevant lineaments intersected by these profiles (e.g. MSFR08021) are also shown in this map.

The modelling has involved lineaments with trends that are either concordant or discordant to the expected main strike of lithology. A lineament with a trend concordant to the main strike may represent a lithological unit with low magnetic susceptibility. However, the general approach for the current work has been to assume that the lineaments represent deformation zones.



**Figure A6-1.** The location of the 19 profiles selected for modelling (red lines). The lineaments in SFR model version 0.1 addressed by the modelling work are marked with thick black-white lines, and labelled. An enhanced version of the magnetic total field image (1st vertical derivative) with the remaining inferred lineaments (black lines) is shown in the background.

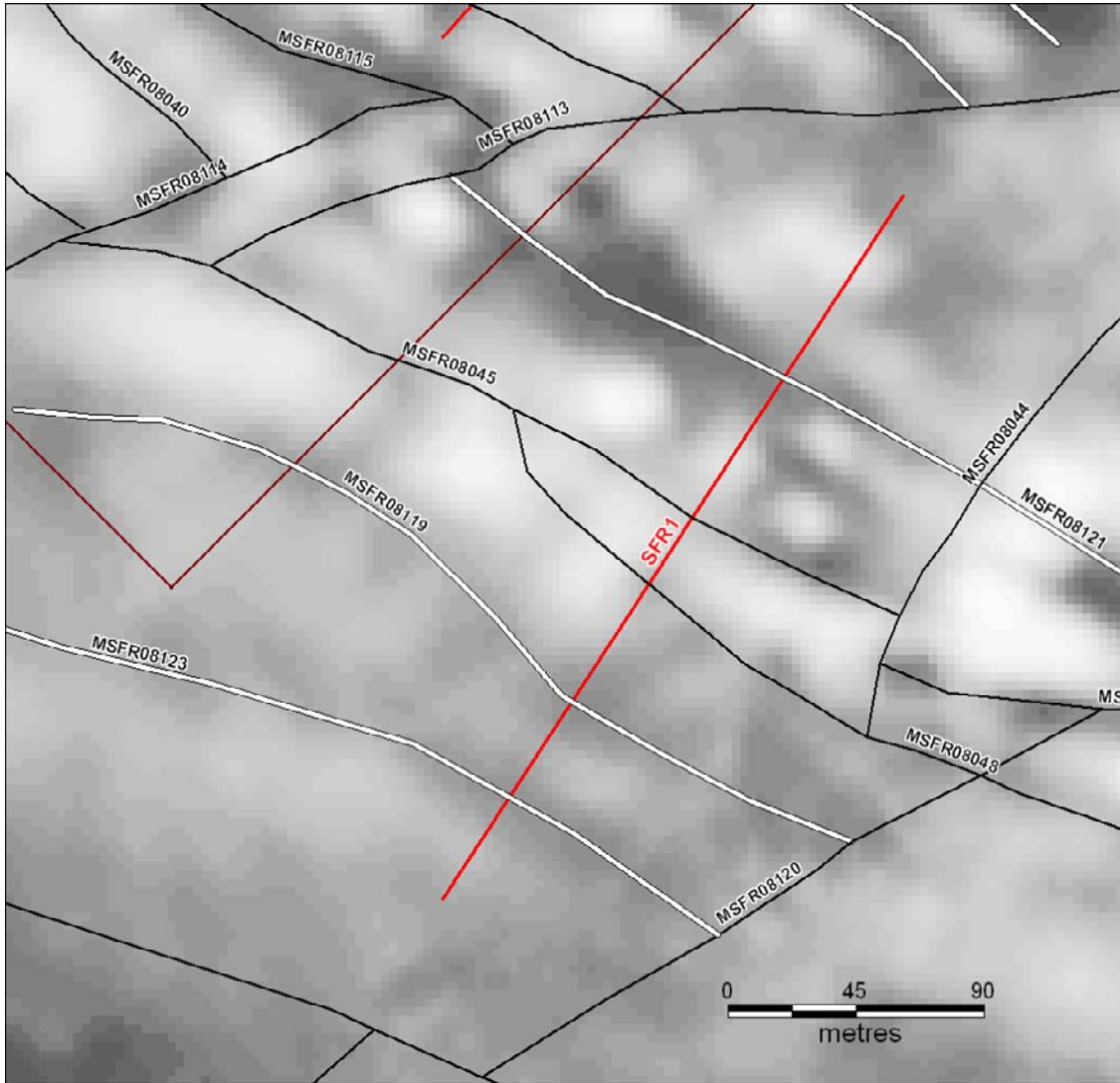
**Profiles for modelling of magnetic anomalies (Coordinates RT90-RHB70)**

SFR1 1633254/6701163 – 1633414/6701409  
SFR2 1633253/6701465 – 1633547/6701793  
SFR3 1633327/6701743 – 1633460/6701974  
SFR4 1633160/6701955 – 1633327/6702109  
SFR5 1633060/6702180 – 1633325/6702180  
SFR6 1633060/6702250 – 1633370/6702250  
SFR7 1633155/6702145 – 1633185/6702050  
SFR8 1633240/6702150 – 1633255/6702090  
SFR9 1633360/6702210 – 1633390/6702130  
SFR10 1633290/6701540 – 1633350/6701590  
SFR11 1633195/6701570 – 1633255/6701500  
SFR12 1633165/6701560 – 1633180/6701665  
SFR13 1632990/6701560 – 1633060/6701620  
SFR14 1632745/6701485 – 1632830/6701525  
SFR15 1632645/6701455 – 1632785/6701600  
SFR16 1632985/6702025 – 1633060/6702005  
SFR17 1633050/6701870 – 1633090/6701945  
SFR18 1632695/6701970 – 1632775/6701935  
SFR19 1632830/6702075 – 1632915/6702115

**SFR1 1633254/6701163 – 1633414/6701409**

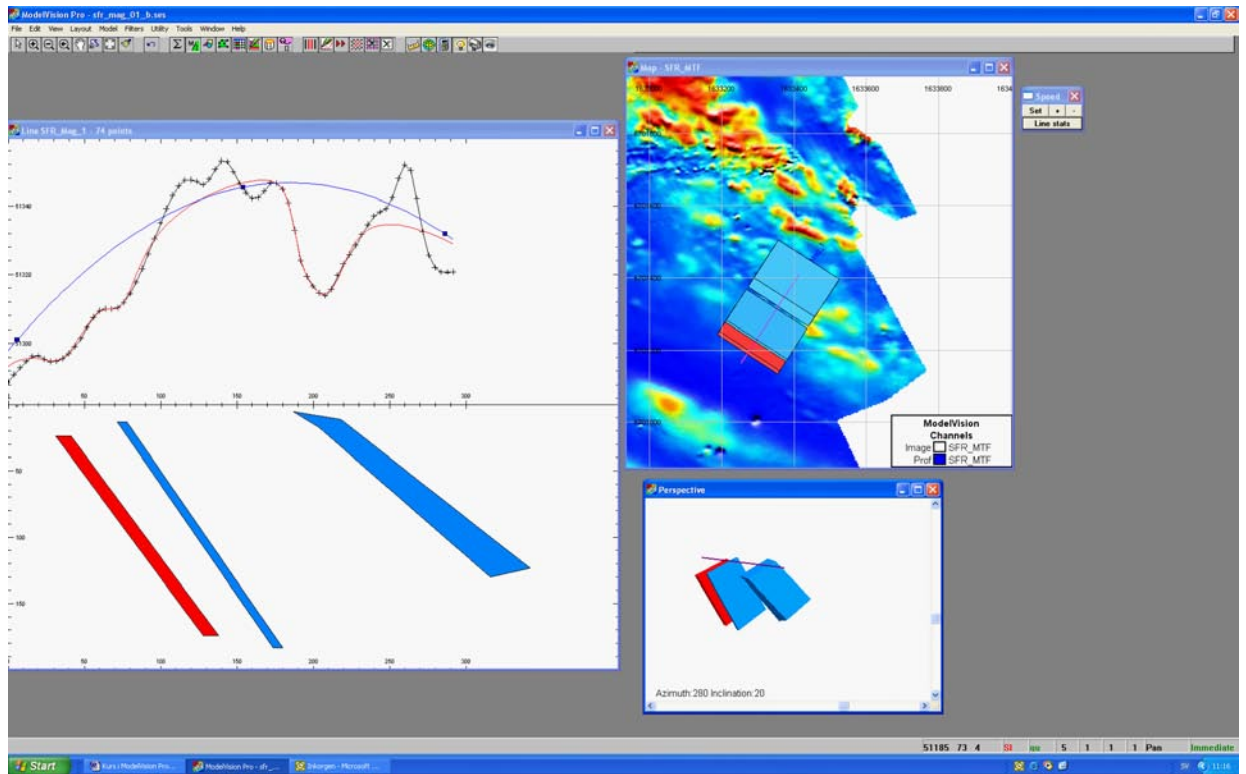
The profile SFR1 crosses the lineaments MSFR08123, MSFR08119, MSFR08048, MSFR08045 and MSFR08121, see Figure A6-2.

The low susceptibility bodies in Figure A6-3 represent lineaments MSFR08123, MSFR08119, MSFR08121. The anomalies from MSFR08048 and MSFR08045 are considered too small for modelling. The dip of all low susceptibility features is towards the north-east with the broadest source body representing the lineament MSFR080121.



*Figure A6-2. Profile SFR1 with associated lineaments. Only the lineaments represented by thick white and black lines crossing the profile have been modelled. The model area of SFR version 0.1 is visible as a brown line.*



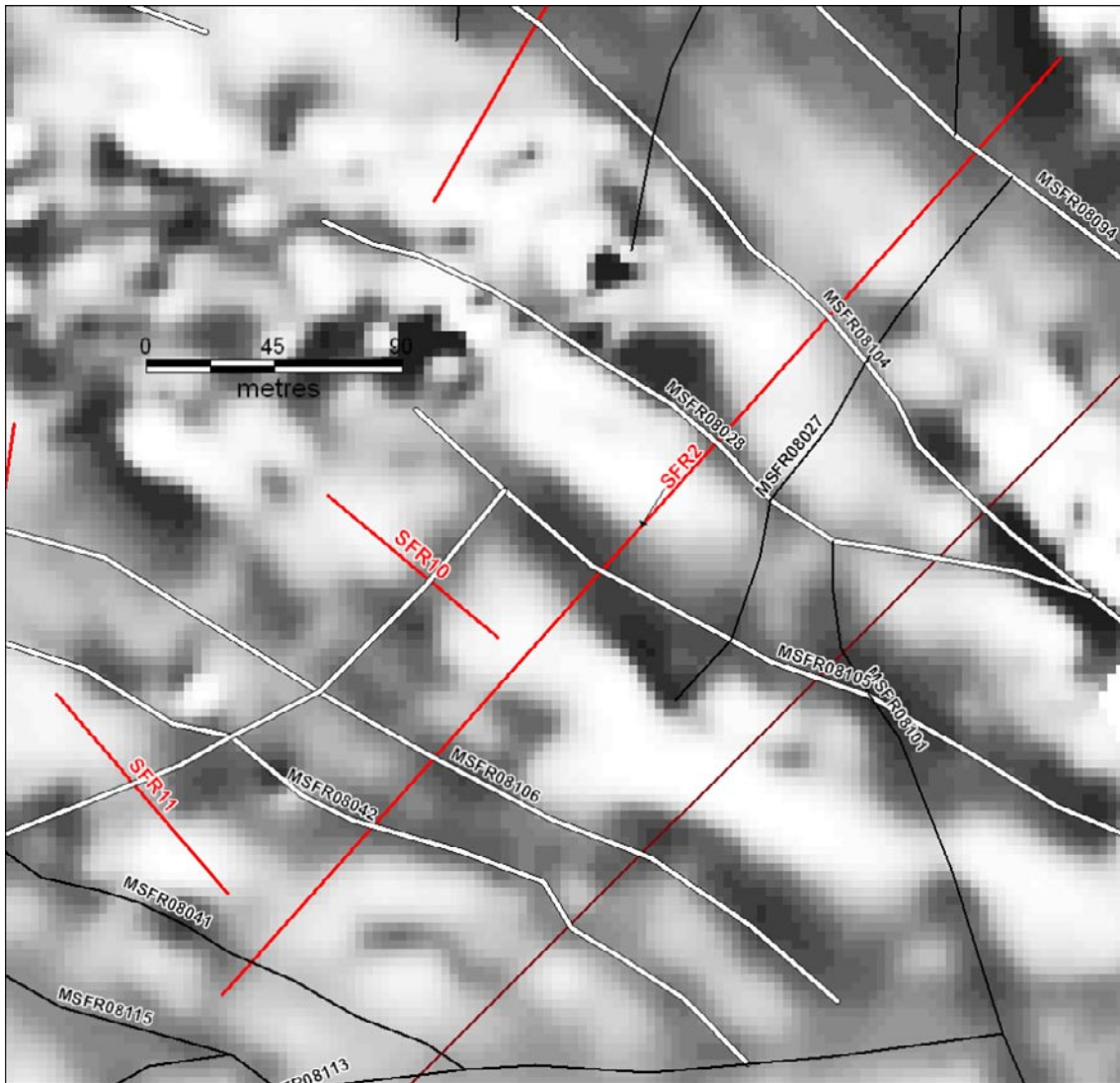


**Figure A6-3.** Modelling result from profile SFR1 with source bodies representing lineaments MSFR08123, MSFR08119, MSFR08121 (from left to right), all have dips towards the north-east. (Screen dump from Encom ModelVision Pro 8, scale on x- and z-axis may differ).

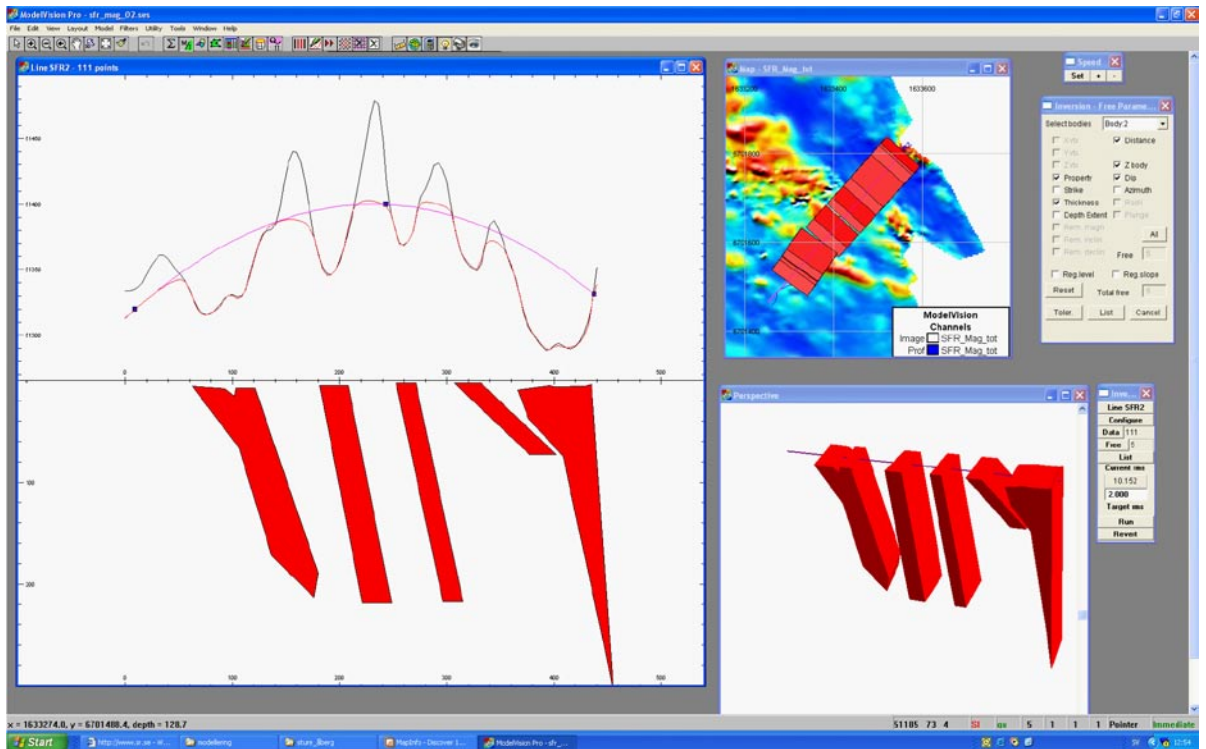
### SFR2 1633253/6701465 – 1633547/6701793

The profile SFR2 crosses the lineaments MSFR08041, MSFR08042, MSFR08106, MSFR08105, MSFR08028, MSFR08104 and MSFR08094, see Figure A6-4.

The low susceptibility bodies in Figure A6-5 represent lineaments MSFR08042 and MSFR08106 (leftmost body), MSFR08105, MSFR08028, MSFR08104, MSFR08094. The anomaly from MSFR08041 is considered too small for modelling. The geometry of the two lineaments MSFR08042 and MSFR08106 is difficult to distinguish as the source bodies appear to coincide at depth.



**Figure A6-4.** Profile SFR2 with associated lineaments. Only the lineaments represented by thick white and black lines crossing the profile have been modelled. The model area of SFR version 0.1 is visible as a brown line.

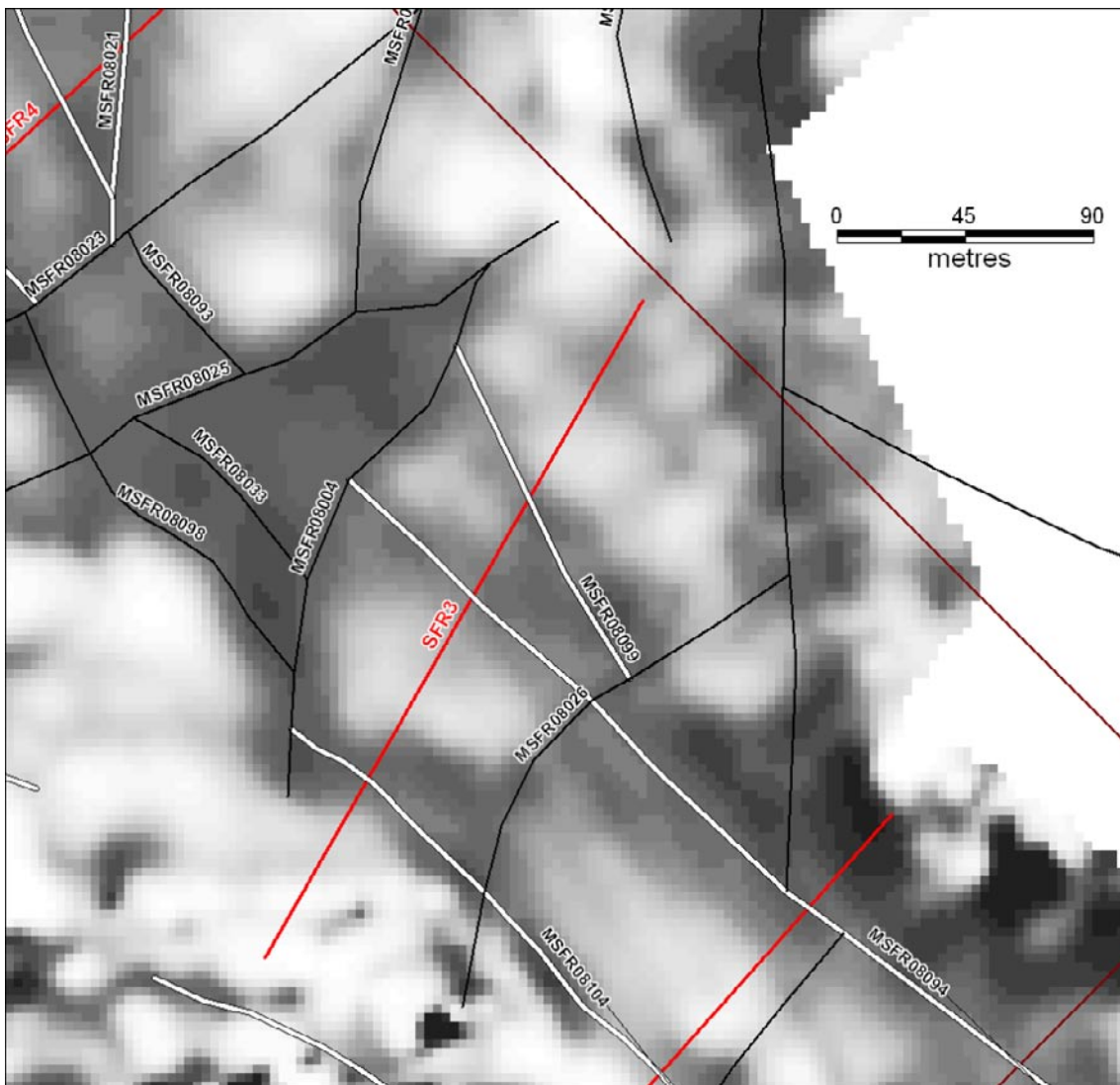


**Figure A6-5.** Modelling result from profile SFR2 with source bodies from left to right representing lineaments MSFR08042 and MSFR08106 (leftmost body), MSFR08105, MSFR08028, MSFR08104, MSFR08094. (Screen dump from Encom ModelVision Pro 8, scale on x- and z-axis may differ).

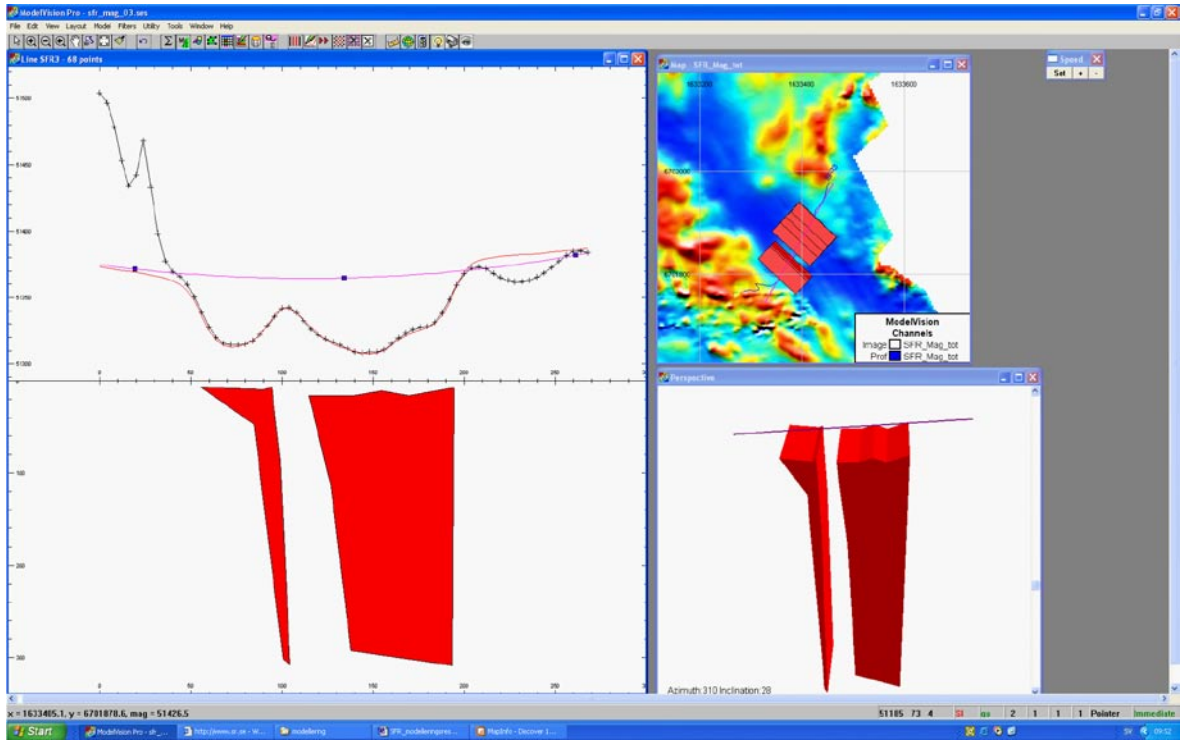
### SFR3 1633327/6701743 – 1633460/6701974

The profile SFR3 crosses the lineaments MSFR08104, MSFR08094 and MSFR08099, see Figure A6-6.

The source bodies representing lineaments MSFR08104, MSFR08094 and MSFR08099 are shown in Figure A6-7. The rightmost body in the figure represents two lineaments (MSFR08094 and MSFR08099), indicating that the whole rock volume in association to the lineaments has a low magnetic susceptibility. The reason could be that the whole unit is affected by tectonic processes. However, a lithological unit with low magnetic susceptibility and without any remarkable tectonic overprint, located between the two lineaments, cannot be ruled out. The thinning of the bodies towards depth should not be taken too literally as the significance level becomes rather low in the prediction of geometry at depth.



**Figure A6-6.** Profile SFR3 with associated lineaments. Only the lineaments represented by thick white and black lines crossing the profile have been modelled. The model area of SFR version 0.1 is visible as a brown line.



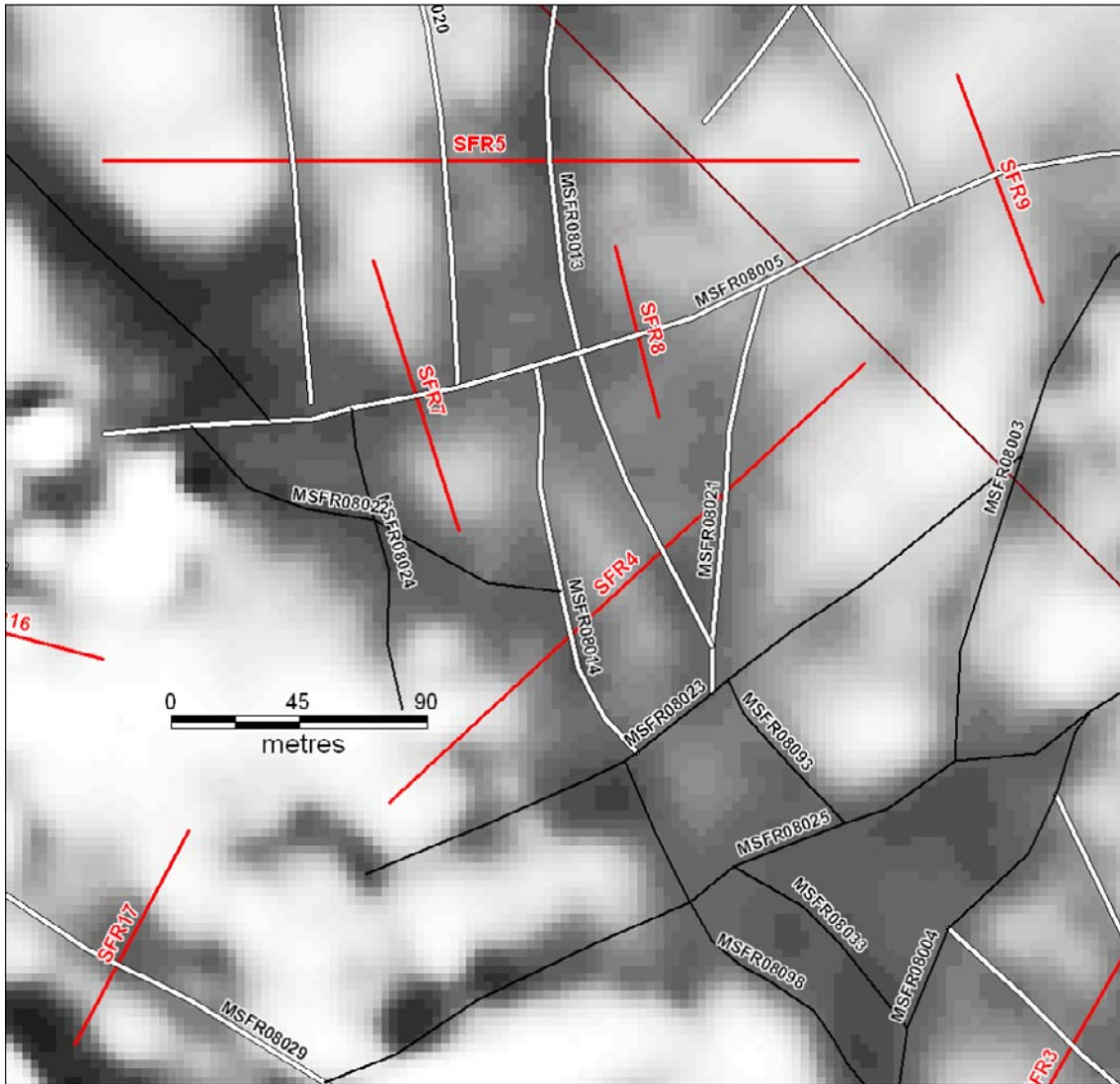
**Figure A6-7.** Modelling result from profile SFR3 with source bodies from left to right representing lineaments MSFR08104, MSFR08094 and MSFR08099, the two latter lineaments are represented by one source body only. (Screen dump from Encom ModelVision Pro 8, scale on x- and z-axis may differ).



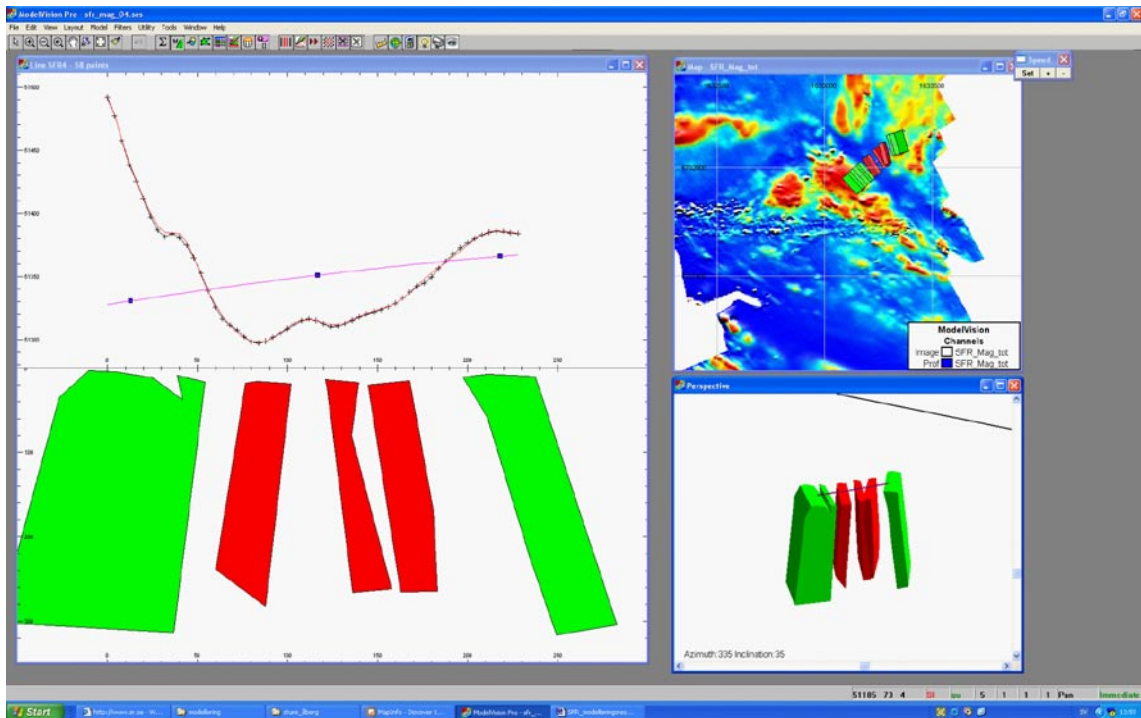
**SFR4 1633160/6701955 – 1633327/6702109**

The profile SFR4 crosses the lineaments MSFR08014, MSFR08013 and MSFR08021, see Figure A6-8.

The model used (see Figure A6-9) consists of three low susceptibility bodies (red) and two high susceptibility bodies (green). The three lineaments are represented by the red source bodies, all three with steep dips.



*Figure A6-8. Profile SFR4 with associated lineaments. Only the lineaments represented by thick white and black lines crossing the profile have been modelled. The model area of SFR version 0.1 is visible as a brown line.*

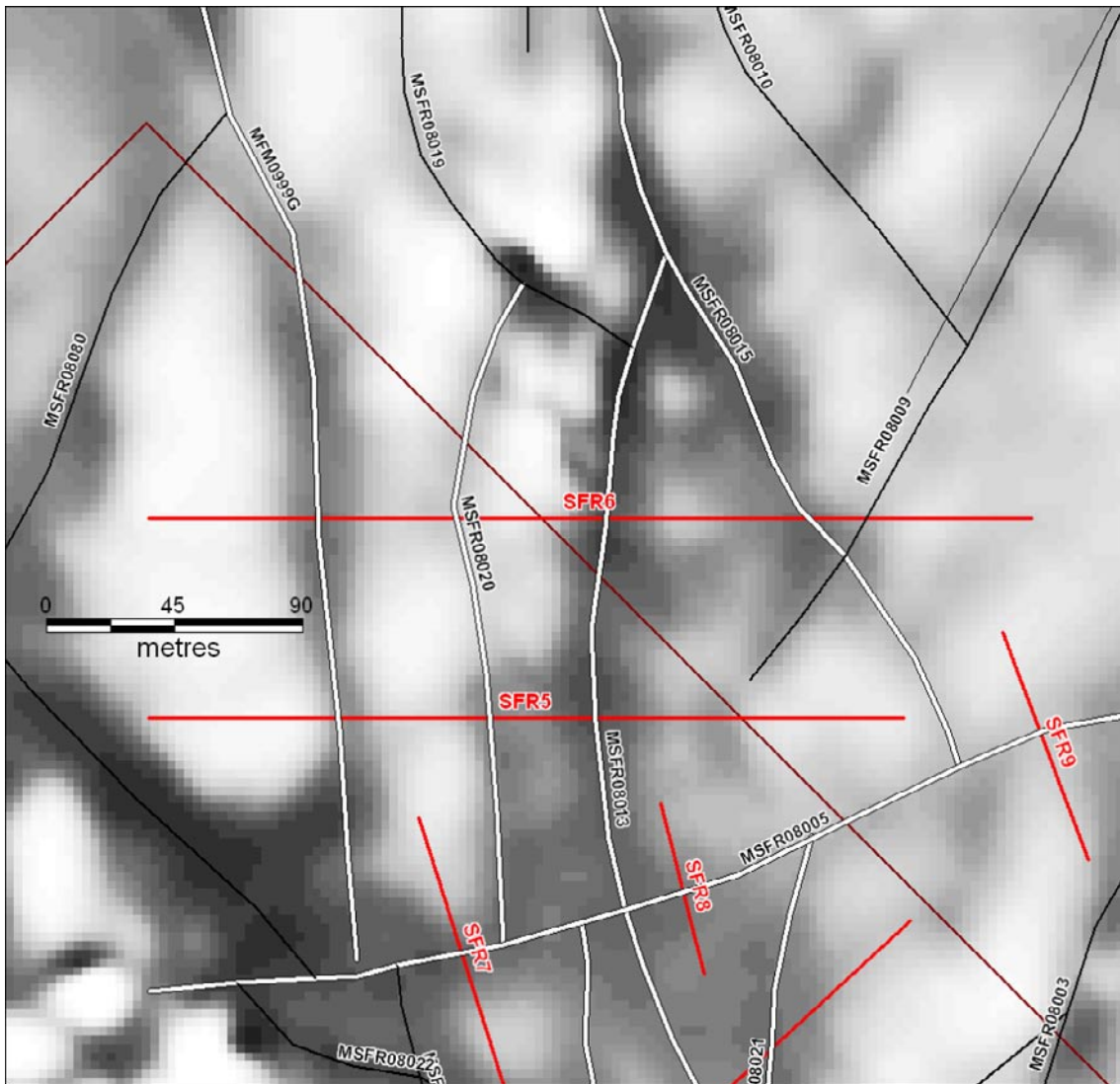


**Figure A6-9.** Modelling result from profile SFR4. In this modelling three low susceptibility bodies (red) have been used, flanked by two high susceptibility rock volumes. The three red source bodies represent the lineaments MSFR08014, MSFR08013 and MSFR08021 (from left to right). (Screen dump from Encom ModelVision Pro 8, scale on x- and z-axis may differ).

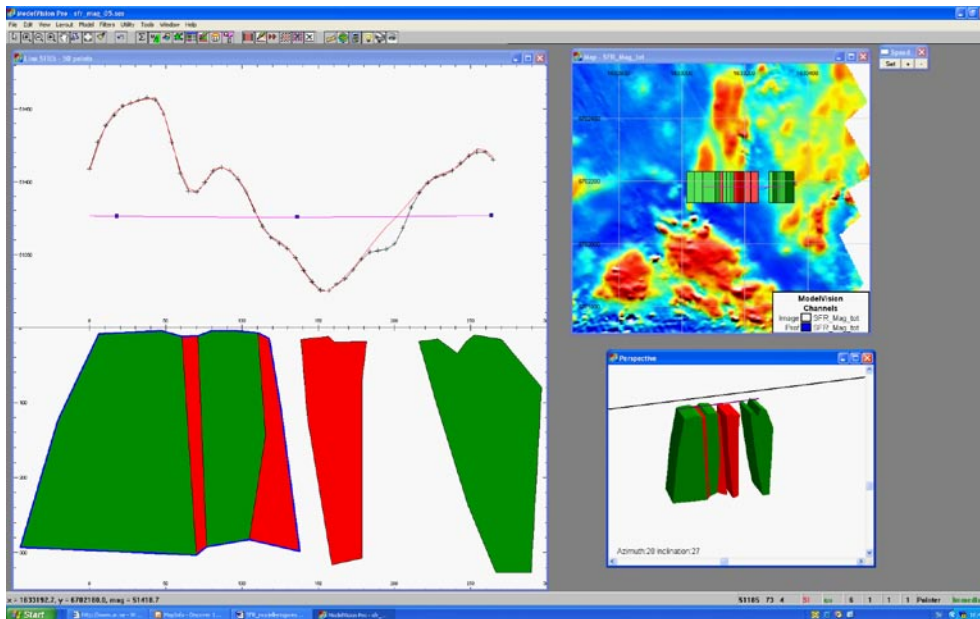
### SFR5 1633060/6702180 – 1633325/6702180

The profile SFR5 crosses the lineaments MFM0999G, MSFR08020, MSFR08013, see Figure A6-10.

The modelling result is shown in Figure A6-11, with the low susceptibility bodies in red and the high susceptibility bodies in green. The low susceptibility source bodies represent the three lineaments; all are steeply dipping, almost vertical. The anomaly connected to lineament MSFR08020 is very faint and difficult to model, since it is located in a gradient of the magnetic total field. The predicted geometry of the source body is consequently of rather low confidence.



**Figure A6-10.** Profile SFR5 with associated lineaments. Only the lineaments represented by thick white and black lines crossing the profile have been modelled. The model area of SFR version 0.1 is visible as a brown line.

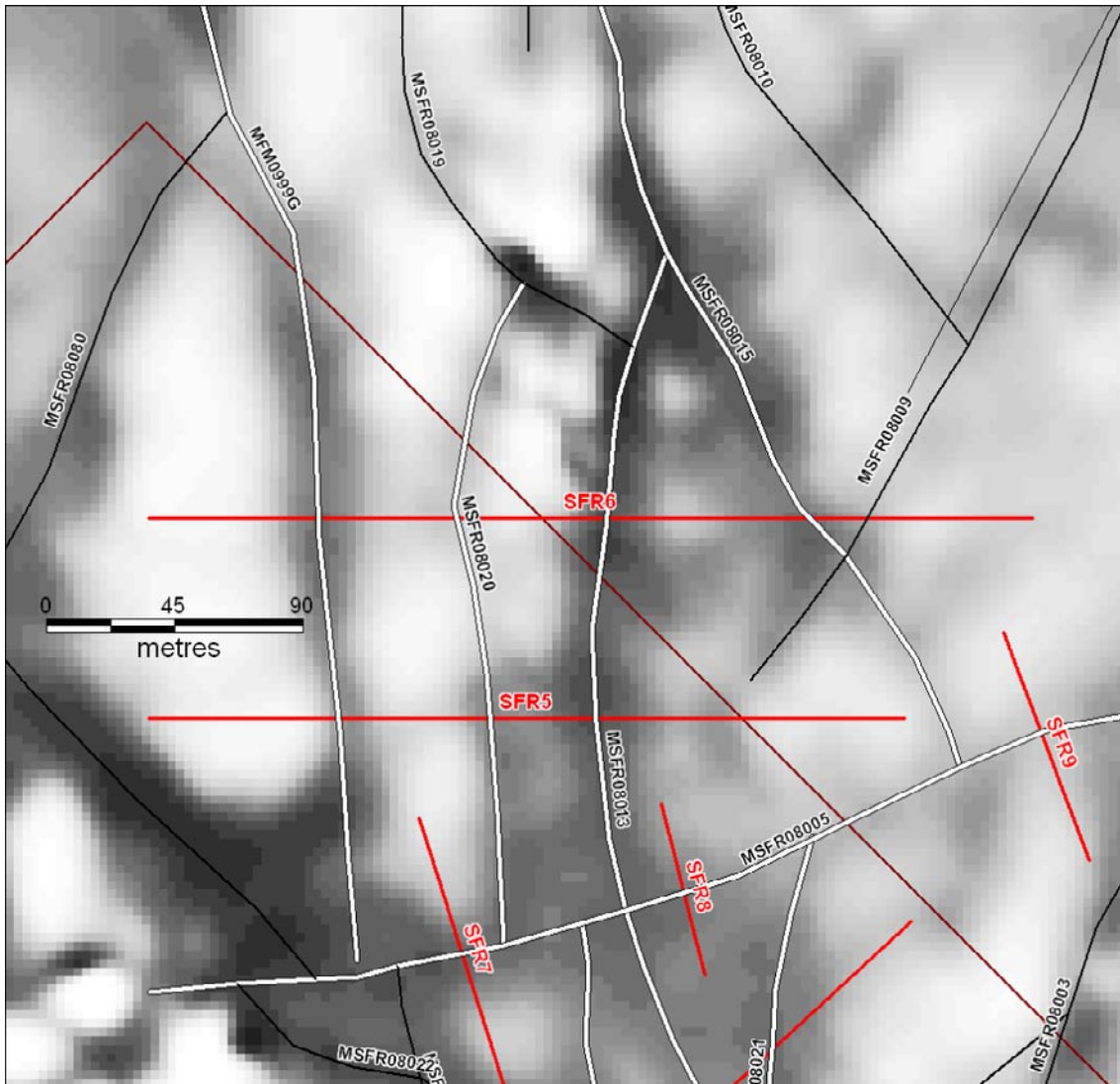


**Figure A6-11.** Modelling result from profile SFR5. In this modelling three low susceptibility bodies (red) have been used, representing the lineaments MFM0999G, MSFR08020, MSFR08013 (from left to right). (Screen dump from Encom ModelVision Pro 8, scale on x- and z-axis may differ).

## SFR6 1633060/6702250 – 1633370/6702250

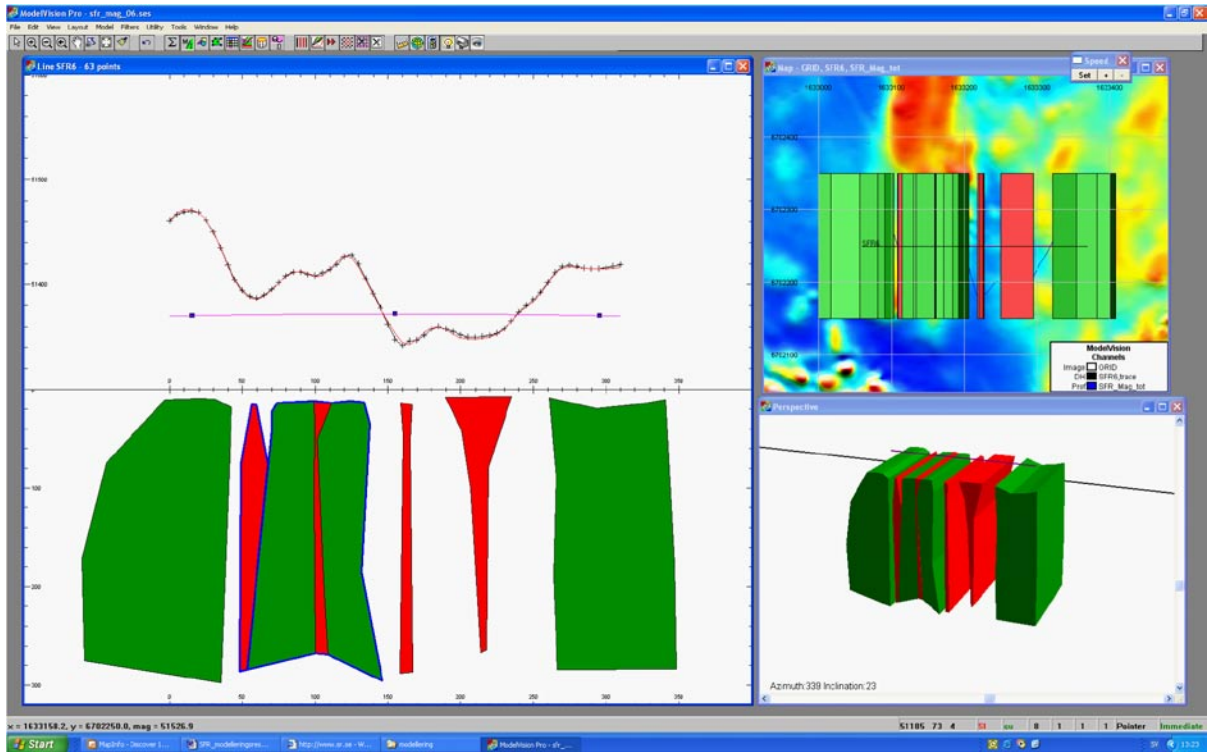
The profile SFR6 crosses the lineaments MFM0999G, MSFR08020, MSFR08013, MSFR08015 and MSFR08009, see Figure A6-12.

The low susceptibility source bodies (in red) and high susceptibility bodies (in green) are shown in Figure A6-13. The lineaments MFM0999G, MSFR08020, MSFR08013 and MSFR08015 are represented by source bodies with almost vertical dipoles. The anomaly associated with MSFR08009 is too weak to be modelled. If the neighbouring source bodies are considered to represent the dips in the area, the source body associated with MSFR08009 could be assumed to dip almost vertically.



**Figure A6-12.** Profile SFR6 with associated lineaments. Only the lineaments represented by thick white and black lines crossing the profile have been modelled. The model area of SFR version 0.1 is visible as a brown line.



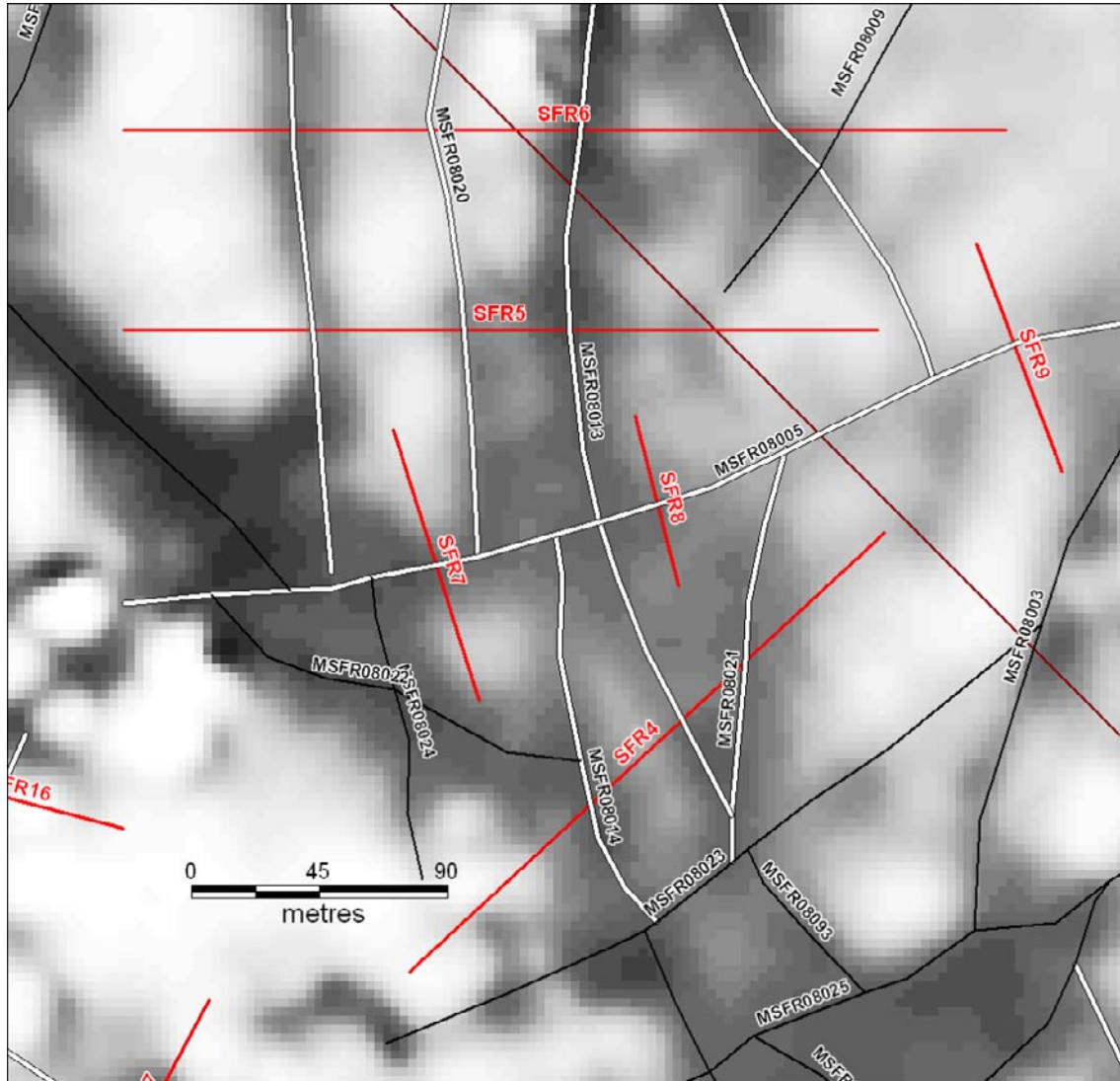


**Figure A6-13.** Modelling result from profile SFR6. Four low susceptibility source bodies (red) have been used together with four high susceptibility bodies (green). The lineaments MF0999G, MSFR08020, MSFR08013 and MSFR08015 are represented by the red bodies (from left to right). (Screen dump from Encom ModelVision Pro 8, scale on x- and z-axis may differ).

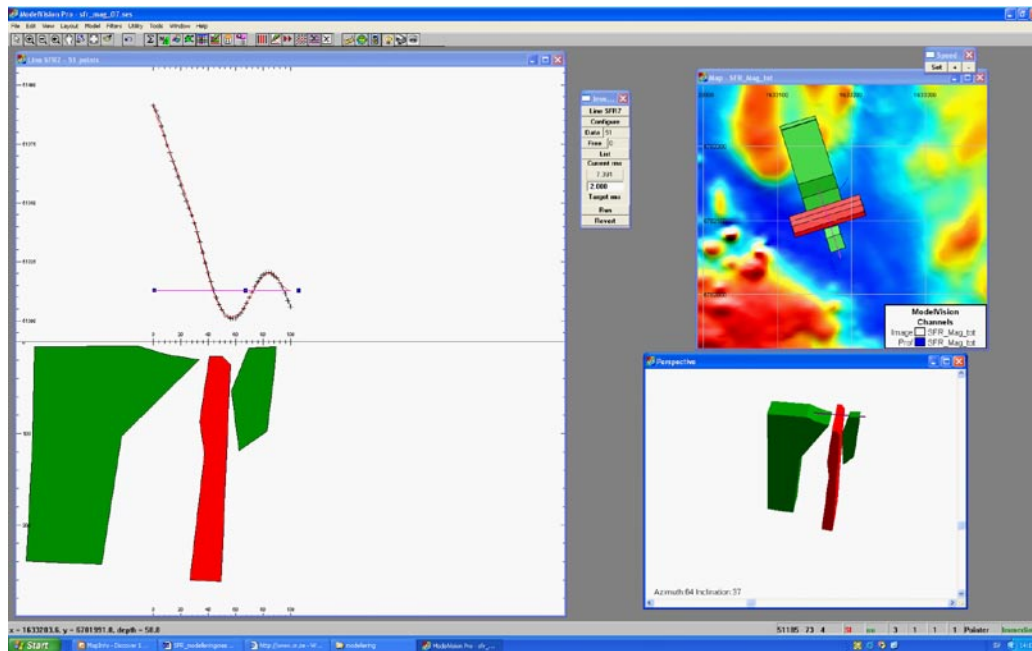
## SFR7 1633155/6702145 – 1633185/6702050

The profile SFR7 crosses the lineament MSFR08005, see Figure A6-14.

The model containing a low susceptibility source body (red) representing the anomaly source to lineament MSFR08005 is shown in Figure A6-15. It is flanked by two high susceptibility bodies (green) on each side. According to the modelling, the source body to the lineament is steeply dipping, possibly slightly towards the NNW.



**Figure A6-14.** Profiles SFR7, SFR8 and SFR9 with associated lineament. Only the lineaments represented by thick white and black lines crossing the profile have been modelled. The model area of SFR version 0.1 is visible as a brown line.

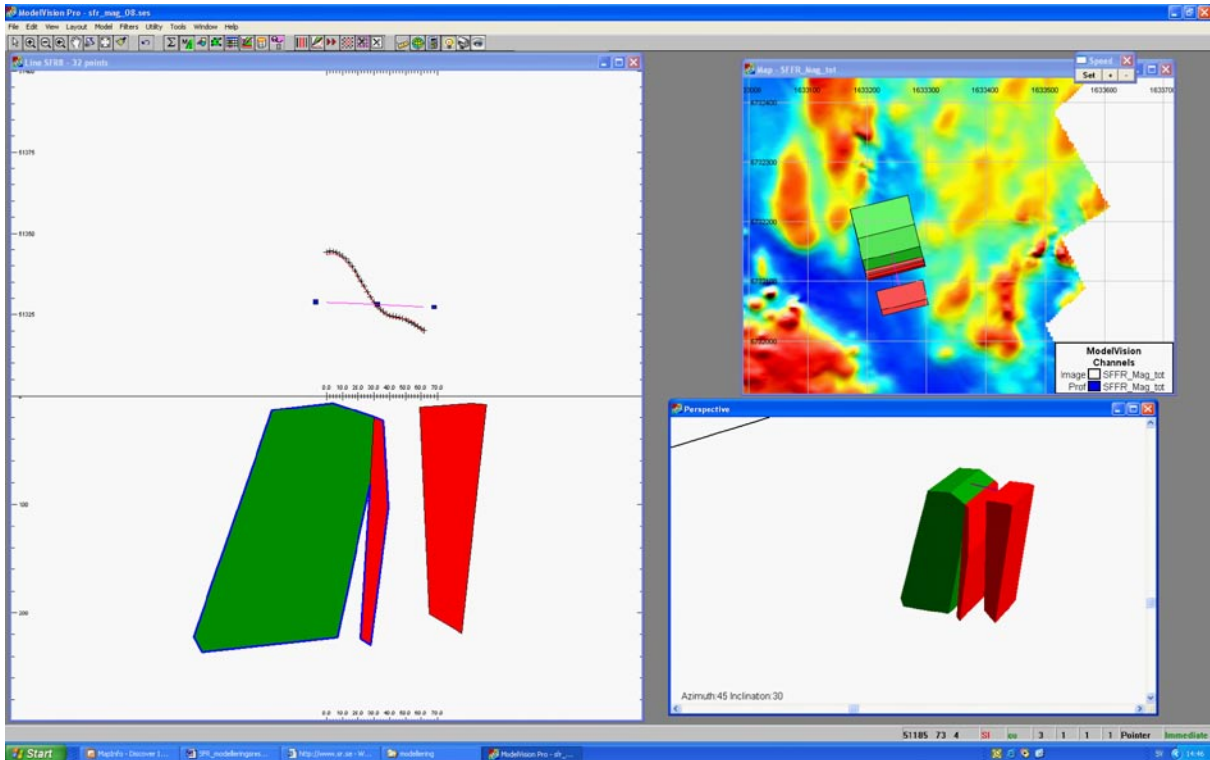


**Figure A6-15.** Modelling result from profile SFR7. In this modelling a low susceptibility body (red), representing lineament MSFR08005, has one high susceptibility body at each side (green). (Screen dump from Encom ModelVision Pro 8, scale on x- and z-axis may differ).

## SFR8 1633240/6702150 – 1633255/6702090

The profile SFR8 with its associated lineament MSFR08005 is shown in Figure A6-14 above. Figure A6-16 shows a model with low susceptibility source bodies (red), and with a high susceptibility body (green). The anomaly associated with the lineament MSFR08005 is represented by the red body closest to the green; the red body is almost vertical. The other red body is inserted for reasons of compensation for another zone not involved in this modelling.

As seen in Figure A6-16, the anomaly associated with the lineament MSFR08005 is located at a gradient in the magnetic total field. Due to this, the level of significance in the modelling is considered to be low.

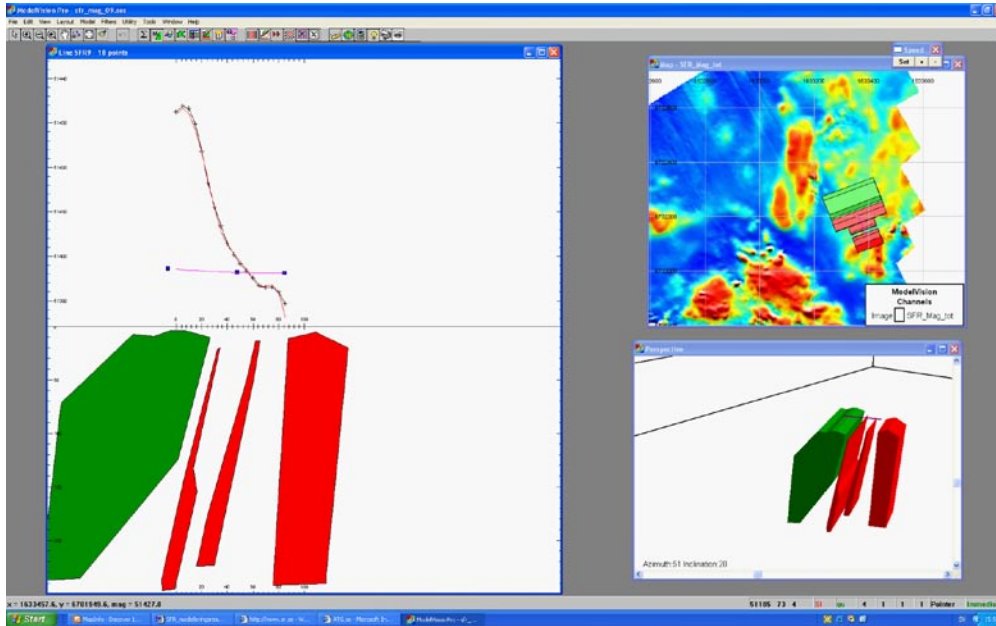


**Figure A6-16.** Modelling result from profile SFR8. In this modelling, the low susceptibility body (red) closest to the high susceptibility body (green) is the primary object representing lineament MSFR08005. The right-most red body is only inserted to compensate for its contribution to the magnetic depression at the side of the step-like lineament anomaly (screen dump from Encom ModelVision Pro 8, scale on x- and z-axis may differ).

### SFR9 1633360/6702210 – 1633390/6702130

The profile SFR9 with its associated lineament MSFR08005 is shown in Figure A6-14 above. Figure A6-17 shows a model with three low susceptibility bodies (red) and one high susceptibility body (green). The zone representing the lineament MSFR08005 (the red one closest to the green) is steeply dipping towards the NW. The other two red bodies are inserted to compensate for other low susceptibility zones not involved in this modelling.

As seen in Figure A6-17, the anomaly associated with the lineament MSFR08005 is located at a gradient in the magnetic total field. Due to this, the level of significance in the modelling is considered to be low.



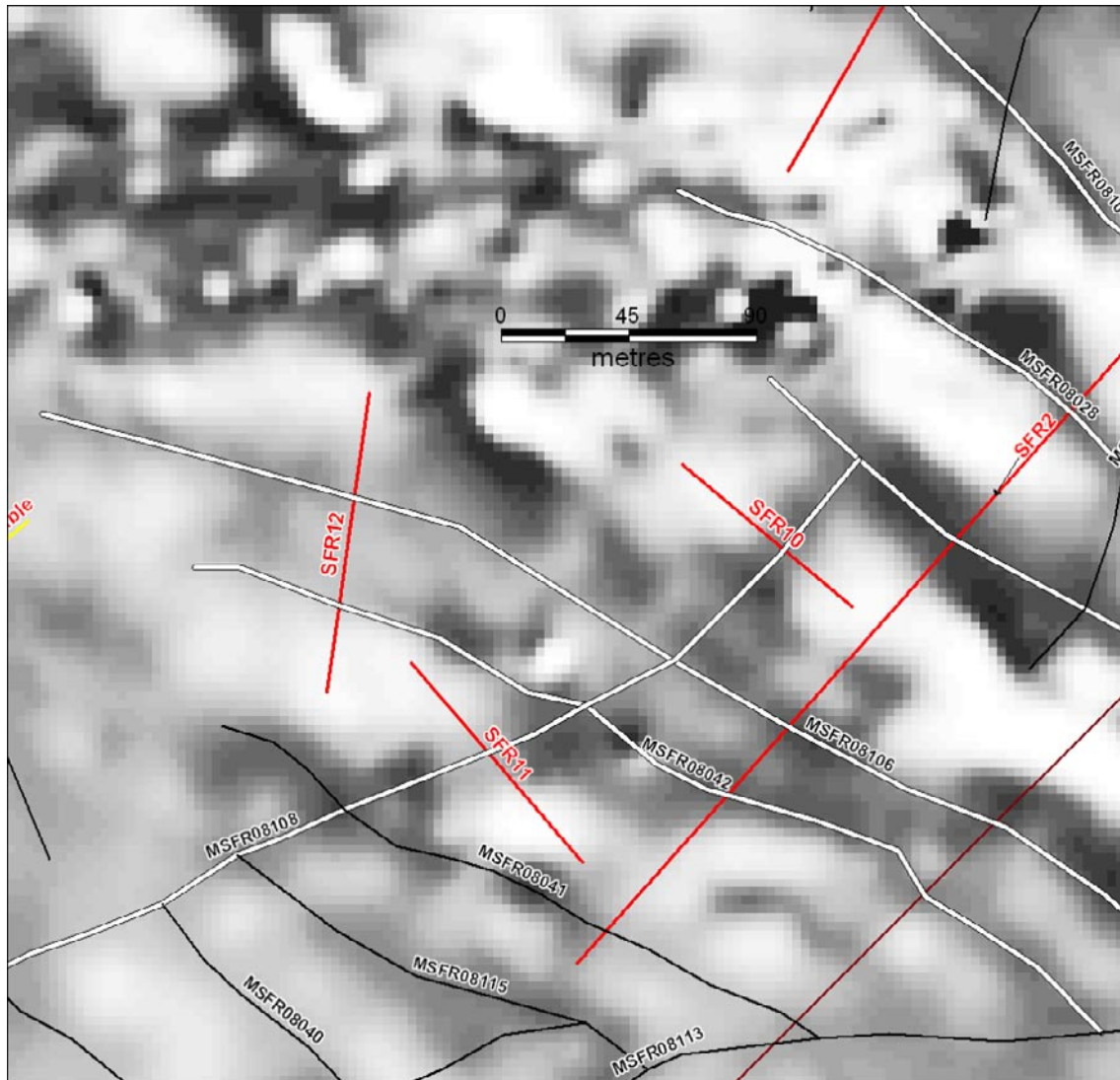
**Figure A6-17.** Modelling result from profile SFR9. In this modelling the low susceptibility body (red) closest to the high susceptibility body (green) is the primary object representing lineament MSFR08005. The right-most two red bodies are only inserted to compensate for their contribution to the magnetic depression at the side of the step-like lineament anomaly (screen dump from Encom ModelVision Pro 8, scale on x- and z-axis may differ).



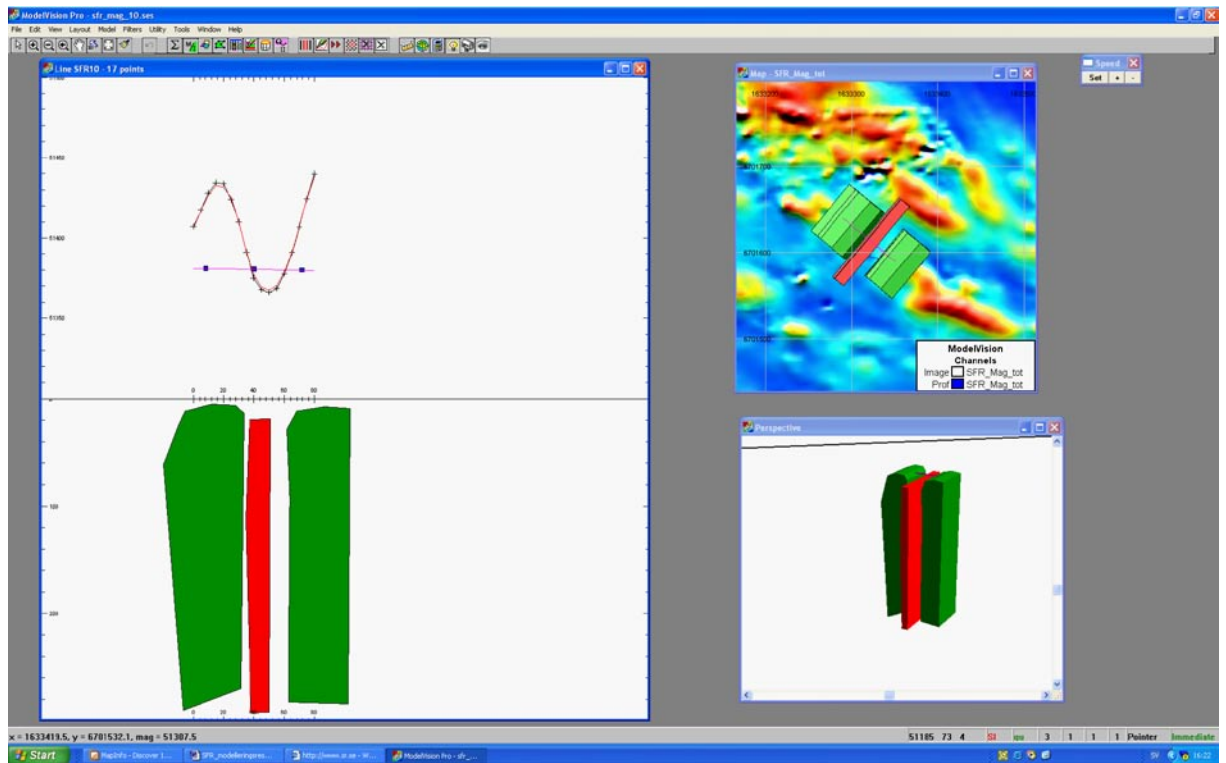
## SFR10 1633290/6701540 – 1633350/6701590

The profile SFR10 crosses the lineament MSFR08108, see Figure A6-18.

A model with one low susceptibility source body (red) and one high susceptibility body at each side (green) is shown in Figure A6-19. The source body to the lineament MSFR08108 (red) is dipping steeply.



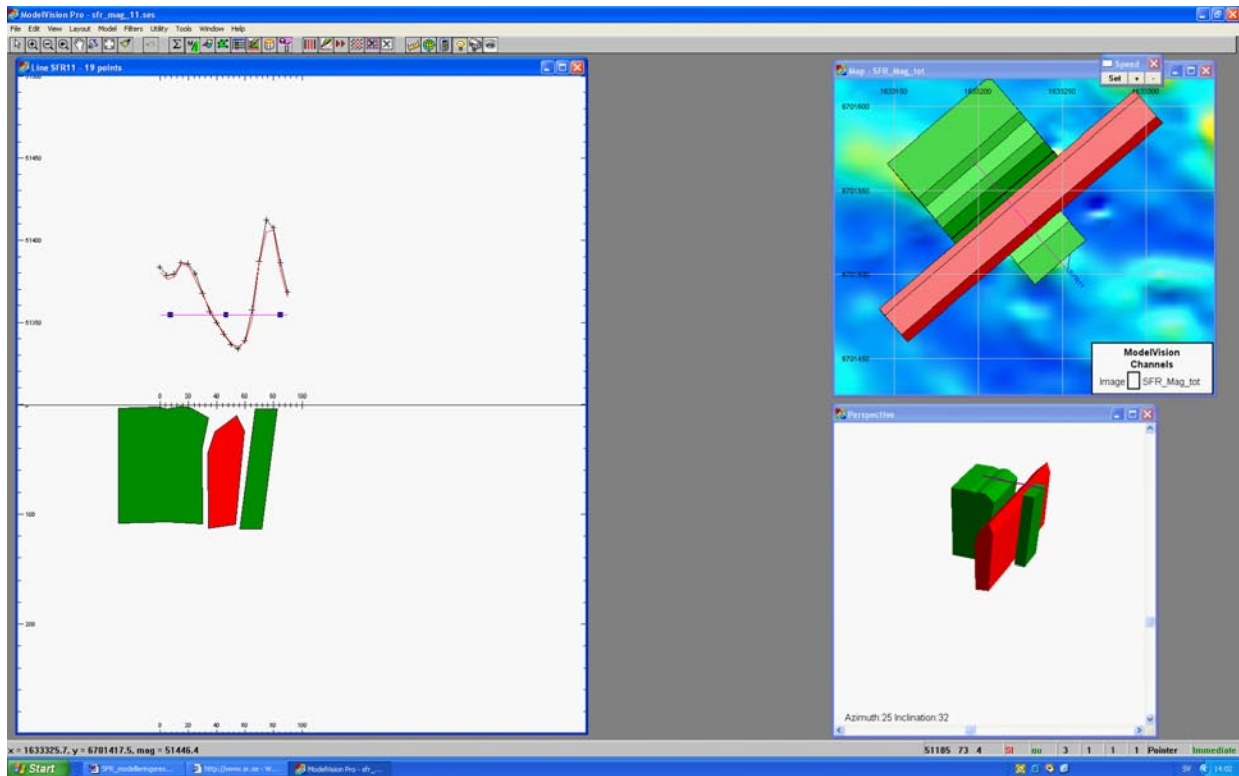
**Figure A6-18.** Profiles SFR10, SFR11 and SFR12 with associated lineament. Only the lineaments represented by thick white and black lines crossing the profile have been modelled. The model area of SFR version 0.1 is visible as a brown line.



**Figure A6-19.** Modelling result from profile SFR10 showing the source body to lineament MSFR08108 (screen dump from Encom ModelVision Pro 8, scale on x- and z-axis may differ).

## SFR11 1633195/6701570 – 1633255/6701500

Profile SFR11 models the anomaly source body to the lineament MSFR08108 (same as profile SFR10). The profile location and its associated lineament are shown above in Figure A6-18. Figure A6-20 shows the model with a low susceptibility source body (red) flanked by two high susceptibility bodies (green). The source body representing the lineament MSFR08108 (in red) is steeply dipping.

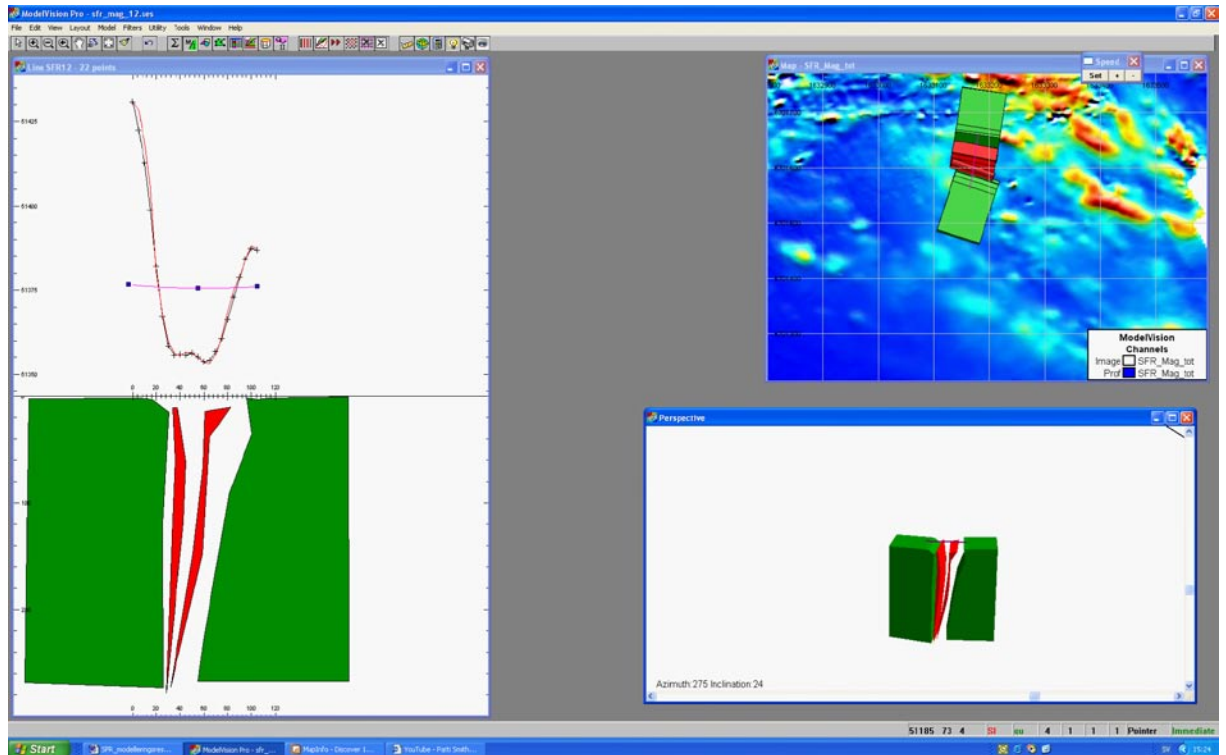


**Figure A6-20.** Modelling result from profile SFR11 with a low susceptibility source body representing the low magnetic anomaly associated with lineament MSFR08108 (screen dump from Encom ModelVision Pro 8, scale on x- and z-axis may differ).

## SFR12 1633165/6701560 – 1633180/6701665

Profile SFR12 models the anomaly sources to the lineaments MSFR08042 and MSFR08106. Profile location and associated lineaments are seen in Figure A6-18 above.

Figure A6-21 shows the model with two low susceptibility source bodies (red), and with bordering high susceptibility bodies (green). The low susceptibility source bodies are located near to each other and are steeply dipping.



**Figure A6-21.** Modelling result from profile SFR12 with two low susceptibility source bodies representing the lineaments MSFR08042 and MSFR08106 (from left to right). (Screen dump from Encom ModelVision Pro 8, scale on x- and z-axis may differ).

**SFR13 1632990/6701560 – 1633060/6701620**

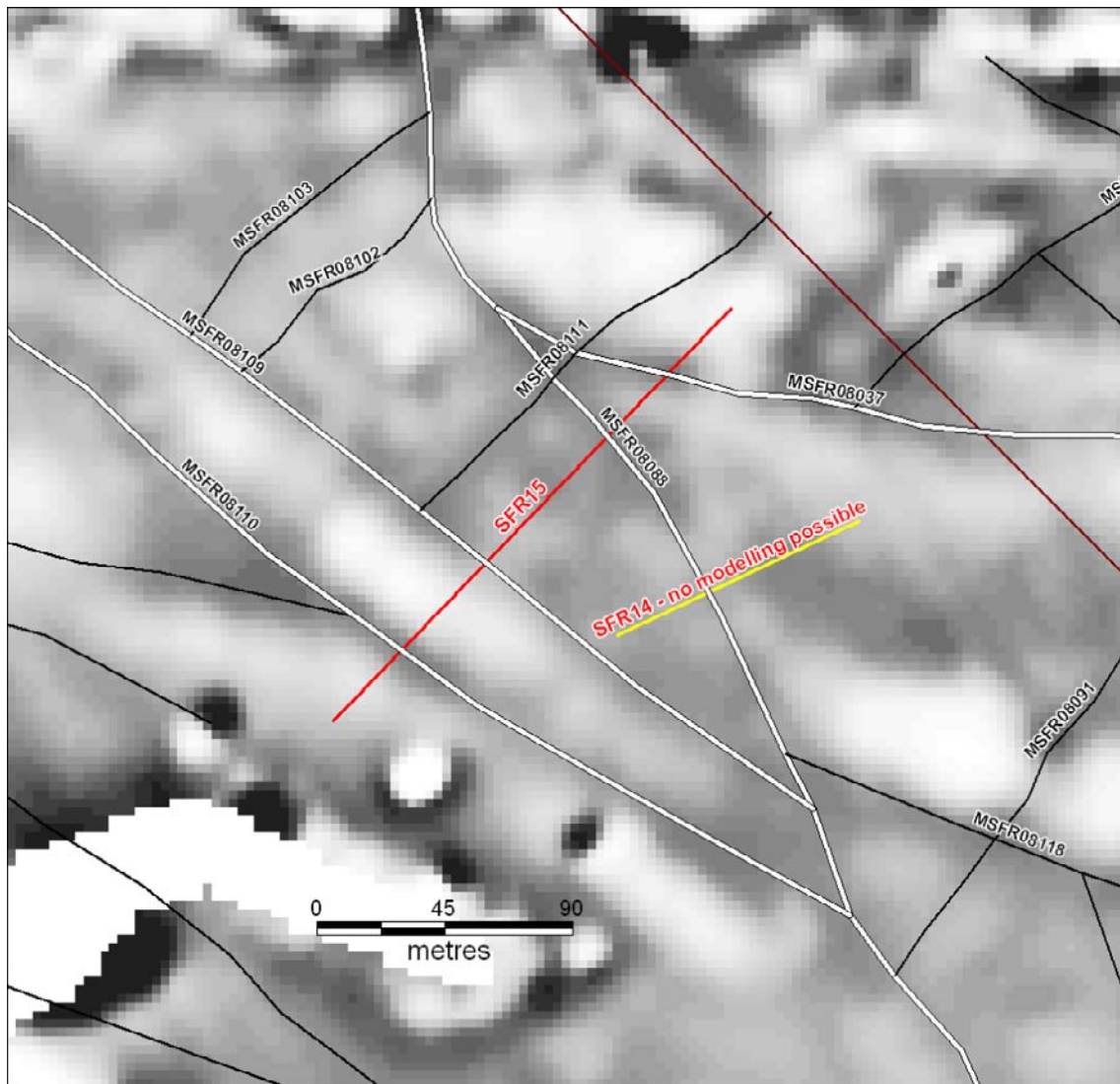
The profile is excluded due to an anomaly too weak for modelling in combination with its position upon a gradient.

**SFR14 1632745/6701485 – 1632830/6701525**

The profile is excluded due to an anomaly too weak for modelling in combination with its position upon a gradient.

**SFR15 1632645/6701455 – 1632785/6701600**

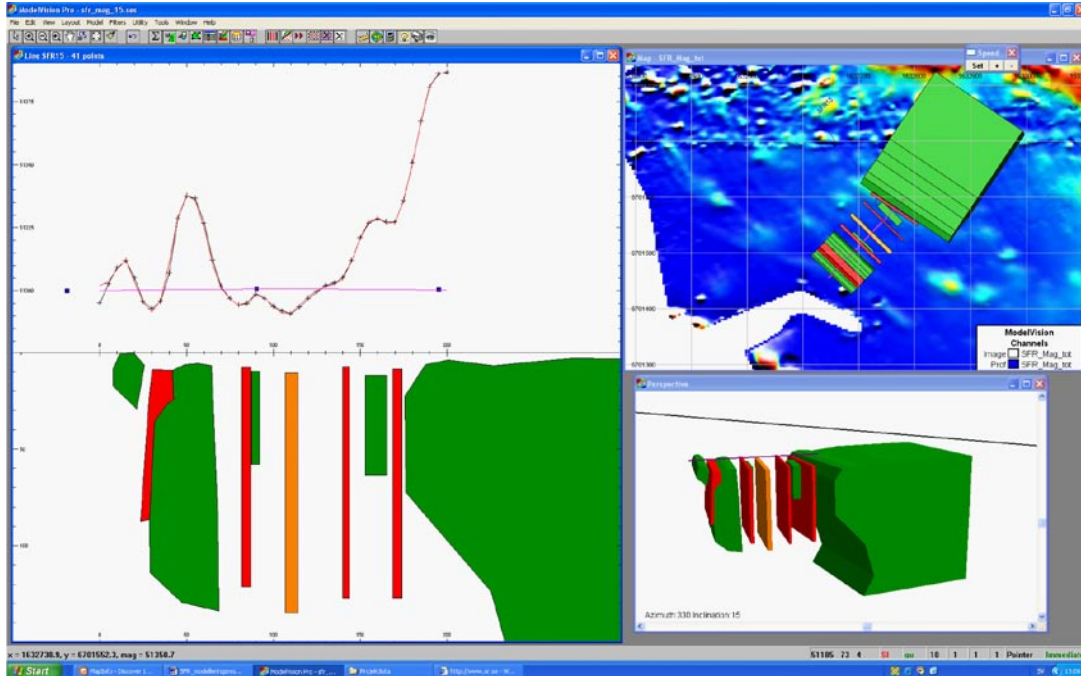
The profile SFR15 crosses the lineaments MSFR08110, MSFR08109, MSFR08088 and MSFR08037, see Figure A6-22.



*Figure A6-22. Profile SFR15 with associated lineament. Only the lineaments represented by thick white and black lines crossing the profile have been modelled. The model area of SFR version 0.1 is visible as a brown line.*



Figure A6-23 shows a model with low susceptibility bodies (red) representing the associated lineaments MSFR08110, MSFR08109, MSFR08088 and MSFR08037. A low susceptibility body is also modelled not coincident with any lineament (orange) and high susceptibility bodies (green). The source body in orange represents a very short linear low magnetic feature not included in the group of lineaments. The source bodies to the lineaments (red) are all steeply dipping.

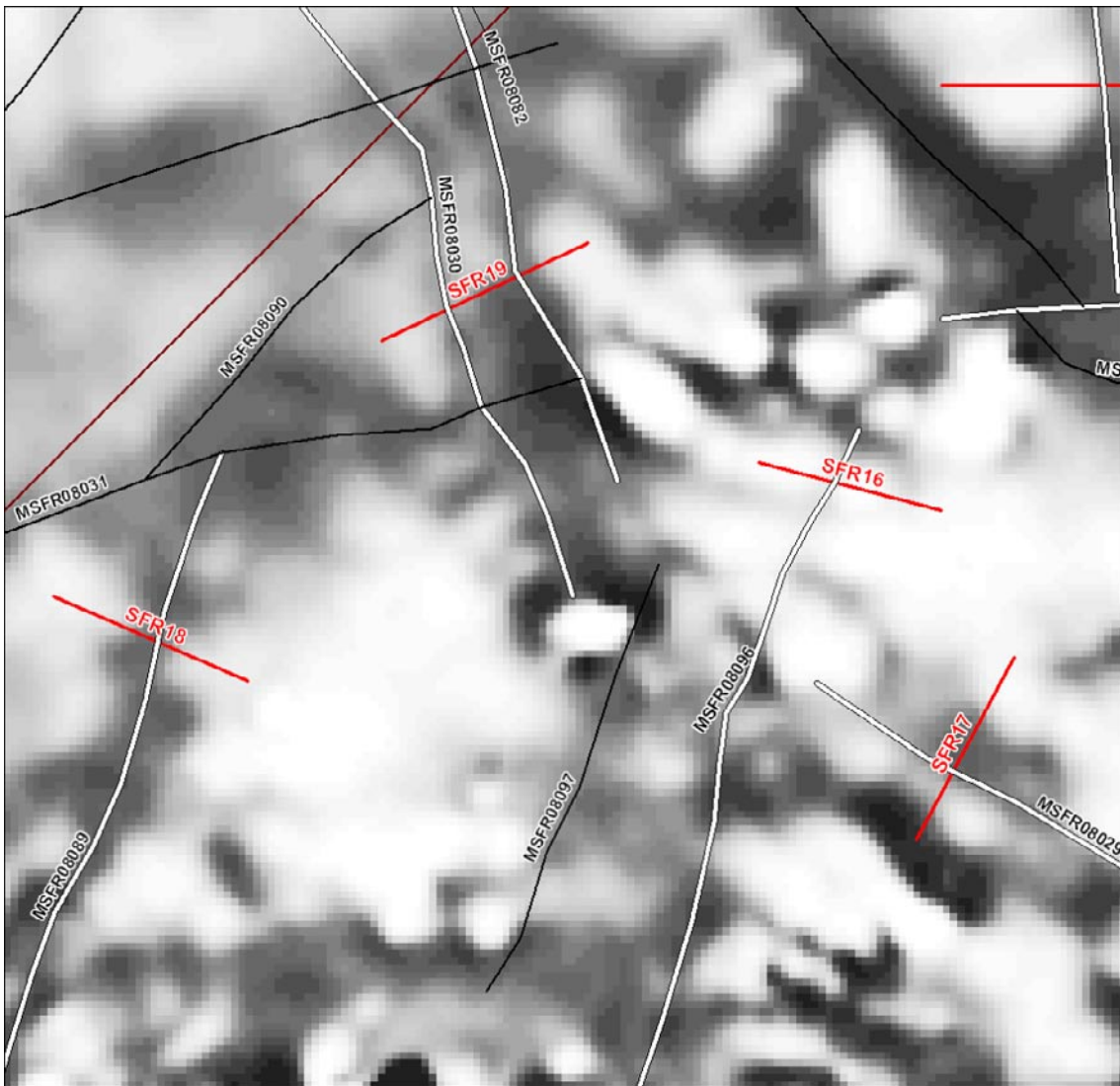


**Figure A6-23.** Modelling result from profile SFR15. The red source bodies represent the lineaments MSFR08110, MSFR08109, MSFR08088 and MSFR08037 (from left to right). The green bodies have high magnetic susceptibilities and are included to compensate for rock volumes with high susceptibilities. The source body in orange is included to model a minimum not associated with any lineament. (Screen dump from Encom ModelVision Pro 8, scale on x- and z-axis may differ).

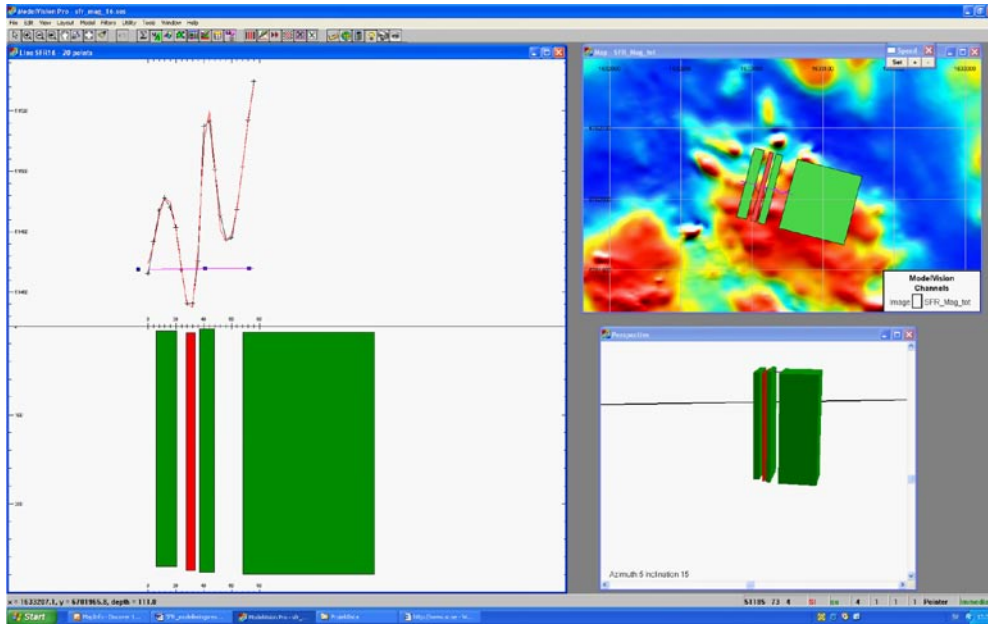
### SFR16 1632985/6702025 – 1633060/6702005

The profile SFR16 crosses the lineament MSFR08096 (see Figure A6-24).

A model with a low susceptibility body (red) and several high susceptibility bodies (green) is shown in Figure A6-25. The source body (red) inferred to represent the lineament MSFR08096 is steeply dipping. A low susceptibility volume is observed between two high susceptibility source bodies in the profile. The minimum is a curved feature in the magnetic total field not included in the lineament identification.



**Figure A6-24.** Profiles SFR16, SFR17, SFR18 and SFR19 with associated lineament. Only the lineaments represented by thick white and black lines crossing the profile have been modelled. The model area of SFR version 0.1 is visible as a brown line.

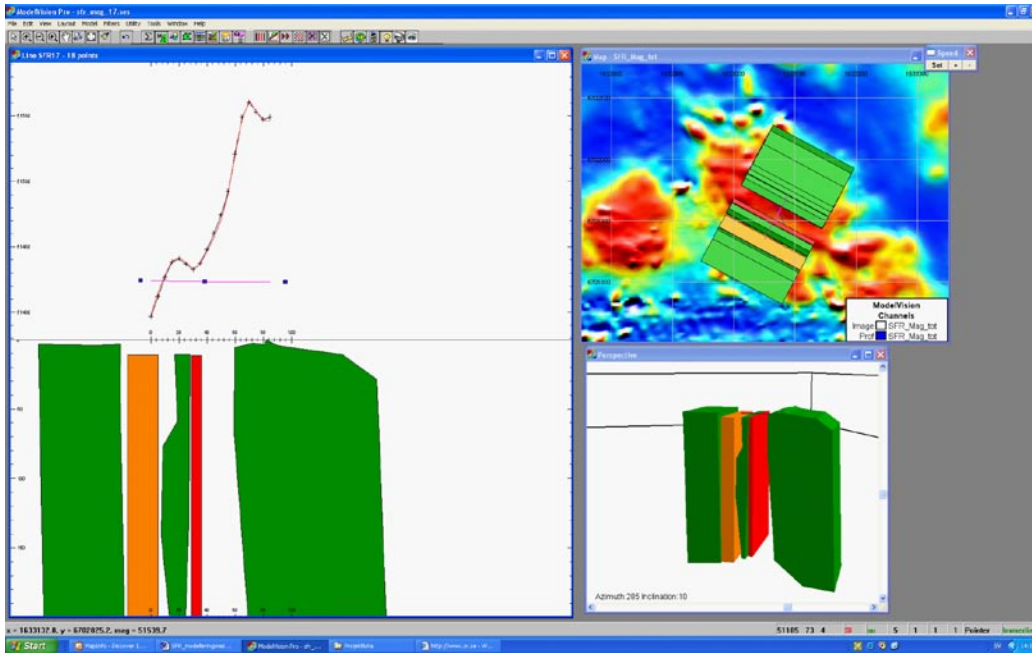


*Figure A6-25. Modelling result from profile SFR16 where the red source body represents the source to the lineament MSFR08096 (screen dump from Encom ModelVision Pro 8, scale on x- and z-axis may differ).*

## SFR17 1633050/6701870 – 1633090/6701945

The location of profile SFR17 and its associated lineament MSFR08029 is shown in Figure A6-24 above.

Figure A6-26 shows the model with one low susceptibility body (red) and several high susceptibility bodies (green) and one body with low susceptibility (orange) not coincident with any lineament. The green bodies and the orange body are inserted to compensate for anomalies in the magnetic field outside the lineament. The source body in red represents the source to lineament MSFR08029, and is dipping vertically.

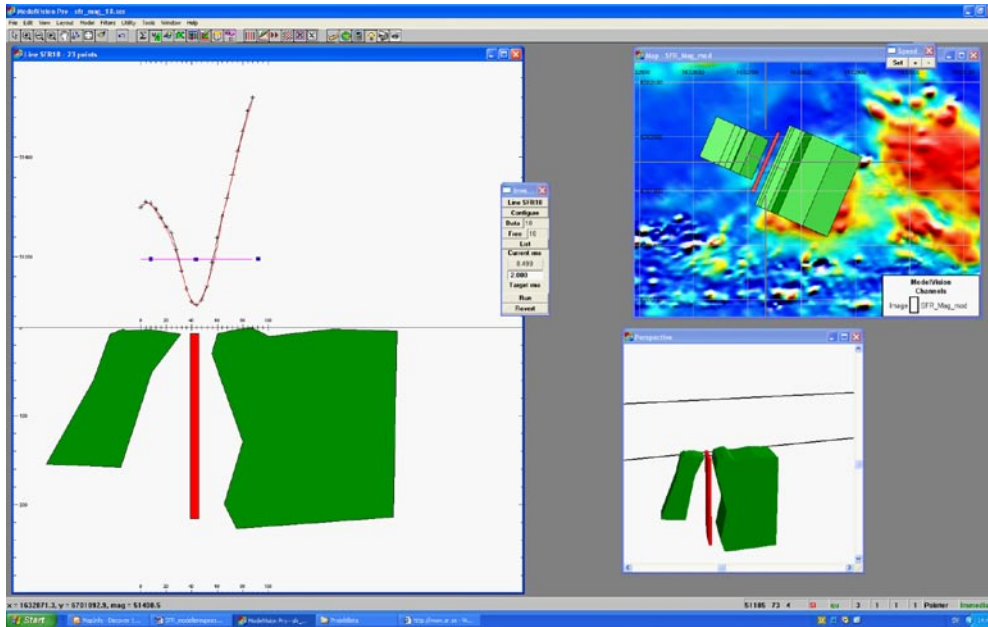


*Figure A6-26. Modelling result from profile SFR17 where the source body in red is representing the source to the lineament MSFR080029. (Screen dump from Encom ModelVision Pro 8, scale on x- and z-axis may differ).*

### SFR18 1632695/6701970 – 1632775/6701935

The location of profile SFR18 and its associated lineament MSFR08089 is shown in Figure A6-24 above.

A model is shown in Figure A6-27 with a low susceptibility body (red) and two high susceptibility bodies (green). The source body (red) is representing the lineament and dips vertically.



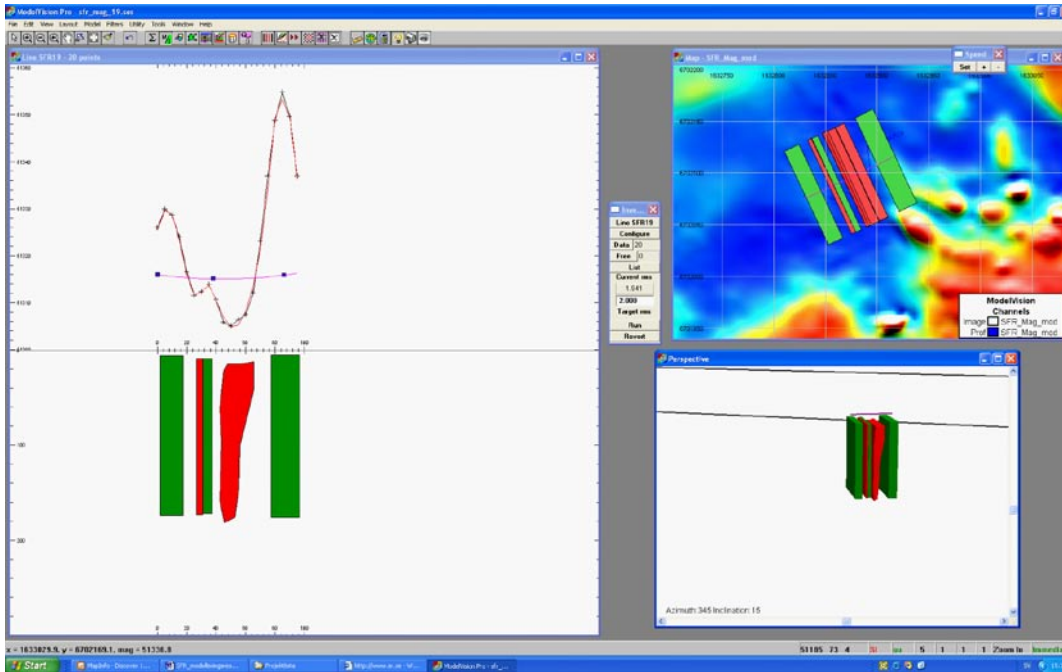
**Figure A6-27.** Modelling result from profile SFR18 with the source body in red representing lineament MSFR08089 (screen dump from Encom ModelVision Pro 8, scale on x- and z-axis may differ).



## SFR19 1632830/6702075 – 1632915/6702115

The location of profile SFR18 and its associated lineaments MSFR08030 and MSFR08082 is shown in Figure A6-24 above.

A model alternative is shown in Figure A6-28 with low susceptibility source bodies (red) and high susceptibility bodies (green). The source bodies in red representing the lineaments dip steeply.



**Figure A6-28.** Modelling result from profile SFR19 with the two source bodies in red representing lineaments MSFR08030 and MSFR08082 (screen dump from Encom ModelVision Pro 8, scale on x- and z-axis may differ).

**Deformation zones on a borehole by borehole and tunnel by tunnel basis**

**Contents**

Table A7-1.	Deformation zones on a borehole by borehole basis
Table A7-2.	Deformation zones on a tunnel by tunnel basis

Table A7-1. Deformation zones on a borehole by borehole basis.

BH	Intercept defined by /Axelsson and Hansen 1997/ (BH length m)		Intercept defined by geological SHI (BH length m)		DZ interception	Geometrical intercept (v0.1) (BH length m)		Target intercept (v0.1) (BH length m)		Comment and SHI Description
	Sec_up	Sec_low	Sec_up	Sec_low		Sec_up	Sec_low	Sec_up	Sec_low	
KFR01	–	–	–	–	zfmWNW0001 Singö	0	eah**	–	–	Entire BH lies within the Singö zone.
KFR02	114.5	124.5	–	–	zfm871_zoneh2_SFR	104.38	129.76	114.5	124.5	Intercept position taken directly from /Axelsson and Hansen 1997/ level 300–290 m.
KFR03	35	35	–	–	zfmNE0870a_zone9a_SFR	32.89	36.88	35	35	/Axelsson and Hansen 1997/ level 380 m.
	86.7	95.5	–	–	zfm871_zoneh2_SFR	74.72	100.10	86.7	95.5	Intercept position taken directly from /Axelsson and Hansen 1997/ level 331–322 m.
	53	53	–	–	zfmNE0870b_zone9b_SFR	51.62	54.62	53	53	/Axelsson and Hansen 1997/ level 365 m.
<b>KFR04</b>	91	100	–	–	zfm871_zoneh2_SFR	80.45	eah	91	100	Intercept position taken directly from /Axelsson and Hansen 1997/ level 326–335 m (control point added at BH length 95.5 m; level 330 m).
	23.5*	23.5*	14	63	zfmNE0807b_zone9b_SFR	21.66	23.94	23	23	<p>Note: SHI interpreted two possible DZs, DZ1 0–3 m and DZ2 14–63 m (BH length) neither of which correlates with ZFM871. However, there are planar chlorite filled fractures from 86 m onwards and some clay filled fractures towards the base of the hole that could be associated with the zone (100.5 m).</p> <p>Intercept position taken directly from /Axelsson and Hansen 1997/, level 400 m. The position falls within a wide SHI possible DZ, DZ2 14–63 m, though since tunnel mapping evidence suggests a much thinner zone the modelled thickness has not been increased to that suggested by the SHI interpretation. The interpreted thickness will be further reviewed during version 1.0.</p> <p>DZ2: Increased frequency of broken and unbroken fractures. One crush at 32.60–32.77 m and one breccia at 33.00–33.22 m. Predominant fracture minerals are laumontite and calcite. Registered <math>\alpha</math>-angles for laumontite-bearing fractures in the interval are generally gently to moderately dipping (&lt; 53°). The occurrence of clay minerals is mainly concentrated to two short sections at 20–23 and 32–36 m length, which corresponds to low single point resistivity anomalies (SPR). The <math>\alpha</math>-angles of these clay filled fractures are moderately to steeply dipping. Generally weak to moderately oxidized. The hydraulic conductivity (measured in sections of about 20–40 m) is low in the whole interval (about 1·10<sup>-8</sup> m/s). Fine to medium grained granite (111058), amphibolite (102017) and felsic to intermediate metavolcanic rock (103076). Confidence level = 2.</p>

BH	Intercept defined by /Axelsson and Hansen 1997/ (BH length m)		Intercept defined by geological SHI (BH length m)		DZ interception	Geometrical intercept (v0.1) (BH length m)		Target intercept (v0.1) (BH length m)		Comment and SHI Description
	Sec_up	Sec_low	Sec_up	Sec_low		Sec_up	Sec_low	Sec_up	Sec_low	
KFR05	85	88	–	–	zfm871_zoneh2_SFR	71.43	95.76	85	88	Intercept position taken directly from /Axelsson and Hansen 1997/ level 343–340 m.
KFR06	–	–	–	–	zfmNE0870b_zone9b_SFR	100.99	112.28	–	–	
KFR08	80*	80*	41	104.4	zfmNW0805a_zone8_SFR	41.18	eoh	41	104.4	The interpreted interval corresponds to KFR08 SHI DZ2.
										SHI DZ2 41–104.4 m: Very high frequency of sealed networks and broken fractures. Nineteen crushed sections. Brittle- to ductile section characterised by fault breccias and cataclasite at 42.25–49.80, 53.83–59.1 and 76–80 m. The predominant fracture filling minerals are calcite, chlorite, laumontite and adularia, typically discoloured by hematite. Registered $\alpha$ -angles for fractures in this interval are variable, but generally moderately dipping. Generally weakly to moderately oxidized with two short sections of quartz dissolution (vuggy rock) at 72.55–73.30 and 77.95–79.55 m. Pegmatitic granite (101061), fine- to medium-grained granite (111058) and moderately foliated metagranite-granodiorite (101057). Confidence level = 3. Moderate hydraulic conductivity (measured in sections of about 20–40 m) of $2\text{--}5\cdot 10^{-7}$ m/s throughout the interval.
	–	–	41	104.4	zfmNW0805b	39.05	49.31	–	–	Note: /Axelsson and Hansen 1997/ approximate position of correlation was BH length 80 m, 407 m level. The interpreted interval corresponds to part of KFR08 SHI DZ2 41–104.4 m. However this interval is inferred as being dominated by ZFMNW0805A and no exclusive evidence for the existence of ZFMNW0805B has been identified. Therefore ZFMNW0805B has been classed as medium confidence.
	–	–	41	104.4	zfmNNW0999	75.72	81.46	–	–	This interval falls within the single thick possible deformation zone interval DZ2 (41–104.4 m) identified in KFR08 SHI. However this interval is inferred as being dominated by ZFMNW0805A and no exclusive evidence for the existence of ZFMNNW0999 has been identified. Therefore ZFMNNW0999 has been classed as medium confidence.

BH	Intercept defined by /Axelsson and Hansen 1997/ (BH length m)		Intercept defined by geological SHI (BH length m)		DZ interception	Geometrical intercept (v0.1) (BH length m)		Target intercept (v0.1) (BH length m)		Comment and SHI Description
	Sec_up	Sec_low	Sec_up	Sec_low		Sec_up	Sec_low	Sec_up	Sec_low	
KFR09	79.5*	79.5*	0	58.7	zfmNNE0869_zone3_SFR	2.53	63.64	0	58.7	Correlated with SHI DZ1 in KFR09, of brittle character.  DZ1: 0–58.7 m. Increased frequency of broken and unbroken fractures and sealed networks. Most intensely fractured between 16–58.7 m. Seven minor intervals of crush. Calcite, chlorite, adularia and laumontite, variably discoloured by microscopic hematite, are the most frequent fracture filling minerals. The occurrence of laumontite is, generally restricted to two distinct sections at 0–24 and 40–45 m, and their $\alpha$ -angles are typically dipping moderately (57–78°). None of the other major mineral phases exhibit such a distinct distribution pattern. Numerous asphalt-bearing fractures have been registered in the length interval 26–61 m. The occurrence of clay mineral fillings is rather scarce. Generally faint to weak oxidation. No hydrogeological investigation data from the upper 7 m of the borehole. The hydraulic conductivity (measured in sections of about 20 m) is moderate to high in the whole interval (above 4·10 <sup>-8</sup> m/s). The maximum measured hydraulic conductivity is 2·10 <sup>-6</sup> m/s in the interval 43–62 m. Felsic to intermediate volcanic rock (103076) with minor occurrences of pegmatitic granite (101061), fine- to medium-grained granite (111058) and amphibolite (102017). Confidence level = 3.  No Control point added.  Note: BH length 79.5 m, level 415 m /Axelsson and Hansen 1997/.
KFR10	–	–	–	–	zfm871_zoneh2_SFR	66.93	95.20	–	–	Intercept position taken directly from /Axelsson and Hansen 1997/ level 350 m. Zone geometry has been defined using SHI BH intercept data. The drill core for this borehole will be inspected during version 1.0 and any target intercept defined. No control point has been in this model version.
	101.5*	101.5*	–	–	zfmNNE0869_zone3_SFR	4.21	97.15	–	–	
KFR11	80*	80*	–	–	zfmNW0805a_zone8_SFR	41.88	eoh	–	–	Note: according to /Axelsson and Hansen 1997/ level 400 m. Zone geometry has been defined using SHI BH intercept data. The drill core for this borehole will be inspected during version 1.0 and any target intercept defined. No control point has been in this model version.
KFR12	–	–	–	–	zfmNW0805b	29.03	40.56	–	–	Intercept position taken directly from /Axelsson and Hansen 1997/ level 391–380 m.
	22	33	–	–	zfm871_zoneh2_SFR	10.65	36.03	22	33	



BH	Intercept defined by /Axelsson and Hansen 1997/ (BH length m)		Intercept defined by geological SHI (BH length m)		DZ interception	Geometrical intercept (v0.1) (BH length m)		Target intercept (v0.1) (BH length m)		Comment and SHI Description
	Sec_up	Sec_low	Sec_up	Sec_low		Sec_up	Sec_low	Sec_up	Sec_low	
KFR13	63.5	65.5	61	68	zfm871_zoneh2_SFR	44.05	69.43	61	68	Intercept position taken directly from DZ4 61.0–68.0 m BH length, with a control point added at BH length 64.5 m. Although the confidence level of DZ4 is low, it shows the general characters of ZFM871, with increased frequency of broken, clay-filled fractures. Moreover, it corresponds largely with the intercept position given by /Axelsson and Hansen 1997/ at level 314–316 m.  61–68 m DZ4: Increased frequency of unbroken and especially broken fractures. Predominant fracture filling minerals are laumontite, chlorite and calcite. A number of broken fractures with clay minerals are concentrated along the section 60.1–64.5 m length. Their $\alpha$ -angles range between 42 and 78°. Increased hydraulic conductivity ( $1-2 \cdot 10^{-7}$ m/s) throughout the interval. Moderately foliated metagranite-granodiorite (101057) and fine- to medium-grained metagranodiorite-tonalite (101051). Confidence level = 1.
KFR14					none					
KFR19					none					
KFR20					none					
KFR21	116	122	–	–	zfm871_zoneh2_SFR	101.67	127.05	116	122	Intercept position taken directly from /Axelsson and Hansen 1997/ level 384–378 m.
KFR22	148	158	–	–	zfm871_zoneh2_SFR	135.57	eoh	148	158	Intercept position taken directly from /Axelsson and Hansen 1997/ level 372–363 m.
KFR23	–	–	–	–	zfm871_zoneh2_SFR	75.96	104.65	–	–	
KFR24	146.5	153	–	–	zfm871_zoneh2_SFR	129.66	157.83	146.5	153	Intercept position taken directly from /Axelsson and Hansen 1997/ level 377–372 m.
	137*	137*	–	–	zfmNW0805a_zone8_SFR	57.53	eoh	–	–	Note: /Axelsson and Hansen 1997/ level 385–385 m. Zone geometry has been defined using SHI BH intercept data. The drill core for this borehole will be inspected during version 1.0 and any target intercept defined. No control point has been in this model version.
	–	–	–	–	zfmNW0805b	59.11	77.60	–	–	
KFR25	133	151	–	–	zfm871_zoneh2_SFR	122.07	148.93	133	151	Intercept position taken directly from /Axelsson and Hansen 1997/ level 404–391 m.

BH	Intercept defined by /Axelsson and Hansen 1997/ (BH length m)		Intercept defined by geological SHI (BH length m)		DZ interception	Geometrical intercept (v0.1) (BH length m)		Target intercept (v0.1) (BH length m)		Comment and SHI Description
	Sec_up	Sec_low	Sec_up	Sec_low		Sec_up	Sec_low	Sec_up	Sec_low	
	174*	174*	–	–	zfmNW0805a_zone8_SFR	52.72	182.93	–	–	Note: according to /Axelsson and Hansen 1997/ level 375–375 m. Zone geometry has been defined using SHI BH intercept data. The drill core for this borehole will be inspected during version 1.0 and any target intercept defined. No control point has been in this model version.
	–	–	–	–	zfmNW0805b	80.66	105.78	–	–	
KFR31	228	232	–	–	zfm871_zoneh2_SFR	214.54	eoh	228	232	Intercept position taken directly from /Axelsson and Hansen 1997/ level349–346 m.
	–	–	–	–	zfmNE0870b_zone9b_SFR	222.29	223.94	–	–	
KFR32	163	186	–	–	zfm871_zoneh2_SFR	153.42	181.76	163	186	Intercept position taken directly from /Axelsson and Hansen 1997/ level 387–370 m.
	–	–	–	–	zfm871_zoneh2_SFR	153.86	eoh	–	–	
KFR33	58*	58*	–	–	zfmNNW1209_zone6_SFR	42.77	106.29	–	–	Note: according to /Axelsson and Hansen 1997/ level 465 m. Zone geometry has been defined using SHI BH intercept data. The drill core for this borehole will be inspected during version 1.0 and any target intercept defined. No control point has been in this model version.
KFR34					none					Base near zfmWNW3262.
KFR35	57.5*	57.5*	32.7	70	zfmNNW1209_zone6_SFR	30.67	72.35	32.7	70	32.7–70 m DZ1: Increased frequency of broken and unbroken fractures and sealed networks. Six crushed intervals in the lower part of the section (57.37–68.15 m). Three intervals at 44.83–46.07, 55.92–56.01 and 60.37–61.60 m include fault breccias and cataclasite. Predominant fracture minerals are adularia, calcite and quartz. $\alpha$ -angles are generally small to moderate (21–61°). Asphaltite, typically associated with calcite, is more or less limited to this section. A black unknown mineral that resembles asphaltite is restricted to 20.1–71.6 m. Locally faint to weak oxidation. One minor core loss at 63.84–64.15 m. Pegmatitic granite (101061) with occurrences of felsic to intermediate metavolcanic rock (103076), fine- to medium-grained granite (111058) and strongly foliated metagranite-granodiorite (101057). Confidence level = 3.
										Note: /Axelsson and Hansen 1997/ approximate position of correlation was 57.5 m BH length, 460 m level.

BH	Intercept defined by /Axelsson and Hansen 1997/ (BH length m)		Intercept defined by geological SHI (BH length m)		DZ interception	Geometrical intercept (v0.1) (BH length m)		Target intercept (v0.1) (BH length m)		Comment and SHI Description
	Sec_up	Sec_low	Sec_up	Sec_low		Sec_up	Sec_low	Sec_up	Sec_low	
KFR36	104*	104*	45	115.5	zfmNNE0869_zone3_SFR	29.58	123.39	45	115.5	<p>One possible deformation zone of brittle character has been recognized with a high degree of confidence in KFR36.</p> <p>45–115.5 m: DZ1: Increased frequency of broken and unbroken fractures and sealed networks. Decreased frequency of broken fractures between 63.5–70 m, which corresponds to the occurrence of pegmatitic granite. The section between 98–115.5 m is the most highly fractured part, with nine crushed sections. The primary infilling minerals in the interval are adularia, calcite and laumontite, together with trace amounts of hematite. Three breccias occur in the interval. <math>\alpha</math>-angles are generally small to moderate (&lt;67°). In the intensely fractured interval at 44–53 m length, there is a majority of fractures filled by calcite and chlorite, with subordinate amounts of hematite. The interval includes one minor crush zone at 49.11–49.15 m. A distinct peak of broken fractures with adularia and chlorite together with a white unidentifiable mineral that might be kaolinite or a zeolite occurs at 60–62 m. Two <math>\alpha</math>-angles at 12 and 30° are registered in the interval. Asphaltite-bearing fractures, concentrated to the interval between 105–114 m. Generally faint to weak oxidation throughout the possible zone. The hydraulic conductivity (measured in 3-m sections) is quite high in the whole interval (<math>6 \cdot 10^{-6}</math>–<math>5 \cdot 10^{-8}</math> m/s). Hydraulic conductivity above <math>1 \cdot 10^{-6}</math> m/s at 48–51, 54–57, 96–99 and 102–108 m.</p> <p>No control point added.</p> <p>Note: BH length 104 m, level 430 m /Axelsson and Hansen 1997/.</p>
KFR37	182	194	–	–	zfm871_zoneh2_SFR	160.27	194.28	182	194	Intercept position taken directly from /Axelsson and Hansen 1997/ level 343–332 m.
KFR38	178	182	–	–	zfm871_zoneh2_SFR	155.04	eoh	178	182	Intercept position taken directly from /Axelsson and Hansen 1997/ level 354–351 m.
KFR51	–	–	–	–	zfmWNNW3145	1.96	7.95	–	–	
KFR52					none					
KFR53	30	30	–	–	zfmNE0870b_zone9b_SFR	29.28	30.51	30	30	Intercept position taken directly from /Axelsson and Hansen 1997/ level 405 m.

BH	Intercept defined by /Axelsson and Hansen 1997/ (BH length m)		Intercept defined by geological SHI (BH length m)		DZ interception	Geometrical intercept (v0.1) (BH length m)		Target intercept (v0.1) (BH length m)		Comment and SHI Description
	Sec_up	Sec_low	Sec_up	Sec_low		Sec_up	Sec_low	Sec_up	Sec_low	
KFR54	38	38	27	40	zfmNE0807b_zone9b_SFR	37.32	39.83	38	38	<p>Intercept position taken directly from /Axelsson and Hansen 1997/, level 390 m. The earlier suggested intercept falls within SHI DZ2 27–40 m though since tunnel mapping evidence suggests a much thinner zone the modelled thickness has not been increased to that suggested by the SHI interpretation. The interpreted thickness will be further reviewed during version 1.0.</p> <p>DZ2: Increased frequency of broken and to a lesser extent unbroken fractures and sealed networks. Decreased frequency of broken fractures between 28.6–33.7 m. Hematite stained clay minerals are restricted to two intervals of anomalously high fracture frequencies at 26.9–28.2 and 31.1–37.4 m, whereas laumontite mainly is restricted to 28.0–31.2 and 37.3–39.1 m. Both assemblages often include calcite. The chlorite content, on the other hand, is very low relative to that in other parts of the drill core. The <math>\alpha</math>-angles of the clay-bearing fractures are typically dipping gently to moderately (30, 37, 60 and 71°). Generally weak to medium oxidation. The hydraulic conductivity is low to very low (<math>10^{-9}</math>–<math>10^{-10}</math> m/s). Generally strongly foliated metagranite-granodiorite (101057) and one occurrence of pegmatitic granite (101061) in the lower most part of the section. Confidence level = 3.</p>
KFR55	48	48	–	–	zfmNE0807b_zone9b_SFR	47.40	48.58	48	48	<p>Intercept position taken directly from /Axelsson and Hansen 1997/, level 365 m. Note that no possible DZ was identified at this position, however, since the zone consists of a single joint for much of its length a control point corresponding to the SHI DZ2, located at a shallower level was not added. Further review may lead to such a point being implemented.</p> <p>8–38 m DZ2: Increased frequency of broken and unbroken fractures and sealed networks, especially in the intervals 8–21 m and 32–38 m. Core loss at 17.86–18.51, 19.13–19.37, 33.48–33.60 and 34.89–35.33 m. The most frequent fracture filling minerals, which occur throughout the interval, are calcite, and to some extent chlorite. Fractures with clay minerals as the primary infilling are generally restricted to the interval at 16.8–19.5 m, with <math>\alpha</math>-angles of 69°. Laumontite <math>\pm</math> calcite filled fractures, on the other hand, occur along three intervals at 8.0–12.6, 16.0–16.5 and 20.4–28.1 m length. Two <math>\alpha</math>-angles are registered in the uppermost (68 and 77°) and three in the lowermost (50, 57 and 65°) intervals. Locally faint to medium oxidation. No hydrogeological investigation data from the upper 22 m of the borehole. The hydraulic conductivity is low in the measured section 22–38 m (<math>10^{-8}</math> m/s). Strongly foliated metagranite-granodiorite (101057) and one occurrence of fine- to medium-grained granite (111058). Confidence level = 3.</p>

BH	Intercept defined by /Axelsson and Hansen 1997/ (BH length m)		Intercept defined by geological SHI (BH length m)		DZ interception	Geometrical intercept (v0.1) (BH length m)		Target intercept (v0.1) (BH length m)		Comment and SHI Description
	Sec_up	Sec_low	Sec_up	Sec_low		Sec_up	Sec_low	Sec_up	Sec_low	
KFR56	68*	68*	–	–	zfmNW0805a_zone8_SFR	63.95	eoh	–	–	Note: according to /Axelsson and Hansen 1997/ level 445 m. Zone geometry has been defined using SHI BH intercept data. The drill core for this borehole will be inspected during version 1.0 and any target intercept defined. No control point has been in this model version.
KFR57	–	–	–	–	zfmNW0805b	59.47	74.87	–	–	
	16.5	22.5	–	–	zfm871_zoneh2_SFR	7.33	eoh	16.5	22.5	Intercept position taken directly from /Axelsson and Hansen 1997/ level 396–390 m.
	12.5*	12.5*	–	–	zfmNNW1209_zone6_SFR	–	–	–	–	Note: according to /Axelsson and Hansen 1997/ level 400 m. Zone geometry has been defined using SHI BH intercept data. The drill core for this borehole will be inspected during version 1.0 and any target intercept defined. No control point has been in this model version.
KFR61	–	–	–	–	zfmWNW0001 Singö	1.4	eoh	–	–	Entire BH lies within the Singö zone.
KFR62	–	–	–	–	zfmWNW0001 Singö	0.5	eoh	–	–	Entire BH lies within the Singö zone.
KFR63					none					
KFR64	–	–	–	–	zfmWNW0001 Singö	0.4	eoh	–	–	Entire BH lies within the Singö zone.
KFR65	–	–	–	–	zfmWNW0001 Singö	0	eoh	–	–	Entire BH lies within the Singö zone.
KFR66	–	–	–	–	zfmWNW0001 Singö	0.5	eoh	–	–	Entire BH lies within the Singö zone.
KFR67	–	–	–	–	zfmWNW0001 Singö	0.6	eoh	–	–	Entire BH lies within the Singö zone.
KFR68	–	–	–	–	zfmWNW1035	0	87.60	–	–	
KFR69	–	–	–	–	zfmNNE0869_zone3_SFR	44.12	eoh	–	–	
	–	–	–	–	zfmWNW3262	155.99	162.99	–	–	
KFR70	–	–	–	–	zfmNE0870a_zon9a_SFR	63.84	68.40	–	–	
KFR71	–	–	–	–	zfmWNW0813	75.66	99.53	–	–	
	–	–	–	–	zfmNNE2308	67.95	85.18	–	–	
KFR80	–	–	–	–	zfm871_zoneh2_SFR	0	17.04	–	–	
KFR83	–	–	–	–	zfm871_zoneh2_SFR	6.27	eoh	–	–	
KFR84	–	–	–	–	zfmWNW0001 Singö	0	eoh	–	–	Entire BH lies within the Singö zone.
KFR85	–	–	–	–	zfmWNW0001 Singö	0	eoh	–	–	Entire BH lies within the Singö zone.
KFR86	–	–	–	–	zfmWNW0001 Singö	0	eoh	–	–	Entire BH lies within the Singö zone.
KFR87	–	–	–	–	zfm871_zoneh2_SFR	0	eoh	–	–	Entire BH lies within zfm871.
KFR88	–	–	–	–	zfm871_zoneh2_SFR	0	eoh	–	–	Entire BH lies within zfm871.



BH	Intercept defined by /Axelsson and Hansen 1997/ (BH length m)		Intercept defined by geological SHI (BH length m)		DZ interception	Geometrical intercept (v0.1) (BH length m)		Target intercept (v0.1) (BH length m)		Comment and SHI Description
	Sec_up	Sec_low	Sec_up	Sec_low		Sec_up	Sec_low	Sec_up	Sec_low	
KFR7A	eoh	eoh	3.5	74.45	zfm871_zoneh2_SFR	3.47	eoh	3.5	74.45	<p>Axelsson and Hansen quote a local elevation corresponding to the approximate end of the borehole (eoh).</p> <p>Intercept position taken directly from the only possible DZ identified in the borehole, DZ1 3.5–74.45 m BH length. While ZFMNW0805A and ZFMNW0805B certainly are present it is considered that this section is dominated by ZFM871. The entire length of DZ1 is thus taken as an intercept with a control point added at BH length 39.0 m.</p> <p>3.5–74.45 m DZ1: Increased frequency of unbroken fractures, sealed networks and especially broken fractures. Nineteen crushes with the most extensive sections at 49.09–74.45 m. Brittle-ductile section characterised by fault breccias and cataclasite at 21–24 m and 64.83–71.29 m. Predominant fracture minerals are clay minerals, calcite and Fe-hydroxide/hematite. The registered <math>\alpha</math>-angles of clay filled fractures are highly variable, ranging from 0 to 85°. Fractures filled with laumontite form swarms throughout the drill core, with the most extensive occurrence at 56.9–64.8 m length. Most of these fractures have gently dipping <math>\alpha</math>-angles less than 25°, with a few ranging up to 55° towards the drill core length axis. Low hydraulic conductivity <math>6 \cdot 10^{-9}</math> m/s in the interval 3.5–19 m. Moderate hydraulic conductivity of <math>5 \cdot 10^{-7}</math> m/s in the interval 20–47 m. High hydraulic conductivity of <math>3 \cdot 10^{-6}</math> m/s in the interval 48–74.45 m. Moderately to strongly foliated metagranite-granodiorite (101057), pegmatitic granite (101061), aplitic metagranite (101058), fine- to medium-grained granite (111058) and amphibolite (102017). Confidence level = 3.</p>
	?	?	3.5	74.45	zfmNW0805a_zone8_SFR	63.61	eoh	64.0	71.3	<p>The target interval corresponds to the lower part of DZ1 that has a brittle ductile character (64.83–71.29 m). The borehole is interpreted to not penetrate the full thickness of the zone.</p> <p>The remainder of the DZ1 interval is interpreted as intercepting both ZFMNW0805B and ZFM871.</p>
	–	–	3.5	74.45	zfmNW0805b	50.32	61.20	–	–	<p>See above for SHI description.</p> <p>This interval falls within the single thick DZ1 (3.5–74.45 m) identified in KFR7A SHI. However this interval is inferred as being dominated by ZFMNW0805A and ZFM871 and no exclusive evidence for the existence of ZFMNW0805B has been identified. Therefore ZFMNW0805B has been classed as medium confidence.</p> <p>See above for SHI description.</p>

BH	Intercept defined by /Axelsson and Hansen 1997/ (BH length m)		Intercept defined by geological SHI (BH length m)		DZ interception	Geometrical intercept (v0.1) (BH length m)		Target intercept (v0.1) (BH length m)		Comment and SHI Description
	Sec_up	Sec_low	Sec_up	Sec_low		Sec_up	Sec_low	Sec_up	Sec_low	
KFR7B	12	16	0	17	zfm871_zoneh2_SFR	1.11	eoh	0	17	<p>Intercept position taken directly from the only possible DZ identified in the borehole, DZ1 0–17 m BH length, with a control point added at BH length 8.5 m.</p> <p>0–17 m DZ1: Increased frequency of unbroken and especially broken fractures. Four crushed sections at 0.67–1.01, 4.14–4.33, 14.34–14.88 and 15.98–16.25 m and two core losses at 14.48–14.88 and 15.98–16.25 m. Predominant fracture minerals are calcite, chlorite and clay minerals, locally with hematite/Fe-hydroxide staining. <math>\alpha</math>-angles are ranging between 43 and 72°. No hydrogeological investigation data from the upper 4 m of the borehole. Moderate hydraulic conductivity of <math>1 \cdot 10^{-8}</math> m/s in the interval 4–7 m. High hydraulic conductivity of <math>2 \cdot 10^{-6}</math> m/s in the interval 8–17 m. Moderately foliated metagranite-granodiorite (101057) and pegmatitic granite (101061). Confidence level = 3.</p> <p>Note: according to /Axelsson and Hansen 1997/ level 355–351 m.</p>
KFR7C	8	22	6	32	zfm871_zoneh2_SFR	7.06	eoh	6	32	<p>Intercept position taken directly from the only possible DZ identified in the borehole, DZ1 6.0–32.0 m BH length, with a control point added at BH length 19.0 m.</p> <p>6–32 m DZ1: Increased frequency of unbroken and especially broken fractures. Five crushes in the intervals 7.89–7.95, 8.11–8.19, 8.47–8.50, 9.25–9.40 and 14.67–14.77 m. Predominant fracture minerals are clay minerals, locally accompanied by Fe-hydroxide/hematite discolouration, chlorite and calcite. Most fractures have <math>\alpha</math>-angles that are moderate (29–74°). Virtually all laumontite-bearing fractures are concentrated in a zone with low <math>\alpha</math>-angles (9 and 10° for individual fractures) at 6.24–7.15 m length. Locally faint oxidation and minor argillization. Moderate hydraulic conductivity <math>2 \cdot 10^{-8}</math> m/s throughout the interval. Strongly foliated metagranite-granodiorite (101057), fine- to medium-grained granite (111058) and pegmatitic granite (101061). Confidence level = 3.</p> <p>Note: according to /Axelsson and Hansen 1997/ level 359–346 m.</p>
	–	–	6	32	zfmNE0870b_zone9b_SFR	0	1.55	–	–	<p>Begins in the zone. The intercept is marginal and in fact there is a corresponding recorded possible DZ in the SHI (DZ1 6–32 m). However, while it is quite possible the zone intercepts at this interval no control point has been added since it is considered that DZ1 is dominated by an intercept with ZFM871.</p>

BH	Intercept defined by /Axelsson and Hansen 1997/ (BH length m)		Intercept defined by geological SHI (BH length m)		DZ interception	Geometrical intercept (v0.1) (BH length m)		Target intercept (v0.1) (BH length m)		Comment and SHI Description
	Sec_up	Sec_low	Sec_up	Sec_low		Sec_up	Sec_low	Sec_up	Sec_low	
HFM34	–	–	37 180	133 184	zfmWNW0001 Singö	6.89	182.52	–	–	The entire borehole intercepts at the junction between the regional Singö zone ZFMWNW0001 and ZFMNNE0869. It is interpreted that ZFMWNW0001 dominates the deformation seen in DZ1 whilst information from DZ2 and DZ3 is too limited to judge.
	–	–	188	192	zfmNNE0869_zone3_SFR	182.52	eoh	–	–	For SHI description see /Carlsten et al. 2007/ and for further details /Stephens et al. 2008a/. The entire borehole intercepts at the junction between the regional Singö zone ZFMWNW0001 and ZFMNNE0869. It is interpreted that ZFMWNW0001 dominates the deformation seen in DZ1 whilst information from DZ2 and DZ3 is too limited to judge.
	–	–	–	–	zfmNW0002	192.37	eoh	–	–	For SHI description see /Carlsten et al. 2007/ and for further details /Stephens et al. 2008a/.
HFM35	–	–	24 47	33 53	zfmNW0002	0	54.17	–	–	For SHI description see /Carlsten et al. 2007/ and for further details /Stephens et al. 2008a/.
	–	–	104	200	zfmWNW1035	152.20	eoh	–	–	For SHI description see /Carlsten et al. 2007/ and for further details /Stephens et al. 2008a/.
KFM11A	–	–	245	824	zfmWNW1035	684.57	767.93	–	–	For SHI description see /Carlsten et al. 2007/ and for further details /Stephens et al. 2008a/.
	–	–	245	824	zfmWNW0001 Singö	552.15	735.52	–	–	For SHI description see /Carlsten et al. 2007/ and for further details /Stephens et al. 2008a/.
	–	–	245	824	zfmNW0002	716.77	814.76	–	–	For SHI description see /Carlsten et al. 2007/ and for further details /Stephens et al. 2008a/.

\* Approximate centre of the zone.

\*\* eoh = end of the borehole.

\*\*\* **KFR04**, bold text indicates a borehole with remapped drillcore in the Boremap system /Pettersson and Andersson 2008, Pettersson et al. 2009/.

**Table A7-2. Deformation zones on a tunnel by tunnel basis. Target intercepts are quoted as tunnel centreline intercepts and are based on inspection of the detailed geological tunnel mapping results as presented in /Christiansson and Bolvede 1987/ after review of the intercepts quoted by /Axelsson and Hansen 1997/. Note /Axelsson and Hansen 1997/ quote the position of deformation zones relative to the tunnel walls rather than to the tunnel centreline.**

SFR Facility part	Intercept defined by /Axelsson and Hansen 1997/ (chainage m)		DZ interception	Geometrical intercept (chainage m)		Target intercept (chainage m)		Comment and SHI Description
DT	1+530	1+570	zfmNE0870a_zone9a_SFR	1+525	1+535	1+530	1+530	
	1+610	1+610	zfmNE0870a_zone9a_SFR	1+610	1+610	1+610	1+610	Connection between DT and BT
	1+470	1+495	zfmNNE0869_zone3_SFR	1+430	1+555	1+430	1+540	
	1+930	1+930	zfmNNW1209_zone6_SFR	1+920	1+945	1+930	1+930	
	–	–	zfmWNW1035	1+430	1+490	1+422	1+490	Tunnel mapping suggests the zone is offset across the NNE striking ZFMNNE0869 and the judgement of thickness is considered low confidence (it could be considerably less)
	–	–	zfmWNW0001 Singö	1+187	1+298	1+208	1+296	
	–	–	zfmNW0002	1+300	1+368	1+300	1+368	
	–	–	zfmWNW3262	1+890	1+896	1+893	1+893	Weak correlation with two, very local, discontinuous crushes
BT	5+640	5+690	zfmNE0870a_zone9a_SFR	5+658	5+670	5+660	5+660	
	–	–	zfmNE0870b_zone9b_SFR	5+890	5+900	5+895	5+895	Connection with NBT
	6+025	6+050	zfmNE0870b_zone9b_SFR	6+032	6+035	6+033	6+033	
	5+390	5+420	zfmNNE0869_zone3_SFR	5+357	5+482	5+350	5+460	
	–	–	zfmNNW1209_zone6_SFR	5+885	5+907	5+893	5+893	
	–	–	zfmWNW1035	5+402	5+463	5+400	5+472	Tunnel mapping suggests the zone is offset across the NNE striking ZFMNNE0869 and the judgement of thickness is considered low confidence (it could be considerably less)
	–	–	zfmWNW0001 Singö	5+173	5+285	5+187	5+275	
	–	–	zfmNW0002	5+288	5+356	5+286	5+350	
–	–	zfmWNW3262	5+883	5+887	5+885	5+885	Weak correlation with a minor gouge filled fracture zone (<2 dm thick) of similar orientation to overlying lineament and also a very local crush	
NBT	8+405	8+435	zfm871_zoneh2_SFR	8+382	>8+432	8+405	8+432	Control point added at chainage 8+405. Position is estimated from the tunnel chainage line, detailed tunnel mapping drawing –017 /Christiansson and Bolvede 1987/ and laser surveyed tunnel profile sections. Due to the gentle dip and nature of the zone the selected central point, representing the zone position, is approximate

Note: /Axelsson and Hansen 1997/ estimate NBT 8+405 to 8+435 and that the zone also occurs in the connecting rock drainage basin (BB)

The modelled zone geometry also encompasses the rock drainage basin (BB), the support shaft (FS) and nearby niches (connection to the NBT at 8+405) but no detailed survey measurements are available for chainage estimates

SFR Facility part	Intercept defined by /Axelsson and Hansen 1997/ (chainage m)		DZ interception	Geometrical intercept (chainage m)		Target intercept (chainage m)		Comment and SHI Description
	8+025	8+025	zfmNE0870b_zone9b_SFR	8+001	8+003	8+002	8+002	
	8+290	8+350	zfmNE0870b_zone9b_SFR	8+357	8+362	8+358	8+358	
	–	–	zfmNNW1209_zone6_SFR	8+000	8+010	–	–	
1 BTF	0+100	0+100	zfmNNW1209_zone6_SFR	0+090	0+117	0+100	0+100	
2 BTF	0+085	0+085	zfmNNW1209_zone6_SFR	0+067	0+090	0+080	0+080	
BLA	0+060	0+060	zfmNNW1209_zone6_SFR	0+048	0+068	0+060	0+060	
BMA	0+030	0+030	zfmNNW1209_zone6_SFR	0+030	0+055	–	–	
TT	–	–	zfmWNW3262	7+066	7+074	7+062	7+075	Weak correlation with a steeply dipping joint swarm of similar orientation to overlying lineament
								Although the modelled geometry intercepts the connecting tunnel between TT and 1-BTF the detailed mapping provides no evidence to support the structure in this location
IST	4+090	4+090	zfmNE0870b_zone9b_SFR	4+088	4+090	4+090	4+090	
STT	6+800	6+820	zfmNE0870b_zone9b_SFR	*	*	*	*	* This location is at the connection between BT and STT



**Basis for interpretation of all deformation zones and property tables for deformation zones focused on during model version 0.1**

**Contents**

Summary of the basis for interpretation of all deformation zones inside the regional model volume

Explanation of descriptive format

ZFM871

ZFMNNE0869

ZFMNE0870A and ZFMNE0870B

ZFMWNW0001

ZFMWNW1035

ZFMWNW3262

ZFMNW0002

ZFMNW0805A and ZFMNW0805B

ZFMNW0805B

ZFMNNW0999

ZFMNNW1209

## Summary of the basis for interpretation of all deformation zones inside the regional model volume

DZ Name	Basis for interpretation
Gently dipping DZs	
zfm871_zoneh2_SFR*	No clearly identified magnetic lineament. Borehole target intercepts with KFR02, KFR03, KFR04, KFR05, KFR7A, KFR7B, KFR7C, KFR12, KFR13, KFR21, KFR22, KFR24, KFR25, KFR31, KFR32, KFR37, KFR38, KFR57. Tunnel target intercept with NBT
ZFMA1**	No surface interception. Based on seismic reflector A1/A0 /Juhlin et al. 2002, Cosma et al. 2003/ and Forsmark stage 2.2 deformation zone model in /Stephens et al. 2007/
Steeply dipping DZs	
NNE to ENE set	
ZFMNNE0725	V2.3 MFM0725G. The earlier Forsmark v2.2 modelled zone /Stephens et al. 2007/ had a lesser extent that did not penetrate the SFR regional model volume. Medium confidence – until further review
zfmNNE0869_zone3_SFR*	MSFR08089 (extended beyond the lineament based on tunnel mapping). Borehole target intercepts with KFR09 and KFR36. Tunnel target intercept with DT and BT
ZFMNNE2308	MFM2308G and its inferred continuation to the north-east /Stephens et al. 2007/. Dip based on comparison with high confidence steeply dipping zones with similar strike /Stephens et al. 2007/
zfmNNE3110	MFM3110G
zfmNNE3117	MFM3117G and MSFR08097
ZFMNNE3130	MFM3130G
zfmNNE3146	MSFR08084 and MFM3146G
zfmNNE3264	MFM3264G and MSFR08001
zfmNNE3265	MFM3265G
zfmNNE3266	MFM3266G
zfmNNE3271	MFM3271G
zfmNNE8027	MSFR08027
zfmNE0870A_zone9a_SFR*	No clearly identified magnetic lineament. Borehole target intercepts with KFR02. Tunnel target intercept with DT and BT.
zfmNE0870B_zone9b_SFR*	No clearly identified magnetic lineament. Borehole target intercepts with KFR03, KFR04, KFR53, KFR54, KFR55, KFR7C. Tunnel target intercept with BT and NBT.
zfmNE3112	MFM3112G
zfmNE3134	MFM3134G
zfmNE3137	MFM3137G and MSFR08091
zfmNE3141	MFM3134G
ZFMNE3153	MFM3153G
zfmNE8026	MSFR08026
zfmENE3109	MFM3109G and MSFR08108
zfmENE3115	MFM3115G and MSFR08116
zfmENE3135	MFM3135G and MSFR08113
zfmENE3151	MFM3151G and MSFR08005
zfmENE8031	MSRF08031
zfmENE8034	MSFR08034 and MSFR08092
WNW to NW set	

DZ Name	Basis for interpretation
ZFMWNNW0001_SFR_Singó*	MFM0803G0, HFM34 and KFM11A (none of the borehole data were directly included in the current work). Tunnel target intercept with DT and BT in addition to Forsmark tunnel intercepts outside of the SFR regional model volume. Essentially based on Forsmark stage 2.2 deformation zone model in /Stephens et al. 2007/ with a local modelled thickness based on SFR tunnel intercepts
ZFMWNNW0813	MFM0813G
zfmWNNW0835	MFM0835BG, MSFR08107 and MSFR08106
ZFMWNNW0836	MFM0836G and MSFR08007
ZFMWNNW1035*	MFM1035G, MSFR08123, MSFR08118 and MSFR08110. Tunnel target intercepts with DT and BT
ZFMWNNW1056	MFM1056G
ZFMWNNW2496	MFM2496G, MSFR08059 and MSFR08060
zfmWNNW3145	MFM3145G. No indication of existence identified in SFR tunnel geometrical intercepts
ZFMWNNW3259	MFM3259G, MSFR08075, MSFR08074 and MSFR08073
zfmWNNW3262*	MFM3262G and MSFR08105, Tunnel target intercepts with DT, BT and TT
zfmWNNW3267	MFM3267G, MSFR08121 and MSFR08115
ZFMWNNW3268	MFM3268G
zfmWNNW8028	MSFR08028
zfmWNNW8037	MSFR08037
zfmWNNW8041	MSFR08041
zfmWNNW8042	MSFR08042
zfmWNNW8043	MSFR08043, MSFR08045 and MSFR08046
ZFMNNW0002*	MFM0804G and MSFR08085; HFM34, HFM35 and KFM11A (none of the borehole data were directly included in the current work). Tunnel target intercept with DT and BT. Essentially based on Forsmark stage 2.2 deformation zone model in /Stephens et al. 2007/ with a local modelled thickness based on SFR tunnel intercepts
zfmNNW0805A_zone8_SFR*	MFM0805G0, MSFR08093, MSFR08094, MSFR08095. Borehole target intercepts with KFR7A and KFR08
zfmNNW0805B*	MFM0805G1, MSFR08104 and MSFR08098
NNW set	
zfmNNW0999*	MFM0999G. Property table included due to its possible intersection of KFR08
zfmNNW1034	MFM1034G, MSFR08100 and MSFR08101
zfmNNW1209_zone6_SFR*	MFM3114G. Borehole target intercept with KFR35. Tunnel target intercepts with DT, BT, NBT, 1 BTF, 2 BTF, 1BLA and 1BMA
zfmNNW3111	MFM3111G and MSFR08099
zfmNNW3113	MFM3113G and MSFR08079
zfmNNW3119	MFM3119G and MSFR08082
zfmNNW3140	MFM3140G and MSFR08067
ZFMNNW3148	MFM3148G
zfmNNW3155	MFM3155G
zfmNS3154***	MFM3154G

\* a separate more detailed property table exists.

\*\* ZFM, upper case indicates that the entire zone lies outside of the local model volume.

\*\*\*zfm, lower case indicates that some part of the DZ falls within the local model volume.

	High confidence (in existence)
	Medium confidence (in existence)
	Low confidence (in existence)

## Explanation of descriptive format

### Deformation zone name (zone XX SFR) xx = zone name from the SFR construction phase

Modelling procedure: A short outline of the basis for the modelled geometry representing the deformation zone

Location figure showing ground surface intersection position of the deformation zone trace in colour (without thickness). All the other deformation zone traces are shown in grey

Confidence of existence: Confidence level rated as high (coloured red in the model) /medium (coloured green in the model) /low (coloured grey in the model) based on the amount of supporting evidence (see section 5.1 of the main report)

Property	Quantitative estimate	Confidence level	Basis for interpretation	Comments
Orientation (strike/dip)	xxx / xx Strike /dip Right-hand rule	x / x Rated as high/medium/low based on a subjective assessment of available background data	Type of data lying behind the interpretation	
Thickness	x m envelope thickness as modelled in RVS (see section 5.1 of the main)	x Rated as high/medium/low based on a subjective assessment of available background data	Type of data lying behind the interpretation	Occasionally supported by a figure showing the modelled zone boundaries and key intercepting boreholes. The position and extent of the relevant SHI DZ's being shown as pink cylinders. The zone boundaries shown are seen to have a variable thickness though this is only due to the 3D perspective
Length (regional model)	x m Total length of the deformation zone trace interception with the ground surface without reference to model boundaries	x Rated as high/medium/low based on a subjective assessment of available background data	Type of data lying behind the interpretation	
Deformation style	Ductile and/or brittle character			
Alteration	Type and degree of alteration			

### Borehole intersections for deformation zone – details

BH	Geometrical intercept		Target intercept		Comment
	Sec_up BH length (m) [z (-m)]	Sec_low BH length (m) [z (-m)]	Sec_up BH length (m) [z (-m)]	Sec_low BH length (m) [z (-m)]	
KFRxx (BH name)	xx= borehole length m	xx= borehole length m	xx= borehole length m	xx= borehole length m	See section 5.1 of the main report for the definition of geometrical and target intercepts
	[xx = elevation (-masl)]	[xx = elevation (-masl)]	[xx = elevation (-masl)]	[xx = elevation (-masl)]	Eoh = end or bottom of borehole BH = borehole

Tunnel intersections for deformation – details					
Tunnel ID	Geometrical intercept		Target intercept		Comment
	Start ch.(m)	End ch. (m)	Start ch.(m)	End ch. (m)	
Tunnel	xxx	xxx	xxx	xxx	DT = operating tunnel
ID	chainage	chainage	chainage	chainage	BT = construction tunnel. See Figure 4-1 for other abbreviations.
	(x+xxx)	(x+xxx)	(x+xxx)	(x+xxx)	Chainage refers to tunnel centreline intersections
	Original chainage*	Original chainage*	Original chainage*	Original chainage*	* The numbering system used during the construction phase /Christiansson and Bolvede 1987/ These chainages are general zone boundary/ tunnel wall intersections

#### Engineering characteristics

Short summary of relevant data. Currently only previously reported data. This section will be expanded during version 1.0

### ZFM871

Zone ZFM871, previously known as zone H2 in earlier SFR models, has been modelled to terminate against ZFMWNW0001A (Singö zone) in the SW and against ZFMNW0805A in the NE. The extension of this zone follows that presented in /Stephens et al. 2007/. However, there has been a minor adjustment to the geometrical configuration of the zone and this modification has led to a change in modelled orientation from 048/15 /Stephens et al. 2007/ to 071/19. However, the difference in dip lies within the span provided in the property table for the zone in /Stephens et al. 2007/ and the change in strike is minor, bearing in mind the gentle dip of the zone.

The zone has been modelled as a best fit plane, based on the interpreted borehole and tunnel intersections, with an applied envelope thickness of 24 m to contain all the interpreted target intercepts. The zone is interpreted as consisting of a group of parallel oriented, smaller hydraulically conductive structures separated by ordinarily fractured rock. The spread of indications suggest that the structure is complex and has a stepped geometry.

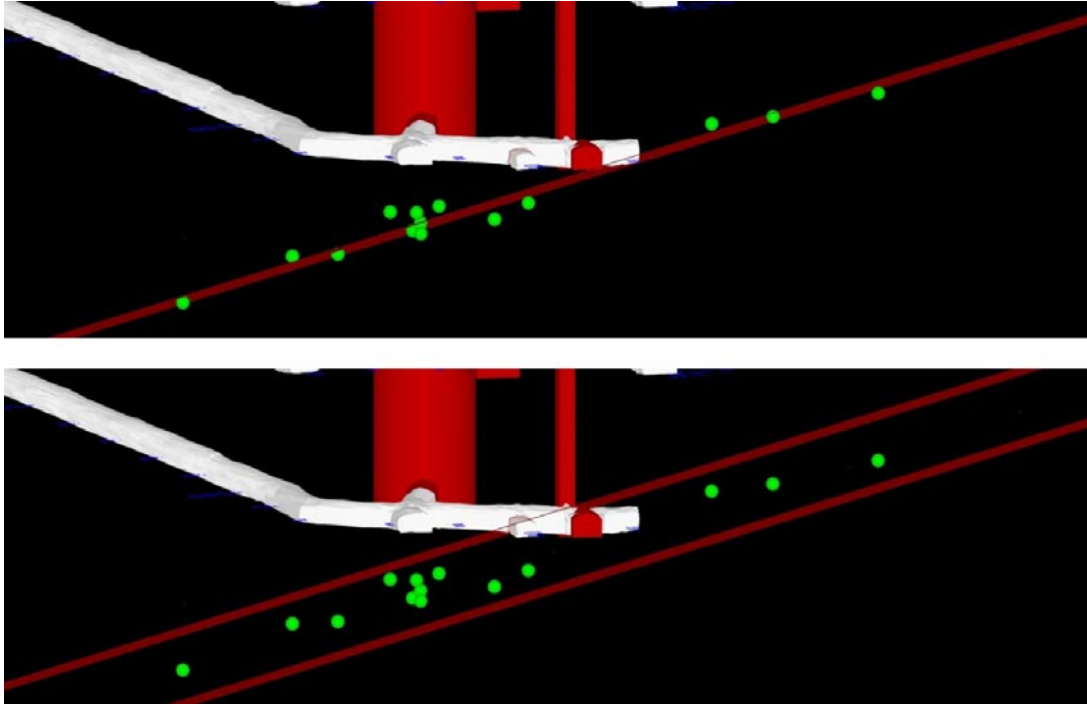
The projected intersection between the modelled deformation zone and the sea floor has no clear coincidence with a lineament. There are two very short lineaments MFM3255G and MFM3256G that have a similar position to the modelled zone but with a different strike. A much longer lineament, MFM0137BG, has a trend that is sub-parallel to the modelled zone strike but with a lateral offset of some 200 m or more. It is considered that there is no clear geometrical correlation with any of these lineaments though it is possible these lineaments could be associated with members of a group of similarly oriented structures. None of these lineaments or the modelled ZFM871 zone geometry coincides with the interpreted 3D position of any seismic reflector as presented in /Cosma et al. 2003, 2006, Balu and Cosma 2005/.

The estimated trace length of the projected surface outcrop based on the current modelled geometry is approximately 1,200 m, i.e. the same as estimated by /Stephens et al. 2007/.

/Christiansson 1986/ reports the zone's character is very variable but generally has two to three gently dipping fracture sets, individually recorded zone thicknesses of up to 10 m and a hydraulic thickness varying from 2 to 20 m; the zone is associated with lenses of weathered and highly fractured rock, along with frequent clay-filled joints. The gently dipping fractures, in combination with an increased frequency of steeply dipping fractures, gives rise to the lenses being hydraulically interconnected.

The earlier interpreted intersections in KFR24 and KFR25 are interpreted in the current model as being dominated by ZFMNW0805A rather than by ZFM871.





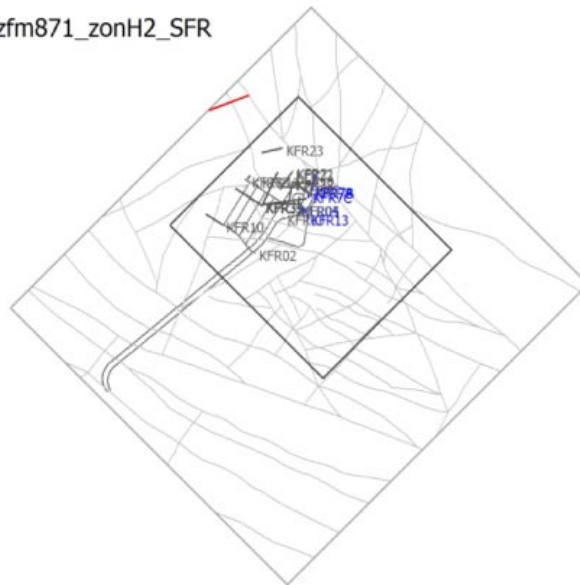
*A8-1. Section view of ZFM871 looking along the strike towards the SW. Green spheres represent correlations with borehole data. The upper view shows how the zone geometry is based on a 'best fit plane' while the lower view shows the 24 m thick envelope applied in the model.*

**Deformation zone ZFM871 (zone H2 SFR)**

Modelling procedure: There is no corresponding magnetic lineament at the ground surface

zfm871\_zonH2\_SFR

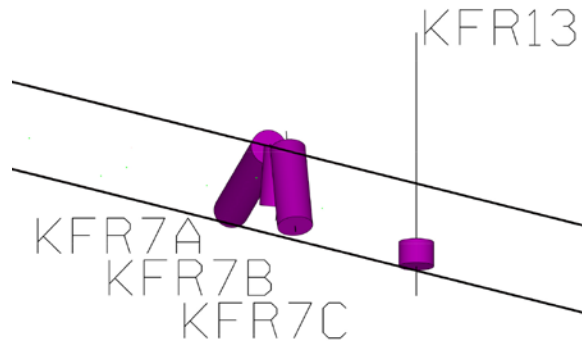
The zone has been modelled as a best fit plane, based on the interpreted borehole and tunnel intersections, with an applied envelope thickness of 24 m to contain all the interpreted target intercepts



Confidence of existence: High

Property	Quantitative estimate	Confidence level	Basis for interpretation	Comments
Orientation (strike/dip)	071 / 19	Medium/medium	Strike and dip based on best fit plane to BH and tunnel data	
Thickness	24 m	Medium	BH and tunnel data.	

Purple cylinders represent SHI DZs interpreted as ZFM871



Note: Individually recorded zone thicknesses of up to 10 m and a hydraulic thickness varying from 2 to 20 m are reported by /Christiansson 1986/

Length (regional model)	1,200 m	Low	Projection of modelled geometry	No corresponding lineament
Deformation style	Brittle			
Alteration	Faint to moderate oxidation and clay alteration			

**Borehole intersections for ZFM871 (zone H2 SFR) – details**

BH	Geometrical intercept		Target intercept		Comment
	Sec_up BH length (m) [z (-m)]	Sec_low BH length (m) [z (-m)]	Sec_up BH length (m) [z (-m)]	Sec_low BH length (m) [z (-m)]	
KFR02	104.38 [189.1]	129.76 [215.19]	114.5	124.5	Intercept position taken directly from /Axelsson and Hansen 1997/ level 290–300 m (control point added at BH length 119.5 m; level 295 m)
KFR03	74.72 [157.09]	100.10 [182.47]	86.7	95.5	Intercept position taken directly from /Axelsson and Hansen 1997/ level 322–331 m (control point added at BH length 91.1 m; level 326 m)
KFR04	80.45 [154.90]	eoh	91	100	Intercept position taken directly from /Axelsson and Hansen 1997/ level 326–335 m (control point added at BH length 95.5 m; level 330 m).  Note: SHI interpreted two possible DZs, DZ1 0–3 m and DZ2 14–63 m (BH length) neither of which correlates with ZFM871. However, there are planar chlorite filled fractures from 86 m onwards and some clay filled fractures towards the base of the hole that could be associated with the zone (100.5 m)
KFR05	71.43 [144.29]	95.76 [167.15]	85	88	Intercept position taken directly from /Axelsson and Hansen 1997/ level 340–343 m (control point added at BH length 86.5 m; level 341 m)
KFR10	66.93 [125.63]	95.20 [145.62]	–	–	This BH has not been assessed during the current modelling phase
KFR12	10.65 [97.77]	36.03 [123.15]	22	33	Intercept position taken directly from /Axelsson and Hansen 1997/ level 380–391 m (control point added at BH length 27.5 m; level 385 m)
KFR13	44.05 [167.39]	69.43 [192.77]	61	68	Intercept position taken directly from DZ4 61.0–68.0 m BH length, with a control point added at BH length 64.5 m. Although the confidence level of DZ4 is low, it shows the general characters of ZFM871, with increased frequency of broken, clay-filled fractures. Moreover, it corresponds largely with the intercept position given by /Axelsson and Hansen 1997/ at level 314–316 m  61–68 m DZ4: Increased frequency of unbroken and especially broken fractures. Predominant fracture filling minerals are laumontite, chlorite and calcite. A number of broken fractures with clay minerals are concentrated along the section 60.1–64.5 m length. Their $\alpha$ -angles range between 42 and 78°. Increased hydraulic conductivity ( $1-2 \cdot 10^{-7}$ m/s) throughout the interval. Moderately foliated metagranite-granodiorite (101057) and fine- to medium-grained metagranodiorite-tonalite (101051). Confidence level = 1
KFR21	101.67 [101.67]	127.05 [125.05]	116	122	Intercept position taken directly from /Axelsson and Hansen 1997/ level 378–384 m (control point added at BH length 119 m; level 381 m)
KFR22	135.57 [117.40]	eoh	148	158	Intercept position taken directly from /Axelsson and Hansen 1997/ level 363–372 m (control point added at BH length 153 m; level 336 m)
KFR23	75.96 [65.78]	104.65 [90.63]	–	–	This BH has not been assessed during the current modelling phase
KFR24	129.66 [108.73]	157.83 [132.37]	146.5	153	Intercept position taken directly from /Axelsson and Hansen 1997/ level 372–377 m (control point added at BH length 149 m; level 375 m)
KFR25	122.07 [87.80]	148.93 [107.12]	133	151	Intercept position taken directly from /Axelsson and Hansen 1997/ level 391–404 m (control point added at BH length 141.5 m; level 398 m)

**Borehole intersections for ZFM871 (zone H2 SFR) – details**

BH	Geometrical intercept		Target intercept		Comment
	Sec_up BH length (m) [z (-m)]	Sec_low BH length (m) [z (-m)]	Sec_up BH length (m) [z (-m)]	Sec_low BH length (m) [z (-m)]	
KFR31	214.54 [141.84]	eoh	228	232	Intercept position taken directly from /Axelsson and Hansen 1997/ level 346–349 m (control point added at BH length 230 m; level 347 m)
KFR32	153.42 [106.27]	181.76 [126.83]	163	186	Intercept position taken directly from /Axelsson and Hansen 1997/ level 370–387 m (control point added at BH length 174.5 m; level 378 m)
KFR33	153.86 [101.38]	eoh	–	–	This BH has not been assessed during the current modelling phase
KFR37	160.27 [137.76]	194.28 [167.92]	182	194	Intercept position taken directly from /Axelsson and Hansen 1997/ level 332–343 m (control point added at BH length 188 m; level 337 m)
KFR38	155.04 [126.40]	eoh	178	182	Intercept position taken directly from /Axelsson and Hansen 1997/ level 351–354 m (control point added at BH length 180 m; level 352 m)
KFR57	7.33 [94.93]	eoh	16.5	22.5	Intercept position taken directly from /Axelsson and Hansen 1997/ level 390–396 m (control point added at BH length 16.5 m; level 393 m)
KFR80	0.00 [136.00]	17.04 [152.02]	–	–	This BH has not been assessed during the current modelling phase
KFR7A	3.47 [132.41]	eoh	3.5	74.45	Intercept position taken directly from the only possible DZ identified in the borehole, DZ1 3.5–74.45 m BH length. While ZFMNW0805A and ZFMNW0805B certainly are present it is considered that this section is dominated by ZFM871. The entire length of DZ1 is thus taken as an intercept with a control point added at BH length 39.0 m
					DZ1: Increased frequency of unbroken fractures, sealed networks and especially broken fractures. Nineteen crushes with the most extensive sections at 49.09–74.45 m. Brittle-ductile section characterised by fault breccias and cataclasite at 21–24 m and 64.83–71.29 m. Predominant fracture minerals are clay minerals, calcite and Fe-hydroxide/hematite. The registered $\alpha$ -angles of clay filled fractures are highly variable, ranging from 0 to 85°. Fractures filled with laumontite form swarms throughout the drill core, with the most extensive occurrence at 56.9–64.8 m length. Most of these fractures have gently dipping $\alpha$ -angles less than 25°, with a few ranging up to 55° towards the drill core length axis. Low hydraulic conductivity $6 \cdot 10^{-9}$ m/s in the interval 3.5–19 m. Moderate hydraulic conductivity of $5 \cdot 10^{-7}$ m/s in the interval 20–47 m. High hydraulic conductivity of $3 \cdot 10^{-6}$ m/s in the interval 48–74.45 m. Moderately to strongly foliated metagranite-granodiorite (101057), pegmatitic granite (101061), aplitic metagranite (101058), fine- to medium-grained granite (111058) and amphibolite (102017). Confidence level = 3
KFR7B	1.11 [134.32]	eoh	0	17	Intercept position taken directly from the only possible DZ identified in the borehole, DZ1 0.0–17.0 m BH length, with a control point added at BH length 8.5 m
					0–17 m DZ1: Increased frequency of unbroken and especially broken fractures. Four crushed sections at 0.67–1.01, 4.14–4.33, 14.34–14.88 and 15.98–16.25 m and two core losses at 14.48–14.88 and 15.98–16.25 m. Predominant fracture minerals are calcite, chlorite and clay minerals, locally with hematite/Fe-hydroxide staining. $\alpha$ -angles are ranging between 43 and 72°. No hydrogeological investigation data from the upper 4 m of the borehole. Moderate hydraulic conductivity of $1 \cdot 10^{-8}$ m/s in the interval 4–7 m. High hydraulic conductivity of $2 \cdot 10^{-6}$ m/s in the interval 8–17 m. Moderately foliated metagranite-granodiorite (101057) and pegmatitic granite (101061). Confidence level = 3

---

**Borehole intersections for ZFM871 (zone H2 SFR) – details**

BH	Geometrical intercept		Target intercept		Comment
	Sec_up BH length (m) [z (-m)]	Sec_low BH length (m) [z (-m)]	Sec_up BH length (m) [z (-m)]	Sec_low BH length (m) [z (-m)]	
KFR7C	7.06 [140.04]	eoh	6	32	Intercept position taken directly from the only possible DZ identified in the borehole, DZ1 6.0–32.0 m BH length, with a control point added at BH length 19.0 m  6–32 m DZ1: Increased frequency of unbroken and especially broken fractures. Five crushes in the intervals 7.89–7.95, 8.11–8.19, 8.47–8.50, 9.25–9.40 and 14.67–14.77 m. Predominant fracture minerals are clay minerals, locally accompanied by Fe-hydroxide/hematite discolouration, chlorite and calcite. Most fractures have $\alpha$ -angles that are moderate (29–74°). Virtually all laumontite-bearing fractures are concentrated in a zone with low $\alpha$ -angles (9 and 10° for individual fractures) at 6.24–7.15 m length. Locally faint oxidation and minor argillization. Moderate hydraulic conductivity $2 \cdot 10^{-8}$ m/s throughout the interval. Strongly foliated metagranite-granodiorite (101057), fine- to medium-grained granite (111058) and pegmatitic granite (101061). Confidence level = 3
KFR83	6.27 [90.79]	eoh	–	–	This BH has not been assessed during the current modelling phase
KFR87	0.00 [135.13]	eoh	–	–	This BH has not been assessed during the current modelling phase
KFR88	0.00 [133.76]	eoh	–	–	This BH has not been assessed during the current modelling phase

---

**Tunnel intersections for ZFM871 (zone H2 SFR) – details**

Tunnel	Geometrical intercept		Target intercept		Comment
NBT	0+382 (8+382)	0+842 (>8+432 End of tunnel)	0+405 (8+405)	0+432 (8+432)	Control point added at chainage 8+405. Position is estimated from the tunnel chainage line, detailed tunnel mapping drawing 017 /Christiansson and Bolvede 1987/ and laser surveyed tunnel profile sections. Due to the gentle dip and nature of the zone the selected central point, representing the zone position, is approximate  Note: /Axelsson and Hansen 1997/ estimate NBT 8+405 to 8+435 and that the zone also occurs in the connecting rock drainage basin (BB)  The modelled zone geometry also encompasses the rock drainage basin (BB), the support shaft (FS) and nearby niches (connection to the NBT at 8+405) but no detailed survey measurements are available for chainage estimates

---

**Engineering characteristics**

Common characteristics for the borehole intercepts are increased hydraulic conductivity, flush water loss, high fracture frequency and occurrence of sub-horizontal fractures. In some boreholes, alteration and crushed rock also occur. However, some of the horizons with a high frequency of horizontal and vertical fractures are separated by ordinarily fractured rock /Axelsson and Hansen 1997/.

Fracture frequency 15 m<sup>-1</sup>, span 8–25 m<sup>-1</sup> based on SFR boreholes /Stephens et al. 2007/. /Christianson 1986/ reports the worst sections of the zone are associated with fine- to medium-grained granite. Clay-filled fractures

---



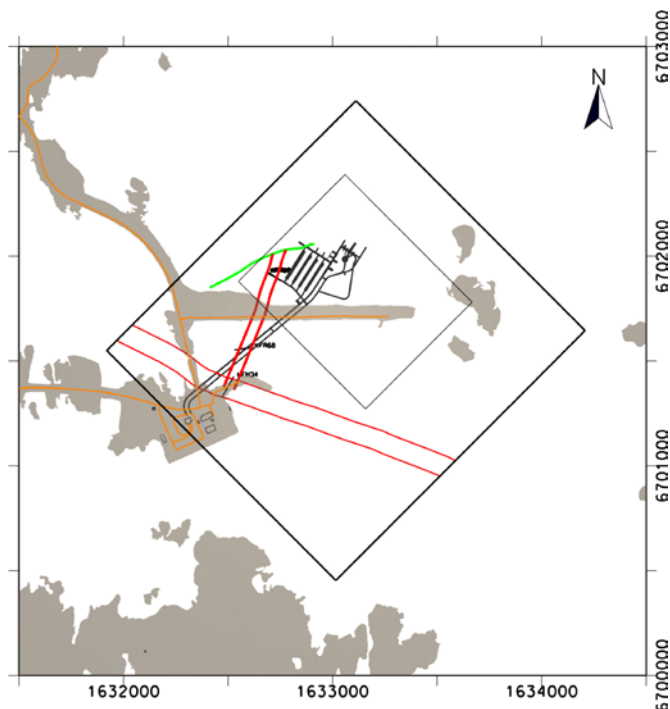
## ZFMNNE0869

Zone ZFMNNE0869, previously known as zone 3 in earlier SFR models, has been modelled to terminate against ZFMWNW0001A (Singö zone) in the SSW and against ZFMENE8031 in the NNE. The termination against ZFMENE3031, based on lineament interpretation and review of the magnetic data (lineament MSFR08089, SFR version 0.1), involves a significant reduction in length to the zone when compared to that modelled by /Axelsson and Hansen 1997/ where the zone had a longer extent to the north east and terminated against ZFMNW0805A.

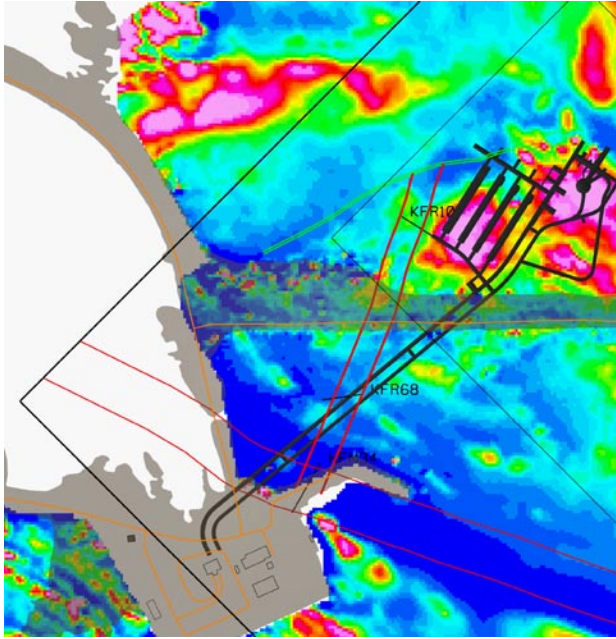
The surface position is based on a combination of magnetic lineament MSFR08089 and tunnel mapping results supported to a certain extent by seismic refraction results. The orientation 201/86 involves only a slight adjustment compared to earlier models (200/80 /Stephens et al. 2007/). However, the zone thickness as well as the NNE extent has been modified. The thickness has been increased from 10 m to 60 m based on the results of the geological SHI from KFR09 and KFR36 and the indications as presented on the tunnel mapping overview drawings, all of which consistently support the increased modelled thickness. The earlier thinner interpretation /Axelsson and Hansen 1997/ did not include the mapped parallel structures shown in the tunnel mapping though the reasoning is not clear. The associated magnetic lineament MSFR08089 has a length of 322 m, while the modelled zone is more extensive based on the inferred correlation with tunnel data. The zone is interpreted to be a composite zone consisting of several narrower high-strain segments (sub-zones) that diverge and converge in a complex pattern /Axelsson and Hansen 1997/.

In the tunnels the zone has been reported as associated with moisture, dripping and occasionally running water.

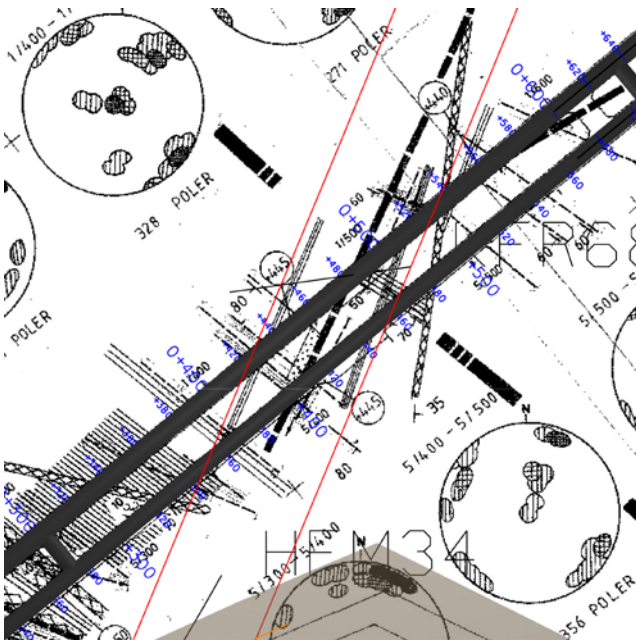
The zone is crossed by four seismic refraction profiles /Keisu and Isaksson 2004/. Two profiles indicate minor low velocity anomalies while generally velocities lie in the range of 4,000–5,000 m/s.



*A8-2. ZFMNNE0869, shown with thickness, terminates against ZFMENE8031 in the NE and ZFMWNW0001 in the SW.*



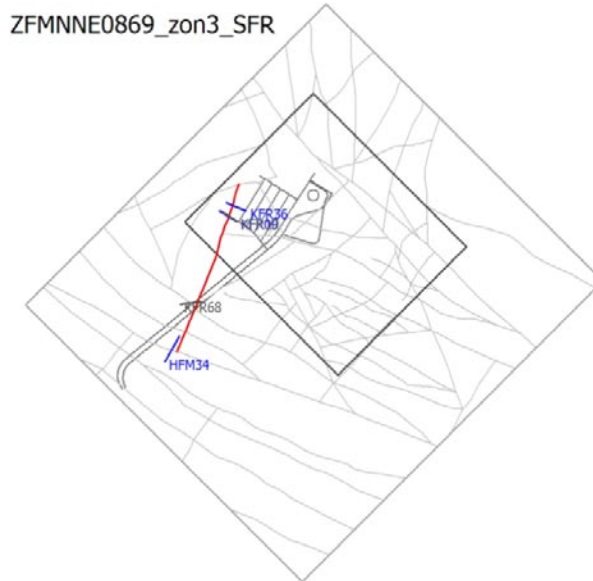
*A8-3. ZFMNNE0869 in relation to the magnetic survey map.*



*A8-4. ZFMNNE0869 as it is intercepted by the existing SFR tunnels (current interpreted thickness DT 430–540, BT350-460) as shown in the tunnel mapping overview drawing /Christiansson and Bolvede 1987/.*

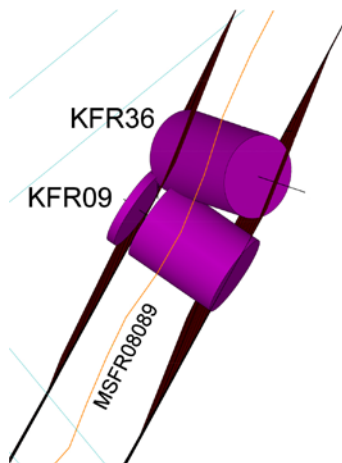
**Deformation zone ZFMNNE0869 (zone 3 SFR)**

Modelling procedure: At the surface, partly corresponds to the low magnetic lineament MSFR08089. The lineament has a length of 322 m however the DZ has an interpreted trace length of 710 m, with approximately 280 m within the local model area. The zone extent to the SW, beyond the lineament, is based on a correlation with tunnel data. The zone thickness is based the SHI DZ intervals in KFR09 and KFR36 along with tunnel mapping results



Confidence of existence: High

Property	Quantitative estimate	Confidence level	Basis for interpretation	Comments
Orientation (strike/dip)	201 / 86	High / medium	Strike based on trend of lineament. Dip based on tunnel, KFR09 and KFR36	
Thickness	60 m	High	Basis: SHI DZs KFR09, and KFR36 along with tunnel mapping. Only DZ1 from KFR09 is incorporated though possible that DZ2 is a further splay of the zone (technical note: modelled with an asymmetrical thickness in RVS (20+40 m) to best fit with BH SHI intervals)	



Modelled ZFMNNE0869 with a 60 m thickness, looking down dip to the NW, and the SHI DZ interceptions in KFR36 and KFR09

Length (regional model)	694 m	Medium	Linked lineaments and tunnel mapping	
Deformation style	Brittle character			
Alteration	Generally faint to weak oxidation			

Borehole intersections for ZFMNNE0869 (zone 3 SFR) – details

BH	Geometrical intercept		Target intercept		Comment
	Sec_up BH length (m) [z (-m)]	Sec_low BH length (m) [z (-m)]	Sec_up BH length (m) [z (-m)]	Sec_low BH length (m) [z (-m)]	
KFR09	2.53 [77.66]	63.64 [82.98]	0	58.7	<p>Correlated with SHI DZ1 in KFR09, of brittle character</p> <p>DZ1: 0–58.7 m. Increased frequency of broken and unbroken fractures and sealed networks. Most intensely fractured between 16–58.7 m. Seven minor intervals of crush. Calcite, chlorite, adularia and laumontite, variably discoloured by microscopic hematite, are the most frequent fracture filling minerals. The occurrence of laumontite is, generally restricted to two distinct sections at 0–24 and 40–45 m, and their <math>\alpha</math>-angles are typically dipping moderately (57–78°). None of the other major mineral phases exhibit such a distinct distribution pattern. Numerous asphalt-bearing fractures have been registered in the length interval 26–61 m. The occurrence of clay mineral fillings is rather scarce. Generally faint to weak oxidation. No hydrogeological investigation data from the upper 7 m of the borehole. The hydraulic conductivity (measured in sections of about 20 m) is moderate to high in the whole interval (above <math>4 \cdot 10^{-8}</math> m/s). The maximum measured hydraulic conductivity is <math>2 \cdot 10^{-6}</math> m/s in the interval 43–62 m. Felsic to intermediate volcanic rock (103076) with minor occurrences of pegmatitic granite (101061), fine- to medium-grained granite (111058) and amphibolite (102017). Confidence level = 3</p> <p>No Control point added</p> <p>Note: BH length 79.5 m, level 415 m /Axelsson and Hansen 1997/</p>
KFR10	4.21 [81.27]	97.15 [147.00]	–	–	<p>This BH has not been assessed during the current modelling phase</p> <p>Note: BH length 101.5 m, level 350 m /Axelsson and Hansen 1997/</p>
KFR36	29.58 [16.28]	123.39 [83.75]	45	115.5	<p>One possible deformation zone of brittle character has been recognized with a high degree of confidence in KFR36</p> <p>45–115.5 m: DZ1: Increased frequency of broken and unbroken fractures and sealed networks. Decreased frequency of broken fractures between 63.5–70 m, which corresponds to the occurrence of pegmatitic granite. The section between 98–115.5 m is the most highly fractured part, with nine crushed sections. The primary infilling minerals in the interval are adularia, calcite and laumontite, together with trace amounts of hematite. Three breccias occur in the interval. <math>\alpha</math>-angles are generally small to moderate (&lt;67°). In the intensely fractured interval at 44–53 m length, there is a majority of fractures filled by calcite and chlorite, with subordinate amounts of hematite. The interval includes one minor crush zone at 49.11–49.15 m. A distinct peak of broken fractures with adularia and chlorite together with a white unidentifiable mineral that might be kaolinite or a zeolite occurs at 60–62 m. Two <math>\alpha</math>-angles at 12 and 30° are registered in the interval. Asphaltite-bearing fractures, concentrated to the interval between 105–114 m. Generally faint to weak oxidation throughout the possible zone. The hydraulic conductivity (measured in 3-m sections) is quite high in the whole interval (<math>6 \cdot 10^{-6}</math>–<math>5 \cdot 10^{-8}</math> m/s). Hydraulic conductivity above <math>1 \cdot 10^{-6}</math> m/s at 48–51, 54–57, 96–99 and 102–108 m</p> <p>No control point added</p> <p>Note: BH length 104 m, level 430 m /Axelsson and Hansen 1997/</p>

KFR68	44.12 [31.20]	eoh	–	–	This BH has not been assessed during the current modelling phase
HFM34	182.52 [352.05]	eoh	–	–	The entire borehole intercepts at the junction between the regional Singö zone ZFMWNW0001 and ZFMNNE0869. It is interpreted that ZFMWNW0001 dominates the deformation seen in DZ1 whilst information from DZ2 and DZ3 is too limited to judge

---

#### Tunnel intersections for ZFMNNE0869 (zone 3 SFR) – details

Tunnel DT/BT	Geometrical intercept		Target intercept		Comment
	Start ch.(m)	End ch. (m)	Start ch.(m)	End ch. (m)	
DT	0+430 (1+430)	0+555 (1+555)	0+430 (1+430)	0+540 (1+540)	Note: earlier interpreted as 1+470–1+495 /Axelsson and Hansen 1997/
BT	0+357 (5+357)	0+482 (5+482)	0+350 (5+350)	0+460 (5+460)	Note: earlier interpreted as 5+390–5+420 /Axelsson and Hansen 1997/

---

#### Engineering characteristics

Fracture frequency 15 m<sup>-1</sup>, span estimated as 10–25 based on intersection along SFR BHs as reported in /Stephens et al. 2007/

### ZFMNE0870A and ZFMNE0870B

Zone ZFMNE0870A, previously known as zone 9 in earlier SFR models, has been modelled to terminate against ZFMWNW1035 in the SW and against ZFMWNW3262 in the NE. After a minor offset along ZFMWNW3262, the zone continues in a NE direction as ZFMNE0870B, finally terminating at ZFMNW0805A. This differs somewhat from the geometrical configuration in earlier models where there was no such subdivision. The minor adjustment at the SW end of the zone and the subdivision described above are judged to provide the best fit with the data but these changes are not considered to be significant. The total inferred length of the zone is similar to that in /Stephens et al. 2007/.

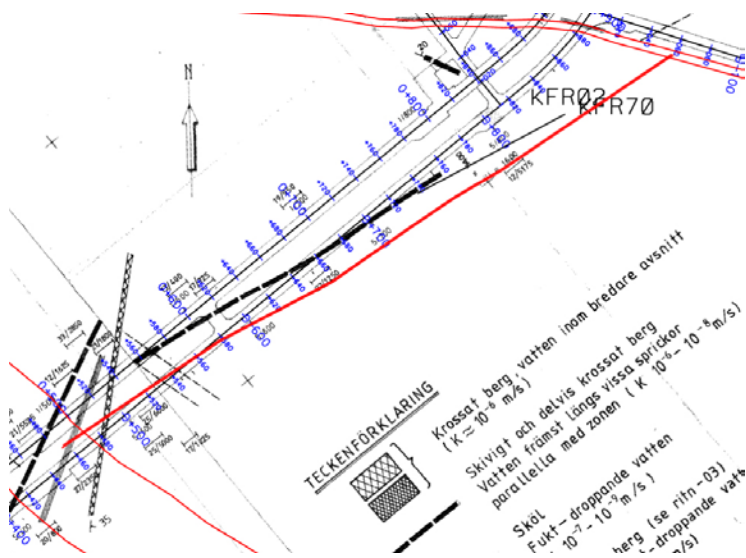
The section of zone 9 that corresponds to ZFMNE0870A has earlier been recorded as dipping steeply to the SE in /Axelsson and Hansen 1997/ and this information steered the evaluation of dip in /Stephens et al. 2007/. There are no clear dip measurements marked on the detailed mapping drawings and the way the zone is presented geometrically on the tunnel walls indicates no more than generally ‘steep to sub-vertical’. Earlier modelling work by /Axelsson and Hansen 1997/ includes a correlation with KFR02, borehole length 35 m (HK2, 380 m level in earlier SFR terminology). This is the only control on the dip along this section of the zone and leads to a dip of 75° to the NW. Such a dip has been implemented in the current model and is consistent with the earlier work reported in /Christiansson 1986/. Since it is reported that this zone is, for most of its length, a water-bearing, gouge-filled joint, occasionally with increased fracturing on one or both sides, i.e. a minor structure, it is likely to undulate and the earlier general description of ‘steep to sub-vertical’ remains valid.

There are also records of mylonite /cf. Christiansson 1986/, but comparison with data from remapped drill cores suggests that the term refers to brittle rather than ductile features, such as cataclasite. The clay gouge indicates brittle reactivation. Flush-water loss and water leakage in the BT from 5+640–5+690 were also recorded.

Essentially the zone has been adopted from the geological model for SFR by /Axelsson and Hansen 1997/, with a correction to the dip direction based on the interpretation of the intercept in KFR02 by /Axelsson and Hansen 1997/. The surface position, based on a projection of tunnel mapping results, lacks a corresponding magnetic lineament and ZFMNE0870A is not crossed by a seismic refraction survey profile.

The second leg of the zone, ZFMNE0870B, extends from ZFMWNW3262 in the SW to ZFMNW0805A in the NE. It has been modelled with an orientation of 227/74 and a thickness of 1 m, very similar to ZFMNE0870A. Although essentially the overall interpretation is grounded on /Axelsson and Hansen 1997/, the suggested correlation with NBT 8+290–8+350 is not accepted,





A8-5. A plan view showing the position of ZFMNE0870A in the overview drawing of the tunnel mapping (black dashed line in the centre of the figure) and the surface trace of the zone (offset parallel red line).

since when plotted in 3D it appears likely it represents a parallel feature rather than one with a direct connection. There is no corresponding magnetic lineament. Two seismic refraction profiles intersect the inferred surface position of the zone but no low velocity anomalies are noted /Keisu and Isaksson 2004/. This is probably due to the very narrow character of the zone. In version 0.1, the modelled thickness of the zone is based on the multiple tunnel mapping indications and earlier definition of the zone included in /Axelsson and Hansen 1997/ and not the recent SHI results since the existence of the zone is based on tunnel mapping rather than borehole information. In two of the three boreholes with SHIs (KFR04, KFR54), the intercepts interpreted by /Axelsson and Hansen 1997/ and used in the current model fall within the SHI DZ intervals. However, since the tunnel mapping evidence suggests a much thinner zone, even allowing for differences due to the updated SKB methodology, the modelled thickness in version 0.1 corresponds to the construction interpretation rather than the thickness from SHI results. The definition and in particular the thickness of this zone will be reviewed during version 1.0 based on inspection of drill core from additional older boreholes along with the more recent SHI results /Pettersson et al. 2009/.

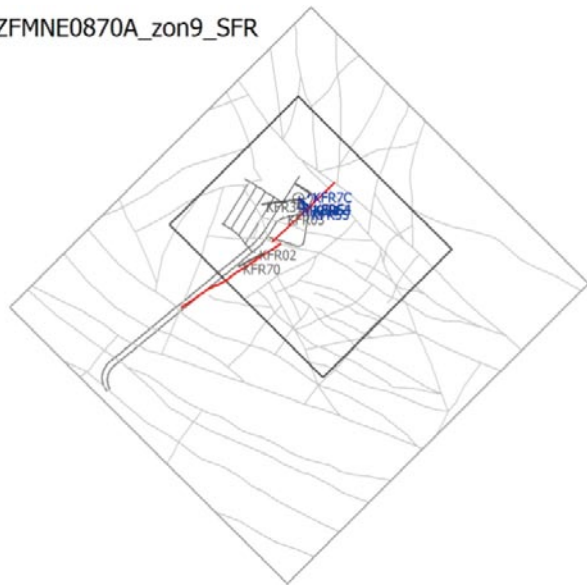


A8-6. A plan view showing the position of ZFMNE0870B in the overview drawing of the tunnel mapping (black dashed line in the centre of the figure) and the surface trace of the zone (offset parallel red line).

**Deformation zone ZFMNE0870A and B (zone 9 SFR)**

Modelling procedure: At the surface, the zone does not correspond to a particular low magnetic lineament. However, the central portion of the projected surface trace coincides with what is recognized as an area of disturbed magnetic data associated with the man-made pier. The zone has been modelled as two sub-structures, parts A and B that are documented separately. The modelled thickness of the zone is based on tunnel mapping indications. This thickness will be reviewed during version 1.0 based on inspection of older drill core and correlation with the more recent drilling results

ZFMNE0870A\_zon9\_SFR



The DZ trace (part A) has a length of 482 m, and straddles the local model boundary.

Modelled using dip that has been inferred from tunnel mapping and boreholes. The DZ trace (part B) has a length of 340 m and dip inferred from tunnel mapping and boreholes

Confidence of existence: High

Property	Quantitative estimate	Confidence level	Basis for interpretation	Comments
Orientation (strike/dip)	A= 238 / 75 B= 227 / 73	High / medium	Strike based on tunnel mapping. Dip based on tunnel mapping and BH intersections	
Thickness	1 m	High	Tunnel mapping and BH intercepts	Sensitive to the interpretation methodology applied. This value will be reviewed during V1.0 based on additional available data
Length (regional model)	A= 482 m B= 340 m	Medium	Tunnel mapping	
Deformation style	Brittle.			
Alteration	–			

**Borehole intersections for ZFMNE0870A and B – details**

BH	Geometrical intercept		Target intercept		Comment
	Sec_up BH length (m) [z (-m)]	Sec_low BH length (m) [z (-m)]	Sec_up BH length (m) [z (-m)]	Sec_low BH length (m) [z (-m)]	
KFR02	32.89 [118.32]	36.88 [122.31]	35	35	ZFMNE0870A. Intercept position taken directly from /Axelsson and Hansen 1997/ 380 m level
KFR70	63.84 [47.32]	68.40 [50.88]	–	–	ZFMNE0870A. This BH has not been assessed during the current modelling phase
KFR03	51.62 [133.99]	54.62 [136.99]	53	53	ZFMNE0870B. Intercept position taken directly from /Axelsson and Hansen 1997/ level 365 m
KFR04	21.66 [98.11]	23.94 [100.31]	23	23	ZFMNE0870B. Intercept position taken directly from /Axelsson and Hansen 1997/, level 400 m. The position falls within a wide SHI possible DZ, DZ2 14–63 m. However, since tunnel mapping evidence suggests a much thinner zone the modelled thickness has not been increased to that suggested by the SHI interpretation. The interpreted thickness will be further reviewed during version 1.0

Borehole intersections for ZFMNE0870A and B – details

BH	Geometrical intercept		Target intercept		Comment
	Sec_up BH length (m) [z (-m)]	Sec_low BH length (m) [z (-m)]	Sec_up BH length (m) [z (-m)]	Sec_low BH length (m) [z (-m)]	
					DZ2: Increased frequency of broken and unbroken fractures. One crush at 32.60–32.77 m and one breccia at 33.00–33.22 m. Predominant fracture minerals are laumontite and calcite. Registered $\alpha$ -angles for laumontite-bearing fractures in the interval are generally gently to moderately dipping ( $< 53^\circ$ ). The occurrence of clay minerals is mainly concentrated to two short sections at 20–23 and 32–36 m length, which corresponds to low single point resistivity anomalies (SPR). The $\alpha$ -angles of these clay filled fractures are moderately to steeply dipping. Generally weak to moderately oxidized. The hydraulic conductivity (measured in sections of about 20–40 m) is low in the whole interval (about $1 \cdot 10^{-8}$ m/s). Fine to medium grained granite (111058), amphibolite (102017) and felsic to intermediate metavolcanic rock (103076). Confidence level = 2
KFR05	100.99 [172.07]	112.28 [182.67]	–	–	ZFMNE0870B. This BH has not been assessed during the current modelling phase
KFR31	222.29 [147.15]	223.94 [148.28]	–	–	ZFMNE0870B. This BH has not been assessed during the current modelling phase
KFR53	29.28 [94.77]	30.51 [95.34]	30	30	ZFMNE0870B. Intercept position taken directly from /Axelsson and Hansen 1997/, level 405 m
KFR54	37.32 [109.25]	39.83 [111.11]	38	38	ZFMNE0870B. Intercept position taken directly from /Axelsson and Hansen 1997/, level 390 m. The earlier suggested intercept falls within SHI DZ2 27–40 m though since tunnel mapping evidence suggests a much thinner zone the modelled thickness has not been increased to that suggested by the SHI interpretation. The interpreted thickness will be further reviewed during version 1.0
					DZ2: Increased frequency of broken and to a lesser extent unbroken fractures and sealed networks. Decreased frequency of broken fractures between 28.6–33.7 m. Hematite stained clay minerals are restricted to two intervals of anomalously high fracture frequencies at 26.9–28.2 and 31.1–37.4 m, whereas laumontite mainly is restricted to 28.0–31.2 and 37.3–39.1 m. Both assemblages often include calcite. The chlorite content, on the other hand, is very low relative to that in other parts of the drill core. The $\alpha$ -angles of the clay-bearing fractures are typically dipping gently to moderately (30, 37, 60 and $71^\circ$ ). Generally weak to medium oxidation. The hydraulic conductivity is low to very low ( $10^{-9}$ – $10^{-10}$ m/s). Generally strongly foliated metagranite-granodiorite (101057) and one occurrence of pegmatitic granite (101061) in the lower most part of the section. Confidence level = 3
KFR55	47.40 [134.62]	48.58 [137.84]	48	48	ZFMNE0870B. Intercept position taken directly from /Axelsson and Hansen 1997/, level 365 m. Note that no possible DZ was identified at this position, however, since the zone consists of a single joint for much of its length a control point corresponding to the SHI DZ2, located at a shallower level was not added. Further review may lead to such a point being implemented.
					8–38 m DZ2: Increased frequency of broken and unbroken fractures and sealed networks, especially in the intervals 8–21 m and 32–38 m. Core loss at 17.86–18.51, 19.13–19.37, 33.48–33.60 and 34.89–35.33 m. The most frequent fracture filling minerals, which occur throughout the interval, are calcite, and to some extent chlorite. Fractures with clay minerals as the primary infilling are generally restricted to the interval at 16.8–19.5 m, with $\alpha$ -angles of $69^\circ$ . Laumontite $\pm$ calcite filled fractures, on the other hand, occur along three intervals at 8.0–12.6, 16.0–16.5 and 20.4–28.1 m length. Two $\alpha$ -angles are registered in the uppermost (68 and $77^\circ$ ) and three in the lowermost (50, 57 and $65^\circ$ ) intervals. Locally faint to medium oxidation. No hydrogeological investigation data from the upper 22 m of the borehole. The hydraulic conductivity is low in the measured section 22–38 m ( $10^{-8}$ m/s). Strongly foliated metagranite-granodiorite (101057) and one occurrence of fine- to medium-grained granite (111058). Confidence level = 3

---

**Borehole intersections for ZFMNE0870A and B – details**

BH	Geometrical intercept		Target intercept		Comment
	Sec_up BH length (m) [z (-m)]	Sec_low BH length (m) [z (-m)]	Sec_up BH length (m) [z (-m)]	Sec_low BH length (m) [z (-m)]	
KFR7C	0.0	1.55 [133.40]	–	–	ZFMNE0870B. Begins in the zone. The intercept is marginal and in fact there is a corresponding recorded possible DZ in the SHI (DZ1 6–32 m). However, while it is quite possible the zone intercepts at this interval no control point has been added since it is considered that DZ1 is dominated by an intercept with ZFM871

---



---

**Tunnel intersections for ZFMNE0870A and B (zone 9)- details**

Tunnel	Geometrical intercept		Target intercept		Comment
DT	525 (1+525)	535 (1+535)	530 (1+530)	530 (1+530)	ZFMNE0870A. Based on detailed mapping drawing –006.  Note: earlier interpreted as 1+530–1+570 /Axelsson and Hansen 1997/
DT	DT-BT connection tunnel at 0+610 (1+610)		DT-BT connection tunnel at 0+610 (1+610)		ZFMNE0870A Note: earlier interpreted as DT-BT connection tunnel at 0+610 /Axelsson and Hansen 1997/
BT	0+658 (5+658)	0+670 (5+670)	0+660 (5+660)	0+660 (5+660)	ZFMNE0870A Note: earlier interpreted as 5+640-5+690 /Axelsson and Hansen 1997/
BT	0+890 (5+890)	0+900 (5+900)	0+895 (5+895)	0+895 (5+895)	ZFMNE0870B. Connection with NBT  Control point added near tunnel connection.
BT	1+038 (6+032)	1+040 (6+035)	1+039 (6+033)	1+039 (6+033)	ZFMNE0870B  Note: earlier interpreted as 6+025–6+050 /Axelsson and Hansen 1997/
NBT	0+001 (8+001)	0+003 (8+003)	0+002 (8+002)	0+002 (8+002)	ZFMNE0870B. Connection with BT  Control point added near tunnel connection.  Note: earlier interpreted as 8+025 (as a branch of zone 9) /Axelsson and Hansen 1997/
NBT	0+357 (8+357)	0+362 (8+362)	0+358 (8+358)	0+358 (8+358)	ZFMNE0870B  Note: earlier interpreted as 8+290–8+350 (as a branch of zone 9) /Axelsson and Hansen 1997/
IST	0+088 (4+088)	0+090 (4+090)	0+090 (4+090)	0+090 (4+090)	ZFMNE0870B  Control point added at 0+090.  Note: earlier interpreted as 4+090 (as a branch of zone 9) /Axelsson and Hansen 1997/. This location is at the connection between BT and STT

---



---

**Engineering characteristics**

Fracture frequency 15 m<sup>-1</sup>, range 10–25 m<sup>-1</sup>

Fracture fillings: quartz, clay minerals, chlorite, calcite, laumontite and Fe bearing mineral.

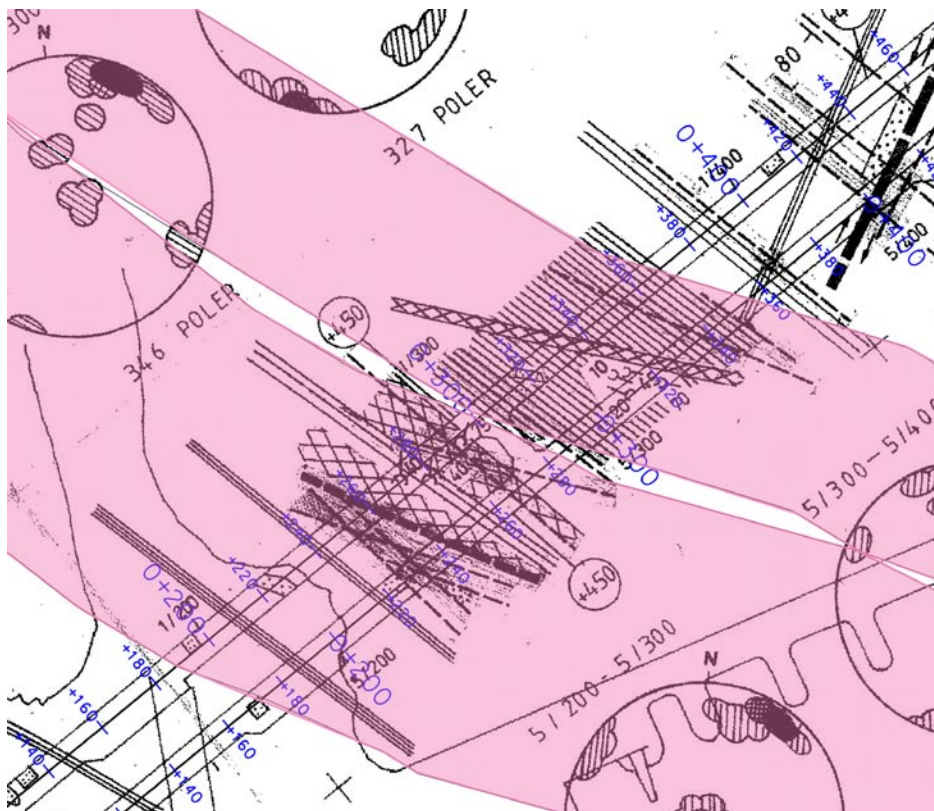
Water-bearing clay, gouge-filled joint, occasionally with increased fracturing on one or both sides. /Axelsson and Hansen 1997/

---

## ZFMWNW0001

Zone ZFMWNW0001, referred to as the Singö deformation zone in earlier SFR models, is a major regional deformation zone interpreted as having a total length of greater than 30 km. The zone crosses the entire regional model volume. The interpretation is largely based on that presented in /Stephens et al. 2007/, itself based on earlier work by /Christianson 1986, Axelsson and Hansen 1997/. However, the position of the Singö deformation zone and a nearby major splay, ZFMNW0002, inside the SFR regional model area, have been modified slightly, based on the updated interpretation of lineaments MFM0803G0 and MFM0804G, respectively, during Forsmark stage 2.3 /Isaksson et al. 2007/. The thicknesses have also been modified with reference to the mapping in the SFR operation and construction tunnels, with the Singö zone corresponding to a complex series of crush zones and ZFMNW0002 corresponding to a secondary, more isolated crush zone lying within a section of closely spaced, sub-vertical parallel fractured rock mapped in the tunnels. Data from the cooling water tunnels 1–2 and 3, northwest of SFR, have not been considered in this procedure. ZFMWNW0001 has also been the subject of a detailed study in the context of the Forsmark site investigation /Glamheden et al. 2007/. A thickness of 165 m with a thickness span of 53–200 m was indicated by /Stephens et al. 2007/. The thickness of 100 m presented here lies within this span.

The results from boreholes KFM11A and HFM34 will provide input to the modelling work for version 1.0. None of the data from these boreholes were directly included in the current modelling work due to time constraints. Inspection of the borehole SHIs, along with the lineaments and tunnel mapping results, revealed a more extensive detailed review was required than that anticipated. The review will need to include how the tectonic belt that includes the Singö deformation zone should be modelled, with possible influence on the planned update of the stage 2.2 Forsmark deformation zone model. These boreholes were drilled to provide information on the Singö deformation zone and neighbouring splays at depth. An evaluation of the data from these boreholes was presented in /Stephens et al. 2008a/.



*A8-7. ZFMWNW0001 (lower pink block) and a nearby splay ZFMNW0002 (upper pink block) as interpreted to intercept the SFR operation and construction tunnels.*



**Deformation zone ZFMWNW0001 Singö zone**

Modelling procedure: At the surface, corresponds to the low magnetic lineament MFM0803G0 with a slight modification where it crosses the SFR tunnels to better fit mapping evidence. The total length of the zone is over 30km with 1678 m falling within the regional model area

The zone dip is based on /Stephens et al. 2007/ while the thickness is based on the SFR tunnel mapping, considered most relevant to the SFR regional model volume



Confidence of existence: High

Property	Quantitative estimate	Confidence level	Basis for interpretation	Comments
Orientation (strike/dip)	120 / 90	High / high	Intersections along Forsmark outlet tunnels 1–2, 3 and SFR, BHs, seismic refraction data and low magnetic lineament MFM0803G0	
Thickness	100 m	High	Intersection along SFR tunnels.	Complex zone, inferred thickness refers to total zone thickness, ductile and brittle, damage zones and core
Length (regional model)	30 km	Medium	Low magnetic lineament MFM0803G0 /Stephens et al. 2007/	Total trace length at the ground surface. Extends outside the regional model volume
Deformation style	Ductile origin followed by brittle reactivation			
Alteration	Red stained bedrock with fine-grained hematite dissemination /Stephens et al. 2007/			

---

**Borehole intersections for ZFMWNW0001 Singö zone – details**

BH	Geometrical intercept		Target intercept		Comment
	Sec_up BH length (m) [z (-m)]	Sec_low BH length (m) [z (-m)]	Sec_up BH length (m) [z (-m)]	Sec_low BH length (m) [z (-m)]	
	HFM34	6.89 [3.42]	182.52 [147.94]	–	
KFM11A	552.15 [474.13]	735.52 [622.09]	–	–	This BH has not been assessed during the current modelling phase
KFR01	0 [48.0]	eoh [101.9]	–	–	This BH has not been assessed during the current modelling phase
KFR61	1.4 [-0.4]	eoh [47.0]	–	–	This BH has not been assessed during the current modelling phase
KFR62	0.5 [-0.3]	eoh [58.0]	–	–	This BH has not been assessed during the current modelling phase
KFR64	0.4 [0.1]	eoh [35.5]	–	–	This BH has not been assessed during the current modelling phase
KFR65	0 [0.0]	eoh [28.9]	–	–	This BH has not been assessed during the current modelling phase
KFR66	0.5 [0.5]	eoh [14.2]	–	–	This BH has not been assessed during the current modelling phase
KFR67	0.6 [0.5]	eoh [31.9]	–	–	This BH has not been assessed during the current modelling phase
KFR84	0.0 [42.0]	Eoh [29.5]	–	–	This BH has not been assessed during the current modelling phase
KFR85	0.0 [43.0]	Eoh [44.1]	–	–	This BH has not been assessed during the current modelling phase
KFR86	0.0 [45.0]	Eoh [59.7]	–	–	This BH has not been assessed during the current modelling phase

---

**Tunnel intersections for ZFMWNW0001 <singö zone- details**

Tunnel DT/BT	Geometrical intercept		Target intercept		Comment
	Start ch.(m)	End ch. (m)	Start ch.(m)	End ch. (m)	
DT	187 (1+187)	298 (1+298)	208 (1+208)	296 (1+296)	
BT	173 (5+173)	285 (5+285)	187 (5+187)	275 (5+275)	

---

**Engineering characteristics**

ZFMWNW0001 has been the subject of detailed studies including engineering characteristics as reported by /Glamheden et al. 2007/

Fracture orientations: 140/80 (closely spaced parallel fractures), 210/75, 055/75, 170/40, sub-horizontal.

Fracture frequency: 10 m<sup>-1</sup>, span + 4 m<sup>-1</sup>

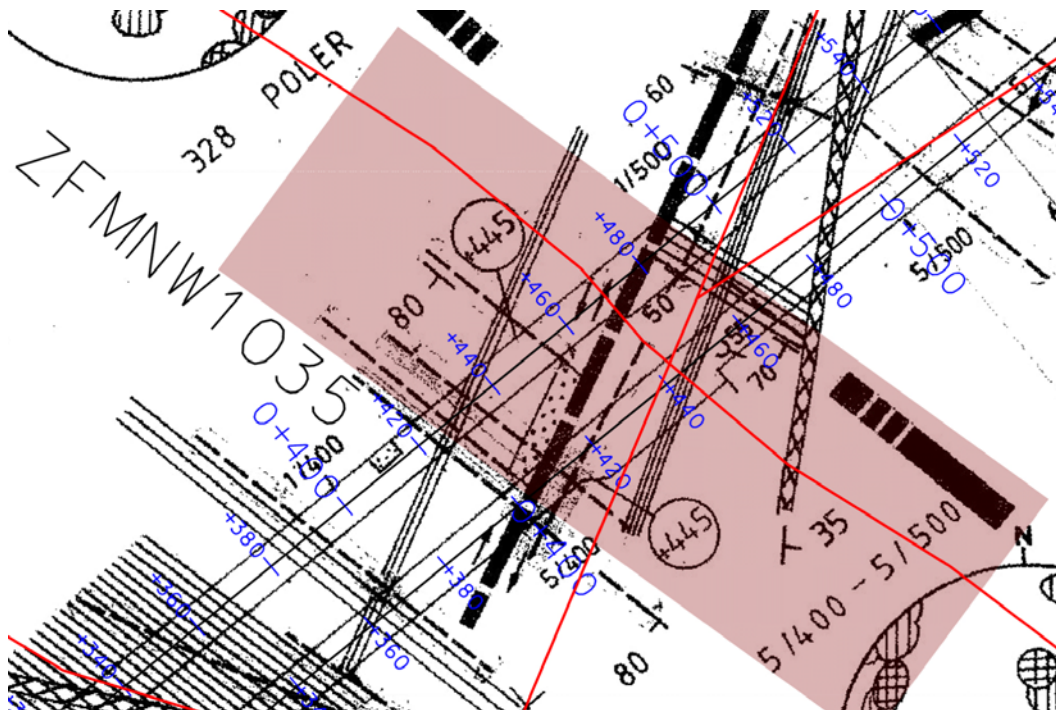
Fracture filling: chlorite, calcite, quartz, clay minerals, sandy material

Further data is available from KFR11A and HFR34, though this information is not represented in the above figures and will be integrated in v0.2. It should be noted that the ZFMWNW001A intercept in KFM11A is at some 500–700 m well below the elevation of focused interest for the current project

---

## ZFMWNW1035

ZFMWNW1035 is based on the magnetic lineament MFM1035G /Isaksson et al. 2007/ and an attempted correlation with SFR tunnel mapping results. There are a number of structures mapped in the tunnels that dip steeply to the SSW with strikes parallel to that of the lineament. However, the situation is complicated by the presence of a more clearly defined group of NNE trending structures, modelled as ZFMNNE0869 (SFR zone 3) that generate a series of offsets along the NW-trending structures. The lineament has been taken as giving an overall indication to the existence and lateral extent of the inferred zone away from the tunnels and a thickness of 60 m has been applied to reflect the spread of the inferred related structures seen in the tunnel mapping. In a similar way as for zone ZFMNNE0869, the zone appears to be an associated group of sub-parallel smaller structures rather than a single discrete major structure. In addition to this, the offsets mean that this is an apparent thickness for the group and, for this reason, the applied thickness is considered conservative with a confidence level judged to be low.

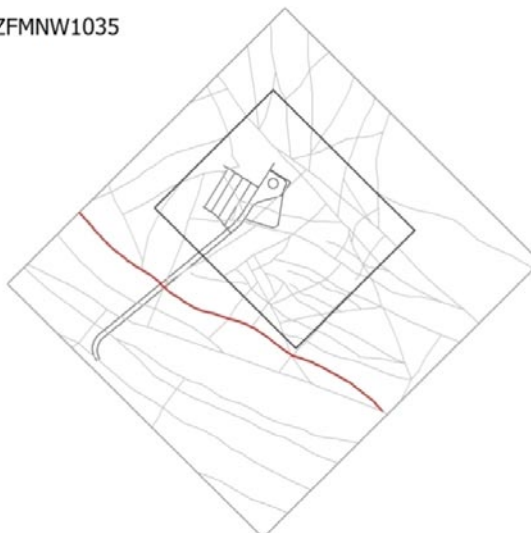


*A8-8. Overview drawing of the tunnel mapping results showing ZFMWNW1035 (pink transparent block) representing the zone thickness and position at tunnel level, along with the corresponding magnetic lineament. Note the dominance of the NE-trending structures offsetting the NW structures.*

### Deformation zone ZFMWNW1035

Modelling procedure: At the surface, corresponds to the low magnetic lineament MFM1035G. The length of the lineament and modelled deformation zone is 1615 m (including extent outside the regional model boundary). The zone lies outside of the local model area

ZFMWNW1035



The zone thickness and dip are based on tunnel mapping results

Confidence of existence: High

Property	Quantitative estimate	Confidence level	Basis for interpretation	Comments
Orientation (strike/dip)	121 / 80	High / medium	Strike based on trend of lineament. Dip based on tunnel mapping	
Thickness	60 m	Low	SFR tunnel mapping	Compound zone, inferred to be a group of smaller sub-parallel structures. Tunnel mapping suggests the zone is offset across the NNE striking ZFMNNE0869 and the judgement of thickness is considered low confidence
Length (regional model)	1,615 m	Medium	Linked lineaments	
Deformation style	Inferred ductile origin with brittle reactivation based on orientation and tunnel mapping			
Alteration				

#### Borehole intersections for ZFMWNW1035 – summary

BH	Geometrical Intercept		Target intercept		Comment
	Sec_up BH length (m) [z (-m)]	Sec_low BH length (m) [z (-m)]	Sec_up BH length (m) [z (-m)]	Sec_low BH length (m) [z (-m)]	
HFM35	152.20 [116.29]	eoh	–	–	This BH has not been assessed during the current modelling phase
KFM11A	684.57 [581.41]	767.93 [647.80]	–	–	This BH has not been assessed during the current modelling phase
KFR68	0.00	87.60 [61.94]	–	–	This BH has not been assessed during the current modelling phase

#### Tunnel intersections for ZFMWNW1035 – details

Tunnel	Geometrical intercept		Target intercept		Comment
	Start ch.(m)	End ch.(m)	Start ch.(m)	End ch.(m)	
DT	0+430 (1+430)	0+490 (1+490)	0+422 (1+422)	0+490 (1+490)	Tunnel mapping suggests the zone is offset across the NNE striking ZFMNNE0869 and the judgement of thickness is considered low confidence (it could be considerably less)
BT	0+402 (5+402)	0+463 (5+463)	0+400 (5+400)	0+472 (5+472)	Tunnel mapping suggests the zone is offset across the NNE striking ZFMNNE0869 and the judgement of thickness is considered low confidence (it could be considerably less)

---

**Engineering characteristics**

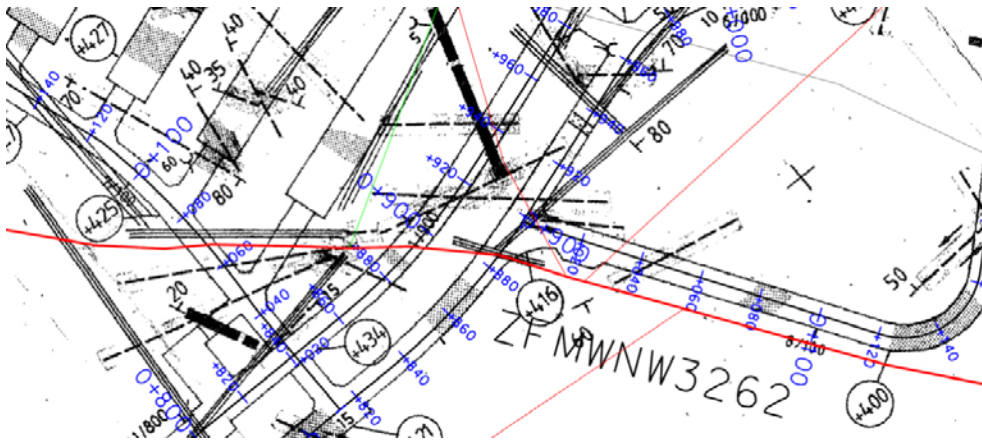
---

To be based on HFM35 and KFM11A, not yet assessed

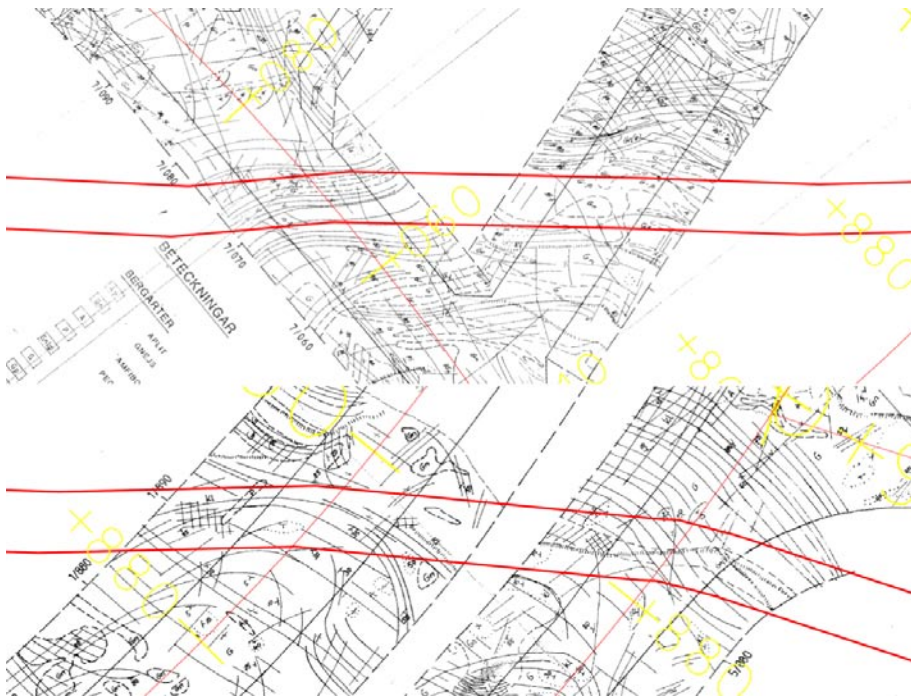
---

**ZFMWNW3262**

ZFMWNW3262 is based on magnetic lineament MFM3262G and a weak correlation with tunnel mapping results. The zone is modelled as terminating against ZFMNW0805B in the east and ZFMNNE0869 in the west. Although there are mapped subvertical structures in the tunnels (BT, DT and TT) which may correlate with the lineament position, they are intermittent and very thin with moisture recorded only locally. Since the lineament is over 1,000 m in length and the position is sensitive to the project, a corresponding zone has been included in the model. However, no evidence has been found to suggest it is anything other than a minor discontinuous structure.



*A8-9. The modelled ZFMWNW3262 centre-line surface trace shown with the overview tunnel mapping figure.*



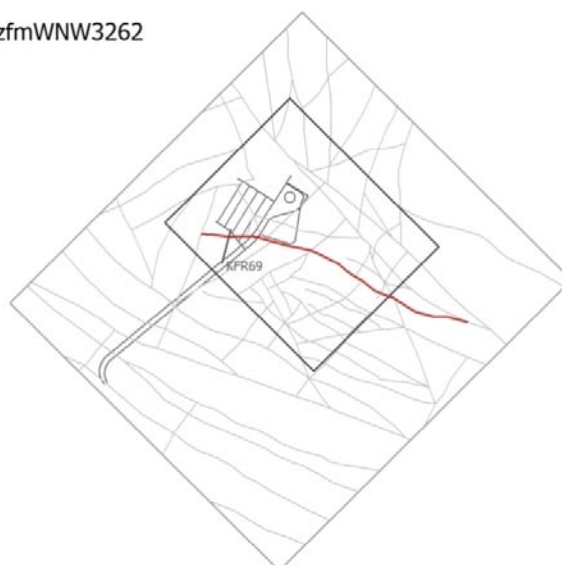
*A8-10. Top views of the modelled ZFMWNW3262 shown with the detailed mapping figures.*



## Deformation zone ZFMWNW3262

Modelling procedure: At the surface, corresponds to the low magnetic lineament MFM3262G, with an applied vertical dip based on tunnel mapping results.

zfmWNW3262



The length of the DZ is 1,173 m on the surface and lies partially within the local model area.

Confidence of existence: High

Property	Quantitative estimate	Confidence level	Basis for interpretation	Comments
Orientation (strike/dip)	111 / 90	Medium/medium	Strike based on trend of lineament. Dip based on tunnel mapping.	Interpreted as a minor diffuse and discontinuous structure.
Thickness	5 m	Medium	Based on tunnel mapping.	Interpreted as a minor diffuse and discontinuous structure.
Length (regional model)	1,171 m	Medium	Linked lineaments	Appears discontinuous
Deformation style				
Alteration				

### Borehole intersections for ZFMWNW3262 – details

BH	Geometrical intercept		Target intercept		Comment
	Sec_up BH length (m) [z (-m)]	Sec_low BH length (m) [z (-m)]	Sec_up BH length (m) [z (-m)]	Sec_low BH length (m) [z (-m)]	
KFR69	155.99 [108.66]	162.99 [113.64]	–	–	This BH has not been assessed during the current modelling phase

### Tunnel intersections for ZFMWNW3262 – details

Tunnel DT/BT	Geometrical intercept		Target intercept		Comment
	Start ch.(m)	End ch. (m)	Start ch.(m)	End ch. (m)	
DT	0+890 (1+890)	0+896 (1+896)	0+893 (1+893)	0+893 (1+893)	Weak correlation with two, very local, discontinuous crushes
BT	0+883 (5+883)	0+887 (5+887)	0+885 (5+885)	0+885 (5+885)	Weak correlation with a minor gouge filled fracture zone (<2 dm thick) of similar orientation to overlying lineament and also a very local crush
TT	0+066 (7+066)	0+074 (7+074)	0+062 (7+062)	0+075 (7+075)	Weak correlation with a steeply dipping joint swarm of similar orientation to overlying lineament

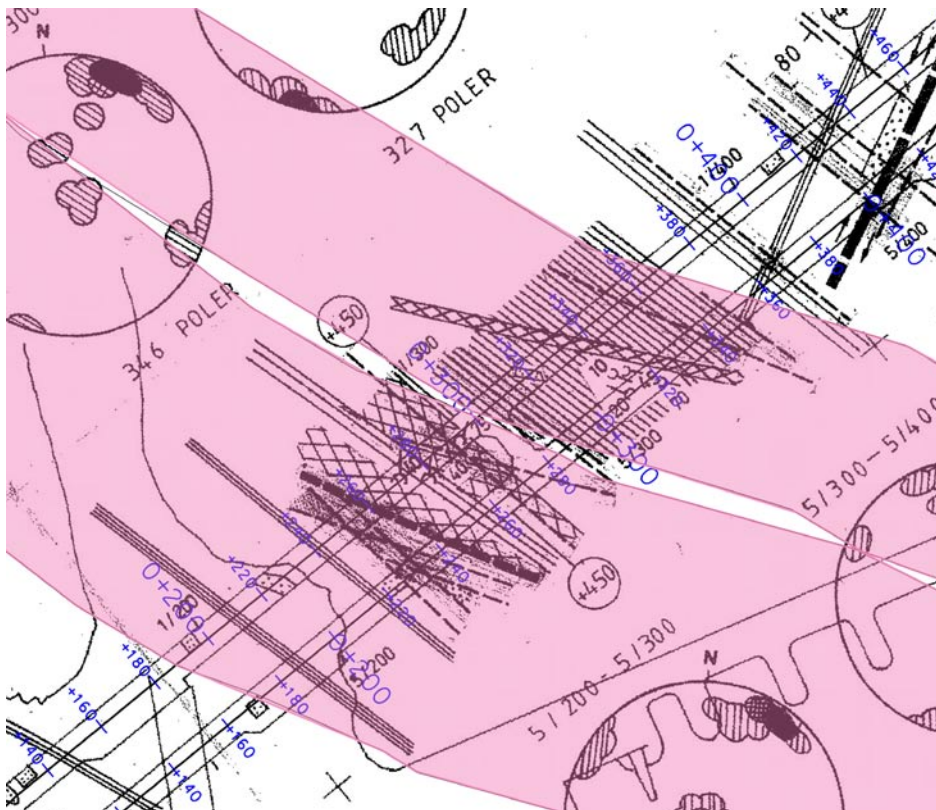
Although the modelled geometry intercepts the connecting tunnel between TT and 1-BTF the detailed mapping provides no evidence to support the structure in this location

**ZFMNW0002**

Zone ZFMNW0002, a splay of the major, regionally significant Singö deformation zone, is itself a regional deformation zone interpreted as having a length of 18 km /Stephens et al. 2007/. However, the position of the zone as it crosses the SFR regional model area has been modified slightly, based on the updated interpretations of lineament MFM0804G in /Isaksson et al. 2007/ and later in this study.

The zone is interpreted as having a close association with the neighbouring ZFMWNW0001 and being part of the same tectonic belt within the SFR regional model area. The thickness has been modified with reference to the mapping in the SFR operation and construction tunnels, with the Singö zone corresponding to the complex series of crush zones and ZFMNW0002 corresponding to secondary, more isolated crush zone lying within a section of closely spaced, sub-vertical parallel fractured rock mapped in the tunnels. Data from the cooling water tunnel 3, northwest of SFR, have not been considered in this procedure. A thickness of 75 m with a thickness span of 53–200 m was indicated by /Stephens et al. 2007/. The thickness of 58 m presented here lies within this span.

The results from boreholes KFM11A, HFM34 and HFM35 will provide input to the modelling work for model version 1.0. These data were not assessed in model version 0.1. These three boreholes were drilled to provide information on the Singö zone and neighbouring splays at depth. An evaluation of the data from these three boreholes was presented in /Stephens et al. 2008a/.



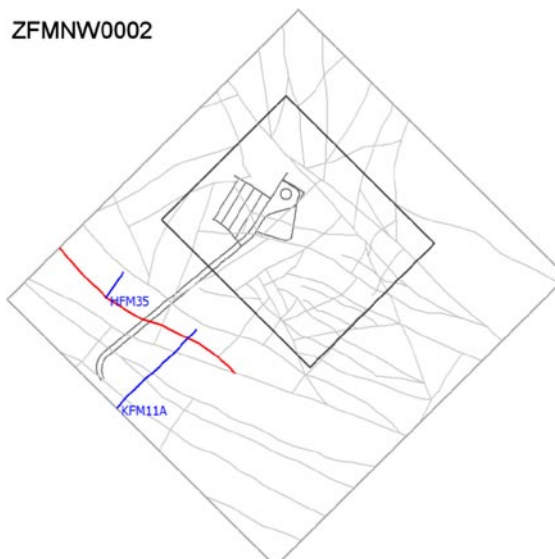
*A8-11. ZFMWNW0001 (lower pink block) and a nearby splay ZFMNW0002 (upper pink block) as interpreted to intercept the SFR operations and construction tunnels.*

---

**Deformation zone ZFMNW0002**


---

Modelling procedure: At the surface, corresponds to the low magnetic lineament MFM0804G. The length of the lineament is 3,940 m. The DZ extends outside the regional model area having a total length of 18 km.



Confidence of existence: High

Property	Quantitative estimate	Confidence level	Basis for interpretation	Comments
Orientation (strike/dip)	123 / 90	High / high	Strike based on trend of lineament. Dip based on SFR tunnel mapping	
Thickness	58 m	Medium	SFR tunnel mapping	
Length (regional model)	1,8000 m	Medium	Linked lineaments	
Deformation style	Ductile origin followed by brittle reactivation style			
Alteration				

---

**Borehole intersections for ZFMNW0002 – details**

BH	Geometrical intercept		Target intercept		Comment
	Sec_up	Sec_low	Sec_up	Sec_low	
	BH length (m)	BH length (m)	BH length (m)	BH length (m)	
	[z (-m)]	[z (-m)]	[z (-m)]	[z (-m)]	
HFM34	192.37 [155.18]	eoh	–	–	This BH has not been assessed during the current modelling phase
HFM35	0 [-1.90]	54.17 [42.63]	–	–	This BH has not been assessed during the current modelling phase
KFM11A	716.77 [607.16]	814.76 [684.70]	–	–	This BH has not been assessed during the current modelling phase

---

**Tunnel intersections for ZFMNW0002 – details**

Tunnel DT/BT	Geometrical intercept		Target intercept		Comment
	Start ch.(m)	End ch. (m)	Start ch.(m)	End ch. (m)	
DT	0+300 (1+300)	0+368 (1+368)	0+300 (1+300)	0+368 (1+368)	
BT	0+288 (5+288)	0+356 (5+356)	0+286 (5+286)	0+350 (5+350)	

**ZFMNW0805A and ZFMNW0805B**

Zone ZFMNW0805A, previously known as zone 8 in earlier SFR models, is a local major zone interpreted as having a length of greater than 3 km. The zone crosses the entire regional model volume. ZFMNW0805A is presented in /Stephens et al. 2007/ with an orientation of 134/90, a span in dip of 10°, a thickness of 10 m and a span in thickness of 10–64 m. /Carlsson et al. 1985/ and /Axelsson and Hansen 1997/ interpreted the zone as dipping steeply to the NE with a thickness of approximately 10–45 m. The current interpretation based on the magnetic lineament MFM0805G0 and remapped borehole SHI intersections (KFR08 and KFR7A) results in a zone of orientation 314/83 and a thickness of 60 m, which are inside the span values cited by /Stephens et al. 2007/ and close to the original interpretation.

The Forsmark version 2.3 lineament interpretation /Isaksson et al. 2007/ has led to the inclusion of ZFMNW0805B. The ZFMNW0805B zone geometry 133/90 is based on the magnetic lineament MFM0805G1, a default vertical dip and an applied length-thickness class of 10 m. The modelled zone geometry results in intersections in KFR08 SHI DZ2 and KFR7A SHI DZ1, however these intervals are inferred as being dominated by ZFMNW0805A and ZFM871 and no exclusive evidence for the existence of ZFMNW0805B has been identified. For this reason, ZFMNW0805B has been classed as medium confidence.

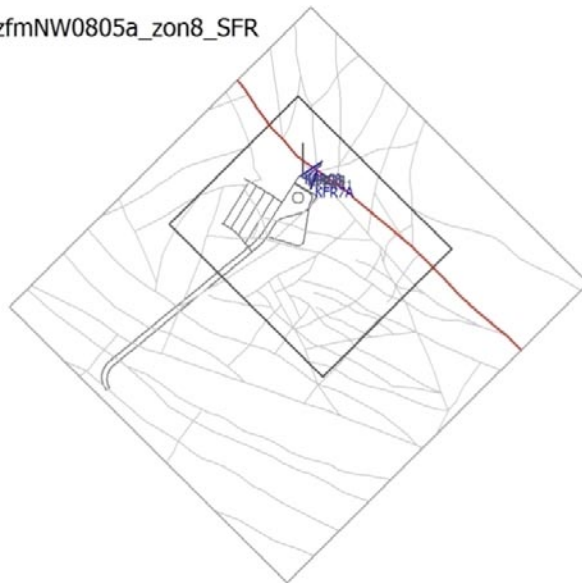
Neither zone intercepts any of the existing SFR tunnels.

**Deformation zone ZFMNW0805A (zone 8 SFR)**

Modelling procedure: At the surface, corresponds to the magnetic lineament MFM0805G0 that crosses and extends beyond the regional model boundary.

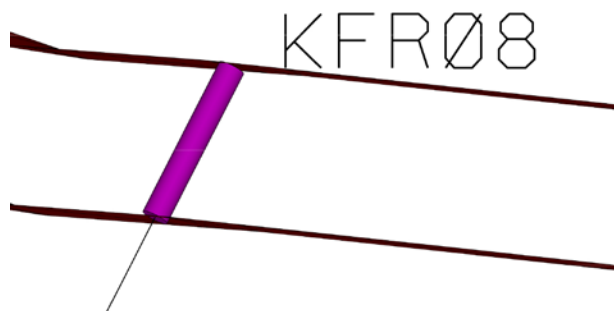
The dip is based on inferred borehole intersections KFR08 DZ2 and the lower part of KFR7A DZ1

zfmNW0805a\_zon8\_SFR



Confidence of existence: High

Property	Quantitative estimate	Confidence level	Basis for interpretation	Comments
Orientation (strike/dip)	314 / 83	High / medium	Strike based on trend of lineament. Dip based on KFR08 DZ2 intercept	
Thickness	60 m	Medium	KFR08 SHI DZ2 intercept	



Purple cylinder represents SHI DZ interpreted as ZFM-NW0805A

Length (regional model)	3643 m	High	Linked lineaments	Lineament possibly continues outside of the study area
Deformation style	Ductile origin followed by brittle reactivation			
Alteration	Generally weakly to moderately oxidized and locally quartz dissolution			



**Borehole intersections for ZFMNW0805A (zone 8 SFR) – details**

BH	Geometrical intercept		Target intercept		Comment
	Sec_up BH length (m) [z (-m)]	Sec_low BH length (m) [z (-m)]	Sec_up BH length (m) [z (-m)]	Sec_low BH length (m) [z (-m)]	
KFR08	41.18 [89.61]	eoh	41	104.4	<p>The interpreted interval corresponds to KFR08 SHI DZ2</p> <p>SHI DZ2 41–104.4 m: very high frequency of sealed networks and broken fractures. Nineteen crushed sections. Brittle- to ductile section characterised by fault breccias and cataclasite at 42.25–49.80, 53.83–59.1 and 76–80 m. The predominant fracture filling minerals are calcite, chlorite, laumontite and adularia, typically discoloured by hematite. Registered <math>\alpha</math>-angles for fractures in this interval are variable, but generally moderately dipping. Generally weakly to moderately oxidized with two short sections of quartz dissolution (vuggy rock) at 72.55–73.30 and 77.95–79.55 m. Pegmatitic granite (101061), fine- to medium-grained granite (111058) and moderately foliated metagranite-granodiorite (101057). Confidence level = 3</p> <p>Moderate hydraulic conductivity (measured in sections of about 20–40 m) of <math>2\text{--}5\cdot 10^{-7}</math> m/s throughout the interval</p> <p>Note: /Axelsson and Hansen 1997/ approximate position of correlation was BH length 80 m, 407 m level</p>
KFR11	41.88 [93.77]	eoh	–	–	<p>/Axelsson and Hansen 1997/ approximate position of correlation was 80 m BH length, 400 m level</p> <p>This BH has not been assessed during the current modelling phase</p>
KFR24	57.53 [48.25]	eoh	–	–	<p>/Axelsson and Hansen 1997/ approximate position of correlation was 137 m BH length, 385 m level</p> <p>This BH has not been assessed during the current modelling phase</p>
KFR25	52.72 [37.92]	182.93 [131.57]	–	–	<p>/Axelsson and Hansen 1997/ approximate position of correlation was 174 m BH length, 375 m level</p> <p>This BH has not been assessed during the current modelling phase</p>
KFR56	63.95 [56.52]	eoh	–	–	<p>/Axelsson and Hansen 1997/ approximate position of correlation was 68 m BH length, 445 m level</p> <p>This BH has not been assessed during the current modelling phase</p>
KFR7A	63.61 [134.50]	eoh	64.0	71.3	<p>The target interval corresponds to the lower part of DZ1 that has a brittle ductile character (64.83–71.29 m). The borehole is interpreted to not penetrate the full thickness of the zone. The remainder of the DZ1 interval is interpreted as intercepting both ZFMNW0805B and ZFM871</p> <p>3.5–74.45 m DZ1: Increased frequency of unbroken fractures, sealed networks and especially broken fractures. Nineteen crushes with the most extensive sections at 49.09–74.45 m. Brittle-ductile section characterised by fault breccias and cataclasite at 21–24 m and 64.83–71.29 m. Predominant fracture minerals are clay minerals, calcite and Fe-hydroxide/hematite. The registered <math>\alpha</math>-angles of clay filled fractures are highly variable, ranging from 0 to 85°. Fractures filled with laumontite form swarms throughout the drill core, with the most extensive occurrence at 56.9–64.8 m length. Most of these fractures have gently dipping <math>\alpha</math>-angles less than 25°, with a few ranging up to 55° towards the drill core length axis. Low hydraulic conductivity <math>6\cdot 10^{-9}</math> m/s in the interval 3.5–19 m. Moderate hydraulic conductivity of <math>5\cdot 10^{-7}</math> m/s in the interval 20–47 m. High hydraulic conductivity of <math>3\cdot 10^{-6}</math> m/s in the interval 48–74.45 m. Moderately to strongly foliated metagranite-granodiorite (101057), pegmatitic granite (101061), aplitic metagranite (101058), fine- to medium-grained granite (111058) and amphibolite (102017). Confidence level = 3</p>

---

**Engineering characteristics**

---

Fracture frequency 15 m<sup>-1</sup>, span + 5 m<sup>-1</sup> /Stephens et al. 2007/. The interpretation is uncertain since more than one DZ may intercept the relevant drill core interval.

Fracture fillings include both clay and laumontite

---

**ZFMNW0805B**

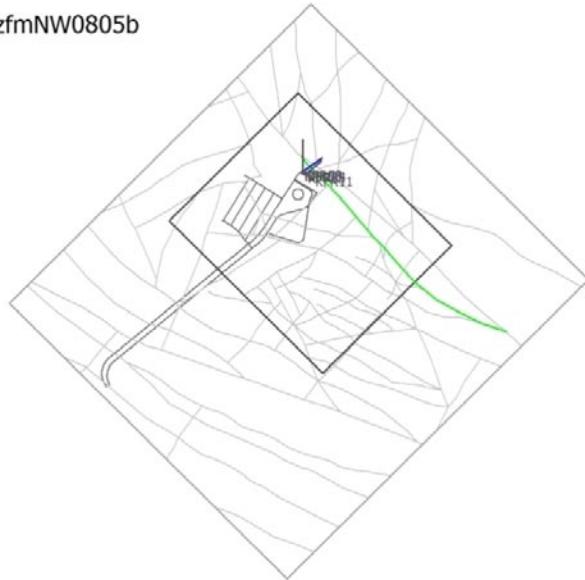
---

**Deformation zone ZFMNW0805B**

---

Modelling procedure: At the surface, corresponds to the low magnetic lineament MFM0805G1. The length of the DZ is 1,111 m with some 678 m inside the local model boundary

zfmNW0805b



A default vertical dip and default length-thickness class of 10 m have been applied to the zone in the model since no specific BH interval correlations have been interpreted

Confidence of existence: High

---

Property	Quantitative estimate	Confidence level	Basis for interpretation	Comments
Orientation (strike/dip)	133 / 90	High / medium	Strike based on trend of lineament. Default vertical dip applied	
Thickness	10 m	Medium	Default length-thickness class applied	
Length (regional model)	1,111 m	Medium	Linked lineament	
Deformation style	Inferred ductile origin with brittle reactivation based on orientation			
Alteration	-			

---

---

**Borehole intersections for ZFMNW0805B – details**

BH	Geometrical intercept		Target intercept		Comment
	Sec_up	Sec_low	Sec_up	Sec_low	
	BH length (m)	BH length (m)	BH length (m)	BH length (m)	
	[z (-m)]	[z (-m)]	[z (-m)]	[z (-m)]	
KFR7A	50.32 [134.04]	61.20 [134.42]	–	–	This interval falls within the single thick DZ1 (3.5 – 74.45 m) identified in KFR7A SHI. However this interval is inferred as being dominated by ZFMNW0805A and ZFM871 and no exclusive evidence for the existence of ZFMNW0805B has been identified. Therefore ZFMNW0805B has been classed as medium confidence
KFR08	39.05 [89.42]	49.31 [90.32]	–	–	The interpreted interval corresponds to part of KFR08 SHI DZ2 41–104.4 m. However this interval is inferred as being dominated by ZFMNW0805A and no exclusive evidence for the existence of ZFMNW0805B has been identified. Therefore ZFMNW0805B has been classed as medium confidence
KFR11	29.03 [91.54]	40.56 [93.54]	–	–	This BH has not been assessed during the current modelling phase
KFR24	59.11 [49.57]	77.60 [65.07]	–	–	This BH has not been assessed during the current modelling phase
KFR25	80.66 [58.02]	105.78 [76.09]	–	–	This BH has not been assessed during the current modelling phase
KFR56	59.47 [58.48]	74.87 [51.73]	–	–	This BH has not been assessed during the current modelling phase

---

**Engineering characteristics**

Not yet assessed

---

## ZFMNNW0999

ZFMNNW0999 is based on lineament MFM0999G (Forsmark version 2.3). The zone has a length of 692 m terminating at ZFMNW0805A in the SE and extending outside of the regional model area to the NW where MFM0999G terminates at MSFR08078 (an update of Forsmark version 2.3 MFM3149G). The modelled zone geometry, 170/90, and a length/thickness class of 5 m, results in an intersection in KFR08 SHI DZ2, however this interval is inferred as being dominated by ZFMNW0805A and no exclusive evidence for the existence of ZFMNNW0999 has been identified. For this reason, ZFMNNW0999 has been classed as medium confidence.

---

### Deformation zone ZFMNNW0999

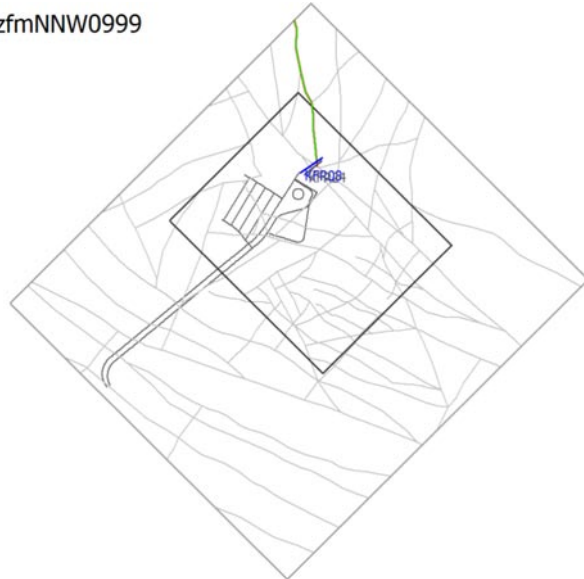
---

Modelling procedure: At the surface, corresponds to the low magnetic lineament MFM0999G

zfmNNW0999

The length of the DZ is 692 m with some 230 m within the local model area

Modelled using a default vertical dip and default length/thickness class of 5 m



Confidence of existence: Medium

Property	Quantitative estimate	Confidence level	Basis for interpretation	Comments
Orientation (strike/dip)	170 / 90	High for strike, medium for dip	Strike based on trend of lineament. Default vertical dip applied	
Thickness	5 m	Medium	Default length/thickness class applied	
Length (regional model)	692 m	Medium	Linked lineaments	
Deformation style	Brittle (inferred from orientation)			
Alteration	-			

---

### Borehole intersections for ZFMNNW0999 – details

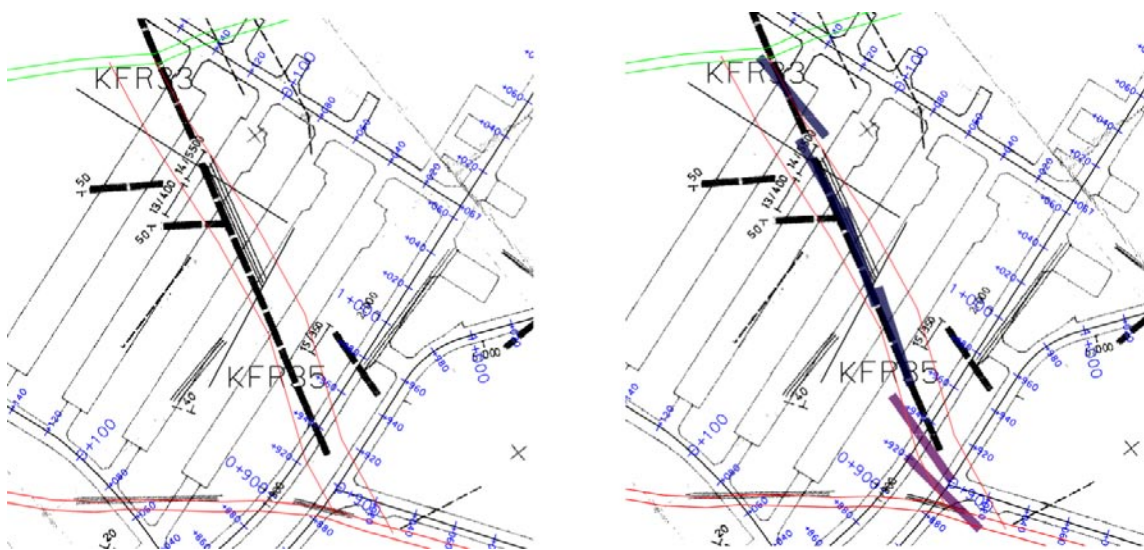
BH	Geometrical intercept		Target intercept		Comment
	Sec_up	Sec_low	Sec_up	Sec_low	
	BH length (m)	BH length (m)	BH length (m)	BH length (m)	
	[z (-m)]	[z (-m)]	[z (-m)]	[z (-m)]	
KFR08	75.72 [92.62]	81.46 [93.12]	-	-	This interval falls within the single thick possible deformation zone interval DZ2 (41–104.4 m) identified in KFR08 SHI. However this interval is inferred as being dominated by ZFMNW0805A and no exclusive evidence for the existence of ZFMNNW0999 has been identified. Therefore ZFMNNW0999 has been classed as medium confidence

## ZFMNNW1209

Zone ZFMNNW1209, previously known as zone 6 in earlier SFR models, has been modelled to extend from ZFMWNW3262 in the south to ZFMENE8031 in the north. Both these zones are medium confidence zones. The extent is based on a modification to the magnetic lineament MFM3114G. Based on inspection of the tunnel mapping results and their visualization in RVS, the existence of this apparently ‘well established’ zone reported in /Axelsson and Hansen 1997/ and earlier reports is difficult to follow as a single discrete structure. It is judged most likely to be a group of loosely associated thin discontinuous structures with a similar trend spread out over a thickness of around 20 m. The evidence quoted in the (northernmost) BMA cavern by /Axelsson and Hansen 1997/ shows a structure that dips steeply (c.70°) to the ENE, whereas indicators in the other caverns (BLA, 2BTF and 1 BTF) are more consistent and dip steeply to the WSW. Modelling work has adopted the steep dip to the WSW and is consistent with that adopted in /Stephens et al. 2007/. Similarly, the southernmost extension of the zone appears less reliable. The existence of the same structure in the DT is uncertain, while extension of the DT structure as a fracture swarm into the BT does appear possible though this has been discounted earlier.

Currently, the modelled geometry has been kept simple based on a partial agreement with the magnetic lineament MFM3114G, three control points from BLA, 2BTF and 1BTF, along with the SHI DZ1 from KFR35 giving a dip of 88° WSW. The lineament needs further review and the SE extension may need modification. The zone has been modelled with a thickness of 20 m to correlate with the thickness indicated by the geological SHI DZ1 in KFR35 and the geometrical spread of the individual, gouge-filled fractures. Individually mapped tunnel locations yield earlier recorded thicknesses between 0.5 and 2 m. Similar, parallel, clay-filled fractures have been reported to the north of the defined zone /Christiansson 1986/.

Essentially the zone has been adopted from the geological model for SFR by /Axelsson and Hansen 1997/. The surface position is based on a combination of magnetic lineament and tunnel mapping results. The zone is crossed by a single seismic refraction profile /Keisu and Isaksson 2004/. However, it does not have a seismic refraction anomaly associated with it, probably due to its diffuse character.



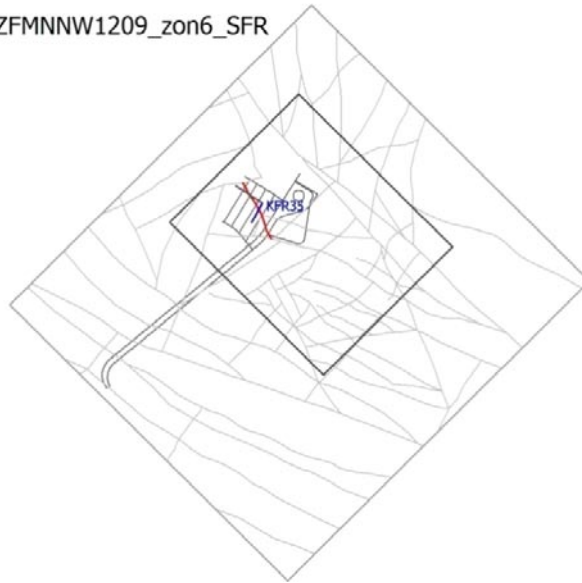
*A8-12. View on left: the tunnel mapping overview drawing showing ZFMNNW1209 as originally presented and the currently modelled envelope surfaces (red lines). View on right shows the modelled individually mapped zone locations. The two purple rectangles show the possible SE extension.*



**Deformation zone ZFMNNW1209 (zone 6 SFR)**

Modelling procedure: At the surface, corresponds to a section of the magnetic lineament MFM3114G, with the zone not extending as far to the NW as the lineament while having a greater extent to the SE. The lineament is currently undergoing review

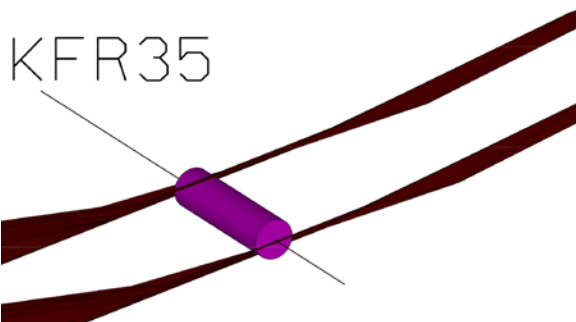
ZFMNNW1209\_zon6\_SFR



Modelled using dip that has been inferred from a combination of the lineament, KFR35 and tunnel mapping results. The modelled thickness is based on KRF35 SHI DZ1

Confidence of existence: High

Property	Quantitative estimate	Confidence level	Basis for interpretation	Comments
Orientation (strike/dip)	151 / 88	High / medium	Strike based on trend of lineament and tunnel mapping. Dip based on tunnel mapping and KFR35 DZ1	
Thickness	20 m	Medium	Individual tunnel mapping results indicate 0.5 to 2 m while KFR35 SHI DZ1 corresponds to a thickness of 20 m	



Purple cylinder represents SHI DZ interpreted as ZFMNNW1209

Length (regional model)	253 m	Medium	Tunnel mapping and magnetic lineament MFM3114G	
Deformation style	Brittle			
Alteration	Locally faint to weak oxidation			

---

**Borehole intersections for ZFMNNW1209 (zone 6 SFR) – details**

BH	Geometrical intercept		Target intercept		Comment
	Sec_up	Sec_low	Sec_up	Sec_low	
	BH length (m)	BH length (m)	BH length (m)	BH length (m)	
	[z (-m)]	[z (-m)]	[z (-m)]	[z (-m)]	
KFR33	42.77 [24.50]	106.29 [68.46]	–	–	Note: /Axelsson and Hansen 1997/ approximate position of correlation was 58 m BH length, 465 m level  This BH has not been assessed during the current modelling phase
KFR35	30.67 [18.90]	72.35 [51.51]	32.7	70	32.7–70 m DZ1: Increased frequency of broken and unbroken fractures and sealed networks. Six crushed intervals in the lower part of the section (57.37–68.15 m). Three intervals at 44.83–46.07, 55.92–56.01 and 60.37–61.60 m include fault breccias and cataclastite. Predominant fracture minerals are adularia, calcite and quartz. $\alpha$ -angles are generally small to moderate (21–61°). Asphaltite, typically associated with calcite, is more or less limited to this section. A black unknown mineral that resembles asphaltite is restricted to 20.1–71.6 m. Locally faint to weak oxidation. One minor core loss at 63.84–64.15 m. Pegmatitic granite (101061) with occurrences of felsic to intermediate metavolcanic rock (103076), fine- to medium-grained granite (111058) and strongly foliated metagranite-granodiorite (101057). Confidence level = 3  Note: /Axelsson and Hansen 1997/ approximate position of correlation was 57.5 m BH length, 460 m level
KFR57	–	–	–	–	Note: /Axelsson and Hansen 1997/ list a possible correlation with a position at 12.5 m BH length, 400 m level  This BH has not been assessed during the current modelling phase

---

**Tunnel intersections for ZFMNNW1209 (zone 6 SFR) – details**

Tunnel	Geometrical intercept		Target intercept		Comment
	Start ch.(m)	End ch. (m)	Start ch.(m)	End ch. (m)	
DT	920 (1+920)	945 (1+945)	930 (1+930)	930 (1+930)	Note:earlier interpreted as 1+930 /Axelsson and Hansen 1998/
BT	885 (5+885)	907 (5+907)	893 (5+893)	893 (5+893)	Additional possible low confidence observation based on detailed drawing -09 /Christiansson and Bolvede 1987/
NBT	0 (8+000)	010 (8+010)	–	–	
1 BTF	0+090	0+117	0+100	0+100	Note:earlier interpreted as 0+100 /Axelsson and Hansen 1997/
2 BTF	0+067	0+090	0+080	0+080	Note:earlier interpreted as 0+085 /Axelsson and Hansen 1997/
BLA	0+048	0+068	0+060	0+060	Note:earlier interpreted as 0+060 /Axelsson and Hansen 1997/
BMA	0+030	0+055	–	–	Note:earlier interpreted as 0+030 /Axelsson and Hansen 1998/

---

---

**Engineering characteristics**

---

Fracture frequency: 12 m-1, span 10–15 m-1, intersection along SFR BHs as reported by /Stephens et al. 2007/

Fracture filling: Clay-rich gouge. Clayey water-bearing gouge, partly with intensely fractured rims. In the tunnels, the zone is reported as having associated moisture and occasionally dripping water. For most of its length, the zone is a slightly water-bearing, gouge-filled joint, occasionally with increased fracturing on one or both sides /Axelsson and Hansen 1997/

/Christiansson 1986/ reports an overall thickness of 2–4 m including weak to moderate weathering and raised fracture frequency. The zone core was reported as having a width of 0.3–1 m including hard clay which, in its turn, had been broken up and surrounded by a younger softer clay. The younger clay appears as the matrix of a breccia. Away from the clay, the fractures have been sealed by calcite. In the rock caverns, the associated water inflow was generally limited to moisture or dripping. At isolated points, inflows in the range of 0.5–1.0 l/min were reported, being associated with blasting and washout of the clay-filled joints

---